May 2020

# Patterns and Processes of Speciation and Phenotypic Diversification in Palm-Pitvipers (Viperidae: *Bothriechis*)

Andrew James Mason
*Clemson University*, masonaj157@gmail.com

# Patterns and Processes of Speciation and Phenotypic diversification in Palm-Pitvipers (Viperidae: *Bothriechis*)

---

A Dissertation
Presented to
the Graduate School of
Clemson University

---

In Partial Fulfillment
of the Requirements for the Degree
Doctor of Philosophy
Biological Sciences

---

by
Andrew James Mason
May 2020

---

Accepted by:
Dr. Christopher L. Parkinson, Committee Chair
Dr. Margaret B. Ptacek
Dr. Samantha A. Price
Dr. Mahmood Sasa

# Abstract

Diversification is primarily a function of two processes—speciation and adaptation—that shape the history and trajectory of evolutionary lineages. These processes are often interdependent and are shaped by biotic and abiotic factors including existing and evolvable genetic variation, selection, and genetic connectivity among lineages. Genomic datasets present a means of disentangling complex evolutionary signals by sampling hundreds or thousands of loci to interrogate lineage and/or trait diversification. Palm-pitvipers (*Bothriechis*) are well suited for testing evolutionary hypotheses related to speciation and adaption. This group of arboreal vipers is well-recognized as monophyletic with a contentious phylogeographic history. Moreover, these species' venoms are an ideal adaptive trait for examining genotype-phenotype interactions. To understand the processes affecting speciation in palm-pitvipers, I estimated the group's phylogeny using an anchored phylogenomics approach and tested for evidence of reticulate evolution (i.e., ancient gene-flow) in the group's history. The recovered phylogeny conflicted with key relationships inferred by mitochondrial genes and tests for reticulate evolution revealed strong support for historic gene flow among geographically proximate lineages. To examine the mechanisms promoting macroevolutionary divergence of venom phenotypes, I first focused on two sister taxa with strongly divergent venom types: The Black-Speckled (*B. nigroviridis*) and Talamancan (*B. nubestris*) Palm-Pitvipers. I tested whether toxins underlying venom differentiation would be associated with modular transcript expression. I found that toxins responsible for specific phenotypes segregate into distinct co-expression modules, which may permit rapid differentiation of venoms. To expand my investigation, I assembled venom gland transcriptomes from all recognized species of palm-pitvipers and assessed how gene family evolution affected patterns of toxin expression. Toxin expression was highly variable within toxin families but more variable following speciation events than gene duplications. Additionally, I identified multiple lineage specific regimes of expression for specific $PLA_2$ and SVMP genes. Despite the broad expression

variation characteristic of toxin genes, lineage-specific patterns of toxin expression emphasize the effect of shared evolutionary history on underlying genetic architecture. More broadly, the complexities of speciation and venom phenotype evolution observed in palm-pitvipers demonstrate the variety of processes that can influence evolutionary trajectories.

# Dedication

To my wife Alania and my parents James and Gail for their love and support, and the friends who have helped me along the way.

# Acknowledgments

Throughout my PhD experience I have been fortunate to interact with many wonderful people who have shaped my research and education. I would first like to thank my advisor, Dr. Chris Parkinson, for taking a chance by accepting a semi-qualified Master's student and supporting six years of research across four countries and several U.S. states. I would also like to thank the members of my Clemson and UCF dissertation committees: Dr. Mahmood Sasa, Dr. Margaret Ptacek, Dr. Sam Price, Dr. Shibu Yooseph, Dr. Anna Savage, and Dr. Eric Hoffman. Thank you all for your consideration and patience with me as I stumbled through graduate school and the construction of this dissertation.

I have been extremely lucky to work with fantastic collaborators, many of whom helped me with the difficult task of collecting samples and generating data. I would especially like to thank Felipe Grazziotin, Fabián Bonilla, the Chacón and Sandi Harmon families, Joe Townsend, Luis Herrera, Jocelyn Analid Castro, Emmanuel Orellana Murillo, Carlos Augusto Andino, Jose Vindel, Carlos R. Vásquez-Almazán, Hector A. Rosales, Denis Padilla Raudales, Chris Grünwald, Jason Jones, Ricardo Ramírez Chaparro, Héctor Franz, Ivan Ahumada Carrillo, Miguel Borja, Juan Castañeda-Gaytán, and Gamaliel Castañeda-Gaytán who provided invaluable assistance collecting specimens. I would like to give special thanks to the Rokyta lab members Carl Whittington, Micaiah Ward, Mike Hogan, Schyler Ellsworth, and Gunnar Nystrom for being great collaborators. I would also like to express my gratitude to Dr. Darin Rokyta for allowing me to invade his lab space on several occasions and for introducing me to bioinformatic analyses.

My research has been supported by many hardworking people at Clemson and UCF. Patrick Larabee of UCFIT and Ashwin Srinath of Clemson's CITI group helped me struggle through my frequent computer problems and navigating the Palmetto cluster. I would also like to thank Dr. Melissa Dagely and the EXCEL/COMPASS/iSTEM team at UCF who provided a unique TA ex-

perience that I was fortunate to be a part of. Dr. Rooksie Noorai and Jaime Randise of the Clemson Genomics and Bioinformatics Facility have been exceptional teammates during my time as a graduate bioinformatics mentor.

I would not have made it through my dissertation without the help of my friends and lab mates, who made every day more fun and did a very great deal of editing. Jason Strickland, Rhett Rautsaw, Matt Lawrence, Alexa Trujillo, Katie Mercier, Mark DiMeo, Eric Hofmann, Matt Holding, Erin Steirs, Mark Margres, Tristan Schramer, Alex Robertson, Hollis Dahn, Alejandra Osorio, Shelly Gaynor, Bridget Vincent, Katelyn Lanctot, Carly Grimison, Millie Baylac, Jade Mellor, Anna Hewitt, and William Rumfelt, you have all been such an important part of my graduate school experience. I owe each of you a great deal and I can only say I hope I have been as good a friend to you all as you have been to me.

Finally, I would like to thank my wife Nia, Ziggy, my mother and father for their unconditional love and support.

# Table of Contents

# List of Tables

# List of Figures

# Chapter 1

# Introduction

Global biodiversity is primarily the result of two processes that shape the diversification of form and function: speciation and adaptation. Speciation is the process by which genetically continuous lineages take on evolutionarily independent trajectories, typically through the establishment of reproductive isolation (Mayr, 1982; Coyne, 1992). Through time, repeated speciation events result in the hierarchical ancestor-descendent relationships, which are represented by the branching patterns of a phylogeny. The information on evolutionary relationships and the non-independence of terminals associated with phylogenies has made them invaluable tools for the study of speciation and diversification (Hennig, 1966). Consequently, establishing a reliable phylogeny for any study group has become a crucial prerequisite in many sub-fields of biology (Felsenstein, 1985; Wanntorp et al., 1990; Monson, 1996; Bermingham and Moritz, 1998). However, recovering a robust phylogeny is often not trivial. Despite its conceptual simplicity, speciation is a complex process that is affected by a variety of factors that can initiate, reinforce, or erode species boundaries (Nosil et al., 2003; Arnegard et al., 2014; Abbott et al., 2016). Although phylogenies were once assumed to be purely the result of bifurcating processes, it is being increasingly recognized that there are many forces of evolution that produce discordant phylogenetic signals (Doyle, 1992; Dowling and Secor, 1997; Maddison, 1997; Degnan and Rosenberg, 2009; Bonnet et al., 2017). As a result, resolving recalcitrant nodes and identifying sources of phylogenetic discordance has become a focal area for phylogenetic development in recent years (Planet, 2005; Jeffroy et al., 2006; Than et al., 2008; Salichos et al., 2014; Ai and Kang, 2015; Solís-Lemus and Ané, 2016; Arcila et al., 2017). Moreover, the resolution or understanding of the processes shaping a phylogeny becomes particularly critical to any kind of

comparative study.

Acting adjacent to speciation is adaptation, the process by which a species is modified to increase its survival and reproduction, typically by natural selection (Dobzhansky, 1956). Adaptation can take place through a variety of mechanisms to produces behaviors, physiologies, morphologies or any combination thereof to optimize the function of organisms' phenotypic traits in response to their environments (Dobzhansky, 1956). However, the capacity for adaptation can be restricted by limited genetic variation or constrained by physiological and developmental characteristics which are usually closely tied to phylogeny (Arnold, 1992; Futuyma, 2010). Accounting for the non-independence of evolutionary constraint represented in the phylogeny becomes particularly important in studies of adaptation (Felsenstein, 1985; Blomberg and Garland Jr, 2002; Butler and King, 2004; Losos, 2011). However, studying macro-evolutionary patterns of diversity in adaptive traits can lend a great deal of insight into species' evolution, ecology, and life history. Adaptation can generate key innovations, which can open previously inaccessible dimensions of niche space to a lineage, thereby accelerating speciation (Alfaro, 2013). Such local adaptation can lead to ecological adaptation and specialization (Futuyma and Moreno, 1988; Losos, 2011). In tractable systems, understanding patterns of evolution in adaptive traits will provide insight into the selective forces that shape adaptation and the genetic mechanisms underlying diversification.

An opportunity to examine the processes affecting speciation and the mechanisms of adaptation exists in the Middle American palm-pitviper group (genus *Bothriechis*). Pitvipers have provided a model system for testing hypotheses of speciation, adaptation, and biogeography due to their diverse distributions and variety of ecomorphs (Parkinson et al., 2000; Castoe et al., 2009; Schield et al., 2015; Alencar et al., 2016, 2017). Palm-pitvipers are unique among New World pitvipers as a completely arboreal genus (Campbell and Lamar, 2004). The 11 recognized species are broadly distributed across Middle America, although 10 of the 11 species are mid-high elevation specialists restricted to montane habitats (Campbell and Lamar, 2004; Townsend et al., 2013; Doan et al., 2016). The exception among palm-pitvipers is *B. schlegelii* which occupies a largely continuous distribution from northern South America to southern Mexico and ranges in habitat from lowland wet forests to high-elevation cloud forests in Colombia and Ecuador. Despite being well-recognized as monophyletic (Castoe and Parkinson, 2006), the phylogeny of palm-pitvipers has been incongruently recovered by studies using different data types. However, the specific sources of phylogenetic incongruence have not been well-explored and present an opportunity to examine the forces generating

discordance in a group with a complex geographic history. Additionally, palm-pitvipers possess an ideal trait for studying adaptation: venom.

Venoms are complex secretions of toxins produced in a specialized gland tissue that function together for prey acquisition and/or defense (Casewell et al., 2013). In snakes, venom is made up of 30-100 individual secreted toxins most of which are from well-characterized toxin gene families (Mackessy, 2010; Casewell et al., 2013). Additionally, the majority of venom proteins can be traced back to single genes, which facilitates genotype-phenotype mapping. Venom is vital to the life histories of viperid snakes and experiences strong selection (Margres et al., 2017). Venom has been shown to vary based on diet composition (Daltry et al., 1996; Barlow et al., 2009; Davies and Arbuckle, 2019; Healy et al., 2019; Lyons et al., 2020), and other environmental pressures (Strickland et al., 2018b; Zancolli et al., 2019). Venoms can be highly variable in composition and function among species (Mackessy, 2010). For instance, three palm-pitviper species occurring in Costa Rica exhibit three differentiated venom phenotypes. *Bothriechis schlegleii* venoms exhibit high proportions of phospholipase $A_2$s ($PLA_2$s), moderate proportions of several venom toxins including snake venom metalloproteinases (SVMPs), snake venom serine proteinases (SVSPs), bradykinin-potentiating peptides (BPPs), and L-amino acid oxidases (LAAOs), and the pharmacological effects of the venom are primarily myotoxic and hemorrhagic (Lomonte et al., 2008). In contrast, the venom of *B. lateralis* is dominated by SVMPs, which induce substantial hemorrhage but little to no myotoxicity (Lomonte et al., 2008). The venom of *B.nigroviridis* also exhibits striking differentiation, being composed primarily of a neurotoxic $PLA_2$ complex that produces neurotoxic pharmacological effects, but few other symptoms (Fernández et al., 2010). Notably, these venom phenotypes are similar to those observed in other pitviper species (Mackessy, 2008, 2010), suggesting that palm-pitvipers can serve as an effective model for venom evolution in pitvipers in general. While there has been widespread interest in characterizing the venoms of snake species (Calvete et al., 2007, 2009; Calvete, 2014; Sunagar et al., 2016), there has been limited progress in understanding the evolutionary dynamics shaping these complex phenotypes (Casewell et al., 2012; Sunagar et al., 2014; Barua and Mikheyev, 2019).

Massively high-throughput sequencing technologies and genomic tools have revolutionized biological inference by allowing one to leverage unprecedented amounts of data to test hypotheses with very high resolution. For instance, RNAseq has fundamentally changed the study of snake venoms by enabling the simultaneous sequencing of toxin transcripts expressed at a given time (Rokyta

et al., 2011; Durban et al., 2011; Brahma et al., 2015). High-throughput venom gland transcriptomes provide a more precise picture of venom composition than is recovered through qualitative proteomic comparisons and are an informative intermediate between genotype and phenotype. Similarly, next-generation phylogenetic methods can utilize hundreds of loci simultaneously to capture phylogenetic signal from across the genome (Lemmon et al., 2012; Lemmon and Lemmon, 2013; McCormack et al., 2013, 2012). Unfortunately, as sequencing technologies have evolved and improved rapidly, analytical methods and approaches that can capitalize on these data have been slower to develop. Thus, analyses of genome-scale datasets still requires careful study design, consideration, and interpretation. Nonetheless, leveraging emerging methods and novel analytical approaches offer the potential to resolve challenging questions and test comprehensive hypotheses on the nature of diversification processes like speciation and adaptation.

Here, I leverage palm-pitvipers as a model system and employ multiple genomic approaches to discern historic evolutionary forces, selective processes, and genetic mechanisms that mediate speciation and adaptation. In this pursuit I will meet the following three goals:

1. Use anchored phylogenomic data to resolve the phylogeny of palm-pitvipers and identify processes leading to conflicting phylogenetic hypotheses.

2. Test whether modular expression of key toxin families provides a mechanism for extreme differentiation in venom phenotypes observed between *B. nigroviridis* and *B. nubestris*.

3. Examine the extent to which genes and species-specific phenotypes interact to shape variation in toxin expression among palm-pitvipers.

# References


Abbott, R. J., Barton, N. H., and Good, J. M. (2016). Genomics of hybridization and its evolutionary consequences. *Molecular Ecology*, 25(11):2325–2332.

Ai, B. and Kang, M. (2015). How many genes are needed to resolve phylogenetic incongruence? *Evolutionary Bioinformatics*, 11:EBO–S26047.

Alencar, L. R. V., Martins, M., Burin, G., and Quental, T. B. (2017). Arboreality constrains morphological evolution but not species diversification in vipers. *Proceedings of the Royal Society B: Biological Sciences*, 284(1869).

Alencar, L. R. V., Quental, T. B., Grazziotin, F. G., Alfaro, M. L., Martins, M., Venzon, M., and Zaher, H. (2016). Diversification in vipers: Phylogenetic relationships, time of divergence and shifts in speciation rates. *Molecular Phylogenetics and Evolution*, 105:50–62.

Alfaro, M. E. (2013). Key evolutionary innovations. In Losos, J. B., editor, *Princeton guide to evolution*, pages 392–398. Princeton University Press, Princeton, New Jersey.

Arcila, D., Ortí, G., Vari, R., Armbruster, J. W., Stiassny, M. L., Ko, K. D., Sabaj, M. H., Lundberg, J., Revell, L. J., and Betancur-R, R. (2017). Genome-wide interrogation advances resolution of recalcitrant groups in the tree of life. *Nature Ecology & Evolution*, 1(2):1–10.

Arnegard, M. E., McGee, M. D., Matthews, B., Marchinko, K. B., Conte, G. L., Kabir, S., Bedford, N., Bergek, S., Chan, Y. F., Jones, F. C., Kingsley, D. M., Peichel, C. L., and Schluter, D. (2014). Genetics of ecological divergence during speciation. *Nature*, 511(7509):307–311.

Arnold, S. J. (1992). Constraints on phenotypic evolution. *American Society of Naturalists*, 140:S85–S107.

Barlow, A., Pook, C. E., Harrison, R. A., and Wüster, W. (2009). Coevolution of diet and prey-specific venom activity supports the role of selection in snake venom evolution. *Proceedings of the Royal Society B*, 276(1666):2443–2449.

Barua, A. and Mikheyev, A. S. (2019). Many options, few solutions: Over 60 my snakes converged on a few optimal venom formulations. *Molecular biology and evolution*, 36(9):1964–1974.

Bermingham, E. and Moritz, C. (1998). Comparative phylogeography: concepts and applications. *Molecular Ecology*, 7(4):367–369.

Blomberg, S. P. and Garland Jr, T. (2002). Tempo and mode in evolution: phylogenetic inertia, adaptation and comparative methods. *Journal of Evolutionary Biology*, 15(6):899–910.

Bonnet, T., Leblois, R., Rousset, F., and Crochet, P.-A. (2017). A reassessment of explanations for discordant introgressions of mitochondrial and nuclear genomes. *Evolution*, 71(9):2140–2158.

Brahma, R. K., McCleary, R. J., Kini, R. M., and Doley, R. (2015). Venom gland transcriptomics for identifying, cataloging, and characterizing venom proteins in snakes. *Toxicon*, 93:1–10.

Butler, M. A. and King, A. A. (2004). Phylogenetic comparative analysis: a modeling approach for adaptive evolution. *American Naturalist*, 164(6):683–695.

Calvete, J. J. (2014). Next-generation snake venomics: protein-locus resolution through venom proteome decomplexation. *Expert Review of Proteomics*, 11(3):315–29.

Calvete, J. J., Juárez, P., and Sanz, L. (2007). Snake venomics. Strategy and applications. *Journal of Mass Spectrometry*, 42(11):1405–1414.

Calvete, J. J., Sanz, L., Angulo, Y., Lomonte, B., and Gutiérrez, J. M. (2009). Venoms, venomics, antivenomics. *FEBS Letters*, 583(11):1736–1743.

Campbell, J. A. and Lamar, W. W. (2004). *Venomous Reptiles of the Western hemisphere*. Cornell University Press, Ithaca, NY, 2 edition.

Casewell, N. R., Huttley, G. a., and Wüster, W. (2012). Dynamic evolution of venom proteins in squamate reptiles. *Nature Communications*, 3(1066):1–10.

Casewell, N. R., Wüster, W., Vonk, F. J., Harrison, R. a., and Fry, B. G. (2013). Complex cocktails: The evolutionary novelty of venoms. *Trends in Ecology and Evolution*, 28(4):219–229.

Castoe, T. A., Daza, J. M., Smith, E. N., Sasa, M. M., Kuch, U., Campbell, J. A., Chippindale, P. T., and Parkinson, C. L. (2009). Comparative phylogeography of pitvipers suggests a consensus of ancient Middle American highland biogeography. *Journal of Biogeography*, 36(1):88–103.

Castoe, T. A. and Parkinson, C. L. (2006). Bayesian mixed models and the phylogeny of pitvipers (Viperidae: Serpentes). *Molecular Phylogenetics and Evolution*, 39(1):91–110.

Coyne, J. A. (1992). Genetics and speciation. *Nature*, 355:511–515.

Daltry, J. C., Wüster, W., and Thorpe, R. S. (1996). Diet and snake venom evolution. *Nature*, 379:537–540.

Davies, E.-L. and Arbuckle, K. (2019). Coevolution of Snake Venom Toxic Activities and Diet: Evidence that Ecological Generalism Favours Toxicological Diversity. *Toxins*, 11(12):711.

Degnan, J. H. and Rosenberg, N. A. (2009). Gene tree discordance, phylogenetic inference and the multispecies coalescent. *Trends in Ecology & Evolution*, 24(6):332–340.

Doan, T. M., Mason, A. J., Castoe, T. A., Sasa, M., and Parkinson, C. L. (2016). A cryptic palm-pitviper species (Squamata: Viperidae: *Bothriechis*) from the Costa Rican highlands, with notes on the variation within *B. nigroviridis*. *Zootaxa*, 4138(2):271–290.

Dobzhansky, T. (1956). What is an Adaptive Trait? *The American Naturalist*, 90(855):337–347.

Dowling, T. E. and Secor, C. L. (1997). The role of hybridization and introgression in the diversification of animals.

Doyle, J. J. (1992). Gene Trees and Species Trees: Molecular Systematics as One-Character Taxonomy. *Systematic Botany*, 17(1):144–163.

Durban, J., Juárez, P., Angulo, Y., Lomonte, B., Flores-Diaz, M., Alape-Girón, A., Sasa, M., Sanz, L., Gutiérrez, J. M., Dopazo, J., Conesa, A., and Calvete, J. J. (2011). Profiling the venom gland transcriptomes of Costa Rican snakes by 454 pyrosequencing. *BMC genomics*, 12:259.

Felsenstein, J. (1985). Phylogenies and the Comparative Method. *The American Naturalist*, 125(1):1–15.

Fernández, J., Lomonte, B., Sanz, L., Angulo, Y., and Calvete, J. J. (2010). Snake Venomics of *Bothriechis nigroviridis* Reveals Extreme Variability among Palm Pitviper Venoms : Different Evolutionary Solutions for the Same Trophic Purpose. *Journal of Proteome Research*, 9:4234–4241.

Futuyma, D. J. (2010). Evolutionary constraint and ecological consequences. *Evolution: International Journal of Organic Evolution*, 64(7):1865–1884.

Futuyma, D. J. and Moreno, G. (1988). The Evolution of Ecological Specialization. *Annual Review of Ecology and Systematics*, 19(1):207–233.

Healy, K., Carbone, C., and Jackson, A. L. (2019). Snake venom potency and yield are associated with prey-evolution, predator metabolism and habitat structure. *Ecology letters*, 22(3):527–537.

Hennig, W. (1966). *Phylogenetic Systematics*. University of Illinois Press.

Jeffroy, O., Brinkmann, H., Delsuc, F., and Philippe, H. (2006). Phylogenomics: the beginning of incongruence? *Trends in Genetics*, 22(4):225–231.

Lemmon, A. R., Emme, S. A., and Lemmon, E. M. (2012). Anchored hybrid enrichment for massively high-throughput phylogenomics. *Systematic Biology*, 61(5):727–744.

Lemmon, E. M. and Lemmon, A. R. (2013). High-throughput genomic data in systematics and phylogenetics. *Annual Review of Ecology, Evolution, and Systematics*, 44:99–121.

Lomonte, B., Escolano, J., Fernández, J., Sanz, L., Angulo, Y., Gutiérrez, J. M., and Calvete, J. J. (2008). Snake venomics and antivenomics of the arboreal neotropical pitvipers *Bothriechis lateralis* and *Bothriechis schlegelii*. *Journal of Proteome Research*, 7(6):2445–2457.

Losos, J. B. (2011). Convergence, adaptation, and constraint. *Evolution*, 65(7):1827–1840.

Lyons, K., Dugon, M. M., and Healy, K. (2020). Diet Breadth Mediates the Prey Specificity of Venom Potency in Snakes. *Toxins*, 12(2):74.

Mackessy, S. P. (2008). Venom composition in rattlesnakes: trends and biological significance. In Hayes, W. K., Beaman, K. R., Cardwell, M. D., and Bush, S. P., editors, *The Biology of Rattlesnakes*, pages 495–510. Loma Linda University Press, Loma Linda, CA.

Mackessy, S. P. (2010). *Venoms and Toxins of Reptiles*.

Maddison, W. P. (1997). Gene trees in species trees. *Systematic Biology*, 46(3):523–536.

Margres, M. J., Bigelow, A. T., Lemmon, E. M., Lemmon, A. R., and Rokyta, D. R. (2017). Selection To Increase Expression, Not Sequence Diversity, Precedes Gene Family Origin and Expansion in Rattlesnake Venom. *Genetics*, 206(3):1569–1580.

Mayr, E. (1982). Speciation and Macroevolution. *Evolution*, 36(6):1119–1132.

McCormack, J. E., Faircloth, B. C., Crawford, N. G., Gowaty, P. A., Brumfield, R. T., and Glenn, T. C. (2012). Ultraconserved elements are novel phylogenomic markers that resolve placental mammal phylogeny when combined with species-tree analysis. *Genome research*, 22(4):746–754.

McCormack, J. E., Hird, S. M., Zellmer, A. J., Carstens, B. C., and Brumfield, R. T. (2013). Applications of next-generation sequencing to phylogeography and phylogenetics. *Molecular phylogenetics and evolution*, 66(2):526–38.

Monson, R. K. (1996). The Use of Phylogenetic Perspective in Comparative Plant Physiology and Development. *Annals of the Missouri Botanical Garden*, 83(1):3–16.

Nosil, P., Crespi, B. J., and Sandoval, C. P. (2003). Reproductive isolation driven by the combined effects of ecological adaptation and reinforcement. *Proceedings of the Royal Society of London. Series B: Biological Sciences*, 270(1527):1911–1918.

Parkinson, C. L., Zamudio, K., and Greene, H. W. (2000). Phylogeography of the pitviper clade *Agkistrodon*: historical ecology, species status, and conservation of cantils. *Molecular Ecology*, 9:411–420.

Planet, P. J. (2005). Tree disagreement: Measuring and testing incongruence in phylogenies. *Journal of Biomedical Informatics*.

Rokyta, D. R., Wray, K. P., Lemmon, A. R., Lemmon, E. M., and Caudle, S. B. (2011). A high-throughput venom-gland transcriptome for the Eastern Diamondback Rattlesnake (*Crotalus adamanteus*) and evidence for pervasive positive selection across toxin classes. *Toxicon*, 57(5):657–671.

Salichos, L., Stamatakis, A., and Rokas, A. (2014). Novel information theory-based measures for quantifying incongruence among phylogenetic trees. *Molecular Biology and Evolution*, 31(5):1261–1271.

Schield, D. R., Card, D. C., Adams, R. H., Jezkova, T., Reyes-Velasco, J., Proctor, F. N., Spencer, C. L., Herrmann, H. W., Mackessy, S. P., and Castoe, T. A. (2015). Incipient speciation with biased gene flow between two lineages of the Western Diamondback Rattlesnake (*Crotalus atrox*). *Molecular Phylogenetics and Evolution*, 83:213–223.

Solís-Lemus, C. and Ané, C. (2016). Inferring Phylogenetic Networks with Maximum Pseudolikelihood under Incomplete Lineage Sorting. *PLOS Genetics*, 12(3):e1005896.

Strickland, J. L., Smith, C. F., Mason, A. J., Schield, D. R., Borja, M., Castañeda-Gaytán, G., Spencer, C. L., Smith, L. L., Trápaga, A., Bouzid, N. M., Campillo-García, G., Flores-Villela, O. A., Antonio-Rangel, D., Mackessy, S. P., Castoe, T. A., Rokyta, D. R., and Parkinson, C. L. (2018). Evidence for divergent patterns of local selection driving venom variation in Mojave Rattlesnakes (*Crotalus scutulatus*). *Scientific Reports*, 8(1):17622.

Sunagar, K., Casewell, N. R., Varma, S., Kolla, R., Antunes, A., and Moran, Y. (2014). Deadly Innovations: Unraveling the Molecular Evolution of Animal Venoms. In Gopalakrishnakone, P. and Calvete, J. J., editors, *Venom Genomics and Proteomics*, pages 1–23. Springer.

Sunagar, K., Morgenstern, D., Reitzel, A. M., and Moran, Y. (2016). Ecological venomics: How genomics, transcriptomics and proteomics can shed new light on the ecology and evolution of venom. *Journal of Proteomics*, 135:62–72.

Than, C., Ruths, D., and Nakhleh, L. (2008). PhyloNet: a software package for analyzing and reconstructing reticulate evolutionary relationships. *BMC Bioinformatics*, 9(1):322.

Townsend, J. H., Medina-Flores, M., Wilson, L. D., Jadin, R. C., and Austin, J. D. (2013). A relict lineage and new species of green palm-pitviper (Squamata, Viperidae, *Bothriechis*) from the Chortís Highlands of Mesoamerica. *ZooKeys*, 298:77–106.

Wanntorp, H.-E., Brooks, D. R., Nilsson, T., Nylin, S., Ronquist, F., Stearns, S. C., and Wedell, N. (1990). Phylogenetic Approaches in Ecology. *Oikos*, 57(1):119–132.

Zancolli, G., Calvete, J. J., Cardwell, M. D., Greene, H. W., Hayes, W. K., Hegarty, M. J., Herrmann, H.-W., Holycross, A. T., Lannutti, D. I., Mulley, J. F., et al. (2019). When one phenotype is not enough: divergent evolutionary trajectories govern venom variation in a widespread rattlesnake species. *Proceedings of the Royal Society B*, 286(1898):20182735.

# Chapter 2

# Reticulate evolution in Nuclear Middle America causes discordane in the phylogeny of palm-pitvipers (Viperidae: *Bothriechis*)

## 2.1 Abstract

A number of processes can lead to weak or conflicting phylogenetic signals, especially in geographically dynamic regions where unstable landscapes and climates promote complex evolutionary histories. The Middle American pitviper genus *Bothriechis* has a complex biogeographic distribution and previous phylogenetic analyses have recovered conflicting topologies based on the data type used. Here, we tested whether historic conflicts in the phylogeny were the result of reticulate evolution and whether the inferred biogeographic history of the group would enable contact among reticulate lineages. We generated a phylogenomic dataset using an anchored phylogenomics approach and inferred a genomics-based species tree and mitochondrial tree to assess incongruence among datasets. We then generated a dated phylogeny and conducted ancestral area reconstruction to examine the biogeographic history surrounding the diversification of these species. We addition-

ally tested whether the discordance among trees is better explained by lineage sorting or reticulate evolution by testing models of reticulate evolution inferred through multiple methods. We found strong support for discordance in the phylogeny of *Bothriechis* and corresponding evidence for reticulate evolution among lineages with incongruent placement. Ancestral area reconstruction placed these taxa in adjacent regions during the time period when reticulation was projected to take place and suggested a biogeographic history heavily influenced by vicariant processes. Reticulation among geographically proximate lineages has driven apparent genomic discordance in *Bothriechis* and is responsible for historical incongruence in the phylogeny. Inference of the order of events suggests that reticulation in Nuclear Middle American occurred during a time of geologic upheaval, promoting lineage divergence and secondary contact. Reticulate evolution and similar processes can have substantial impacts on the evolutionary trajectory of taxa and are important to explicitly test for in biogeographically complex regions.

## 2.2 Introduction

A variety of systematic and inherent biases can contribute to phylogenetic instability and discordance (Pamilo and Nei, 1988; Funk and Omland, 2003; Jeffroy et al., 2006). The use of next-generation sequencing and genome-scale datasets were expected to provide resolution for recalcitrant nodes, and, while genomic datasets have resolved some relationships (Arcila et al., 2017; Breinholt et al., 2017), many systems remain challenged by discordance and conflicting phylogenetic signals (Smith et al., 2015).

Many processes can lead to weak phylogenetic signal or discordance (Doyle, 1992; Maddison, 1997; Rieseberg et al., 2000; Giarla and Esselstyn, 2015), especially in historically dynamic geographic regions where unstable landscapes and climate promote complex evolutionary histories (Daza et al., 2009; Boissin et al., 2011; Ornelas et al., 2013). Changing landscapes can create novel habitats and open niches allowing for rapid radiations where the order of diversification can be difficult or impossible to determine (Weissing et al., 2011; Giarla and Esselstyn, 2015). Similarly, disjunct habitats such as island archipelagos and isolated montane "sky-islands" can lead to intricate patterns of speciation through vicariance or dispersal (Savage, 1982; Juan et al., 2000; Zaher et al., 2018).

While many geographic regions have complicated histories, few are as biologically rich and geologically complex as Middle America. Middle America lies at the junction of several tectonic

blocks, whose movement and the associated volcanic activity have produced a diverse topographic landscape (MacMillan et al., 2004; Marshall, 2007; Townsend, 2014). For example, the formation of Middle American cordilleras and volcanic sky islands has promoted complex patterns of diversification in a number of taxa. In these habitats, connectivity and secondary gene flow often erode phylogenetic signal or introduce gene tree discordance (Rieseberg et al., 2000; Sardell et al., 2016; Thom et al., 2018). Thus, when examining evolution in regions with complex climatic or geologic histories where several evolutionary processes affect speciation simultaneously or in succession, many hypotheses may require evaluation to identify and explain sources of discordance and/or conflicting signal.

Phylogenetic discordance among data types may indicate a role of historic gene flow in shaping evolutionary histories. If gene flow is sufficiently high between ancestral lineages, a group's phylogeny may be considered reticulate such that it can no longer be characterized by strictly bifurcating processes. However, inferring trees for groups with gene flow can be problematic as multispecies coalescent methods that account for discordance due to incomplete lineage sorting (ILS) can fail in the face of moderate gene flow (Leaché et al., 2014a). To this end, several methods have been proposed to model reticulate evolution among lineages, some of which can simultaneously account for ILS (Than et al., 2008; Pickrell and Pritchard, 2012; Yu and Nakhleh, 2015; Solís-Lemus and Ané, 2016). These methods offer an opportunity to explicitly test introgression as a source of discordance by comparing optimality criteria, as well as infer a phylogenetic network that can more accurately reflect a group's history. Moreover, phylogenomic datasets using hundreds of loci from across the genome provide a robust input for reticulate inference, lending confidence to network assessment in the face of discordance (Solís-Lemus and Ané, 2016).

One Middle American group with a complex biogeographic distribution and disputed evolutionary history is the pitviper genus *Bothriechis*. This clade of 11 species is mainly restricted to mid to high elevation habits, which has led to a mosaic of species distributions across Middle American montane habitats (Campbell and Lamar, 2004)(Fig. 2.1). Speciation in this group is thought to have progressed largely allopatrically as montane populations were separated by changing topologies or other biogeographic breaks (Doan et al., 2016). For instance, the Nicaraguan Depression has been implicated as a biogeographic break separating the Nuclear Middle American species (*B. aurifer*, *B. bicolor*, *B.guifarroi*, *B. marchi*, *B. rowleyi*, and *B. thalassinus*) from those species restricted to the southern Middle American Isthmus (*B. lateralis*, *B. nigroviridis*, *B. nubestris*, and *B. supra-*

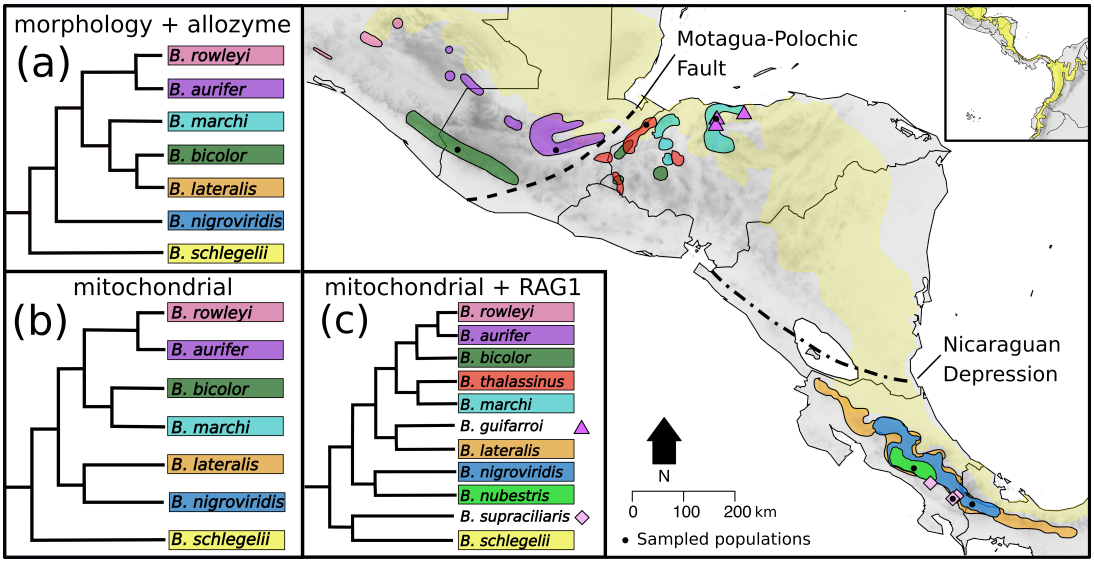


Figure 2.2.1: Phylogenetic hypotheses (a, b, c) for the evolution of *Bothriechis* in relation to their geographic to distributions. (a) Phylogeny of Crother et al. 1992 based on morphological and allozyme characters. Notably, *B. lateralis* is nested with northern Middle American taxa suggesting a southward dispersion of this taxon to Costa Rica. (b) Phylogeny of Taggart et al. 2001 based on 12S sequences with a monophyletic northern Middle American clade suggesting a northward invasion. (c) Phylogeny of Doan et al. 2016 including all currently described species. Ranges are based on Campbell and Lamar, 2004; Townsend et al., 2013; and Doan et al. 2016. Species with limited or poorly sample ranges shown as points and sampled populations are denoted with a black dot where known.

*ciliaris*)(Castoe et al., 2009; Daza et al., 2010). Similarly, the Motagua-Paolochic fault has been proposed as a break dividing *B. aurifer*, *B. bicolor*, and *B. rowleyi* from *B. guifarroi*, *B. marchi*, and *B. thalassinus* (Castoe et al., 2009; Daza et al., 2010). However, within and among these groups the order of diversification is questionable based on historic incongruences in inferred phylogenies.

The earliest phylogeny of *Bothriechis* was based on morphology and allozyme data (Crother et al., 1992) and suggested a complex biogeographic history based on a recovered clade containing both Nuclear Middle American and southern Middle American taxa (Fig. 2.1A). Later, the incorporation of mitochondrial data resulted in the recovery of an incongruent topology (Taggart et al., 2001), with monophyletic Nuclear Middle American clades (Fig. 2.1B). Subsequent phylogenies supported this, but were similarly driven by mitochondrial sequence data. It is therefore unclear whether the incongruences in these results are due to differences in analytical approach and total sequence data, or if they reflect biological discordance in the system. Additionally, the description of several new species, some of which add biogeographic-phylogenetic conflict (Fig. 2.1C), further

call into question the evolutionary processes shaping this group (Solórzano et al., 1998; Campbell and Smith, 2000; Townsend et al., 2013; Doan et al., 2016).

The historical incongruences and growing evidence of a complex evolutionary history in *Bothriechis* make it an ideal group to test for discordance among data types and test for specific processes generating discordance in a biogeographic context. Here, we generated a phylogenomic dataset using an anchored phylogenomics approach (Lemmon et al., 2012) and inferred a genomics-based species tree and mitochondrial tree to assess incongruence among phylogenomic and mitochondrial datasets. We then generated a dated phylogeny and conducted ancestral area reconstruction to examine the biogeographic history surrounding diversification of these species. Finally, we tested whether the discordance among trees is better explained by lineage sorting or reticulate evolution. Specifically, we used a model testing approach to compare models of reticulate evolution inferred through multiple methods to strictly bifurcating trees.

## 2.3 Methods

### Sampling & Sequence Generation

We collected 17 tissue samples representing the 11 recognized species of *Bothriechis*, with six species (*B. aurifer*, *B. bicolor*, *B. lateralis*, *B. nubestris*, *B. schlegelii*, and *B. supraciliaris*) represented by two samples. We additionally included sampling from nine outgroup taxa representing each genus of Middle American viper, as well as *Crotalus cerastes* and *Agkistrodon contortrix* as representatives of the Northern American pitvipers. For biogeographic analyses, *Bitis nasicornis*, *Pareas margaritophorus*, *Bungaris multicinctus*, *Causus maculatus* and *Oxybelis aeneus* were also included for tree calibration. Data for sampled taxa are available in Appendix A, Table A.1 in Supporting Information.

We used the Anchored Hybrid Enrichment method described in Lemmon et al. (2012) with probe kit improvements for squamate taxa described in Ruane et al. (2015) and Tucker et al. (2016) to generate genomic sequences for phylogenomic analyses (additional details in Appendix A). Libraries were sequenced on a HiSeq 2500 at the FSU College of Medicine's Translational Science Laboratory and approximately 1Gb of 150bp pair-end sequence data were collected per sample.

## Data Processing

We processed data following the bioinformatics pipeline of Breinholt et al. (2017) (additional details in Appendix A). Briefly, we cleaned raw reads using TrimGalore! 0.4.4 (Krueger, 2015) assembled anchored loci using the IBA.py script (Breinholt et al., 2017). Assembled sequences for each individual were reorganized by locus and aligned to the probe region with MAFFT 7.035b (Katoh and Standley, 2013). To determine orthology of trimmed probe regions, we mapped sequences to the Burmese python genome with NCBI BLASTn 2.7.1 (Camacho et al., 2009), filtered BLAST results by bit score, and selected single hit sequences mapped to the same region of the python genome.

Orthologous copies for each taxon were then aligned with MAFFT and FASconCAT-G 1.04 (Kück and Longo, 2014) was used to generate strict consensus sequences for taxa with multiple isoforms. Duplicates were removed and the remaining sequences were aligned using MAFFT to generate the final alignment set for each locus. Final alignments were trimmed by density and entropy using Trim_DE.py (Breinholt et al., 2017) to remove sites with a density of less than 0.6% or entropy >1.5 and were checked manually in Geneious 10.2.3 (Kearse et al., 2012).

## Species Tree Estimation

We used concatenation and species tree approaches in phylogenetic estimation to assess potential conflict in phylogenetic signal and ensure robust inferences. Both concatenation and species tree estimation were carried out using the Palmetto high performance computing cluster at Clemson University. For concatenated analyses, alignments for all loci were first concatenated in Geneiout. We then determined the most appropriate data partitioning scheme and model of nucleotide substitution using PartitionFinder2 2.1.1 (Lanfear et al., 2016), specifying the relaxed hierarchical clustering algorithm (rclust) and AICc as the optimality criterion. We obtained our best-tree estimate in RAxML 8.2.11 (Stamatakis, 2014) using 100 independent searches and a GTRGAMMA model for each partition. Nodal support values were calculated by performing 1000 bootstrap replicates that were mapped to the best tree. To assess the degree of incongruence at internal nodes we calculated internode certainty (IC), tree certainty (TC), and relative tree certainty (RTC) based on trees estimated for each locus using RAXML with independent GTRGAMMA models and 100 independent searches.

Coalescent and coalescent-based inference of the species tree was conducted using *BEAST2 0.13.5 (Ogilvie et al., 2017) and ASTRAL III 5.6.1, respectively (Mirarab et al., 2014; Zhang et al., 2017). For *BEAST2 analyses we followed Leaché et al. (2014b) in selecting the 20 loci with the highest number of parsimony informative sites. Site models, clock models, and trees were unlinked across all loci and each locus was assigned an uncorrelated log-normal clock and appropriate substitution model determined in PartitionFinder2. The tree prior was set to Yule with a linear with constant root population size parameter. We ran *BEAST four independent times for 1.5 billion generations and assessed convergence among runs in TRACER 1.6.0 (Rambaut et al., 2015). For ASTRAL analyses we used the gene trees to assess internal node incongruence with nodal support estimated with 1000 bootstrap replicates. Gene trees for each locus were then used as input for ASTRAL to estimate the species tree. To better assess gene tree discordance across nodes in the tree, we annotated quartet support for each node by specifying the -t 8 option. The resulting species trees for concatenated and coalescent analyses were visualized using FigTree 1.4.3 (Rambaut, 2012).

## Mitochondrial Genome Analyses

We extracted mitochondrial sequence data captured as a by-product of the anchored phylogenomics workflow and conducted mitochondrial genome-based analyses. We inferred mitochondrial genomes for all specimens of *Bothriechis* and representatives of Middle American genera by mapping trimmed readsets to the *Bothrops jararaca* mitochondrial genome (GenBank accession: NC030760, (Almeida et al., 2016)) in Geneious with a minimum read coverage of 5x.

Sequences for each of the 13 protein coding loci and the 12S and 16S ribosomal RNAs were extracted from each individual and a partitioning scheme and nucleotide substitution model for each locus determined by PartitionFinder2. We then inferred a gene tree for each locus using RAxML with 1000 bootstrap replicates. Gene trees were checked individually for their support for the species tree or an alternate hypothesis. For a mitogenome-wide approach, we used HomBlocks 1.1.1 (Bi et al., 2017) to construct a reduced, phylogenetically informative multiple sequence alignment based on locally colinear synteny blocks of the mitochondrial genome. The HomBlocks alignment was then used to infer a mitochondrial phylogeny in RAxML using a GTRGAMMA model based on PartitionFinder2 output of HomBlocks with 1000 bootstrap replicates.

## Phylogenetic Dating

To examine the historical biogeography underlying the speciation of *Bothriechis*, we produced a dated phylogeny using MCMCtree in PAML 4.9 (Yang, 2007) . For MCMCtree analyses, we used the North American Crotalinae dataset and additionally included five outgroup taxa as nodal-calibration points. The reference topology used for MCMCtree was based on ML analyses of the concatenated anchored dataset. Four calibration points were used to calibrate the clock (see Appendix A) and estimates of branch lengths were obtained using BASEML with the GTR+G model. The autocorrelated rates model was used to set the rate prior on internal nodes. MCMCtree was run for 5,000,000 iterations as burn-in and then sampled every 1,000 generations to collect 50,000 samples. MCMCtree was run three times with different random seeds and checked for convergence.

## Biogeographic Inference

To assess the historical biogeography of *Bothriechis*, we used the recovered time calibrated phylogeny and estimated ancestral areas of each species with the R package "BioGeoBEARS" (Matzke, 2013). We first pruned the dated tree to single representatives of only *Bothriechis* species using the droptip function of the R package "APE" (Paradis et al., 2004). We then assigned each *Bothriechis* species to a biogeographic distribution based on their occupation of four biogeographic regions, which correspond to known biogeographic breaks in Middle America (see Appendix A). We modeled differential dispersion probability across these regions with three categories based on likelihood of dispersal (0.1-unlikely, 0.5-moderately likely, 1-very likely) as in Feng et al. (2017). Assignment to one or more biogeographic regions was determined based on verified, georeferenced specimens on VertNet and positively identified species on iNaturalist. To infer ancestral areas, we evaluated the DEC, DIVA, and BAYAREA models based on AIC. We used the best model to visualize the conditional probabilities of ancestral *Bothriechis* occupying various biogeographic ranges and compared the most likely occupation of ancestors surrounding discordant nodes.

## Reticulation Analyses

We tested the hypothesis that recent and/or historic gene flow has led to conflicting phylogenetic signals in *Bothriechis* using three programs PhyloNet 3.6.2 (Than et al., 2008), SNaQ implemented in the Julia package "PhyloNetworks" (Solís-Lemus and Ané, 2016), and TreeMix 1.13

(Pickrell and Pritchard, 2012). PhyloNet and SNaQ infer phylogenetic networks using sequence data, gene trees, or 4-taxon concordance factors while TreeMix uses a statistical algorithm incorporating allele frequency data to determine the most likely tree with a specified number of migration events (i.e., gene flow) (Pickrell and Pritchard, 2012). Additional details on these analyses are available in Appendix A.

To evaluate the relative contribution of reticulations events, we inferred networks and trees with between 0-9 reticulations for each method, which also served as explicit tests of whether ILS alone sufficiently explains gene tree discordance. We calculated AIC for each model based on log likelihood or log pseudo-likelihood score treating each reticulation as a free parameter in the model and determined the optimal number of reticulations based on the relative change in AIC. Where models with one or more reticulations performed better, we concluded that ILS alone insufficiently explained observed gene tree discordance.

All PhyloNet and SNaQ analyses used gene trees inferred for each anchored locus in RAxML as in the species tree estimation analyses (above). To implement TreeMix, we phased alleles for each sample using bash and python wrappers for BWA 0.7.16 (Li and Durbin, 2009) and GATK 3.8.1 (McKenna et al., 2010) based on scripts from (Alexander, 2015) and extracted independent SNPs from each locus. For PhyloNet analyses, we used the maximum pseudo-likelihood criterion for network selection (Yu and Nakhleh, 2015) and performed 25 iterations of 500 independent searches of network space retaining the top five models in each iteration For SNaQ analyses we conducted 500 searches of network space and retained the network with the highest pseudolikelihood as the best network. We used the ASTRAL topology as the starting tree for the first network search, with the resulting best networks as starting networks for subsequent searches with additional reticulation edges. TreeMix was run with each *Bothriechis* species defining a population and specifying 0-9 migration edges and we used the three-population and four-population tests to calculate the f3 and f4 statistics for all population combinations. Finally, to assess the number and signal of informative SNPs across all loci, calculated Patterson's D-statistic for all population combinations with an alignment of SNPs from all loci with all terminals using the R package "evobiR" (Blackmon and Adams, 2015).

## 2.4 Results

### Bioinformatic Processing

After sequencing we obtained an average of 3,148,191bp pair-end reads per sample (range 316,456-6,178,333) (see Appendix A, Table A.2). Bioinformatic processing recovered 405 anchored loci for phylogenetic inference, the most extensive dataset to date for phylogenomic analysis of palm-pitvipers. The average alignment length per locus was 668 bp (range 434-1185). The final concatenated alignment consisted of 269,957 base-pairs.

### Species Tree Analyses

Both species tree and concatenation methods of analysis recovered trees with strong support and largely consistent topologies (Fig. 2, see Fig. A.1 and Fig. A.2 in Appendix A). Though the relationships among genera, were not fully resolved, *Bothriechis* was recovered as monophyletic in all analyses. The clade composed by *B. schlegelii* and *B. supraciliaris* was found as the most basal lineage. The clade formed by *B. nigroviridis* and *B. nubestris* is sister to a clade containing the Nuclear Middle American *Bothriechis* and *B. lateralis*, reflecting an early divergence of this morphologically distinct lineage. *Bothriechis aurifer*, *B. bicolor*, and *B. rowleyi* were recovered as a strongly supported clade, though their order of diversification varied among methods and was comparatively poorly supported. ASTRAL triplet scores and *BEAST analyses for this node showed similar support for each of the three possible topologies among gene trees. The lack of congruence in the order of diversification of these taxa may reflect a lack of power in the dataset for resolving this node, or a high degree of ILS as a result of a rapid speciation of these three taxa.

Among both concatenation and species tree analyses of anchored loci, *B. marchi* + *B. thalassinus* formed a clade with *B. lateralis* + *B. guifarroi*. This topology disagrees with the relationship recovered with morphological and allozyme data-which place *B. lateralis* sister to *B. bicolor* (Crother et al., 1992), and also contradicts the relationships observed from later phylogenies placing *B. marchi* + *B. thalassinus* with the *B. aurifer* + *B. bicolor* + *B. rowleyi* clade. The ASTRAL triplet scores for this node were inconsistent with what would be expected under strict lineage sorting (e.g., strong support for one topology, and lower but approximately equal support for the other two) (see Fig. A.2 in Appendix A). This suggests that processes other than strict ILS are impacting the relationships of taxa at this node.

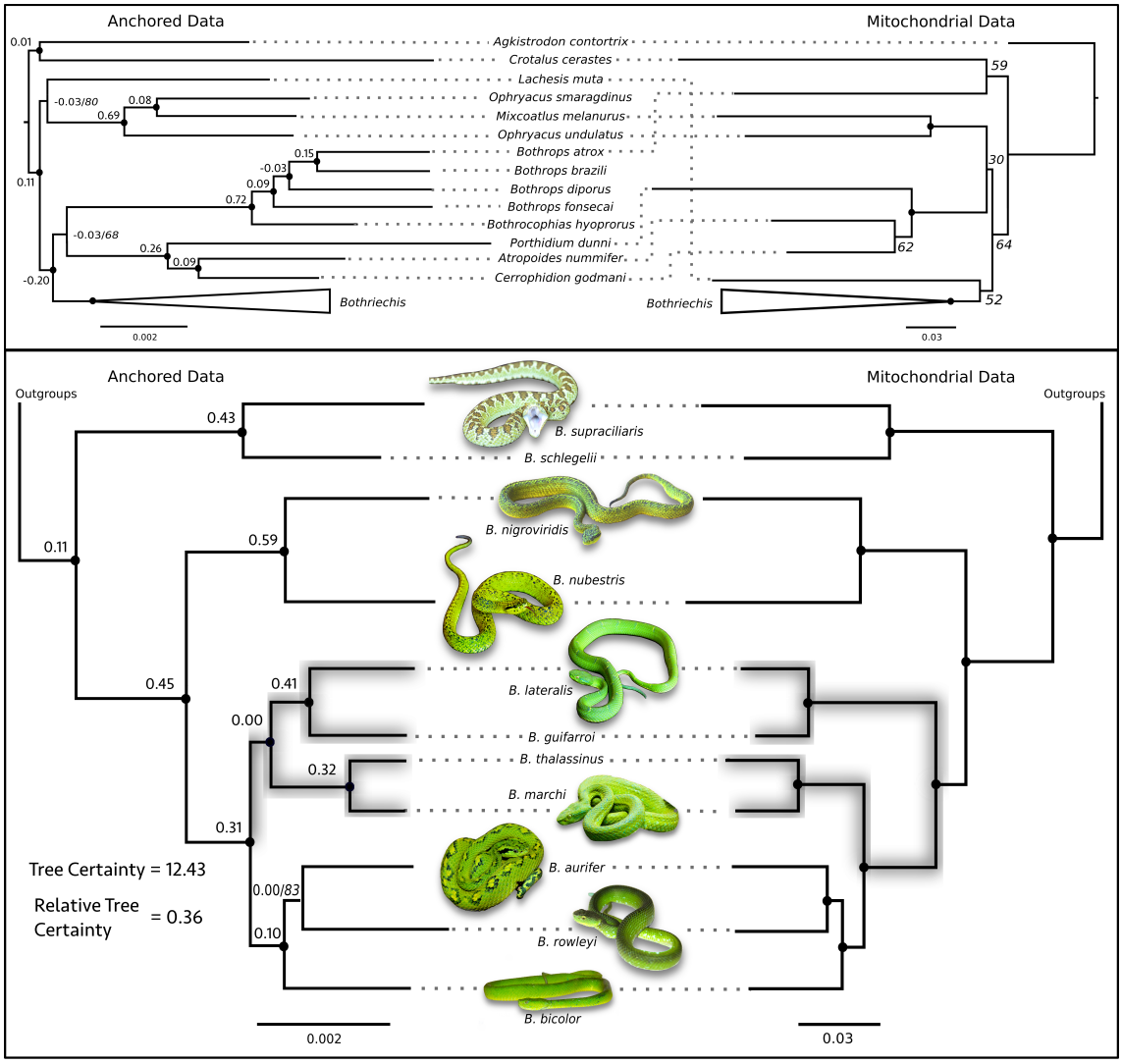


Figure 2.4.1: Concatenated anchored loci phylogeny (left) and mitochondrial phylogeny (right) of New World pitviper genera and *Bothriechis* species. Values by nodes show internode certainty and bootstrap support below 95 (italics). Dots on nodes indicate bootstrap support above 95. Discrepancies in the interspecific relationships of *Bothriechis* when using anchored loci versus mitochondrial data are shaded.

## Mitochondrial Analyses

Mitochondrial genome coverage averaged 95.5% per sample (range 85.8-98.7%). Mitochondrial sequence accession numbers and recovered lengths are given Tables A.1 and A.2, respectively, in Appendix A.

The interspecific relationships within *Bothriechis* were strongly supported and most relationships were consistent with those of the anchored loci analyses. However, in the mitochondrial tree, the clade *B. marchi* + *B. thalassinus* was found as sister to the clade composed by *B. aurifer*, *B. bicolor* and *B. rowleyi* instead of the clade *B. lateralis* + *B. guifarroi* (shaded branches in Fig. 2.2). Single mitochondrial gene phylogenies lacked the resolution of the HomBlocks alignment, but similarly supported this conflicting relationship (Fig. A.3 in Appendix A). This topology is consistent with other mitochondrially driven phylogenies (Castoe et al., 2009; Daza et al., 2010; Townsend et al., 2013; Doan et al., 2016).

## Dating and Biogeographic Inference

Results of time calibration analyses were generally consistent with those of recent work (Alencar et al., 2016). We inferred that the common ancestor of *Bothriechis* arose approximately 18 mya, with many instances of diversification occurring in the late Miocene-early Pliocene (Fig. 2.3, see Fig. A.4 in Appendix A). The *B. nigroviridis* + *B. nubestris* lineage was found to have diverged from the other *Bothriechis* approximately 7.5-13 mya, which may have been a result of a shift to higher elevation habitats. Divergence of a Mayan block clade (*B. aurifer*, *B. bicolor*, and *B. rowleyi*) and a largely Chortís block clade (*B. guifarroi*, *B. lateralis*, *B. marchi*, and *B. thalassinus*) occurred approximately 8.5-10 mya, concordant with the timing of the west to east progression of the Chortís block along the Mayan block to its current position (Rogers et al., 2007; Townsend, 2014). The divergence of the *B. guifarroi* + *B. lateralis* and the *B. marchi* + *B. thalassinus* lineages likely occurred shortly thereafter while speciation of *B. aurifer*, *B. bicolor*, and *B. rowleyi* likely occurred in a contracted time period between 7-9 mya.

Model evaluation in BioGeoBEARS found DEC as the most probable model (see Table A.3 in Appendix A). Ancestral area reconstruction of *Bothriechis* showed low confidence in estimating the distribution of the common ancestor of *Bothriechis* but indicated the ancestor of *B. schlegelii* and *B. supraciliaris* likely inhabited all of Middle America while the common ancestor of the remaining

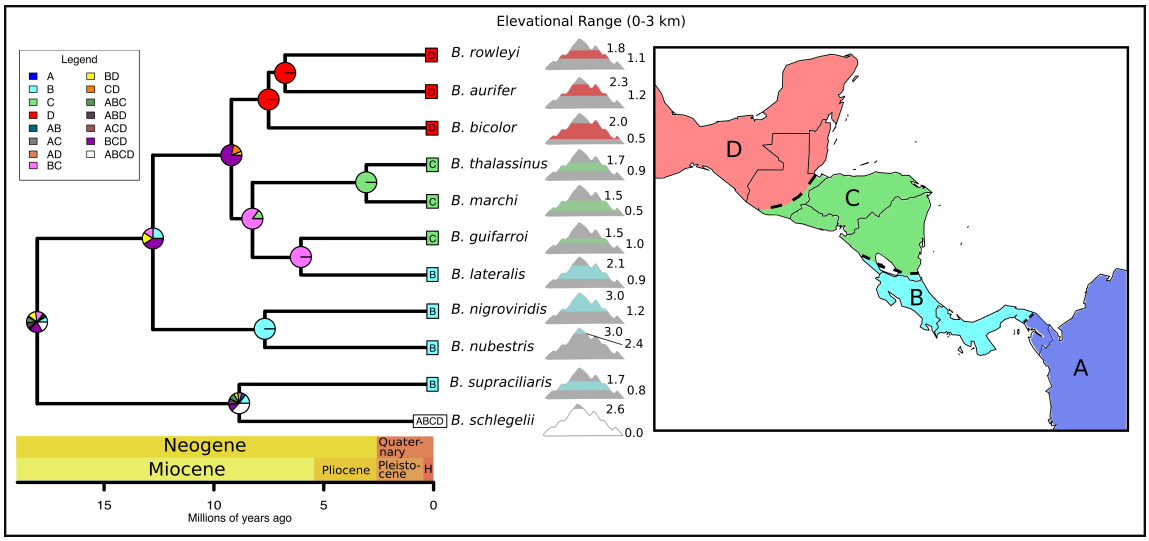


Figure 2.4.2: Ancestral area reconstruction from BioGeoBEARS. Piecharts on nodes indicate likelihood of originating in a given region. Biogeographic regions roughly correspond with South America (A; dark blue), the lower Middle American isthmus (B: light blue), the Chortís block region (C: green), and the Mayan block region (D: red). Mountain icons in the center of the figure indicate the elevational distributions of each species in kilometers above sea level.

taxa was restricted to the region above the Isthmus of Panama (Fig. 2.3). The primarily northern Middle American clade likely retained this distribution, prior to splitting into the Mayan block and Chortís block + Southern Middle American clades. Most species in this latter group later became restricted to the Chortís block, while *Bothriechis lateralis'* occupation of Southern Middle America was found to be the result of vicariant processes.

## Reticulation Analyses

Reticulation analyses in all three methods supported a role for historical gene flow in the diversification of *Bothriechis*. Trees recovered by specifying zero reticulation events (i.e., bifurcating trees) were consistent with those recovered using concatenation and species tree approaches, thus establishing an appropriate baseline for evaluating the effect of adding reticulation. Due to computational limitations we were only able to effectively evaluate networks with one or two reticulation events in PhyloNet and networks with more than five reticulations were not recovered by SNaQ. Overall, model comparisons of species tree and reticulation models supported a model of two reticulation events (Fig. A.5 in Appendix A), which performed better than the species tree in all three

methods.

The top networks with two reticulation events inferred by PhyloNet, SNaQ, and TreeMix are shown in Fig. 2.4. The topologies outside of reticulation events were generally consistent with the species tree topology, although the specific relationships among *B. aurifer*, *B. bicolor*, and *B. rowleyi* did vary. The three methods recovered different reticulate relationships, though several nuclear Middle American lineages, especially *B. aurifer*, *B. marchi*, and *B. thalassinus*, were implicated in multiple methods. PhyloNet recovered a reticulation from *B. aurifer* (minor edge) to *B. thlassinus* (major edge) and from an ancestral nuclear Middle American lineage to the ancestor of *B. bicolor* and *B. rowleyi*. In contrast, SNaQ inferred reticulations from *B. aurifer* (minor edge) to the ancestor of *B. marchi* and *B. thalassinus* and a second, more genetically limited transfer between *B. supraciliaris* (minor edge) and the ancestor of the montane *Bothriechis*.

For TreeMix inference, we extracted 368 putatively independent SNPs (i.e., one SNP per locus) excluding loci for which there were missing taxa. The overall topology inferred from TreeMix reflected the relationships recovered in phylogenetic analyses of the anchored loci, with the addition of a migration edge between *B. marchi* and the ancestor of *B. aurifer*, *B. bicolor* (Fig. 2.4) and migration between *B. rowleyi* and *B. nubestris*. Three-population and four-population tests did not show definitive admixture or gene flow among taxa, although this may reflect our usage of species rather than populations, or these tests limited ability to detect gene flow occurring before speciation events which was suggested in network analyses (see Tables A.4 and A.5 in Appendix A). In contrast, D-statistics showed strong evidence for admixture among many population combinations, including several of the Nuclear Middle American lineages identified in previous analyses (see Table A.7 in Appendix A).

## 2.5 Discussion

As genomic datasets have become increasingly available, there has been a corresponding rise in the identification and recognition of complex evolutionary histories (Jeffroy et al., 2006; Arcila et al., 2017; Thom et al., 2018). Our phylogenomic analysis of *Bothriechis* reveals reticulate evolution in Nuclear Middle America leading to conflict in the phylogenetic placement of some lineages. Biogeographic dating and ancestral area reconstruction indicate that the taxa most often implicated were present in adjacent regions during the time when reticulation occurred. Finally, the inferred

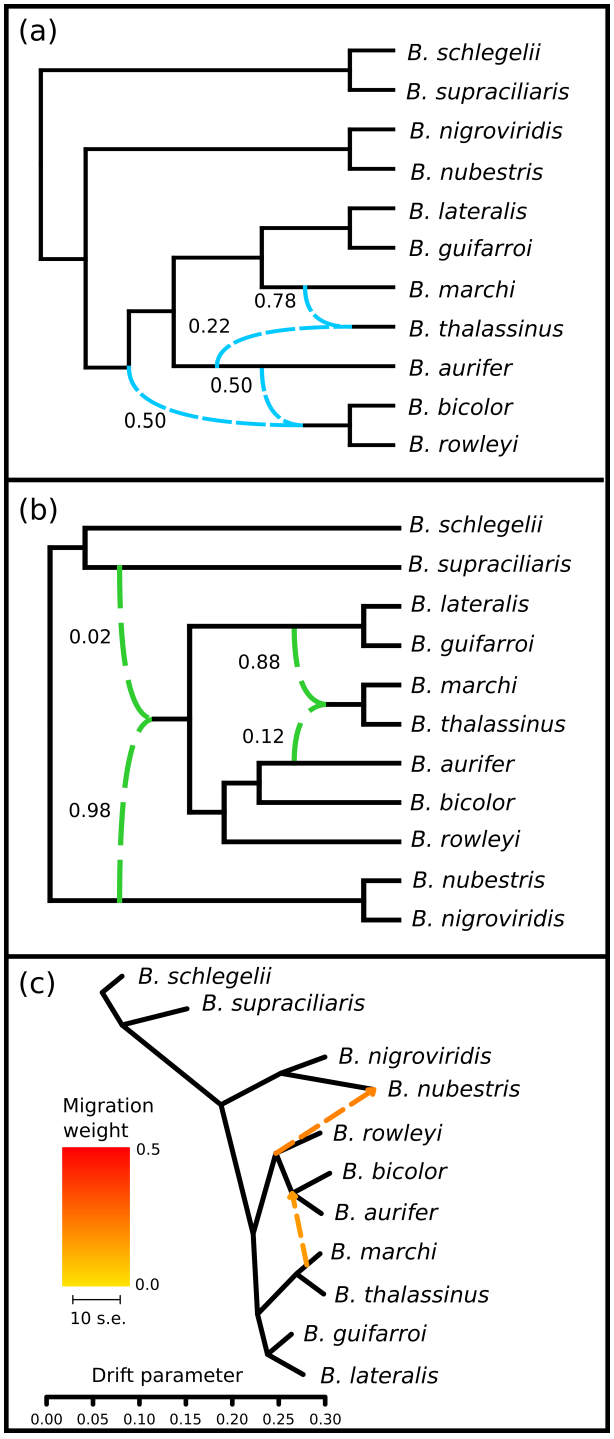


Figure 2.4.3: Top phylogenetic networks inferred by (a) PhyloNet, (b) SNaQ, and (c) TreeMix for *Bothriechis*. Dashed edges represent reticulation among lineages. Numbers adjacent to reticulation edges show inheritance probabilities for PhyloNet and SNaQ. Color of reticulation edges in (c) indicate migration (i.e., geneflow) weights.e

reticulations in the phylogeny resolve historical incongruences in the phylogeny of *Bothriechis*.

The prevailing hypothesis for the biogeographic history of *Bothriechis* has been the northern dispersal model suggested by mitochondrial data (Castoe et al., 2009; Daza et al., 2010), but our phylogenomic sampling shows that this model does not effectively explain the patterns of diversification and phylogenetic conflict in these data. In contrast, our biogeographic reconstruction suggests that the common ancestor of *Bothriechis* was likely widely distributed. The common ancestor of the 'montane' *Bothriechis*, which includes all species outside of *B. schlegelii* and *B. supraciliaris*, likely range from the Isthmus of Panama to southern Mexico. Speciation within this group then occurred through a combination of sympatric and vicariant process. The high-elevation species *B. nigroviridis* and *B. nubestris* became restricted to the cordilleras of Costa Rica and Panama, perhaps as a result of specialization for higher elevational distributions and niche partitioning with mid-elevation taxa (Fig. 2.3). Speciation in Nuclear Middle America appears to have occurred largely through vicariance, especially in the divergence of the montane Chortís block species. Here, tectonic activity (Rogers et al., 2007) and possible climatic fluctuations such as those associated with the final closure of the Isthmus of Panama (Lunt et al., 2008), likely promoted isolation and speciation while later allowing secondary contact and gene flow among lineages.

We find strong support for several general conclusions regarding gene flow in nuclear Middle America which likely involved at least *B. aurifer* and either *B. marchi*, *B. thalassinus*, or their common ancestor. Though the specifics of which lineages were involved and the extent of inferred genomic exchange varied among methods, gene flow among lineages in this region appears to have been substantial enough to cause the conflicting phylogenetic signals observed in this study and previous work (Taggart et al., 2001). While the variation in networks recovered by PhyloNet, SNaQ, and TreeMix is partially due to technical differences among methods, it likely also reflects limited or conflicting biological signal due to low numbers of informative sites or weak signal of introgression among sampled gene trees. In the latter case, improved sampling at the genomic level and/or population level may add clarity to the direction and magnitude of inferred reticulation. Regardless, for gene flow to occur, lineages must occupy (or have occupied) geographically proximate regions that would allow secondary contact (Burbrink and Gehara, 2018). Our ancestral area reconstruction, as well as the modern distributions of these taxa, place the lineages putatively involved in this reticulation in adjacent regions on either side of the Motagua-Polochic fault. Moreover, based on our fossil calibrated tree, this reticulation likely occurred between 8-3 mya. This time period

corresponds to an interval of high volcanic and tectonic activity in the region; conditions which could lead to repeated instances of isolation and secondary contact (Rogers et al., 2007). Regardless of the mechanisms promoting contact, the reticulate evolution observed in this group and the phylogenetic conflict it introduced underscores the importance of these processes to the *Bothriechis* phylogeny.

Hybridization can lead to adaptive introgression, wherein natural selection maintains introgressed alleles, which may allow for rapid adaptation in dynamic environments (Suarez-Gonzalez et al., 2018). If adaptive introgression plays a role in the reticulate evolution identified in *Bothriechis*, identifying loci that have introgressed from across the genome and determining how these have impacted phenotypes would be informative for our understanding of adaptation and trait evolution. The addition of genetic variation attained through hybridization and introgression has also been proposed as an important driver of speciation (Seehausen, 2004; Abbott et al., 2013), even leading to adaptive radiations as seen in some systems (Salzburger et al., 2002; Meier et al., 2017; Grummer et al., 2018). While this does not appear to be the case in *Bothriechis*, much of the genera's range is poorly sampled and future surveys of currently unsampled populations may lead to recognition of additional species and stronger support for the role of reticulate evolution in the diversification of this group. Unfortunately, due to the highly disjunct distributions of *Bothriechis* and the logistical challenges associated with reaching them, many species' ranges and populations remain under sampled (Savage, 2002; Campbell and Lamar, 2004; Wilson and McCranie, 2004; McCranie, 2011). This may be a promising avenue for future study, though it is beyond the scope of the current work.

Phylogenomic approaches have led to increased resolution in many taxonomic groups, especially when combined with explicit tests of complex or non-treelike evolutionary processes (Burbrink and Gehara, 2018; Grummer et al., 2018; Thom et al., 2018). Dynamic geologic and climatic histories are often associated with diversification and speciation processes, but these conditions can also promote complex evolutionary interactions that make it difficult to infer a strictly bifurcating tree. The increasing appearance of approaches for identifying and testing for reticulate evolution and gene flow among lineages corresponds with a growing appreciation for the role of these processes in evolutionary biology and speciation. However, the ability to detect and characterize ancient hybridization events is highly dependent on the characteristics of a given dataset as well as the specific analytical methods used, each of which have their own strengths and weaknesses (see Appendix A for additional discussion on this topic). Complex histories can occur at any taxonomic level, are not apparent with every dataset, nor detectable with every analytical method making their true

prevalence in the tree of life unclear. Though genomic resources can provide the raw materials for resolving complex evolutionary processes, explicitly testing alternative hypotheses using several approaches and multiple lines of evidence remains the best strategy for bringing these histories into focus.

## 2.6 Acknowledgments

We thank the University of Texas at Arlington Amphibian and Reptile Diversity Research Center, Dr. Jonathon A. Campbell, and Dr. Eric N. Smith for tissue loans. We thank Dr. Mahmood Sasa for assistance in field collection of additional species used here. We thank Dr. Jason L. Strickland and Dr. Mark Margres for comments, and discussion, which improved the manuscript. This work was funded by National Science foundation grants DEB-0416000, DEB-1638879, DEB-1822417 and Clemson University start-up funds to CLP; National Science Foundation grant DEB-1120516 to EML; National Science Foundation grant IIP-1313554 to ARL and EML; São Paulo Research Foundation (FAPESP) grants 2011/50206-9 and 2016/50127-5 to HZ; and the Southwestern Association of Naturalists McCarley Research Grant, the Theodore Roosevelt Memorial Fund through the American Museum of Natural History, and The Explorers Club Exploration Fund-Mamont Scholars Program Grant to AJM. FGG thanks FAPESP post-doctoral grant (2012/08661-3). We also thank Michelle Kortyna and Sean Holland at Florida State University's Center for Anchored Phylogenomics for assistance with data collection and analysis. The authors declare no conflicts of interest. The contents of this chapter were originally published as "Reticulate evolution in nuclear Middle America causes discordance in the phylogeny of palm-pitvipers (Viperidae:*Bothriechis*)" in *Journal of Biogeography*, volume 46, issue 5. The work has been reused with the permission of the copyright holder (John Wiley and Sons) under licensing agreement 4804430320738 (Appendix D).

# References


Abbott, R., Albach, D., Ansell, S., Arntzen, J. W., Baird, S. J. E., Bierne, N., Boughman, J., Brelsford, A., Buerkle, C. A., Buggs, R., Butlin, R. K., Dieckmann, U., Eroukhmanoff, F., Grill, A., Cahan, S. H., Hermansen, J. S., Hewitt, G., Hudson, A. G., Jiggins, C., Jones, J., Keller, B., Marczewski, T., Mallet, J., Martinez-Rodriguez, P., Möst, M., Mullen, S., Nichols, R., Nolte, A. W., Parisod, C., Pfennig, K., Rice, A. M., Ritchie, M. G., Seifert, B., Smadja, C. M., Stelkens, R., Szymura, J. M., Väinölä, R., Wolf, J. B. W., and Zinner, D. (2013). Hybridization and speciation. *Journal of Evolutionary Biology*, 26(2):229–246.

Alencar, L. R. V., Quental, T. B., Grazziotin, F. G., Alfaro, M. L., Martins, M., Venzon, M., and Zaher, H. (2016). Diversification in vipers: Phylogenetic relationships, time of divergence and shifts in speciation rates. *Molecular Phylogenetics and Evolution*, 105:50–62.

Alexander, A. (2015). Phase_hybrid_from_next_genv1.0.3.

Almeida, D. D., Kitajima, J. P., Nishiyama Jr, M. Y., Condomitti, G. W., Castro de Oliveira, U., Setúbal, J. C., and Junqueira-de Azevedo, I. L. M. (2016). The complete mitochondrial genome of *Bothrops jararaca* (Reptilia, Serpentes, Viperidae). *Mitochondrial DNA Part B*, 1(1):907–908.

Arcila, D., Ortí, G., Vari, R., Armbruster, J. W., Stiassny, M. L., Ko, K. D., Sabaj, M. H., Lundberg, J., Revell, L. J., and Betancur-R, R. (2017). Genome-wide interrogation advances resolution of recalcitrant groups in the tree of life. *Nature Ecology & Evolution*, 1(2):1–10.

Bi, G., Mao, Y., Xing, Q., and Cao, M. (2017). HomBlocks: A multiple-alignment construction pipeline for organelle phylogenomics based on locally collinear block searching. *Genomics*, 110:18–22.

Blackmon, H. and Adams, R. H. (2015). evobiR: Comparative and Population Genetic Analyses.

Boissin, E., Stöhr, S., and Chenuil, A. (2011). Did vicariance and adaptation drive cryptic speciation and evolution of brooding in *Ophioderma longicauda* (echinodermata: Ophiuroidea), a common atlanto-mediterranean ophiuroid? *Molecular Ecology*, 20(22):4737–4755.

Breinholt, J. W., Earl, C., Lemmon, A. R., Lemmon, E. M., Xiao, L., and Kawahara, A. Y. (2017). Resolving Relationships among the Megadiverse Butterflies and Moths with a Novel Pipeline for Anchored Phylogenmics. *Systematic Biology*, 0(0):78–93.

Burbrink, F. T. and Gehara, M. (2018). The biogeography of deep time phylogenetic reticulation. *Systematic biology*, 67(5):743–755.

Camacho, C., Coulouris, G., Avagyan, V., Ma, N., Papadopoulos, J., Bealer, K., and Madden, T. L. (2009). Blast+: architecture and applications. *BMC bioinformatics*, 10(1):421.

Campbell, J. A. and Lamar, W. W. (2004). *The Venomous Reptiles of the Western Hemisphere*. Comstock Pub. Associates.

Campbell, J. A. and Smith, E. N. (2000). A new species of arboreal pitviper from the Atlantic versant of northern Central America. *Revista de Biología Tropical*, 48(4):1001–1013.

Castoe, T. A., Daza, J. M., Smith, E. N., Sasa, M. M., Kuch, U., Campbell, J. A., Chippindale, P. T., and Parkinson, C. L. (2009). Comparative phylogeography of pitvipers suggests a consensus of ancient Middle American highland biogeography. *Journal of Biogeography*, 36(1):88–103.

Chang, Z., Li, G., Liu, J., Zhang, Y., Ashby, C., Liu, D., Cramer, C. L., and Huang, X. (2015). Bridger: a new framework for de novo transcriptome assembly using RNA-seq data. *Genome Biology*, 16(1):30.

Crother, B. I., Campbell, J. A., and Hillis, D. M. (1992). Phylogeny and historical biogeography of the palm-pitvipers, genus *Bothriechis*: biochemical and morphological evidence. In *Biology of the Pitvipers*, pages 1–19.

Daza, J. M., Castoe, T. A., and Parkinson, C. L. (2010). Using regional comparative phylogeographic data from snake lineages to infer historical processes in middle america. *Ecography*, 33(2):343–354.

Daza, J. M., Smith, E. N., Páez, V. P., and Parkinson, C. L. (2009). Complex evolution in the Neotropics: the origin and diversification of the widespread genus *Leptodeira* (Serpentes: Colubridae). *Molecular Phylogenetics and Evolution*, 53(3):653–67.

Doan, T. M., Mason, A. J., Castoe, T. A., Sasa, M., and Parkinson, C. L. (2016). A cryptic palm-pitviper species (Squamata: Viperidae: *Bothriechis*) from the Costa Rican highlands, with notes on the variation within *B. nigroviridis*. *Zootaxa*, 4138(2):271–290.

Doyle, J. J. (1992). Gene Trees and Species Trees: Molecular Systematics as One-Character Taxonomy. *Systematic Botany*, 17(1):144–163.

Edgar, R. C. (2010). Search and clustering orders of magnitude faster than BLAST. *Bioinformatics*, 26(19):2460–2461.

Feng, Y.-J., Blackburn, D. C., Liang, D., Hillis, D. M., Wake, D. B., Cannatella, D. C., and Zhang, P. (2017). Phylogenomics reveals rapid, simultaneous diversification of three major clades of gondwanan frogs at the cretaceous–paleogene boundary. *Proceedings of the National Academy of Sciences*, 114(29):E5864–E5870.

Funk, D. J. and Omland, K. E. (2003). Species-level paraphyly and polyphyly: frequency, causes, and consequences, with insights from animal mitochondrial dna. *Annual Review of Ecology, Evolution, and Systematics*, 34(1):397–423.

Giarla, T. C. and Esselstyn, J. A. (2015). The Challenges of Resolving a Rapid, Recent Radiation: Empirical and Simulated Phylogenomics of Philippine Shrews. *Systematic Biology*, 64(5):727–740.

Grummer, J. A., Morando, M. M., Avila, L. J., Sites, J. W., and Leaché, A. D. (2018). Phylogenomic evidence for a recent and rapid radiation of lizards in the Patagonian *Liolaemus fitzingerii* species group. *Molecular Phylogenetics and Evolution*.

Hsiang, A. Y., Field, D. J., Webster, T. H., Behlke, A. D., Davis, M. B., Racicot, R. A., and Gauthier, J. A. (2015). The origin of snakes: revealing the ecology, behavior, and evolutionary history of early snakes using genomics, phenomics, and the fossil record. *BMC evolutionary biology*, 15(1):87.

Jeffroy, O., Brinkmann, H., Delsuc, F., and Philippe, H. (2006). Phylogenomics: the beginning of incongruence? *Trends in Genetics*, 22(4):225–231.

Juan, C., Emerson, B. C., Oromı, P., and Hewitt, G. M. (2000). Colonization and diversification: towards a phylogeographic synthesis for the Canary Islands. *Trends in Ecology & Evolution*, 15(3):104–109.

Katoh, K. and Standley, D. M. (2013). MAFFT Multiple Sequence Alignment Software Version 7: Improvements in Performance and Usability. *Molecular Biology and Evolution*, 30(4):772–780.

Kearse, M., Moir, R., Wilson, A., Stones-Havas, S., Cheung, M., Sturrock, S., Buxton, S., Cooper, A., Markowitz, S., Duran, C., Thierer, T., Ashton, B., Meintjes, P., and Drummond, A. (2012). Geneious Basic: An integrated and extendable desktop software platform for the organization and analysis of sequence data. *Bioinformatics Applications Note*, 19(12):34–17.

Krueger, F. (2015). Trim Galore!: A wrapper tool around Cutadapt and FastQC to consistently apply quality and adapter trimming to FastQ files.

Kück, P. and Longo, G. C. (2014). Fasconcat-g: extensive functions for multiple sequence alignment preparations concerning phylogenetic studies. *Frontiers in zoology*, 11(1):81.

Lanfear, R., Frandsen, P. B., Wright, A. M., Senfeld, T., and Calcott, B. (2016). PartitionFinder 2: New Methods for Selecting Partitioned Models of Evolution for Molecular and Morphological Phylogenetic Analyses. *Molecular Biology and Evolution*, 34(3):772–773.

Lawson, R., Slowinski, J. B., Crother, B. I., and Burbrink, F. T. (2005). Phylogeny of the colubroidea (serpentes): new evidence from mitochondrial and nuclear genes. *Molecular phylogenetics and evolution*, 37(2):581–601.

Leaché, A. D., Harris, R. B., Rannala, B., and Yang, Z. (2014a). The influence of gene flow on species tree estimation: A simulation study. *Systematic Biology*, 63(1):17–30.

Leaché, A. D., Wagner, P., Linkem, C. W., Böhme, W., Papenfuss, T. J., Chong, R. A., Lavin, B. R., Bauer, A. M., Nielsen, S. V., Greenbaum, E., Rödel, M.-O., Schmitz, A., LeBreton, M., Ineich, I., Chirio, L., Ofori-Boateng, C., Eniang, E. A., Baha El Din, S., Lemmon, A. R., and Burbrink, F. T. (2014b). A hybrid phylogenetic–phylogenomic approach for species tree estimation in African *Agama* lizards with applications to biogeography, character evolution, and diversification. *Molecular Phylogenetics and Evolution*, 79:215–230.

Lemmon, A. R., Emme, S. A., and Lemmon, E. M. (2012). Anchored hybrid enrichment for massively high-throughput phylogenomics. *Systematic Biology*, 61(5):727–744.

Li, H. and Durbin, R. (2009). Fast and accurate short read alignment with Burrows-Wheeler transform. *Bioinformatics*, 25(14):1754–1760.

Lunt, D. J., Valdes, P. J., Haywood, A., and Rutt, I. C. (2008). Closure of the Panama Seaway during the Pliocene: Implications for climate and Northern Hemisphere glaciation. *Climate Dynamics*, 30(1):1–18.

MacMillan, I., Gans, P. B., and Alvarado, G. (2004). Middle Miocene to present plate tectonic history of the southern Central American Volcanic Arc. *Tectonophysics*, 392(1-4):325–348.

Maddison, W. P. (1997). Gene trees in species trees. *Systematic Biology*, 46(3):523–536.

Marshall, J. S. (2007). Chapter 3 The Geomorphology and Physiographic Provinces of Central America. *Central America: Geology, Resources and Hazards-Bundschuh & Alvarado (Eds) 1*, pages 1–51.

Matzke, N. J. (2013). BioGeoBEARS: BioGeography with Bayesian (and likelihood) evolutionary analysis in R Scripts. *R package, version 0.2*, 1:2013.

McCranie, J. R. (2011). *The snakes of Honduras: systematics, distribution, and conservation.* Society for the Study of Amphibians and Reptiles USA.

McKenna, A., Hanna, M., Banks, E., Sivachenko, A., Cibulskis, K., Kernytsky, A., Garimella, K., Altshuler, D., Gabriel, S., Daly, M., and DePristo, M. A. (2010). The Genome Analysis Toolkit: a MapReduce framework for analyzing next-generation DNA sequencing data. *Genome research*, 20(9):1297–303.

Meier, J. I., Marques, D. A., Mwaiko, S., Wagner, C. E., Excoffier, L., and Seehausen, O. (2017). Ancient hybridization fuels rapid cichlid fish adaptive radiations. *Nature Communications*, 8:14363.

Meyer, M. and Kircher, M. (2010). Illumina sequencing library preparation for highly multiplexed target capture and sequencing. *Cold Spring Harbor Protocols*, 5(6).

Mirarab, S., Reaz, R., Bayzid, M. S., Zimmermann, T., S. Swenson, M., and Warnow, T. (2014). ASTRAL: Genome-scale coalescent-based species tree estimation. *Bioinformatics*, 30(17):541–548.

Ogilvie, H. A., Bouckaert, R. R., and Drummond, A. J. (2017). StarBEAST2 Brings Faster Species Tree Inference and Accurate Estimates of Substitution Rates. *Molecular Biology and Evolution*, 34(8):2101–2114.

Ornelas, J. F., Sosa, V., Soltis, D. E., Daza, J. M., González, C., Soltis, P. S., Gutiérrez-Rodríguez, C., de los Monteros, A. E., Castoe, T. A., Bell, C., and Ruiz-Sanchez, E. (2013). Comparative Phylogeographic Analyses Illustrate the Complex Evolutionary History of Threatened Cloud Forests of Northern Mesoamerica. *PLoS ONE*, 8(2).

Pamilo, P. and Nei, M. (1988). Relationships between Gene Trees and Species Trees. *Molecular Biology and Evolution*, 5(5):568–583.

Paradis, E., Claude, J., and Strimmer, K. (2004). APE: Analyses of phylogenetics and evolution in R language. *Bioinformatics*, 20(2):289–290.

Pickrell, J. K. and Pritchard, J. K. (2012). Inference of Population Splits and Mixtures from Genome-Wide Allele Frequency Data. *PLoS Genetics*, 8(11):e1002967.

Rage, J.-C., Folie, A., Rana, R. S., Singh, H., Rose, K. D., and Smith, T. (2008). A diverse snake fauna from the early eocene of vastan lignite mine, gujarat, india. *Acta Palaeontologica Polonica*, 53(3):391–403.

Rambaut, A. (2012). FigTree v1. 4. *Molecular evolution, phylogenetics and epidemiology. Edinburgh, UK: University of Edinburgh, Institute of Evolutionary Biology.*

Rambaut, A., Suchard, M. A., and Drummond, A. J. (2015). Tracer v1. 6. 2014.

Rieseberg, L. H., Baird, S. J. E., and Gardner, K. A. (2000). Hybridization, introgression, and linkage evolution. *Plant Molecular Biology*, 42(1):205–224.

Rogers, R. D., Mann, P., and Emmet, P. A. (2007). Tectonic terranes of the Chortís block based on integration of regional aeromagnetic and geologic data. *Special Papers-Geological Society of America*, 428:65.

Ruane, S., Raxworthy, C. J., Lemmon, A. R., Lemmon, E. M., and Burbrink, F. T. (2015). Comparing species tree estimation with large anchored phylogenomic and small Sanger-sequenced molecular datasets: an empirical study on Malagasy pseudoxyrhophiine snakes. *BMC Evolutionary Biology*, 15(1):221.

Salzburger, W., Baric, S., and Sturmbauer, C. (2002). Speciation via introgressive hybridization in East African cichlids? *Molecular Ecology*, 11(3):619–625.

Sardell, J. M., Albert, J., and Uy, C. (2016). Hybridization following recent secondary contact results in asymmetric genotypic and phenotypic introgression between island species of *Myzomela* honeyeaters. *Evolution*, 70(2):257–269.

Savage, J. (1982). The enigma of the Central American herpetofauna: dispersals or vicariance? *Annals of the Missouri Botanical Garden*, 69(3):464–547.

Savage, J. M. (2002). *The Amphibians and Reptiles of Costa Rica: A Herpetofauna Between Two Continents, Between Two Seas.* University of Chicago press.

Seehausen, O. (2004). Hybridization and adaptive radiation. *Trends in Ecology & Evolution*, 19(4):198–207.

Smith, K. T. (2013). New constraints on the evolution of the snake clades Ungaliophiinae, Loxocemidae and Colubridae (Serpentes), with comments on the fossil history of erycine boids in North America. *Zoologischer Anzeiger - A Journal of Comparative Zoology*, 252:157–182.

Smith, S. A., Moore, M. J., Brown, J. W., and Yang, Y. (2015). Analysis of phylogenomic datasets reveals conflict, concordance, and gene duplications with examples from animals and plants. *BMC Evolutionary Biology*, 15(1):150.

Solís-Lemus, C. and Ané, C. (2016). Inferring Phylogenetic Networks with Maximum Pseudolikelihood under Incomplete Lineage Sorting. *PLoS Genetics*, 12(3):e1005896.

Solórzano, A., Gómez, L. D., Monge-Nájera, J., and Crother, B. I. (1998). Redescription and validation of *Bothriechis supraciliaris* (Serpentes: Viperidae). *Revista de Biologia Tropical*, 46(2):453–462.

Stamatakis, A. (2014). RAxML version 8: A tool for phylogenetic analysis and post-analysis of large phylogenies. *Bioinformatics*, 30(9):1312–1313.

Suarez-Gonzalez, A., Lexer, C., and Cronk, Q. C. B. (2018). Adaptive introgression: a plant perspective. *Biology Letters*, 14(3):20170688.

Taggart, T. W., Crother, B. I., and White, M. E. (2001). Palm-Pitviper (*Bothriechis*) Phylogeny, mtDNA, and Consilience. *Cladistics*, 17(4):355–370.

Tchernov, E., Rieppel, O., Zaher, H., Polcyn, M. J., and Jacobs, L. L. (2000). A fossil snake with limbs. *Science*, 287(5460):2010–2012.

Than, C., Ruths, D., and Nakhleh, L. (2008). PhyloNet: a software package for analyzing and reconstructing reticulate evolutionary relationships. *BMC Bioinformatics*, 9(1):322.

Thom, G., Amaral, F. R. D., Hickerson, M. J., Aleixo, A., Araujo-Silva, L. E., Ribas, C. C., Choueri, E., and Miyaki, C. Y. (2018). Phenotypic and genetic structure support gene flow generating gene tree discordances in an amazonian floodplain endemic species. *Systematic biology*, 67(4):700–718.

Townsend, J. H. (2014). Characterizing the Chortís Block Biogeographic Province: geological, physiographic, and ecological associations and herpetofaunal diversity. *Mesoamerican Herpetology*, 1(2).

Townsend, J. H., Medina-Flores, M., Wilson, L. D., Jadin, R. C., and Austin, J. D. (2013). A relict lineage and new species of green palm-pitviper (Squamata, Viperidae, *Bothriechis*) from the Chortís Highlands of Mesoamerica. *ZooKeys*, 298:77–106.

Tucker, D. B., Colli, G. R., Giugliano, L. G., Hedges, S. B., Hendry, C. R., Lemmon, E. M., Lemmon, A. R., Sites, J. W., and Pyron, R. A. (2016). Methodological congruence in phylogenomic analyses with morphological support for teiid lizards (Sauria: Teiidae). *Molecular Phylogenetics and Evolution*, 103:75–84.

Weissing, F. J., Edelaar, P., and van Doorn, G. S. (2011). Adaptive speciation theory: A conceptual review. *Behavioral Ecology and Sociobiology*, 65(3):461–480.

Wilson, L. D. and McCranie, J. R. (2004). The herpetofauna of the cloud forests of Honduras. *Amphibian and Reptile Conservation*, 3(1):34–48.

Yang, Z. (2007). PAML 4: Phylogenetic analysis by maximum likelihood. *Molecular Biology and Evolution*, 24(8):1586–1591.

Yu, Y., Dong, J., Liu, K. J., and Nakhleh, L. (2014). Maximum likelihood inference of reticulate evolutionary histories. *Proceedings of the National Academy of Sciences of the United States of America*, 111(46):16448–53.

Yu, Y. and Nakhleh, L. (2015). A maximum pseudo-likelihood approach for phylogenetic networks. *BMC Genomics*, 16(Suppl 10):S10.

Zaher, H., Grazziotin, F. G., Cadle, J. E., Murphy, R. W., Moura-Leite, J. C. d., and Bonatto, S. L. (2009). Molecular phylogeny of advanced snakes (serpentes, caenophidia) with an emphasis on south american xenodontines: a revised classification and descriptions of new taxa. *Papéis Avulsos de Zoologia*, 49(11):115–153.

Zaher, H., Yánez-Muñoz, M. H., Rodrigues, M. T., Graboski, R., Machado, F. A., Altamirano-Benavides, M., Bonatto, S. L., Grazziotin, F. G., and Anez-Muñoz, M. H. Y. (2018). Origin and hidden diversity within the poorly known Galápagos snake radiation (Serpentes: Dipsadidae). *Systematics and Biodiversity*, 0(0):1–9.

Zhang, C., Sayyari, E., and Mirarab, S. (2017). ASTRAL-III: Increased Scalability and Impacts of Contracting Low Support Branches. In *Comparative Genomics*, pages 53–75. Springer, Cham.

# Chapter 3

# Trait differentiation and modular toxin expression in Palm-Pitvipers

## 3.1 Abstract

Modularity is the tendency for systems to organize into semi-independent units and can be a key to the evolution and diversification of complex biological systems. Snake venoms are highly variable modular systems that exhibit extreme diversification even across very short time scales. One well-studied venom phenotype dichotomy is a trade-off between neurotoxicity versus hemotoxicity that occurs through the high expression of a heterodimeric neurotoxic phospholipase $A_2$ ($PLA_2$) or snake venom metalloproteinases (SVMPs). We tested whether the variation in these venom phenotypes could occur via variation in regulatory sub-modules through comparative venom gland transcriptomics of representative Black-Speckled Palm-Pitvipers (*Bothriechis nigroviridis*) and Talamancan Palm-Pitvipers (*B. nubestris*). We assembled 1517 coding sequences, including 43 toxins for *B. nigroviridis* and 1787 coding sequences including 42 toxins for *B. nubestris*. The venom gland transcriptomes were extremely divergent between these two species with one *B. nigroviridis* exhibiting a primarily neurotoxic pattern of expression, both *B. nubestris* expressing primarily hemorrhagic toxins, and a second *B. nigroviridis* exhibiting a mixed expression phenotype. Weighted gene coexpression analyses identified six submodules of transcript expression variation, one of which was highly associated with SVMPs and a second which contained both subunits of the neurotoxic

$PLA_2$ complex. The sub-module association of these toxins suggest common regulatory pathways underlie the variation in their expression and is consistent with known patterns of inheritance of similar haplotypes in other species. We also find evidence that module associated toxin families show fewer gene duplications and transcript losses between species, but module association did not appear to affect sequence diversification. Sub-modular regulation of expression likely contributes to the diversification of venom phenotypes within and among species and underscores the role of modularity in facilitating rapid evolution of complex traits.

## 3.2 Introduction

Modularity, the tendency for systems to organize into semi-independent discrete units, is a central theme in the evolution of biological systems and complex traits (Wagner et al., 2007). Modularity creates evolvability and the potential to adapt to novel environments rapidly by eliminating or reducing antagonistic pleiotropy while simultaneously permitting advantageous phenotypic changes through the use of conserved genetic machinery (von Dassow and Munro, 1999; Yang, 2001). Gene regulatory networks are an especially common mechanism for modular evolution within and among lineages (Levine and Davidson, 2005). Inducing, increasing, reducing, or eliminating expression of specific sub-modules can create or replicate advantageous phenotypes through the recombination of sub-modular features (Ferguson et al., 2011). As such, modularity is a common characteristic of many adaptive traits because sub-modules associated features can be rapidly modified without evolving 'from scratch' (von Dassow and Munro, 1999). *Heliconius* butterflies provide a classic example where a variety of predator-deterring wing patterns have evolved and diversified through variation in modular elements (e.g., color and spot-pattern) controlled by just a few conserved genes (e.g., the *optix* transcription factor and the *wntA* signaling pathway) (Ferguson et al., 2011; Joron et al., 2006; Van Belleghem et al., 2017). Identifying modules and their sub-modules underlying variation in highly variable modular traits can therefore provide valuable insight on the genetic basis of diversification across micro and macroscales.

Snake venoms are highly variable adaptive traits composed of 10–100 secreted proteins that collectively work to subdue prey or deter predation (Mackessy, 2016; Casewell et al., 2013). Despite the perceived complexity of the venom system, venoms appear to evolve rapidly and respond to local selection pressures over short timescales (Margres et al., 2016; Strickland et al., 2018b).

The exceptional degree of phenotypic variation observed in venoms can partially be contributed by the modularity of the venom system. Because toxin expression and production is localized to a specialized gland (Oron and Bdolah, 1973; Fry et al., 2012; Vonk et al., 2013; Schield et al., 2019) (but see (Hargreaves et al., 2014; Reyes-Velasco et al., 2015)), the venom system is a functional module that is inherently more free to vary with limited pleiotropic effects. Moreover, venom functionality is, at least in part, dependent on the coordinated expression of specific toxins or toxin classes which may covary geographically or among species (Glenn and Straight, 1978; Glenn et al., 1994; Rokyta et al., 2013). In many cases, recurrent patterns of variation in venom compositions suggest that expression of associated toxins represent sub-modules of variation, though empirical tests of sub-modularity of toxins are lacking.

One example of venom variation likely mediated by sub-modular regulation is an apparent phenotypic trade-off between neurotoxicity and hemotoxicity. In crotalid vipers (*Viperidae: Crotalinae*), hemorrhagic venoms are most common and are a function of high proportions of several toxin families, especially snake venom metalloproteinases (SVMPs) (Soto et al., 1988; Mackessy, 2008). However, in some lineages neurotoxicity has emerged as a principal phenotype (Mackessy, 2008). An extremely well-documented manifestation of neurotoxicity in crotalid venoms is based on high expression of a heterodimeric $\beta$-neurotoxic phospholipase $A_2$ ($PLA_2$) complex (Doley et al., 2010; Gutiérrez and Lomonte, 2013). These phenotypes can manifest as interspecific, intraspecific, and/or ontogenetic variation (Glenn and Straight, 1978; Glenn et al., 1994; Mackessy, 2008; Rokyta et al., 2013, 2015; Fernández et al., 2016; Mackessy et al., 2003; Calvete et al., 2010), prompting the establishment of a "Type A/Type B" nomenclature to describe the variation in rattlesnakes. Type A venoms refer those dominated by the neurotoxic $PLA_2$s, and Type B venoms refer to those with high proportions of SVMPs. Notably, there are also descriptions of Type A+B venoms which have high proportions of neurotoxic $PLA_2$s and hemorrhagic SVMPs, but these phenotypes are rare even in Type A - Type B contact zones (Glenn and Straight, 1989; Glenn et al., 1994; Strickland et al., 2018b). Here, recurring phenotypic patterns, the lack of apparent phylogenetic signal (even over ecological time scales), and the usage of common genetic building blocks (i.e., toxin families) is suggestive of modularity mediating the evolution of these phenotypes.

An opportunity to test this exists in the arboreal pitvipers of the genus *Bothriechis*. One species, *B. nigroviridis*, exhibits a neurotoxic venom phenotype driven by the high abundance of a neurotoxic heterodimeric $PLA_2$ named nigroviriditoxin (Fernández et al., 2010; Lomonte et al., 2015).

*Bothriechis nigroviridis* is unique among species with neurotoxic venom because of its ecological differentiation; *B. nigroviridis* is an arboreal high-elevation specialist while most others are mid-low elevation terrestrial species. The sister species to *B. nigroviridis*, *B. nubestris*, appears to occupy an extremely similar ecological niche based on its documented range and conserved morphology (Doan et al., 2016). Although empirical studies of *B.nubestris'* venom have yet to be conducted, its divergence from *B. nigroviridis* 6–10 mya would provide sufficient temporal opportunity for venom diversification (Mason et al., 2019). *Bothriechis nigroviridis* and *B. nubestris* can therefore provide a test case for examining mechanisms of phenotypic diversification in a modular framework.

We sought to describe and compare the venom gland transcriptomes of *B. nigroviridis* and *B. nubestris* to understand toxin evolution in a modular framework. We characterize the venom gland transcriptomes of representatives of each species and identify key dimensions of variation within and between species. We identified conserved and unique toxins and used weighted-gene co-expression network analysis (WGCNA) to test for sub-modules of variation among distinct venom types. Based on the observation that neurotoxic and hemotoxic phenotypes occur independently, in combination, or as ontogenetic changes, we hypothesized that toxins associated with neurotoxic and hemorrhagic phenotypes (i.e., neurotoxic $PLA_2$s and SVMPs) would segregate into distinct sub-modules of correlated expression variation. Additionally, we examine instances of intraspecific transcript duplication and loss and comparative sequence divergence. We hypothesized that if modular expression is a primary driver of variation, gene duplications and sequence diversification would be reduced in sub-module associated toxin families whose function has been selectively optimized and is primarily regulated by expression.

## 3.3 Methods

### 3.3.1 Sample Collection

We collected two individuals of *Bothriechis nigroviridis* and two *B. nubestris* in May-June of 2016 for venom gland extraction and sequencing. Due to the smaller range of *B. nubestris*, both individuals were collected from the same locality (∼1 km apart), San Gerardo de Dota, San Jose province, Costa Rica. *Bothriechis nigroviridis* occupies a wider range than *B. nubestris* and we collected two individuals from distant populations. One of these individuals (CLP1864), was collected from outside of the La Esperanza sector of Parque Tapanati, Cartago province, Costa Rica, a locality

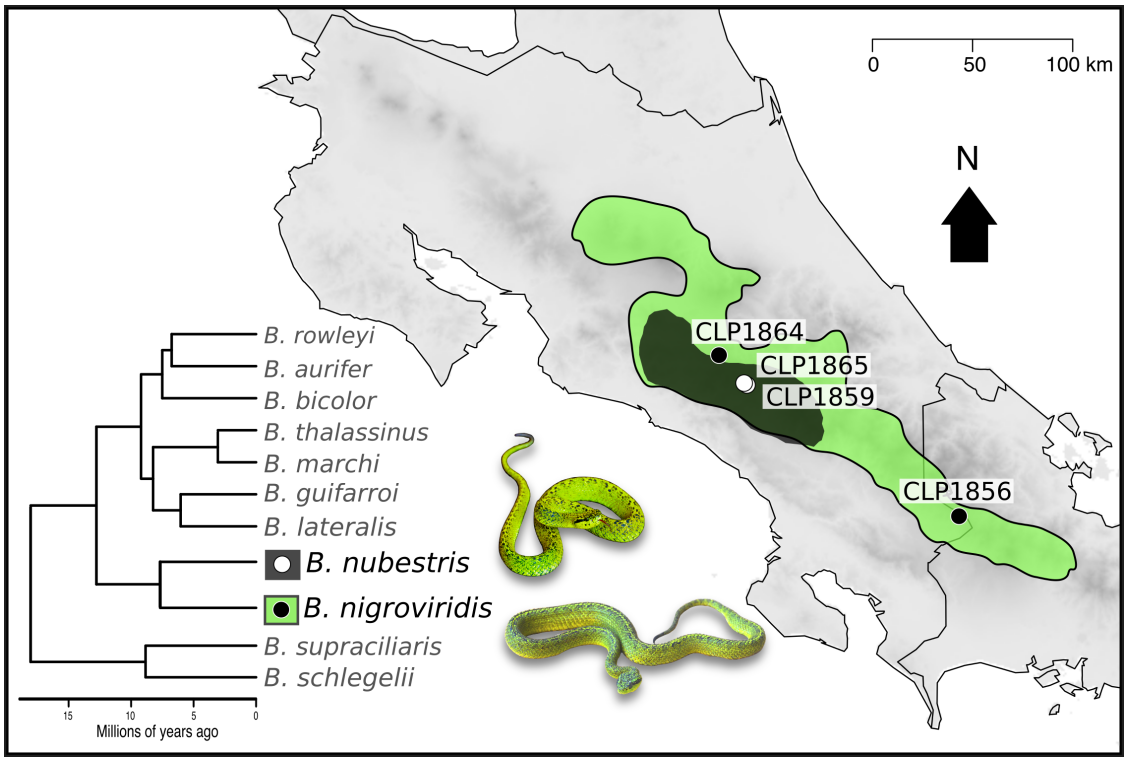


Figure 3.3.1: Phylogeny of *Bothriechis* based on Mason et al. (2019) and a distribution map for *B. nigroviridis* and *B. nubestris* made in R v.3.5.3 (url: https://www.R-project.org/) based on ranges described in Campbell et al. (2004) and Mason et al. (2019) and publicly available specimen localities in Doan et al., 2016. Sampled localities are shown as dots with specimen labels.

that is ∼50 km south of specimens collected and used in previous proteomic studies characterizing the venom of this species (Fernández et al., 2010). The second individual (CLP1856) came from the southern most portion of the species' range in Costa Rica, Las Tablas, Puntarenas province, Costa Rica (Fig. 3.3.1) ∼200 km southeast of specimens used in (Fernández et al., 2010).

Following collection, each individual had its venom collected via manual extraction. Collected venoms were lyophilized and stored at -20 C for later use. Each animal was sacrificed four days later when transcription of venom proteins is at its maximum (Rotenberg et al., 1971), via injection of sodium pentobarbitol (100mg/kg). Venom glands were dissected and stored separately in approximately 2 mL of RNAlater preservative. Animal carcasses were preserved as museum specimens with 10% buffered formalin and deposited in the Universidad de Costa Rica. The above methods were approved by University of Central Florida Institutional Animal Care and Use Committee (IACUC) protocol 16-17W, Clemson University IACUC protocol number 2017-067, and Universi-

dad de Costa Rica Comimté Institucional para el Cuidado y Uso de los Animales (CICUA) permit number CICUA-082-17.

### 3.3.2 Venom Gland Transcriptome Sequencing

Total RNA was extracted from left and right glands independently using a standard, Trizol reagent extraction as described in (Rokyta et al., 2011). Briefly, diced venom gland tissues were submerged in 500 $\mu$L of Trizol, homogenized with a sterile 20-gauge needle, and treated with an additional 500 $\mu$L of Trizol and 200 $\mu$L chloroform. RNA was then separated from tissue, cellular components, and DNA by centrifuging the total mix in a 5Prime phase lock gel heavy tube for 20 minutes at 12,000 g. Supernatant containing the RNA was transferred to a new tube and RNA was precipitated with 500 $\mu$L of isopropyl alcohol. Pelleted RNA was washed in 75 % ethanol and re-suspended in RNAase free water. Extracted total RNA was checked for quality and quantified using either an Agilent 2100 Bioanalyzer or Agilent 2200 TapeStation and stored at -80 C.

We prepared cDNA libraries from 1 $\mu$L high quality total RNA using the NEBNext Ultra RNA library Prep Kit for Illumina following the manufacturer's instructions. Specifically, we isolated polyadenalated RNA with the NEB Poly(A) Magnetic Isolation Module (New England Biolabs) and fragmented resulting mRNA by heat fragmentation at 70° C for 14.5 minutes to attain an average size of approximately 370 bp. mRNA fragments were reverse transcribed to cDNA and each library was ligated with a unique combination of index primers and Illumina adapters. The cDNA libraries were amplified through PCR using the NEBNext High-Fidelity 2X Hot Start PCR Master Mix and 14 cycles of PCR. Amplified cDNA was purified with Agencourt AMPure XP PCR Purification beads. The resulting libraries were checked for quality, fragment size distribution, and concentration on either an Agilent 2100 Bioanalyzer or Agilent 2200 TapeStation. KAPA qPCR was additionally performed on each sample library to determine amplifiable concentrations. Libraries were then pooled in groups of twelve with equal representation of amplifiable cDNA for sequencing.

Sequencing took place on an Illumina HiSeq 2000 at the Florida State University College of Medicine's Translational Science Laboratory. Combined libraries were multiplexed and sequenced with a 150 bp paired-end rapid run lane. Raw reads were demultiplexed and quality checked in FastQC (Andrews, 2010). To account for reads which may have been mis-assigned during demultiplexing, we used jellyfish v.2.2.6 (Marçais and Kingsford, 2011) and KAT v.2.3.4 (Mapleson et al., 2017) to identify and filter reads with kmers that exhibited more than a 500 fold difference in occur-

rence between samples sequenced on the same lane. Adapter sequences and low quality bases were then trimmed using trim-galore v.0.4.4 (Krueger, 2015). Finally, to increase both quality and total length of read sequences, we used PEAR v 0.9.6 (Zhang et al., 2014) to merge paired reads with a 3' overlap of greater than 10 bp.

### 3.3.3 Transcriptome Assembly & Analyses

Previous transcriptome studies have shown the challenges associated with venom gland transcriptome assembly, especially given the contrast in a proportionately low number of highly expressed toxin transcripts compared to the much broader, low expression of house keeping genes (Holding et al., 2018). To overcome this, we performed three independent assemblies using Extender (Rokyta et al., 2011), the DNAstar NGen assembler v.15.0, and Trinity v.2.4.0 (Grabherr et al., 2011) per the strategy suggested in Holding et al. (Holding et al., 2018). Sequence identities of toxins from each assembly were identified via local blastx search of SWISS-prot's curated toxins database. Contigs with a blast match of greater than 90% identity were then clustered against a database of identified snake toxins to annotate coding regions of 90% similarity or greater. Coding regions of remaining toxin contigs were annotated manually in Geneious v.10.2.3 (Kearse et al., 2012). Contigs which were not identified as toxins were annotated by clustering against a database of previously identified snake nontoxins to annotate coding regions of 90% similarity or greater representing nontoxin transcripts used in later analyses. Annotated transcripts from independent assemblies were combined and duplicate sequences as well as coding regions with ambiguous sites were removed. The remaining transcripts were screened for chimeric or mis-assembled coding sequences by mapping merged reads against these sequences with bwa v.0.7.16 (Li and Durbin, 2009) and checking for uneven read distribution across sites. Specifically, sequences with sites where the mean number of bases per read on either side of a site differed by more than 50% of the mean read length were considered likely chimeras, checked manually, and removed accordingly. We clustered the remaining transcripts at a threshold of 98% similarity to account for toxin alleles or recent paralogs that may be present. This represented the final transcriptome for each individual. To account for variation among individuals in a species and for stochastic variation in the assembly process that may have resulted in failure to assemble specific toxins in a given individual, we combined final contig sets for individuals of the same species, removed duplicates, and clustered coding regions of 98% similarity to create a master transcriptome for each species. These species-specific master transcriptomes were then used

for subsequent read mapping and expression analyses.

### 3.3.4 Expression Analyses & Ortholog Identification

To determine relative expression of transcripts, we mapped reads from individuals to their species master transcriptome with Bowtie2 v2.3.2 and calculated relative expression with RSEM v.1.3.0 (Li and Dewey, 2011). Intraspecific differences in expression were assessed using species-specific datasets for *B. nigroviridis* and *B. nubestris*. Because our limited intraspecific sampling precluded formal tests for differential expression within species, we generated pairwise null distributions of expression divergence for each species based on nontoxin expression to identify outlier toxins similar to (Rokyta and Ward, 2017). Data were first centered log-ratio (clr) transformed to normalize the expression distributions while accounting for the compositional nature of relative expression values (e.g., TPM) using the cmultRepl function in the R package zCompositions (Aitchison, 1982; Palarea-Albaladejo and Martin-Fernandez, 2015; Rokyta et al., 2015). Toxins whose pairwise divergence in expression fell outside the 99th percentile of the centered log-ratio transformed nontoxin distributions were considered outliers that are likely differential expression. RSEM can assign non-zero values to transcripts that may not be present in the transcriptome through mis-mapping of reads from other transcripts with regions of high similarity. To verify the extent to which toxins varied in presence or absence within species we aligned merged reads to the species-specific transcript sets to screen for poor read mapping. Toxins that had regions greater than 10% of the total sequence length with less than 5x coverage or highly anomalous read distributions (determined by manual review) were considered absent in the transcriptome of a given individual.

Toxin families in snakes are notorious for undergoing rapid expansions and losses, which is problematic for interspecific comparisons which assume orthology among matched transcripts. To overcome this we identified orthologous groups of transcripts using OrthoFinder v.2.3.1 (Emms and Kelly, 2015) specifying multisequence alignments with mafft. OrthoFinder identifies groups of sequences derived from a single gene in the common ancestor of compared species (i.e., orthogroups), as well as identifies conserved orthologs within orthogroups. We classified transcripts as orthologs or paralogs by parsing the OrthoFinder "orthologs" output to identify single copy orthologs and one-to-one orthologs within orthogroups using a custom python script (orthocombiner.py). For interspecific comparisons, expression data for orthologous and paralogous transcripts were combined into a single dataset where paralogous transcripts were given an expression value of zero where absent for a given

species. We used estimates of read counts from RSEM to test for differences in transcript expression with DESeq2 in R v.3.5.3 (Love et al., 2014).

### 3.3.5 Network Analyses

We performed weighted gene coexpression network analysis using the R package CEMitool (Russo et al., 2018) in R. A variance stabilizing transformation (vst) was used and transcripts were filtered to reduce correlation between variance and gene expression. We used pearson's coefficient as the correlation method and a beta value of 10 was automatically selected. The minimum module size was set to 1 to allow the greatest flexibility in identifying modules of correlated expression. Because of the high variability in venom composition observed among *B. nigroviridis* (see above), we annotated samples as one of three venom types which correspond to venom phenotypes observed in rattlesnakes: *B. nigroviridis* Type A (CLP1864), *B. nigroviridis* Type A+B (CLP1856), and *B. nubestris* type B (CLP1859 and CLP1865).

### 3.3.6 Gene Family Analyses

To more closely examine how toxin family expansion, duplications, and loss have shaped venom composition, we constructed phylogenies for the four most highly expressed toxin families: C-type lectins (CTLs), $PLA_2$s, snake venom serine proteases (SVSPs), and SVMPs. Alignments for each family were generated with mafft v.7.407 (Katoh and Standley, 2013) and checked manually in Geneious. Partitioning schemes for each gene family were determined using PartitionFinder v.2 (Lanfear et al., 2016). Phylogenies were then recovered with MrBayes v.3.2.6 (Ronquist et al., 2012). MrBayes was run using one cold and three heated chains for 10 million generations with a variable rate prior. We then identified and mapped species-specific deletion and duplication events onto the trees based on the output of OrthoFinder. We considered toxins that were unassigned an ortholog to be indicative of gene loss in one species while one to many ortholog assignments indicated duplications within a species. We tested for differences in expression of one-to-one orthologs versus conserved and duplicated toxins with a two-way factorial with toxin type and species as factors in R. TPM values were used as the metric for expression and were centered log-ratio transformed to linearize the data while preserving their compositional nature (Rokyta et al., 2015; Aitchison, 1982).

### 3.3.7 Sequence Analyses

We compared divergence of orthologous toxin and nontoxin transcripts by calculating $dN/dS$ ratios ($\omega$). Orthologous transcripts were first aligned by codon using PRANK v.170427 (Löytynoja and Goldman, 2008). PRANK alignments were then used as input to estimate $\omega$, $dS$, and $dN$ with codeml in paml v. 4.9 (Yang, 2007).

We compared $\omega$, $dS$, and $dN$ of toxin genes against a background of nontoxins as in (Rokyta et al., 2013) to discern if toxin genes exhibited higher synonymous and/or nonsynonymous substitution rates and if toxins displayed high rates of positive selection (i.e., higher values of $\omega$). We excluded sequences with $dS$ <0.001 due to the possibility of estimating excessively inflated values of $\omega$, and sequences with $dS$ >0.10 to reduce the risk of including misidentified orthologs. Statistical differences in $\omega$, $dS$, and $dN$ values between toxins and nontoxins were tested with a wilcoxon sign rank test in R.

## 3.4 Results

### 3.4.1 Transcriptome Characterization

To examine the evolutionary mechanisms underlying venom divergence we sequenced, assembled, and characterized the venom gland transcriptomes of two *Bothriechis nigroviridis* (CLP1856 and CLP1864) and two *B. nubestris* (CLP1859 and CLP1865) (Table 1). The number of recovered toxins and recovered families were generally consistent with those of other viperid transcriptomes (Rokyta et al., 2012, 2015; Aird et al., 2015; Strickland et al., 2018a; Hofmann et al., 2018) and with estimates of toxin family size in early high-throughput transcriptomes of *B. schlegelii* and *B. lateralis* (Durban et al., 2011) (Table 3.4.2, Table 3.4.3).

We recovered 1517 total transcripts for *B. nigroviridis*, which included 43 toxins from 13 toxin families. The venom transcriptome of *B. nigroviridis* was largely dominated by the expression of the heterodimeric neurotoxic $PLA_2$, nigroviriditoxin (Lomonte et al., 2015), especially in the northern individual where it accounted for 60.3% of toxin expression (Fig. 3.4.1, Table 3.4.2). BPPs and SVSPs were also abundant in *B. nigroviridis* venoms, accounting for 7.6% and 14.6% of toxin expression, respectively (Fig. 3.4.1, Table 3.4.2). The high expression of the neurotoxic $PLA_2$ complex observed in the northern individual is consistent with the neurotoxic phenotype previously

| Species | Specimen ID | Museum ID | Total Reads | Merged | Total Unique CDS | CDS Passing QC | SRR |
|---|---|---|---|---|---|---|---|
| *B. nigroviridis* | CLP1856 | MZUCR23264 | 20002019 | 17227317 | 3177 | 807 | SRR9968896 |
| *B. nigroviridis* | CLP1864 | MZUCR23270 | 24641535 | 21035386 | 3323 | 1416 | SRR9968897 |
| *B. nubestris* | CLP1859 | MZUCR23267 | 20628335 | 16855601 | 3125 | 1476 | SRR9968894 |
| *B. nubestris* | CLP1865 | MZUCR23271 | 23443610 | 20108934 | 3297 | 1461 | SRR9968895 |

Table 3.4.: Specimen information for *Bothriechis* individuals used in this work.

described in individuals from a similar locality (∼50 km north of CLP1864's locality, though from a different cordillera) (Fernández et al., 2010) (Type A based on the rattlesnake nomenclature). Consistent with the Type A phenotype, there was low expression of CTL and SVMP variants which, in a previous proteomic study of *B. nigroviridis*, were not detected in the venom (Fernández et al., 2010).

Unlike the northern *B. nigroviridis*, the southern *B. nigroviridis* showed substantial expression of the nigroviriditoxin subunits as well as SVMPs (Fig. 3.4.1, Table 3.4.2). Both subunits of nigroviriditoxin and seven of the nine SVMPS were identified as outliers in expression comparisons between the two individuals; nigroviriditoxin and one SVMP were found to be expressed outside of the 99th percentile of the null distribution in the northern *B. nigroviridis* while six SVMPs were expressed outside of the 99th percentile of the null distribution in the southern *B. nigroviridis* (Table 3.4.2). In addition to the toxin family differences, four CTL and 11 SVSP variants fell outside of the 99th percentile of the null distribution of expression divergence between individuals (Table 3.4.2). Of the 43 total toxins assembled for *B. nigroviridis*, 27 were expressed outside of the 99th percentile of the nontoxin null distribution. In many cases, expression differences could be explained by toxin absence. Overall, 14 toxins were found to be absent in one individual with six absences in the southern *B. nigroviridis* and eight absences in the northern *B. nigroviridis*. The overall pattern of toxin expression is more characteristic of a Type A+B phenotype than Type A

For *B. nubestris* we recovered 1787 transcripts which included 42 toxins from 14 toxin families (Table 3.4.3). In contrast to *B. nigroviridis*, toxin expression and presences/absences were generally similar between the two sequenced individuals of *B. nubestris* (Fig. 3.4.2, Table 3.4.3). In total, 14 toxins were expressed outside of the 99th percentile of the nontoxin null distribution. Toxins whose expression was outside the 99th percentile spanned all major families including BPP, CTLs, $PLA_2$s, SVMPs, and SVSPs. However, only two toxins, Bnube-BPP-1 and Bnube-SVMPIII-1, were found to be absent in one individual. The overall expression pattern for both individuals was broadly

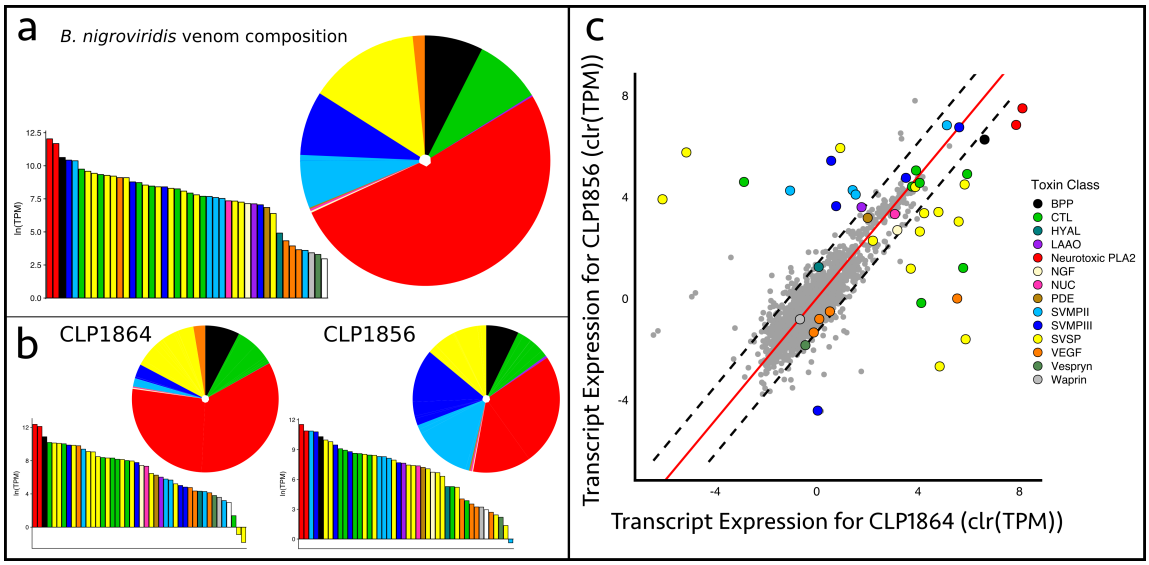


Figure 3.4.1: Venom characterization for *Bothriechis nigroviridis*. (a) Venom transcriptome compositions for *B. nigroviridis* based on average expression between two individuals. (b) Venom transcriptome compositions of each individual used. The venom of *B. nigroviridis* CLP1864 is largely consistent with the published proteome for this species. The high proportion of snake venom metalloproteinases (SVMPs) observed in the venom gland transcriptome of *B. nigroviridis* CLP1856 has not been described previously. (c) Intraspecific variation in transcript expression for *B. nigroviridis*. Data have been centered log-ratio transformed to account for their compositional nature. Dashed lines denote the 99% confidence interval of nontoxin expression and red lines are lines of best fit based on orthogonal residuals. *B. nigroviridis* displays substantially more variation in toxin expression, primarily in C-Type lectins (CTLs), SVMPs, and snake venom serine proteinases (SVSPs).

consistent with observed Type B venoms (Glenn and Straight, 1978). SVMPs and CTLs were highly abundant components in the venom making up, on average 34.9% and 40.4% of toxin expression, respectively. In addition to SVMPs and CTLs, *B. nubestris* also expressed three $PLA_2$s at lower levels. Two of these $PLA_2$s were orthologous to the alpha and beta subunits of nigroviriditoxin on average accounting for 0.2% and 0.5% of toxin expression, respectively. The third $PLA_2$, Bnube-PLA2-3, made up 15.7% of toxin expression in one *B. nubestris* individual (CLP1865) and appears homologous to a non-enzymatic, myotoxic $PLA_2$ in *B. schlegelii* (Angulo et al., 1997; Tsai et al., 2001). (Glenn et al., 1983).

| Toxin ID | Ortholog/ Paraloge | TPM | | Likely Over Expression | Presence/Absence | |
|---|---|---|---|---|---|---|
| | | CLP1856 | CLP1864 | | CLP1856 | CLP1864 |
| Bnigro-BPP-1 | Ortholog | 29752.98 | 52897.54 | CLP1864 | + | + |
| Bnigro-CTL-1 | Ortholog | 5601.97 | 3.99 | CLP1856 | + | - |
| Bnigro-CTL-2 | Ortholog | 47.42 | 4353.63 | CLP1864 | - | + |
| Bnigro-CTL-3 | Ortholog | 4669.5 | 3027.69 | - | + | + |
| Bnigro-CTL-4 | Paralog | 5395.92 | 4095.4 | - | + | + |
| Bnigro-CTL-5 | Paralog | 7653.39 | 26592.73 | CLP1864 | + | + |
| Bnigro-CTL-6 | Paralog | 8809.55 | 3537.01 | - | + | + |
| Bnigro-CTL-7 | Paralog | 0 | 22739.95 | CLP1864 | - | + |
| Bnigro-HYAL-1 | Ortholog | 196.31 | 76.03 | - | + | + |
| Bnigro-LAAO-1 | Ortholog | 2070.21 | 412.19 | CLP1856 | + | + |
| Bnigro-NGF-1 | Ortholog | 836.47 | 1692.1 | - | + | + |
| Bnigro-NUC-1 | Ortholog | 1575.76 | 1532.59 | - | + | + |
| Bnigro-PDE-1 | Ortholog | 1356.81 | 524.9 | - | + | + |
| Bnigro-$PLA_2$-1 | Ortholog | 53023.62 | 183732.85 | CLP1864 | + | + |
| Bnigro-$PLA_2$-2 | Ortholog | 102035.05 | 235935.29 | CLP1864 | + | + |
| Bnigro-SVMPII-1 | Ortholog | 3405.08 | 327.07 | CLP1856 | + | - |
| Bnigro-SVMPII-2 | Ortholog | 4055.07 | 290.21 | CLP1856 | + | - |
| Bnigro-SVMPII-3 | Ortholog | 3980.17 | 24.59 | CLP1856 | + | - |
| Bnigro-SVMPII-4 | Paralog | 52404.14 | 11942.88 | - | + | + |
| Bnigro-SVMPIII-1 | Ortholog | 0.68 | 73.09 | CLP1864 | - | + |
| Bnigro-SVMPIII-2 | Ortholog | 2157.48 | 151.17 | CLP1856 | + | + |
| Bnigro-SVMPIII-3 | Ortholog | 12908.06 | 124.4 | CLP1856 | + | + |
| Bnigro-SVMPIII-4 | Ortholog | 6587.36 | 2375.96 | CLP1856 | + | - |
| Bnigro-SVMPIII-5 | Ortholog | 48324.54 | 19456.86 | - | + | + |
| Bnigro-SVSP-1 | Ortholog | 5067.97 | 24092.29 | CLP1864 | + | + |
| Bnigro-SVSP-2 | Ortholog | 4588.27 | 3441.02 | - | + | + |
| Bnigro-SVSP-3 | Ortholog | 1633.58 | 4877.37 | CLP1864 | + | + |
| Bnigro-SVSP-4 | Ortholog | 1174.85 | 19016.69 | CLP1864 | + | + |
| Bnigro-SVSP-5 | Ortholog | 552.15 | 644.59 | - | + | + |
| Bnigro-SVSP-6 | Ortholog | 1712.44 | 8567.09 | CLP1864 | - | + |
| Bnigro-SVSP-7 | Ortholog | 792.67 | 4112.06 | CLP1864 | + | + |
| Bnigro-SVSP-8 | Ortholog | 17931.94 | 0.41 | CLP1856 | + | - |
| Bnigro-SVSP-9 | Paralog | 11.35 | 25032.15 | CLP1864 | - | + |
| Bnigro-SVSP-10 | Paralog | 183.43 | 2875.45 | CLP1864 | + | + |
| Bnigro-SVSP-11 | Paralog | 2827.4 | 0.16 | CLP1856 | + | - |
| Bnigro-SVSP-12 | Paralog | 3.89 | 8988.68 | CLP1864 | - | + |
| Bnigro-SVSP-13 | Paralog | 21317.45 | 0 | CLP1856 | + | - |
| Bnigro-VEGF-1 | Ortholog | 56.56 | 17963.5 | CLP1864 | + | + |
| Bnigro-VEGF-2 | Ortholog | 33.93 | 117.99 | - | + | + |
| Bnigro-VEGF-3 | Ortholog | 14.81 | 62.5 | - | + | + |
| Bnigro-VEGF-4 | Ortholog | 25.22 | 77.81 | - | + | + |
| Bnigro-Vespryn-1 | Paralog | 8.98 | 45.01 | - | + | + |
| Bnigro-Waprin-1 | Ortholog | 24.92 | 36.31 | - | + | + |

Table 3.4.2: Toxin transcripts recovered for *Bothriechis nigroviridis* and associated classifications as orthologs or paralogs, expected transcripts per million reads (TPM) estimated by RSEM, likely over expression classification as detected in intraspecific variation comparisons (i.e., above the 99th percentile of expected variance in expression based on a nontoxin null distribution), and coverage-based assessment of likely presence or absence

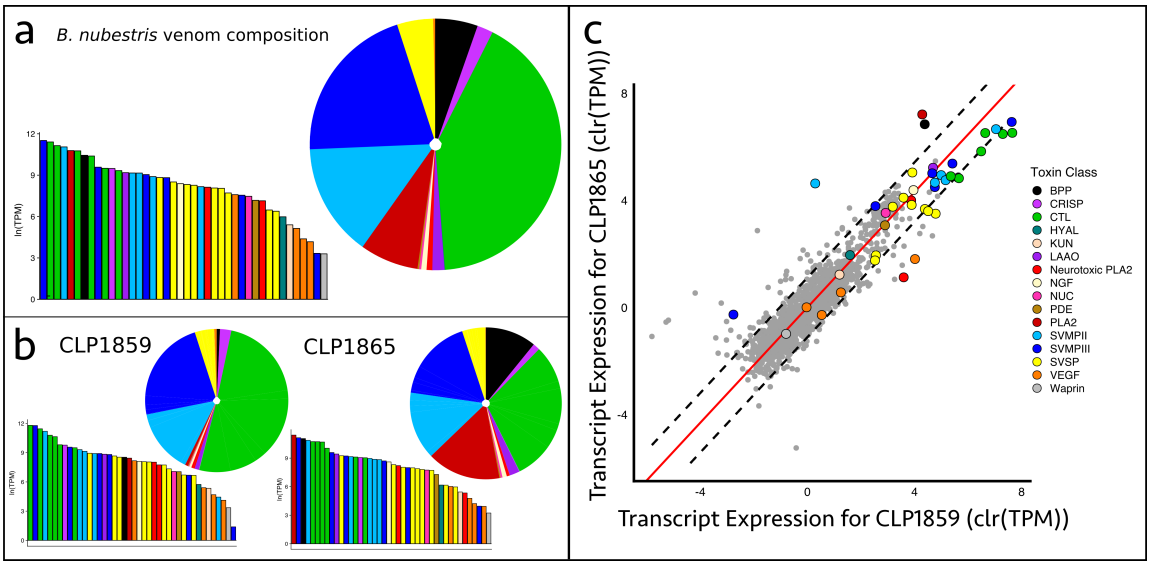


Figure 3.4.2: Venom characterization for *Bothriechis nubestris*. (a) Venom transcriptome compositions for *B. nubestris* based on average expression between two individuals for each species. (b) Venom transcriptome compositions of each individual used. The venom of *B. nubestris* is dominated by SVMPs and CTLs. (c) Intraspecific variation in transcript expression for *B. nubestris*. Data have been centered log-ratio transformed to account for their compositional nature. Dashed lines denote the 99% confidence interval of nontoxin expression and red lines are lines of best fit based on orthogonal residuals. The venoms of *B. nubestris* CLP1859 and CLP1865 are largely similar, though CLP1865 displays elevated expression of a basic $PLA_2$ and BPPs.

Table 3.4.3: Toxin transcripts recovered for *Bothriechis nubestris* and associated classifications as orthologs or paralogs, expected transcripts per million reads (TPM) estimated by RSEM, over expression classification as detected in intraspecific variation comparisons (i.e., above the 99th percentile of expected variance in expression based on a nontoxin null distribution), and coverage-based assessment of likely presence or absence

| Toxin ID | Ortholog/ Paralog | TPM | | Likely Over Expression | Presence/Absence | |
|---|---|---|---|---|---|---|
| | | CLP1859 | CLP1865 | | CLP1859 | CLP1865 |
| Bnubes-BPP-1 | Ortholog | 5097.77 | 63484.01 | CLP1865 | - | + |
| Bnubes-CRISP-1 | Paralog | 17682.06 | 8634.01 | CLP1859 | + | + |
| Bnubes-CTL-1 | Ortholog | 48790.4 | 45771.89 | - | + | + |
| Bnubes-CTL-2 | Ortholog | 13469.89 | 9134.83 | - | + | + |
| Bnubes-CTL-3 | Ortholog | 18273.91 | 8462.73 | CLP1859 | + | + |
| Bnubes-CTL-4 | Paralog | 134247.25 | 46096.08 | CLP1859 | + | + |
| Bnubes-CTL-5 | Paralog | 93992.03 | 44194.92 | CLP1859 | + | + |
| Bnubes-CTL-6 | Paralog | 41975.1 | 23098.03 | CLP1859 | + | + |
| Bnubes-HYAL-1 | Ortholog | 312.56 | 480.7 | - | + | + |
| Bnubes-KUN-1 | Paralog | 211.54 | 231.29 | - | + | + |
| Bnubes-LAAO-1 | Ortholog | 6946.11 | 12529.4 | - | + | + |
| Bnubes-NGF-1 | Ortholog | 3347.21 | 5435.31 | - | + | + |
| Bnubes-NUC-1 | Ortholog | 1184.42 | 2318.22 | - | + | + |
| Bnubes-PDE-1 | Ortholog | 1156.15 | 1461.55 | - | + | + |
| Bnubes-$PLA_2$-1 | Ortholog | 3073.31 | 3700.01 | - | + | + |
| Bnubes-$PLA_2$-2 | Ortholog | 2321.73 | 209.08 | CLP1859 | + | + |
| Bnubes-$PLA_2$-3 | Paralog | 4646.1 | 91726.32 | CLP1865 | + | + |
| Bnubes-SVMPII-1 | Ortholog | 11115.83 | 7867.18 | - | + | + |
| Bnubes-SVMPII-2 | Ortholog | 7446.39 | 7182.3 | - | + | + |
| Bnubes-SVMPII-3 | Ortholog | 85.26 | 6966.13 | CLP1865 | + | + |
| Bnubes-SVMPII-4 | Paralog | 9408.28 | 9519.11 | - | + | + |
| Bnubes-SVMPII-5 | Paralog | 72976.3 | 52932.86 | - | + | + |
| Bnubes-SVMPIII-1 | Ortholog | 4.02 | 52.08 | CLP1865 | - | + |
| Bnubes-SVMPIII-2 | Ortholog | 7436.41 | 6075.36 | - | + | + |
| Bnubes-SVMPIII-3 | Ortholog | 14334.66 | 14644.25 | - | + | + |
| Bnubes-SVMPIII-4 | Ortholog | 6744.23 | 10192.23 | - | + | + |
| Bnubes-SVMPIII-5 | Ortholog | 131295.22 | 69281.92 | CLP1859 | + | + |
| Bnubes-SVMPIII-6 | Paralog | 808.43 | 2990.11 | - | + | + |
| Bnubes-SVSP-1 | Ortholog | 5793.23 | 2477.48 | CLP1859 | + | + |
| Bnubes-SVSP-2 | Ortholog | 1544.31 | 2924.28 | - | + | + |
| Bnubes-SVSP-3 | Ortholog | 3126.56 | 3125.05 | - | + | + |
| Bnubes-SVSP-4 | Ortholog | 7665.15 | 2252.2 | CLP1859 | + | + |
| Bnubes-SVSP-5 | Ortholog | 2301.11 | 4094.43 | - | + | + |
| Bnubes-SVSP-6 | Ortholog | 5123.44 | 2684.33 | - | + | + |
| Bnubes-SVSP-7 | Ortholog | 795.14 | 393.28 | - | + | + |
| Bnubes-SVSP-8 | Ortholog | 3207.97 | 10487.13 | - | + | + |
| Bnubes-SVSP-9 | Paralog | 823.13 | 475.48 | - | + | + |
| Bnubes-VEGF-1 | Ortholog | 3542.02 | 413.99 | CLP1859 | + | + |
| Bnubes-VEGF-2 | Ortholog | 222.72 | 119.16 | - | + | + |
| Bnubes-VEGF-3 | Ortholog | 109.03 | 51.22 | - | + | + |
| Bnubes-VEGF-4 | Ortholog | 61.69 | 68.27 | - | + | + |
| Bnubes-Waprin-1 | Ortholog | 28.73 | 25.35 | - | + | + |

### 3.4.2 Interspecific Variation & Submodule Identification

OrthoFinder (Emms and Kelly, 2015) identified 1282 one-to-one orthologs, which included 32 orthologous toxins. Due to the high variability in toxin expression observed between individuals of *B. nigroviridis*, we compared toxin expression of each individual to the average expression of *B. nubestris* (Fig. 3.4.3). High variation in ortholog expression was observed between the northern *B. nigroviridis* and *B. nubestris*, with 14 toxins detected as differentially expressed by DESeq2 (Fig. 3.4.3, Table 3.4.4). The most prominent pattern was the variation in expression of nigroviriditoxin subunits and SVMPs (Fig. 3.4.3); a pattern which supports the classification of the northern *B. nigroviridis'* venom as Type A and *B. nubestris'* venom as Type B. In contrast, only 8 orthologous toxins were detected as differentially expressed between the southern *B. nigroviridis* and *B. nubestris* (Fig. 3.4.3, Table 3.4.5). Moreover, the variance in orthologous expression between the southern

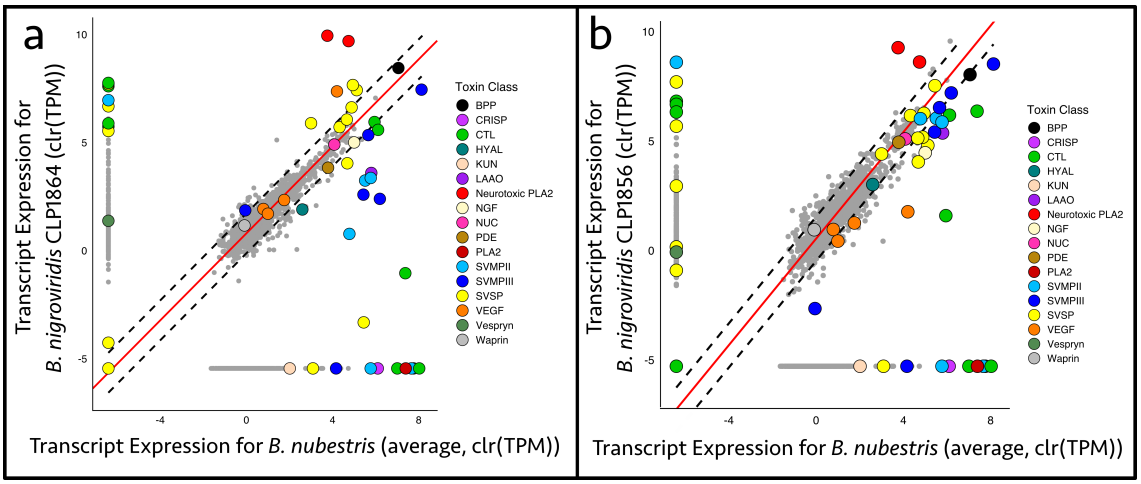


Figure 3.4.3: Interspecific comparisons of toxin expression between average *Bothriechis nubestris* toxin expression and (a) Type A *B. nigroviridis* and (b) Type A+B *B. nigroviridis*. TPM values have been centered log-ratio transformed to account for the compositional nature of the data. Dashed lines denote the 99% confidence interval of nontoxin expression and red lines are lines of best fit based on orthogonal residuals. Paralogs are shown near axes for each species.

*B.nigroviridis* and *B. nubestris* was substantially lower than observed in the previous comparison, due largely to increased expression of several SVMPs.

We implemented WGCNA assigning three venom phenotypes as "treatments": Type A (*B. nigroviridis* CLP1864), Type A+B (*B. nigroviridis* CLP1856), and Type B (*B. nubestris* CLP1859 and CLP1865). After transcript filtering, 83 transcripts, including 22 toxin transcripts, were segregated into six modules (Fig. 3.4.4, Table B.7 in Appendix B). Most of the toxins associated with the Type A/Type B phenotypes segregated into two distinct modules. Module 2 contained five of the seven orthologous SVMPs while Module 3 contained both nigroviriditoxin subunits. SVSPs were distributed across three modules, including module 2 and module 3. Similarly, BPPs were the only toxin assigned to module 1 which appeared to primarily capture intraspecific variation in *B. nubestris*. Of the three orthologous CTLs, one was removed during filtering and the remaining two were assigned to modules 2 and 6. Finally, two VEGFs were assigned to two separate modules as well. We did not identify any transcription factors associated with the putatively Type A or Type B modules. However, we did identify a translation initation factor, TIF-4E1, associated with module 2.

| Toxin | baseMean | log2FoldChange | lfcSE | stat | p-value | p-adj |
|---|---|---|---|---|---|---|
| SVSP-4 | 56149.550 | -2.041 | 0.790 | -2.582 | 0.010 | 0.136 |
| SVSP-1 | 62813.029 | -2.650 | 0.676 | -3.920 | <0.001** | 0.003** |
| SVSP-2 | 14843.268 | -0.759 | 0.651 | -1.166 | 0.243 | 0.819 |
| SVSP-6 | 31232.805 | -1.245 | 0.643 | -1.935 | 0.053 | 0.405 |
| SVSP-7 | 10256.001 | -2.901 | 0.713 | -4.069 | <0.001** | 0.002** |
| SVSP-3 | 21197.683 | -0.765 | 0.534 | -1.433 | 0.152 | 0.685 |
| SVSP-8 | 24729.723 | 13.915 | 1.148 | 12.121 | <0.001** | <0.001** |
| VEGF-2 | 575.456 | 0.408 | 0.512 | 0.798 | 0.425 | 0.968 |
| VEGF-4 | 176.204 | -0.412 | 0.432 | -0.953 | 0.341 | 0.913 |
| VEGF-3 | 329.392 | 0.240 | 0.558 | 0.429 | 0.668 | 0.983 |
| CTL-2 | 21966.999 | 1.227 | 0.588 | 2.087 | 0.037 | 0.322 |
| CTL-1 | 75597.100 | 13.412 | 0.619 | 21.666 | <0.001** | <0.001** |
| SVMPII-3 | 26046.537 | 7.004 | 3.014 | 2.324 | 0.020* | 0.228 |
| SVMPII-2 | 58055.510 | 4.545 | 0.471 | 9.658 | <0.001** | <0.001** |
| CTL-3 | 27445.563 | 2.004 | 0.682 | 2.940 | 0.003** | 0.061 |
| LAAO-1 | 81941.767 | 4.437 | 0.564 | 7.862 | <0.001** | <0.001** |
| NGF-1 | 17559.052 | 1.241 | 0.606 | 2.047 | 0.041 | 0.350 |
| NUC-1 | 24635.841 | 0.0662 | 0.630 | 0.105 | 0.916 | 0.999 |
| PDE-1 | 22815.921 | 1.204 | 0.537 | 2.242 | 0.025* | 0.258 |
| $PLA_2$-1 | 153799.239 | -5.920 | 0.508 | -11.652 | <0.001** | <0.001*** |
| $PLA_2$-2 | 193031.819 | -7.691 | 1.132 | -6.796 | <0.001** | <0.001*** |
| SVMPIII-5 | 1120896.609 | 2.273 | 0.848 | 2.681 | 0.007 | 0.115 |
| SVMPIII-3 | 146258.094 | 6.755 | 0.495 | 13.645 | <0.001** | <0.001** |
| SVMPIII-2 | 68851.762 | 5.381 | 0.499 | 10.779 | <0.001** | <0.001** |
| SVMPIII-4 | 96830.991 | 1.714 | 0.522 | 3.286 | 0.001** | 0.025* |
| SVSP-5 | 12727.207 | 2.176 | 0.638 | 3.408 | 0.001** | 0.019* |
| SVMPII-1 | 75173.762 | 4.756 | 0.534 | 8.899 | <0.001** | <0.001** |
| BPP-1 | 162148.870 | -0.756 | 1.137 | -0.665 | 0.506 | 0.982 |
| HYAL-1 | 3084.833 | 2.260 | 0.587 | 3.853 | <0.001** | 0.004** |
| SVMPIII-1 | 676.400 | -1.536 | 2.179 | -0.705 | 0.481 | 0.982 |
| VEGF-1 | 19141.242 | -3.323 | 1.095 | -3.036 | 0.002** | 0.050 |
| Waprin-1 | 65.350 | -0.587 | 0.626 | -0.938 | 0.348 | 0.915 |

Table 3.4.4: DESeq2 expression analyses for *B. nigroviridis* A versus *B. nubestris* toxins comparison. Statistically significant $p$-values are denoted with asterisks

| Toxin | baseMean | log2FoldChange | lfcSE | stat | $p$-value | $p$-adj |
|---|---|---|---|---|---|---|
| SVSP-4 | 17900.673 | 1.529 | 0.879 | 1.740 | 0.082 | 0.327 |
| SVSP-1 | 23976.545 | -0.846 | 0.744 | -1.136 | 0.256 | 0.562 |
| SVSP-2 | 17011.775 | -1.609 | 0.720 | -2.234 | 0.025* | 0.171 |
| SVSP-6 | 15736.775 | 0.634 | 0.743 | 0.854 | 0.393 | 0.704 |
| SVSP-7 | 3569.069 | -0.970 | 0.718 | -1.351 | 0.177 | 0.483 |
| SVSP-3 | 13267.220 | 0.373 | 0.656 | 0.569 | 0.570 | 0.805 |
| SVSP-8 | 61332.390 | -1.966 | 0.681 | -2.886 | 0.004** | 0.053 |
| VEGF-2 | 398.593 | 1.786 | 0.519 | 3.445 | 0.001** | 0.012* |
| VEGF-4 | 113.051 | 0.845 | 0.535 | 1.580 | 0.114 | 0.391 |
| VEGF-3 | 218.467 | 1.899 | 0.590 | 3.220 | 0.001** | 0.021* |
| CTL-2 | 15138.097 | 7.366 | 0.698 | 10.557 | <0.001** | <0.001** |
| CTL-1 | 68552.480 | 2.542 | 0.432 | 5.890 | <0.001** | <0.001** |
| SVMPII-3 | 40750.244 | -0.784 | 3.020 | -0.260 | 0.795 | 0.908 |
| SVMPII-2 | 67043.525 | 0.277 | 0.433 | 0.641 | 0.522 | 0.780 |
| CTL-3 | 25464.314 | 0.979 | 0.707 | 1.384 | 0.166 | 0.469 |
| LAAO-1 | 77794.353 | 1.648 | 0.514 | 3.206 | 0.001** | 0.022* |
| NGF-1 | 13847.466 | 1.826 | 0.701 | 2.606 | 0.009** | 0.088 |
| NUC-1 | 23423.714 | -0.436 | 0.683 | -0.638 | 0.523 | 0.782 |
| PDE-1 | 27866.068 | -0.637 | 0.571 | -1.115 | 0.265 | 0.572 |
| $PLA_2$-1 | 50595.962 | -4.499 | 0.465 | -9.673 | <0.001** | <0.001*** |
| $PLA_2$-2 | 90982.168 | -6.867 | 2.083 | -3.296 | 0.001** | 0.018* |
| SVMPIII-5 | 1147158.941 | 0.489 | 0.697 | 0.702 | 0.483 | 0.766 |
| SVMPIII-3 | 202400.932 | -0.410 | 0.438 | -0.937 | 0.349 | 0.661 |
| SVMPIII-2 | 70220.557 | 1.077 | 0.453 | 2.377 | 0.017* | 0.134 |
| SVMPIII-4 | 111332.469 | -0.222 | 0.472 | -0.470 | 0.638 | 0.837 |
| SVSP-5 | 10829.466 | 1.964 | 0.726 | 2.707 | 0.007** | 0.074 |
| SVMPII-1 | 77902.986 | 0.911 | 0.480 | 1.898 | 0.058 | 0.273 |
| BPP-1 | 120779.234 | -0.334 | 2.184 | -0.153 | 0.878 | 0.954 |
| HYAL-1 | 3203.542 | 0.434 | 0.624 | 0.696 | 0.487 | 0.767 |
| SVMPIII-1 | 236.935 | 4.758 | 2.234 | 2.130 | 0.033* | 0.197 |
| VEGF-1 | 2696.561 | 4.593 | 1.031 | 4.457 | <0.001** | <0.001** |
| Waprin-1 | 51.896 | -0.411 | 0.679 | -0.606 | 0.545 | NA |

Table 3.4.5: DESeq2 expression analyses for *B. nigroviridis* A + B versus *B. nubestris* toxins comparison. Statistically significant $p$-values are denoted with asterisks

### 3.4.3 Gene Family Analyses

To better understand the dynamics of transcript turnover (i.e., gene duplications and transcript losses through either gene loss or gene silencing) in relation to families associated with specific modules, we inferred toxin family phylogenies for four highly expressed and diverse toxin families and identified species-specific gene duplication and transcript loss events. As expected, our results suggest that the majority of toxin genes in *B. nigroviridis* and *B. nubestris* were likely present in their common ancestor. In three of the four toxin families, OrthoFinder identified one-to-one orthologs for the majority of toxins, although expression levels were not necessarily conserved (Fig. 3.4.5). However, each toxin family exhibited at least one species-specific toxin loss and three of the families showed evidence of both losses and duplications.

Transcript turnover was lower in families with a higher proportion of toxins sorted into a specific submodule. The two CTLs were split between two expression submodules (M2 and M6) and had four deletions and one duplication. Similarly, five SVSPs were split between three modules with three SVSPs assigned to module 2. SVMPs were inferred to have a single duplication and loss and were similarly assigned to three modules (M2, M4, and M6), though the five consistently highly expressed SVMPs were assigned to M2. $PLA_2$s were the only family to experience a single species-specific toxin transcript loss, and the two orthologous toxins were assigned to M3.

In both SVMPs and SVSPs, we observed sequence divergence that occurred in one or more toxin copies following a duplication event (Fig. 3.4.5). In the case of SVSPs, nucleotide sequence divergence was sufficient to give conflicting phylogenetic signal when compared to the amino acid-based phylogeny inferred by OrthoFinder (Fig. 3.4.5, Fig. B.7 in Appendix B). Although we did not find a significant difference in expression of one-to-one toxin orthologs compared to duplicated or conserved toxins ($p = 0.28$), we did find a marginally significant interaction between species and expression of one-to-one orthologs versus duplicated or conserved toxins ($p = 0.08$, Fig. 3.4.6). More specifically, *B. nubestris* appeared to exhibit proportionately higher expression of toxins, but also disproportionately higher expression of duplicated and conserved toxins (Fig. 3.4.6).

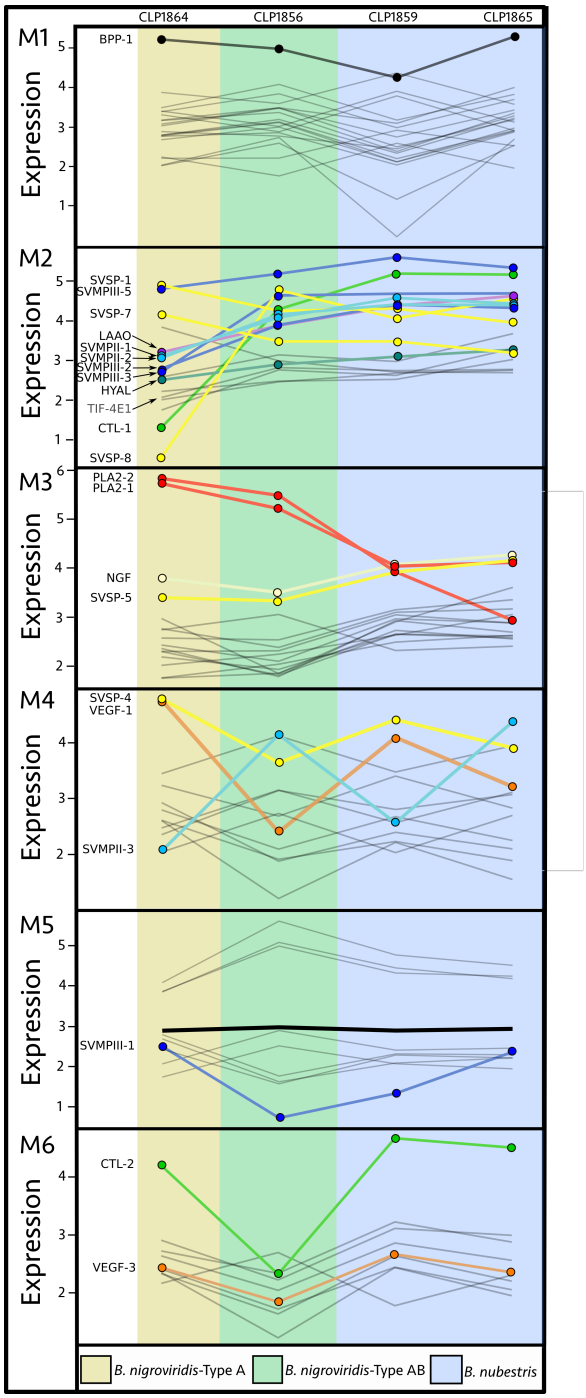


Figure 3.4.4: Expression profiles for the six expression modules identified by CEMiTool. Each line represents a transcript and its change in expression across treatments. Toxins assigned to each module are colored by class and labelled. Nontoxins associated with a module are shown as grey lines. Toxins generally associated with the Type A and Type B venom phenotypes (neurotoxic $PLA_2$ subunits and SVMPs, respectively) largely separated into two modules: M2 and M3. *B. nigroviridis* with Type A+B venom showed generally intermediate expression of A-B associated toxins.

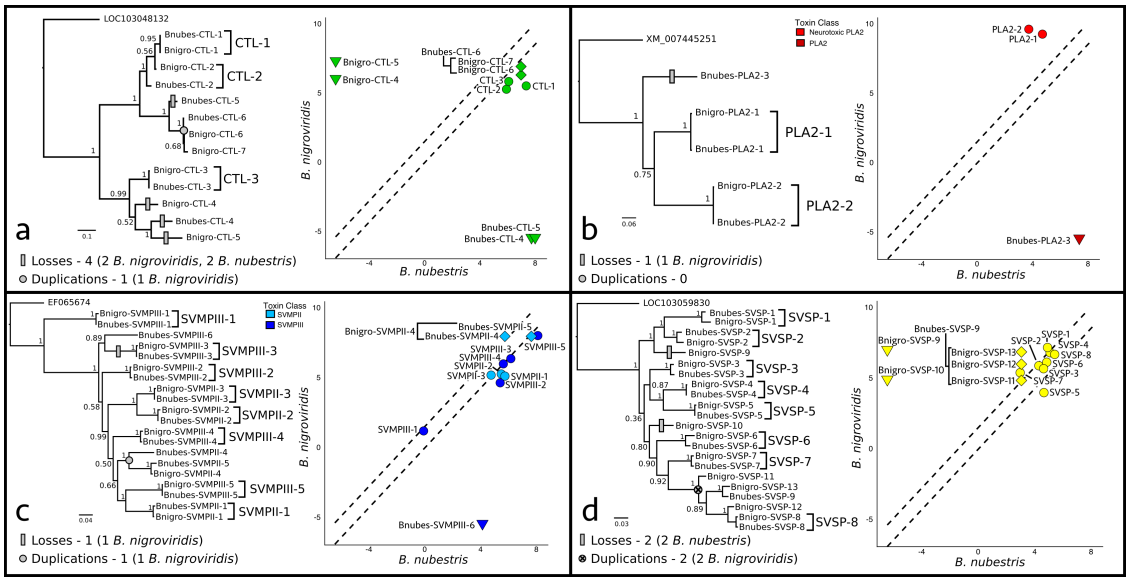


Figure 3.4.5: Toxin family phylogenies and expression plots of (a) C-Type lectins (CTLs), (b) phospholipase $A_2$s ($PLA_2$s), (c) snake venom metalloproteinases (SVMPs), and (d) snake venom serine proteases (SVSPs). Single copy toxin orthologs identified by OrthoFinder are marked by brackets in the phylogeny. Toxin transcript gains and losses were inferred based on a simple parsimony model and are shown on phylogenies as grey circles and rectangles, respectively. Expression plots are based on average expression of each toxin for each species and dashed lines denote 99% confidence interval established by nontoxin expression. Identified orthologs are shown as colored circles and losses as colored inverted triangles. Duplicated toxins are shown as colored diamonds and expression of each copy is plotted against expression of their orthologous counter part in the other species (identified with bracketing on plots).

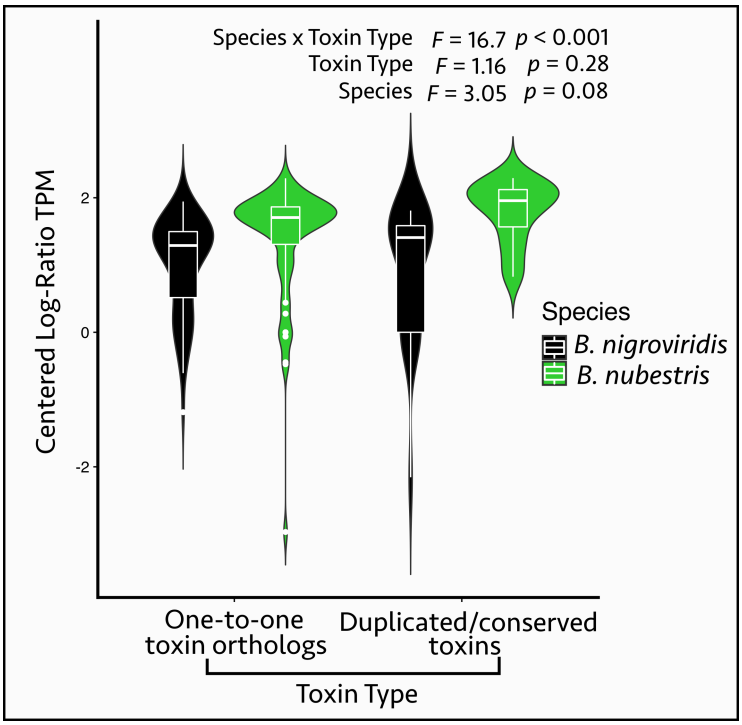


Figure 3.4.6: Violin plots comparing expression of orthologous and paralogous toxins for *Bothriechis nigroviridis* and *B. nubestris*. Orthologous and paralogous toxins were not differentially expressed between the species.

### 3.4.4 Sequence Based Selection Analyses

To determine the extent and role of sequence diversification in differentiating venoms, we compared pairwise values of $\omega$, $dS$, and $dN$ between toxin and nontoxin orthologs. Toxin sequences exhibited significantly higher values of $\omega$ ($p$ <0.001) with three toxins, CTL-2, SVMPII-1, and SVMPIII-5, having $\omega$ values >1 indicating positive selection (Fig. 3.8). Despite having a higher $\omega$ ratio than the background nontoxins, the overall mean $\omega$ for toxin sequences was 0.56. Additionally, we tested for differences in synonymous and nonsynonymous substitution rates between toxins and nontoxins under the expectation that toxins and nontoxins should display similar background synonymous substitution rates but differ in nonsynonomous substitutions resulting in diversifying selection. As expected, we found no differences in synonymous substitution rates between toxins and nontoxins ($p$ = 0.252) but significantly higher nonsynonymous substitution rates ($p$ <0.001). Moreover, nine toxins had nonsynonymous substitution above the 95th percentile of nontoxin sequences; nearly double the number of toxins above the 95th percentile of $\omega$. However, four of these toxins were found to have synonymous substitution above the 95th percentile of nontoxin sequences.

## 3.5 Discussion

We tested the hypothesis that dimensions of the neurotoxic-hemorrhagic venom phenotype were associated with specific submodules of toxin expression. We identified six submodules of expression variation, which included a primarily Type A submodule containing both nigroviridi-toxin homolog subunits and a primarily Type B submodule containing the majority of orthologous SVMPs. The findings supported our hypothesis and implicate submodular regulation as a mechanism for rapid venom diversification. Modular expression regimes would allow rapid transitions between phenotypes while avoiding or minimizing occurrence of low-fitness intermediates (von Dassow and Munro, 1999) and facilitate ontogentic shifts observed in many groups (Mackessy et al., 2003; Calvete et al., 2010; Durban et al., 2017; Pla et al., 2017). In the *Bothriechis* system, modularity effectively explains many of the toxin expression differences between *B. nigroviridis* and *B. nubestris*. The patterns of modularity observed here are also consistent with on-going genomic research to elucidate the genomic architecture mediating venom phenotype evolution (Dowell et al., 2016, 2018; Schield et al., 2019). Taken together these findings provide strong support for a role of sub-modular variation mediating changes in snake venom phenotypes.

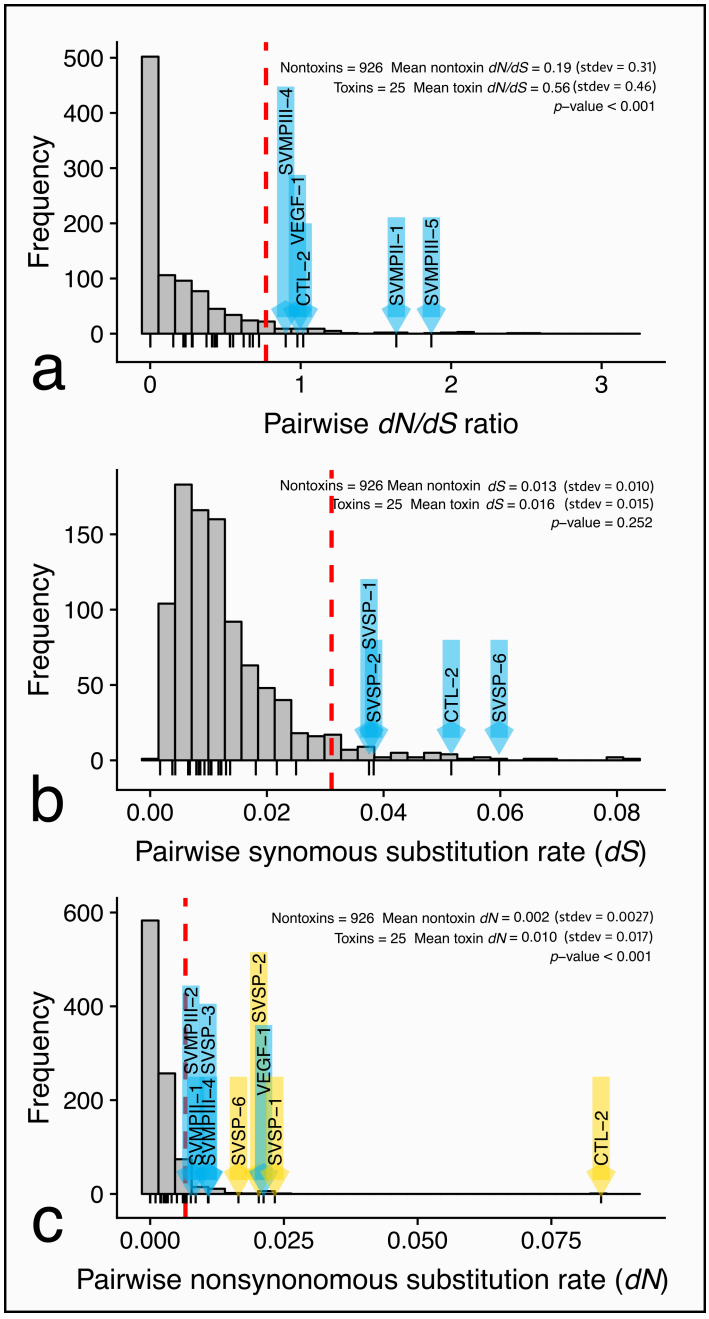


Figure 3.4.7: Distribution of (a) pairwise $dN/dS$ ratios, (b) synonymous substitution rates, and (c) nonsynonymous substitution rates of orthologous transcripts. Dashed red lines denote 95 percentiles based on distribution of nontoxins. Lines beneath plots indicate toxins, and toxins with values greater than the 95 percentile are marked with blue arrows. In (c), toxins above the 95th percentile with elevated synonymous mutation rates (i.e., above the 95th percentile in (b) are colored yellow. Toxins had statistically higher $dN/dS$ ratios and nonsynonymous substitution rates based on a Wilcoxon signed rank test. Toxin and nontoxin synonymous mutation rates were not significantly different.

### 3.5.1 Modularity Underlying the Neurotoxic-Hemorrhagic Dichotomy

The patterns of modularity and submodular organization inferred by WGCNA analyses explained much of the inter- and intraspecific variation in toxin expression we observed for *B. nigroviridis* and *B. nubestris*. We recovered a venom gland transcriptome for the northern *B. nigroviridis* consistent with the published proteomic venom phenotype and Type A venom expression. The increase in expression of nigroviriditoxin/nigroviriditoxin homologs is accomplished primarily through modification of regulatory patterns in module 3. Similarly, modifications to regulatory elements in module 2 can mediate expression regime shifts of many toxins, especially SVMPs. The strong association of these modules with species-specific patterns of inheritance demonstrate how modularity can promote rapid phenotypic transition among recently diverged and/or eco-morphically conserved species.

Of note was the Type A+B expression pattern in the southern *B. nigroviridis* which suggested intermediate or combined expression of the Type A and Type B submodules. Although Type A+B venoms have been documented in multiple species (Glenn et al., 1983, 1994) they are primarily associated with species exhibiting population level neurotoxic-hemorrhagic dichotomies and often occur at lower frequency than either the Type A or Type B phenotypes (Strickland et al., 2018b). If this pattern holds true in *B. nigroviridis*, it would suggest the existence of individuals or populations of *B. nigroviridis* that have primarily Type B venom. Population level sampling has been difficult to attain due to the inherent rarity of this species and the logistical challenges of sampling many of the undisturbed, high-elevation regions of its distribution. However, population level sampling will be key for understanding the ecological and evolutionary dynamics of venom variation in this species. More importantly, the occurrence of the Type A+B phenotype in *B. nigroviridis* and other species suggests that the Type A and B submodules are not mutually exclusive. Rather, each module likely has independent genetic architectures which can occur in variable combinations among populations and species.

Modular expression effectively explains Type A/Type B toxin variation among these two species, but several toxin families such as CTLs, SVSPs, and VEGFs did not fit this framework. The variation observed in these families underscores the diversity of expression patterns in venom toxins and presents an ongoing challenge for the future. Although a great deal of work has been devoted to dissecting broad patterns of venom variation (e.g., neurotoxic-hemorrhagic dichotomy),

the mechanisms influencing variation in other diverse toxin families such as SVSPs and CTLs deserves further investigation.

While our findings present evidence for submodularity of toxin expression, it is important to note their limitations as well. WGNCA identifies submodular clusters based on positive and negative correlations in transcript expression across assigned treatments with the expectation that these transcripts may be influenced by common regulatory elements. Because coexpression network analyses are based on observed patterns of expression rather than experimental validation, they are better regarded as hypotheses of submodular association rather than empirical findings. Moreover, WGCNA are ideally implemented using thousands of candidate transcripts derived from thoroughly assembled and annotated genomes with tens of replicates across treatments for robust inference. Unfortunately, genomic resources remain limited for snakes and such large sample sizes are difficult to attain for many species. Here, we have implemented WCGNA with a much reduced sample size and far fewer candidate genes than is typically ideal, which may make module assignment less powerful and robust, especially for lowly expressed transcripts. Nevertheless, our analyses assigned many highly expressed toxins to biologically plausible submodules corresponding to known axes of phenotypic variation in snake venom. Thus, we believe that WGCNA as implemented here represent an important proof-of-concept in the relevance and potential of these methods and the conceptual framework of modularity for evolutionary study of venom differentiation.

### 3.5.2 Mechanisms Promoting Modularity

Although our WGCNA and similar approaches identify submodules of variation based on phenomenological rather than mechanistic models, observed patterns of expression and recent genomic work implicate several general mechanisms contributing to modularity of the system. For instance, one of the primary advantages of co-expression network approaches is the ability to identify regulatory components such as transcription factors that potentially mediate the identified expression differences. In sub-module 2, we identified one translation initiation factor that showed increased expression with progression towards the Type B phenotype. Translation initiation factors enhance translation by stabilizing mRNA and facilitating assembly of ribosomal complexes (Sonenberg and Hinnebusch, 2009). In mammals, TIF-4E is required for efficient translation and acts as a translational regulatory mechanism (Sonenberg and Hinnebusch, 2009). Here, its association with module 2 may reflect an effort to promote rapid translation of the relatively large and highly ex-

pressed SVMPs. Though concordant expression of TIF-4E and module 2 toxins does not necessarily imply a causative link, it does present a hypothesis to test through functional validation.

The identification of primarily neurotoxic and hemorrhagic submodules are also consistent with recent genomic evidence which show that Type A and Type B toxins are inherited as independent haplotypes (Dowell et al., 2016, 2018; Schield et al., 2019). In some cases, presence and absence differences in these genes have been implicated as the primary drivers of variance in Type A/Type B phenotypes. In the case of the northern *B. nigroviridis*, absence of the SVMP tandem array could account for both the low expression of SVMPs and their inferred absence from the transcriptome (Table 3.4.2). In contrast, both *B. nubestris* individuals express low levels of a nigroviriditoxin homolog. Despite patterns of low expression, the sequences of the *B. nubestris* $PLA_2$s were highly conserved with respect to nigroviriditoxin; both subunits had over 99% nucleotide sequence similarity with three nonsynonomous substitutions occurring in the beta subunit and one synonymous substitution occurring in the alpha subunit. The conservation of these sequences suggests that the *B. nubestris* variants of nigroviriditoxin have likely retained their neurotoxic function and that convergence on a "low neurotoxicity" phenotype therefore occurs through regulatory evolution in *Bothriechis* rather than through gene loss/gain as is observed in other species (Dowell et al., 2016, 2018; Schield et al., 2019).

If expression patterns of the Type A and Type B submodules are inherited as independent haplotypes with additive effects, we can hypothesize that combined phenotypes are possible and should exhibit intermediate expression of of each module. The expression patterns apparent in the southern *B. nigroviridis* support these predictions as it displayed intermediate expression between the Type A *B. nigroviridis* and the Type B *B. nubestris* for the majority of Type A and Type B associated toxins. Additive expression of species-specific toxins has also been observed in interspecific hybrids where the putatively heterozygous offspring exhibit lower expression levels than presumably homozygous parents (Aird et al., 2015). In the case of *B. nigroviridis*, intermediate expression observed in the southern *B. nigroviridis* could feasibly be the result of heterozygosity at Type A and Type B loci, though such a hypothesis is largely postulation without genomic evidence. As such, comparative genomics approaches that test architectural mechanisms promoting and mediating modularity are a promising avenue for future work.

### 3.5.3 Transcript Turnover & Diversification in a Modular System

We expected selective optimization for modularity of toxins expression to affect toxin transcript turnover and sequence diversification. We tested for these effects in four toxin families and found that although all three toxin families had experienced some turnover, rates of duplication and loss were higher in toxins less associated with specific modules. Many snake toxin families have experienced dramatic expansions since their common ancestor (Casewell et al., 2013) though the frequency of toxin duplications and losses within species is not clear. The marginal decrease in transcript-turnover with increased association with a specific submodule suggests selection for maintaining these toxins. Duplications are often implicated as having a primary role in toxin neofunctionalization by creating functional redundancy that allows toxins to 'explore' the phenotype space (Wong and Belov, 2012; Casewell et al., 2013; Aird et al., 2017), but can also occur as a mechanism to increase expression of beneficial toxins (Margres et al., 2017). We observed both increased sequence divergence following duplication and a marginal increase in expression of duplicated or conserved (i.e., not deleted or silenced) toxins specific to the *B. nubestris* lineage. Whether the possible emphasis on expression of paralogous versus orthologous toxins reflect phenomena unique to the *B. nubestris* lineage or a broader trend in the evolution of the more complex, hemorrhagic venom types is not clear, especially given our limited sample size. However, increased sampling of lineages and their toxin compositions will provide improved resolution to test the extent and role of gene duplication and loss in venom diversification

We expected sequence diversification to be lowest in module associated toxins, but we did not find evidence to support this. Two of the three toxins with $\omega$ above one were SVMPs associated with Module 2, suggesting that although regulation may be conserved/coordinated, functionality is not. Many of the toxins with elevated rates of nonsynonymous substitution had similarly high rates of synonymous substitutions, which may indicate an overall higher substitution rate than the genomic background. Notably, SVSPs, which were generally less associated with a specific module, displayed some of the highest values of both $dN$ and $dS$. The overall elevated substitution rates of these toxins and the lack of correspondence to clear expression regimes may reflect higher rates of substitution and recombination in these gene regions, though patterns of gene expression and the organization of the genetic architecture of SVSP regions is not well understood. Overall, toxin $\omega$ values were generally below what is expected under positive selection with just a few toxins displaying

$\omega$ values greater than 1. Instead, toxin evolution between species appears to function under a model of relaxed purifying selection, which has been similarly noted in other interspecific comparisons of toxin sequence evolution (Rokyta et al., 2013).

## 3.6 Conclusions

Snake venoms are key innovations that have allowed the diversification of species across the globe. Unfortunately, many of the genomic mechanisms governing rapid variation of phenotypes remain uncertain. Through comparative transcriptomics and coexpression network analyses, we demonstrated how rapid transition between a common phenotypic venom dichotomy can occur through submodular regulation of the associated toxins. Modularity of the venom system and submodular variation of venom classes likely contribute to broader patterns of variation observed across taxonomic levels (Barua and Mikheyev, 2019). As genomic and transcriptomic resources become more available for venomous snakes, systems-based approaches such as the co-expression network analyses used here will yield more comprehensive understanding of the evolution of venoms and other complex, modular traits. Although our work presents these findings in the limited context of a single species pair, it highlights the importance of considering how complex traits function and evolve as a modular system. Our understanding of the selective forces that generate modularity and how modularity in turn mediates and facilitates the evolution of complex traits remains incomplete. However, as we have shown here, on-going efforts to address these questions in dynamic adaptive systems can provide key insights that lead to a more integrated understanding of the genomics of rapid adaptation in complex traits.

# Availability of Data & Materials

Raw sequence data and transcript sequences generated during the current study are available on the National Center for Biotechnology Information (NCBI) under accession numbers given in Table 1. Consensus transcriptomes have been to submitted to the NCBI Transcriptome Shotgun Assembly (TSA) database under GIBL00000000 (*Bothriechis nigroviridis*) and GIBM00000000 (*B. nubestris*). Scripts used in data analyses are available on GitHub at:https://github.com/masonaj157/Trait_differentiation_and_modular_expression_in_palm-pitvipers

## 3.7 Acknowledgments

We thank Fabian Bonilla and the Chacón and Sandi Harmon families for assistance collecting specimens used in this work. The project and its protocols were submitted to and approved by University of Central Florida Institutional Animal Care and Use Committee (IACUC) protocol 16-17W and Clemson University IACUC protocol number 2017-067. Project protocols were also submitted to and approved locally in Costa Rica by the Universidad de Costa Rica's Animal Care Office (Comité Institucional para el Cuidado y Uso de los Animales) permit CICUA-082-17. Samples were collected and exported from Costa Rica under Sistema Nacional de áreas conservación (SINAC) Investigation Permit 040-2016-INV-ACAT. Permission to collect samples used in this study was received from SINAC and property owners of sites from which animals were collected. This work was funded by National Science Foundation grants DUE 1161228, DEB 1638879, and DEB 1822417 to C.L.P. and DEB 1638902 to D.R.R. as well as the Southwestern Association of Naturalists McCarley Research Grant, the Theodore Roosevelt Memorial Fund through the American Museum of Natural History, and The Explorers Club Exploration Fund and Mamont Scholars program to A.J.M. The funding bodies played no role in study design; data collection, analysis, or interpretation; or writing the manuscript. The contents of this chapter were originally published as "Trait differentiation and modular toxin expression in palm-pitvipers" in *BMC Genomics*, 21, article 147. 

# References


Aird, S., da Silva, N., Qiu, L., Villar-Briones, A., Saddi, V., Pires de Campos Telles, M., Grau, M., and Mikheyev, A. (2017). Coralsnake venomics: analyses of venom gland transcriptomes and proteomes of six Brazilian taxa. *Toxins*, 9(12):187.

Aird, S. D., Aggarwal, S., Villar-Briones, A., Tin, M. M.-Y., Terada, K., and Mikheyev, A. S. (2015). Snake venoms are integrated systems, but abundant venom proteins evolve more rapidly. *BMC Genomics*, 16(647):1–20.

Aitchison, J. (1982). The statistical analysis of compositional data. *Journal of the Royal Statistical Society Series B*, 44(2):139–177.

Andrews, S. (2010). FastQC: a quality control tool for high throughput sequence data.

Angulo, Y., Chaves, E., Alape, A., Rucavado, A., Gutiérrez, J. M., and Lomonte, B. (1997). Isolation and characterization of a myotoxic phospholipase $A_2$ from the venom of the arboreal snake *Bothriechis* (*Bothrops*) *schlegelii* from Costa Rica. *Archives of Biochemistry and Biophysics*, 339(2):260–266.

Barua, A. and Mikheyev, A. S. (2019). Many options, few solutions: Over 60 my snakes converged on a few optimal venom formulations. *Molecular biology and evolution*, 36(9):1964–1974.

Calvete, J. J., Sanz, L., Cid, P., de la Torre, P., Flores-Díaz, M., Dos Santos, M. C., Borges, A., Bremo, A., Angulo, Y., Lomonte, B., Alape-Girón, A., and Gutiérrez, J. M. (2010). Snake venomics of the Central American Rattlesnake *Crotalus simus* and the South American *Crotalus durissus* complex points to neurotoxicity as an adaptive paedomorphic trend along *Crotalus* Dispersal in South America. *Journal of Proteome Research*, 9(1):528–544.

Casewell, N. R., Wüster, W., Vonk, F. J., Harrison, R. A., and Fry, B. G. (2013). Complex cocktails: the evolutionary novelty of venoms. *Trends in Ecology and Evolution*, 28(4):219–229.

Doan, T. M., Mason, A. J., Castoe, T. A., Sasa, M., and Parkinson, C. L. (2016). A cryptic palm-pitviper species (Squamata: Viperidae: *Bothriechis*) from the Costa Rican highlands, with notes on the variation within *B. nigroviridis*. *Zootaxa*, 4138(2):271–290.

Doley, R., Zhou, X., and Kini, R. M. (2010). Snake venom phospholipase $A_2$ enzymes. *Handbook of venoms and toxins of reptiles*, 1:173–205.

Dowell, N. L., Giorgianni, M. W., Griffin, S., Kassner, V. A., Selegue, J. E., Sanchez, E. E., and Carroll, S. B. (2018). Extremely divergent haplotypes in two toxin gene complexes encode alternative venom types within rattlesnake species. *Current Biology*, 28(7):1016–1026.

Dowell, N. L., Giorgianni, M. W., Kassner, V. A., Selegue, J. E., Sanchez, E. E., and Carroll, S. B. (2016). The deep origin and recent loss of venom toxin genes in rattlesnakes. *Current Biology*, 26(18):2434–2445.

Durban, J., Juárez, P., Angulo, Y., Lomonte, B., Flores-Díaz, M., Alape-Girón, A., Sasa, M., Sanz, L., Gutiérrez, J. M., Dopazo, J., Conesa, A., and Calvete, J. J. (2011). Profiling the venom gland transcriptomes of Costa Rican snakes by 454 pyrosequencing. *BMC genomics*, 12:259.

Durban, J., Sanz, L., Trevisan-Silva, D., Neri-Castro, E., Alagón, A., and Calvete, J. J. (2017). Integrated venomics and venom gland transcriptome analysis of juvenile and adult Mexican Rattlesnakes *Crotalus simus*, *C. tzabcan*, and *C. culminatus* revealed miRNA-modulated ontogenetic shifts. *Journal of Proteome Research*, 16(9):3370–3390.

Emms, D. M. and Kelly, S. (2015). OrthoFinder: solving fundamental biases in whole genome comparisons dramatically improves orthogroup inference accuracy. *Genome Biology*, 16(1):157.

Ferguson, L. C., Maroja, L., and Jiggins, C. D. (2011). Convergent, modular expression of ebony and tan in the mimetic wing patterns of *Heliconius* butterflies. *Development Genes and Evolution*, 221(5-6):297–308.

Fernández, J., Lomonte, B., Sanz, L., Angulo, Y., and Calvete, J. J. (2010). Snake venomics of *Bothriechis nigroviridis* reveals extreme variability among palm pitviper venoms: different evolutionary solutions for the same trophic purpose. *Journal of Proteome Research*, 9:4234–4241.

Fernández, R., Edgecombe, G. D., and Giribet, G. (2016). Exploring phylogenetic relationships within Myriapoda and the effects of matrix composition and occupancy on phylogenomic reconstruction. *Systematic Biology*, 65(5):871–889.

Fry, B. G., Casewell, N. R., Wüster, W., Vidal, N., Young, B., and Jackson, T. N. W. (2012). The structural and functional diversification of the Toxicofera reptile venom system. *Toxicon*, 60(4):434–448.

Glenn, J. and Straight, R. (1978). Mojave rattlesnake *Crotalus scutulatus scutulatus* venom: variation in toxicity with geographical origin. *Toxicon*, 16(1):81–84.

Glenn, J., Straight, R., and Wolt, T. (1994). Regional variation in the presence of canebrake toxin in *Crotalus horridus* venom. *Comparative Biochemistry and Physiology Part C: Pharmacology, Toxicology and Endocrinology*, 107(3):337–346.

Glenn, J. L. and Straight, R. C. (1989). Intergradation of two different venom populations of the Mojave Rattlesnake (*Crotalus scutulatus scutulatus*) in Arizona. *Toxicon*, 27(4):411–418.

Glenn, J. L., Straight, R. C., Wolfe, M. C., and Hardy, D. L. (1983). Geographical variation in *Crotalus scutulatus scutulatus* (Mojave rattlesnake) venom properties. *Toxicon*, 21(1):119–130.

Grabherr, M. G., Haas, B. J., Yassour, M., Levin, J. Z., Thompson, D. A., Amit, I., Adiconis, X., Fan, L., Raychowdhury, R., Zeng, Q., Chen, Z., Mauceli, E., Hacohen, N., Gnirke, A., Rhind, N., di Palma, F., Birren, B. W., Nusbaum, C., Lindblad-Toh, K., Friedman, N., and Regev, A. (2011). Full-length transcriptome assembly from RNA-Seq data without a reference genome. *Nature biotechnology*, 29(7):644–52.

Gutiérrez, J. M. and Lomonte, B. (2013). Phospholipases $A_2$: unveiling the secrets of a functionally versatile group of snake venom toxins. *Toxicon*, 62:27–39.

Hargreaves, A. D., Swain, M. T., Hegarty, M. J., Logan, D. W., and Mulley, J. F. (2014). Restriction and recruitment—gene duplication and the origin and evolution of snake venom toxins. *Genome Biology and Evolution*, 6(8):2088–2095.

Hofmann, E. P., Rautsaw, R. M., Strickland, J. L., Holding, M. L., Hogan, M. P., Mason, A. J., Rokyta, D. R., and Parkinson, C. L. (2018). Comparative venom-gland transcriptomics and venom proteomics of four Sidewinder Rattlesnake (*Crotalus cerastes*) lineages reveal little differential expression despite individual variation. *Scientific Reports*, 8(1):15534.

Holding, M. L., Margres, M. J., Mason, A. J., Parkinson, C. L., and Rokyta, D. R. (2018). Evaluating the performance of de novo assembly methods for venom-gland transcriptomics. *Toxins*, 10(6):249.

Joron, M., Jiggins, C. D., Papanicolaou, A., and McMillan, W. O. (2006). *Heliconius* wing patterns: an evo-devo model for understanding phenotypic diversity. *Heredity*, 97(3):157–167.

Katoh, K. and Standley, D. M. (2013). MAFFT Multiple Sequence Alignment Software Version 7: improvements in performance and usability. *Molecular Biology and Evolution*, 30(4):772–780.

Kearse, M., Moir, R., Wilson, A., Stones-Havas, S., Cheung, M., Sturrock, S., Buxton, S., Cooper, A., Markowitz, S., Duran, C., Thierer, T., Ashton, B., Meintjes, P., and Drummond, A. (2012). Geneious Basic: An integrated and extendable desktop software platform for the organization and analysis of sequence data. *Bioinformatics*, 28(12):1647–1649.

Krueger, F. (2015). Trim Galore!: A wrapper tool around Cutadapt and FastQC to consistently apply quality and adapter trimming to FastQ files.

Lanfear, R., Frandsen, P. B., Wright, A. M., Senfeld, T., and Calcott, B. (2016). PartitionFinder 2: new methods for selecting partitioned models of evolution for molecular and morphological phylogenetic analyses. *Molecular Biology and Evolution*, 34(3):772–773.

Levine, M. and Davidson, E. H. (2005). Gene regulatory networks for development. *Proceedings of the National Academy of Sciences*, 102(14):4936–4942.

Li, B. and Dewey, C. N. (2011). RSEM: accurate transcript quantification from RNA-Seq data with or without a reference genome. *BMC bioinformatics*, 12(1):323.

Li, H. and Durbin, R. (2009). Fast and accurate short read alignment with Burrows-Wheeler transform. *Bioinformatics*, 25(14):1754–1760.

Lomonte, B., Mora-Obando, D., Fernández, J., Sanz, L., Pla, D., María Gutiérrez, J., and Calvete, J. J. (2015). First crotoxin-like phospholipase $A_2$ complex from a New World non-rattlesnake species: Nigroviriditoxin, from the arboreal Neotropical snake *Bothriechis nigroviridis*. *Toxicon*, 93:144–54.

Love, M. I., Huber, W., and Anders, S. (2014). Moderated estimation of fold change and dispersion for RNA-seq data with DESeq2. *Genome Biology*, 15(12):550.

Löytynoja, A. and Goldman, N. (2008). Phylogeny-aware gap placement prevents errors in sequence alignment and evolutionary analysis. *Science*, 320(5883):1632–1635.

Mackessy, S. P. (2008). Venom composition in rattlesnakes: trends and biological significance. In Hayes, W. K., Beaman, K. R., Cardwell, M. D., and Bush, S. P., editors, *The Biology of Rattlesnakes*, pages 495–510. Loma Linda University Press, Loma Linda, CA.

Mackessy, S. P. (2016). *Handbook of Venoms and Toxins of Reptiles*. CRC press, Boca Raton, FL.

Mackessy, S. P., Williams, K., and Ashton, K. G. (2003). Ontogenetic variation in venom composition and diet of *Crotalus oreganus concolor*: a case of venom paedomorphosis? *Copeia*, 2003(4):769–782.

Mapleson, D., Garcia Accinelli, G., Kettleborough, G., Wright, J., and Clavijo, B. J. (2017). Kat: a k-mer analysis toolkit to quality control ngs datasets and genome assemblies. *Bioinformatics*, 33(4):574–576.

Marçais, G. and Kingsford, C. (2011). A fast, lock-free approach for efficient parallel counting of occurrences of k-mers. *Bioinformatics*, 27(6):764–770.

Margres, M. J., Bigelow, A. T., Lemmon, E. M., Lemmon, A. R., and Rokyta, D. R. (2017). Selection to increase expression, not sequence diversity, precedes gene family origin and expansion in rattlesnake venom. *Genetics*, 206(3):1569–1580.

Margres, M. J., Wray, K. P., Seavy, M., McGivern, J. J., Herrera, N. D., and Rokyta, D. R. (2016). Expression differentiation is constrained to low-expression proteins over ecological timescales. *Genetics*, 202(1):273–283.

Mason, A. J., Grazziotin, F. G., Zaher, H., Lemmon, A. R., Moriarty Lemmon, E., and Parkinson, C. L. (2019). Reticulate evolution in nuclear Middle America causes discordance in the phylogeny of palm-pitvipers (Viperidae: *Bothriechis* ). *Journal of Biogeography*, 46(5):833–844.

Oron, U. and Bdolah, A. (1973). Regulation of protein synthesis in the venom gland of viperid snakes. *The Journal of Cell Biology*, 56:177–190.

Palarea-Albaladejo, J. and Martin-Fernandez, J. A. (2015). zCompositions – R package for multivariate imputation of left-censored data under a compositional approach. *Chemometrics and Intelligent Laboratory Systems*, 143:85–96.

Pla, D., Sanz, L., Whiteley, G., Wagstaff, S. C., Harrison, R. A., Casewell, N. R., and Calvete, J. J. (2017). What killed Karl Patterson Schmidt? Combined venom gland transcriptomic, venomic and antivenomic analysis of the South African green tree snake (the boomslang), *Dispholidus typus*. *Biochimica et Biophysica Acta*, 1861(4):814–823.

Reyes-Velasco, J., Card, D. C., Andrew, A. L., Shaney, K. J., Adams, R. H., Schield, D. R., Casewell, N. R., Mackessy, S. P., and Castoe, T. A. (2015). Expression of venom gene homologs in diverse python tissues suggests a new model for the evolution of snake venom. *Molecular Biology and Evolution*, 32(1):173–183.

Rokyta, D. R., Lemmon, A. R., Margres, M. J., and Aronow, K. (2012). The venom-gland transcriptome of the Eastern Diamondback Rattlesnake (*Crotalus adamanteus*). *BMC Genomics*, 13(1):312.

Rokyta, D. R., Margres, M. J., and Calvin, K. (2015). Post-transcriptional mechanisms contribute little to phenotypic variation in snake venoms. *G3 (Bethesda, Md.)*, 5(11):2375–2382.

Rokyta, D. R. and Ward, M. J. (2017). Venom-gland transcriptomics and venom proteomics of the black-back scorpion (*Hadrurus spadix*) reveal detectability challenges and an unexplored realm of animal toxin diversity. *Toxicon*, 128:23–37.

Rokyta, D. R., Wray, K. P., Lemmon, A. R., Lemmon, E. M., and Caudle, S. B. (2011). A high-throughput venom-gland transcriptome for the Eastern Diamondback Rattlesnake (*Crotalus adamanteus*) and evidence for pervasive positive selection across toxin classes. *Toxicon*, 57(5):657–671.

Rokyta, D. R., Wray, K. P., and Margres, M. J. (2013). The genesis of an exceptionally lethal venom in the timber rattlesnake (*Crotalus horridus*) revealed through comparative venom-gland transcriptomics. *BMC genomics*, 14:394.

Ronquist, F., Teslenko, M., Van Der Mark, P., Ayres, D. L., Darling, A., Höhna, S., Larget, B., Liu, L., Suchard, M. a., and Huelsenbeck, J. P. (2012). Mrbayes 3.2: Efficient bayesian phylogenetic inference and model choice across a large model space. *Systematic Biology*, 61(3):539–542.

Rotenberg, D., Bamberger, E., and Kochva, E. (1971). Studies on ribonucleic acid synthesis in the venom glands of *Vipera palaestinae* (ophidia, reptilia). *Biochemical Journal*, 121(4):609–612.

Russo, P. S. T., Ferreira, G. R., Cardozo, L. E., Bürger, M. C., Arias-Carrasco, R., Maruyama, S. R., Hirata, T. D. C., Lima, D. S., Passos, F. M., Fukutani, K. F., Lever, M., Silva, J. S., Maracaja-Coutinho, V., and Nakaya, H. I. (2018). CEMiTool: a Bioconductor package for performing comprehensive modular co-expression analyses. *BMC Bioinformatics*, 19(1):56.

Schield, D. R., Card, D. C., Hales, N. R., Perry, B. W., Pasquesi, G. M., Blackmon, H., Adams, R. H., Corbin, A. B., Smith, C. F., Ramesh, B., Demuth, J. P., Betrán, E., Tollis, M., Meik, J. M., Mackessy, S. P., and Castoe, T. A. (2019). The origins and evolution of chromosomes, dosage compensation, and mechanisms underlying venom regulation in snakes. *Genome research*, 29(4):590–601.

Sonenberg, N. and Hinnebusch, A. G. (2009). Regulation of translation initiation in Eukaryotes: mechanisms and biological targets. *Cell*, 136(4):731–745.

Soto, J. G., Perez, J. C., and Minton, S. A. (1988). Proteolytic, hemorrhagic and hemolytic activities of snake venoms. *Toxicon*, 26(9):875–882.

Strickland, J. L., Mason, A. J., Rokyta, D. R., and Parkinson, C. L. (2018a). Phenotypic variation in Mojave Rattlesnake (*Crotalus scutulatus*) venom is driven by four toxin families. *Toxins*, 10(4):135.

Strickland, J. L., Smith, C. F., Mason, A. J., Schield, D. R., Borja, M., Castañeda-Gaytán, G., Spencer, C. L., Smith, L. L., Trápaga, A., Bouzid, N. M., Campillo-García, G., Flores-Villela, O. A., Antonio-Rangel, D., Mackessy, S. P., Castoe, T. A., Rokyta, D. R., and Parkinson, C. L. (2018b). Evidence for divergent patterns of local selection driving venom variation in Mojave Rattlesnakes (*Crotalus scutulatus*). *Scientific Reports*, 8(1):17622.

Tsai, I.-H., Chen, Y.-H., Wang, Y.-M., Tu, M.-C., and Tu, A. T. (2001). Purification, sequencing, and phylogenetic analyses of novel Lys-49 phospholipases $A_2$ from the venoms of rattlesnakes and other pit vipers. *Archives of Biochemistry and Biophysics*, 394(2):236–244.

Van Belleghem, S. M., Rastas, P., Papanicolaou, A., Martin, S. H., Arias, C. F., Supple, M. A., Hanly, J. J., Mallet, J., Lewis, J. J., Hines, H. M., Ruiz, M., Salazar, C., Linares, M., Moreira, G. R. P., Jiggins, C. D., Counterman, B. A., McMillan, W. O., and Papa, R. (2017). Complex modular architecture around a simple toolkit of wing pattern genes. *Nature Ecology & Evolution*, 1(3):0052.

von Dassow, G. and Munro, E. (1999). Modularity in animal development and evolution: elements of a conceptual framework for EvoDevo. *The Journal of Experimental Zoology*, 285(4):307–325.

Vonk, F. J., Casewell, N. R., Henkel, C. V., Heimberg, A. M., Jansen, H. J., McCleary, R. J. R., Kerkkamp, H. M. E., Vos, R. A., Guerreiro, I., Calvete, J. J., Wüster, W., Woods, A. E., Logan, J. M., Harrison, R. A., Castoe, T. A., de Koning, A. P. J., Pollock, D. D., Yandell, M., Calderon, D., Renjifo, C., Currier, R. B., Salgado, D., Pla, D., Sanz, L., Hyder, A. S., Ribeiro, J. M. C., Arntzen, J. W., van den Thillart, G. E. E. J. M., Boetzer, M., Pirovano, W., Dirks, R. P., Spaink, H. P., Duboule, D., McGlinn, E., Kini, R. M., and Richardson, M. K. (2013). The king cobra genome reveals dynamic gene evolution and adaptation in the snake venom system. *Proceedings of the National Academy of Sciences of the United States of America*, 110(51):20651–6.

Wagner, G. P., Pavlicev, M., and Cheverud, J. M. (2007). The road to modularity. *Nature Reviews Genetics*, 8(12):921–931.

Wong, E. S. and Belov, K. (2012). Venom evolution through gene duplications. *Gene*, 496(1):1–7.

Yang, A. S. (2001). Modularity, evolvability, and adaptive radiations: a comparison of the hemi- and holometabolous insects. *Evolution and Development*, 3(2):59–72.

Yang, Z. (2007). PAML 4: phylogenetic analysis by maximum likelihood. *Molecular Biology and Evolution*, 24(8):1586–1591.

Zhang, J., Kobert, K., Flouri, T., and Stamatakis, A. (2014). PEAR: a fast and accurate Illumina Paired-End reAd mergeR. *Bioinformatics*, 30(5):614–620.

# Chapter 4

# Evolution of gene expression in snake toxin families

## 4.1 Abstract

Complex phenotypes are shaped by phylogenetic inertia and regimes of selection that are affected by their underlying genetic architecture. Despite widespread interest in elucidating how variation arises and is optimized among genes and species, progress has been limited. Snake venoms present a tractable system for comparative analyses because venom toxins arise from a handful of well-characterized venom gene families which can be directly tied to observed phenotypes. Here, we utilized a comparative framework and venom gland transcriptomes from all species of palm-pitvipers to investigate the dynamics of venom gene family evolution and the effects of phylogenetic inertia and lineage-specific selection on toxin gene expression. We inferred time calibrated gene trees for 1352 orthologous groups of transcripts and tested for differences in phylogenetic signal, and variance in expression between toxins and nontoxins. We tested whether higher variance in expression was more associated with gene duplications or speciation events and identified shifts in optimal expression of three toxin gene families: phospholipase $A_2$s ($PLA_2$s), snake venom metalloproteases (SVMPs), and snake venom serine proteases (SVSPs). We found that toxins and nontoxins did not differ in estimates of phylogenetic signal, but that toxins did exhibit significantly higher variance. Higher divergence in expression was associated with speciation events rather than duplication events

indicating that selection acting on species-specific venom phenotypes shapes venom gene expression more then gene-specific regimes of expression. Furthermore, we identified multiple shifts in optimal expression within $PLA_2$s and SVMPs, suggesting that selection acting on specific genes within particular lineages. Variation in snake venom phenotypes is a function of high variation characteristic of toxin genes and lineage-specific shifts in expression optima.

## 4.2 Introduction

A fundamental goal of evolutionary biology is to identify and understand the genetic mechanisms and selective forces that interact to promote phenotypic differentiation. Phenotypes are shaped by selective pressures and phylogenetic inertia which may direct and constrain evolutionary trajectories (Arnold, 1992; Futuyma, 2010). While the definitions of phylogenetic inertia vary (Blomberg and Garland Jr, 2002), here we define it as the influence of a character's ancestral state on its derived condition. The extent and influence of phylogenetic inertia on a derived phenotype depends on many factors, including existing genetic variation, evolutionary and developmental constraints, and the strength and direction of selection (Arnold, 1992; Moczek, 2005; Futuyma, 2010; Losos, 2011). Moreover, phylogenetic inertia also affects, and is affected by, the structure, diversity, and lability of a phenotype's underlying genomic architecture.

Genomic architecture is shaped by a variety of factors such as gene composition, organization, and the evolution of regulatory elements (Hoekstra and Coyne, 2007; Carroll, 2008; Koo; Prasad et al., 2012; Taylor and Ehrenreich, 2015). Of particular importance to genomic architecture are the dynamics of gene family evolution (Nei et al., 1997; Ohno, 2013; Albalat and Cañestro, 2016; Richter et al., 2018; Fernández and Gabaldón, 2020). Gene duplication can create functional redundancy that facilitates neo- or sub-functionalization that increase evolvability and lability (Holland et al., 1994; True and Carroll, 2002; Chang and Duda, 2012). However, gene duplications and losses do not occur uniformly among lineages, resulting in orthologous and paralogous genes which have shared ancestral and derived evolutionary histories, respectively, among lineages (Fernández and Gabaldón, 2020). Based on the assumptions that gene duplications facilitate differentiation, orthologous genes are expected to be more similar to one another than paralogs, particularly with regard to function (Koonin, 2005). This expectation has been formalized as the ortholog conjecture hypothesis (Koonin, 2005). Although, formal tests of the ortholog conjecture hypothesis have

shown mixed evidence for its validity (Nehrt et al., 2011; Altenhoff et al., 2012; Chen and Zhang, 2012; Rogozin et al., 2014; Kryuchkova-Mostacci and Robinson-Rechavi, 2016; Dunn et al., 2018), it remains the null hypothesis for the functional diversification of gene families. Gene duplications can also function in altering expression or permitting greater variation when selectively advantageous (Carroll, 2008; Duncan and Dearden, 2010; Margres et al., 2017). However, selection can act differentially among genes, species, or combinations therein, thus making it difficult to establish the extent to which phylogenetic inertia and selection interact to mediate phenotypic evolution.

Animal venoms present a practical system for investigating how phylogentic inertia interacts with gene family evolution and phenotypic diversification (Whittington et al., 2018; Casewell et al., 2012; Sunagar and Moran, 2015; Haney et al., 2016; Li et al., 2017; Mason et al., 2020). Venoms are complex traits composed of tens to hundreds of secreted toxins collectively used for prey capture and/or defense (Casewell et al., 2013). As secreted proteins, venoms are largely free of developmental and pleiotropic effects that confound mechanistic inference in many traits. In the case of many taxa like snakes, venoms are also highly variable among species (Mackessy, 2008, 2016; Barua and Mikheyev, 2019), providing sufficient phenotypic variation for informative comparisons. Despite their variability in overall composition, most snake venom toxins are derived from a handful of well-described toxin families and individual components can be traced to single genes, facilitating genotype-phenotype mapping (Fry, 2005; Margres et al., 2014; Aird et al., 2015; Margres et al., 2015). Venom gene families evolve rapidly through birth-death processes (Wong and Belov, 2012; Casewell et al., 2013; Hargreaves et al., 2014) and because of venom's role in predator-prey interactions (Daltry et al., 1996; Barlow et al., 2009; Holding et al., 2016) and limited physiological constraint, venom composition is expected to evolve rapidly (Kordis and Gubensek, 2000; Gibbs and Rossiter, 2008; Aird et al., 2015). Although next-generation sequencing techniques have revolutionized our ability to characterize venoms, explicit tests of the evolutionary lability of venom genes and the way selection acts within and among gene and species lineages have been limited.

We sought to identify patterns of gene family and expression evolution affecting venom phenotypes by leveraging genus-wide transcriptomic representation of a highly adapted, venomous snake lineage, the Middle American palm-pitvipers (*Bothriechis*). This genus includes 11 species distributed across Middle America (Campbell and Lamar, 2004; Townsend et al., 2013; Doan et al., 2016). Palm-pitvipers exhibit morphological and behavioral specialization for arboreality including a prehensile tail, laterally compressed body, and strike-and-hold (as opposed to strike-and-release)

feeding behavior (Campbell and Lamar, 2004; Alencar et al., 2017). Despite their shared specializations and presumed similarity in ecological niche, interspecific venom compositions of palm-pitvipers are highly variable (Lomonte et al., 2008; Fernández et al., 2010; Lomonte et al., 2012; Pla et al., 2017; Mason et al., 2020). Palm-pitvipers are also advantageous as a model system for venom evolution because they have a published genome-scale phylogeny (Mason et al., 2019), which provides a phylogenetic context for informative comparisons. High-throughput RNA sequencing techniques like RNAseq offer three advantages for comparative study; first mapping reads to an appropriate reference transcriptome provides estimates of relative expression of toxins, which generally correlates with the venom proteome (Rokyta et al., 2015; Hofmann et al., 2018) (but see (Casewell et al., 2014)). Second, the recovered transcript sequences can be used in evolutionary inference (Rokyta et al., 2013; Hofmann et al., 2018; Barua and Mikheyev, 2019). Third, the wealth of house-keeping proteins recovered can act as a null-distribution to test hypotheses specific to the evolution of venom components (Rokyta et al., 2013; Mason et al., 2020).

Here, we utilized venom gland transcriptomes from all species of palm-pitvipers to investigate the dynamics of venom gene family evolution and the effects of phylogenetic inertia and lineage-specific selection on gene expression. We inferred gene family phylogenies for orthologous groups of transcripts and compared the evolutionary lability and phylogenetic inertia among toxin and nontoxin gene families. Based on our expectation of higher evolutionary lability of toxin genes, we expected greater variation in expression in toxin gene families and lower estimates of phylogenetic inertia, with most of the phylogenetic signal in expression being attributed to variation among species. We further tested whether gene duplications permitted greater variation in toxin expression than did speciation events (i.e., the ortholog conjecture). Finally, to determine whether variation in expression could be attributed to gene-specific and/or lineage-specific effects, we tested for the presence of multiple adaptive optima and identified differential expression regimes in three key toxin families.

## 4.3 Methods

### 4.3.1 Sample Collection

We generated venom gland transcriptomes for 21 individual palm-pitvipers representing each palm-pitviper species. All individuals were wild-caught specimens collected between May 2016

and July 2018 (Table S1). Shortly after capture each individual had venom extracted and was euthanized four days later when transcriptional rate is highest (Rotenberg et al., 1971). Venom glands were removed from each specimen and stored in approximately 2 mL of RNAlater. Carcasses were preserved as museum specimens and deposited in publicly accessible natural history collections (Table S1).

### 4.3.2 Transcriptomics

Venom gland RNA was extracted and prepared for Illumina sequencing following methods described in similar studies (Hofmann et al., 2018; Strickland et al., 2018a). Briefly, total RNA was extracted from right and left venom glands following a standard Trizol protocol. Glands were subsampled and finely diced then placed in 500 microliters of Trizol for 10 minutes then 200 microliters of chloroform was added and the solution was mixed vigorously then vortexed at 12,000g for 20 minutes. The aqueous phase containing total RNA was placed in a clean 1.5 mL tube and 1000 microliters of isopropyl alcohol was added. Solutions were placed in a -20  freezer overnight to facilitate RNA precipitation. The resulting RNA pellets were washed with 80% ethanol and resuspended in RNAase free water. RNA concentration was determined using Qubit 3 broad range RNA assay and RNA quality was checked using an Agilent 2100 Bioanalyer RNA pico assay or Aigilent 2200 Tapestation High Sensitivity RNA ScreenTape assay.

Polyadenylated transcripts were isolated from total RNA using the NEBNext Poly(A) mRNA Magnetic Isolation Module and converted to cDNA and prepared for Illumina sequencing using the NEBNext Ultra RNA Library Prep Kit for Illumina. The concentration of cDNA libraries was determined using a Quibit 3 broad range dsDNA assay and the distribution of fragment sizes was assessed with an Agilent Bioanalyzer 2100 High Sensitivity DNA assay or Aigilent 2200 Tapestation High Sensitivity DNA ScreenTape assay. To verify adapter ligation and the concentration of sequencable cDNA for each library we performed KAPA q-PCR. Libraries were pooled and sequenced on either an Illumina HiSeq 2500 or an Illumina Novaseq 6000 at the Florida State University College of Medicine's Translational Science Laboratory with 150 bp paired-end sequencing.

Following sequencing, sample reads were demultiplexed and quality checked in FastQC v.0.10.1 (Andrews, 2010). Illumina adapters and low-quality base pairs were trimmed using TrimGalore! v.0.4.4 (Krueger, 2015). Finally, to increase total fragment sizes used in transcriptome assembly

we used PEAR v 0.9.6 (Zhang et al., 2014) to merge reads with a 3' overlap greater than 10 bp. Transcripts were *de novo* assembled for each species following the recommendations of Holding et al., 2018. Briefly, three *de novo* transcriptome assemblers, Extender (Rokyta et al., 2012), DNAstar NGen v.15.0, and Trinity v.2.4.0 (Grabherr et al., 2011), were used for each sample and the resulting transcripts were annotated via local blastx search of the curated Swiss-Prot database (downloaded 2 July 2019). Transcripts with a blast match of greater than 90% were clustered against a database of known snake transcripts using cd-hit (Fu et al., 2012) to annotate coding regions with greater than 90% identity with a known sequence. Coding regions of toxin sequences <90% similar to our curated toxin transcripts were annotated manually in Geneious v.10.2.3 (Kearse et al., 2012). Coding regions were extracted and combined from each assembly and duplicate sequences and those with ambiguous base calls were removed from the candidate transcript set. The combined assemblies for each individual were screened for chimeric or mis-assembled transcripts by mapping merged reads to the transcript set with bwa v.0.7.16 (Li and Durbin, 2009) and identifying and removing sequences with highly uneven read distributions across the sequence lengths. The remaining transcripts were clustered at 98% sequence identity using cd-hit to group alleles and recent paralogs. Transcript sets from each individual of each species were then similarly clustered at 98% sequence identity to create a master transcript set for each species that was used for subsequent analyses.

We approximated transcript expression by mapping reads from each individual to the corresponding species assembly using bowtie2 (Langmead and Salzberg, 2012) in RSEM v.1.3.1 (Li and Dewey, 2011). Transcript expression in transcripts per million reads (TPM) were centered log-ratio (CLR) transformed prior to comparisons to free these data from a constant sum constraint that would otherwise create statistical non-independence.

### 4.3.3 Ortholog Identification & Gene Tree Reconciliation

We identified orthologous groups of transcripts among *Bothriechis* species using OrthoFinder v.2.2.7 (Emms and Kelly, 2015, 2019) with a less conservative MCL inflation parameter of 1.2 because preliminary analyses indicated a tendency to segregate some toxin transcripts into orthogroups inconsistent with amino-acid or nucleotide based gene family phylogenies. To assess the evolution of expression within orthogroups, we first inferred phylogenies for each orthogroup based on nucleotide sequences, which are expected to provide greater resolution at shallow nodes than the correspond-

ing amino acid sequences (Townsend et al., 2008). For each orthogroup, nucleotide sequences were aligned with PRANK v.170 (Löytynoja and Goldman, 2008) specifying a codon alignment. Phylogenies were inferred for each alignment with IQ-TREE v.1.6.12 (Nguyen et al., 2015). Alignments were partitioned by codon position and the optimal partitioning scheme and model were inferred by ModelFinder (Kalyaanamoorthy et al., 2017). Nodal support was assessed with 1000 ultrafast bootstraps for each orthogroup.

To identify and annotate lineage divergences that were the result of speciation versus duplication events, we reconciled orthogroup phylogenies with the palm-pitviper species tree of Mason et al., (2019) using Generax v.1.1.0 (Morel et al., 2020) under a gene duplication and gene loss (DL) model which infers a reconciled genetree based on a maximum likelihood optimization of gene duplication and loss parameters. Orthogroup phylogenies inferred by IQ-TREE were used as the starting tree and for orthogroups with incomplete species representation, species were pruned from the dated species tree using the python ete3 library.

### 4.3.4 Macroevolutionary Comparisons

We followed the approach of Dunn et al., 2018, to place transcriptomic comparisons in a phylogenetic context. Briefly, reconciled genetrees were read into R with Treeio (Wang et al., 2019) and nodes were labelled as speciation or duplication events based on Generax annotations. Expression data and $\omega$ estimates from codeml were attached to their respective gene family trees. We filtered trees with <9 species represented. We then time calibrated gene family phylogenies with the 'chronos()' function in ape (Paradis et al., 2004) using node ages of the species tree as corresponding calibration points in the gene family tree. We excluded the ancestor of *B. aurifer* + *B. rowleyi* as a calibration point because of the generally low support for this node in previous phylogenetic studies (Mason et al., 2019). Of the successfully calibrated trees, we further filtered trees based on divergence estimates, excluding trees with divergence events >90 mya as likely mis-clustered orthogroups.

We fit Brownian motion (BM) and Ornstein-Uhlenbeck (OU) models of expression evolution to each calibrated gene family tree using the fitContinuous function in geiger (Harmon et al., 2008) and calculated phylogenetic independent contrasts (PIC's) under a BM model.

We tested whether transcript expression evolves more rapidly in toxins than nontoxins by

testing whether toxins had statistically higher rates of $\sigma^2$ estimated under BM than nontoxins with a Wilcoxon signed rank test in R. Similarly, we tested support for the ortholog conjecture hypothesis with regard to expression evolution within toxin and nontoxin transcripts with two Wilcoxon signed rank tests for differences in PICs of CLR transformed TPM values between nodes arising from speciation and duplication events.

We tested whether expression evolved differentially among genes/species with a toxin family using the Bayesian reversible-jump model of multiple optima using the R package bayou (Uyeda and Harmon, 2014). We focused on three toxin families, $PLA_2$s, SVMPs, and SVSPs, which were the three largest gene families (i.e., had the most terminals) and have previously been identified as key families in the diversification of venom phenotypes (Strickland et al., 2018a; Barua and Mikheyev, 2019). We fit multi-optimal models of expression evolution to each family with bayou's RJMCMC algorithm using uninformative, default priors and allowing a measurement standard error of 0.1. RJMCMC chains were run for 10,000,000 generations and checked for convergence in R.

## 4.4 Results

### 4.4.1 Transcriptome Recovery

We generated transcriptomes from 21 wild-caught palm-pitviper specimens representing all recognized palm-pitviper species (Table S1). Two specimens were used to represent each species, except for *Bothriechis bicolor* which we were only able to represent with one specimen. In total, 1812–2932 transcripts were recovered per species, with 43–56 toxins recovered. Orthology assessment with Orthofinder2 identified 2989 orthologous groups of transcripts, of which 1185 had all 11 species represented and 1752 had >8 species represented. Most toxin families were placed in a single orthogroup which reflected their shared homology from ancestral nontoxin genes. However, two families, C-type lectins (CTLs) and vascular endothelial growth factor (VEGF's), were clustered into multiple orthogroups.

### 4.4.2 Toxin Expression

Toxin family expression was highly variable across palm-pitviper species though was broadly consistent with patterns of toxin expression seen in other pitviper groups (Fig. 4.4.1). Phospholipase

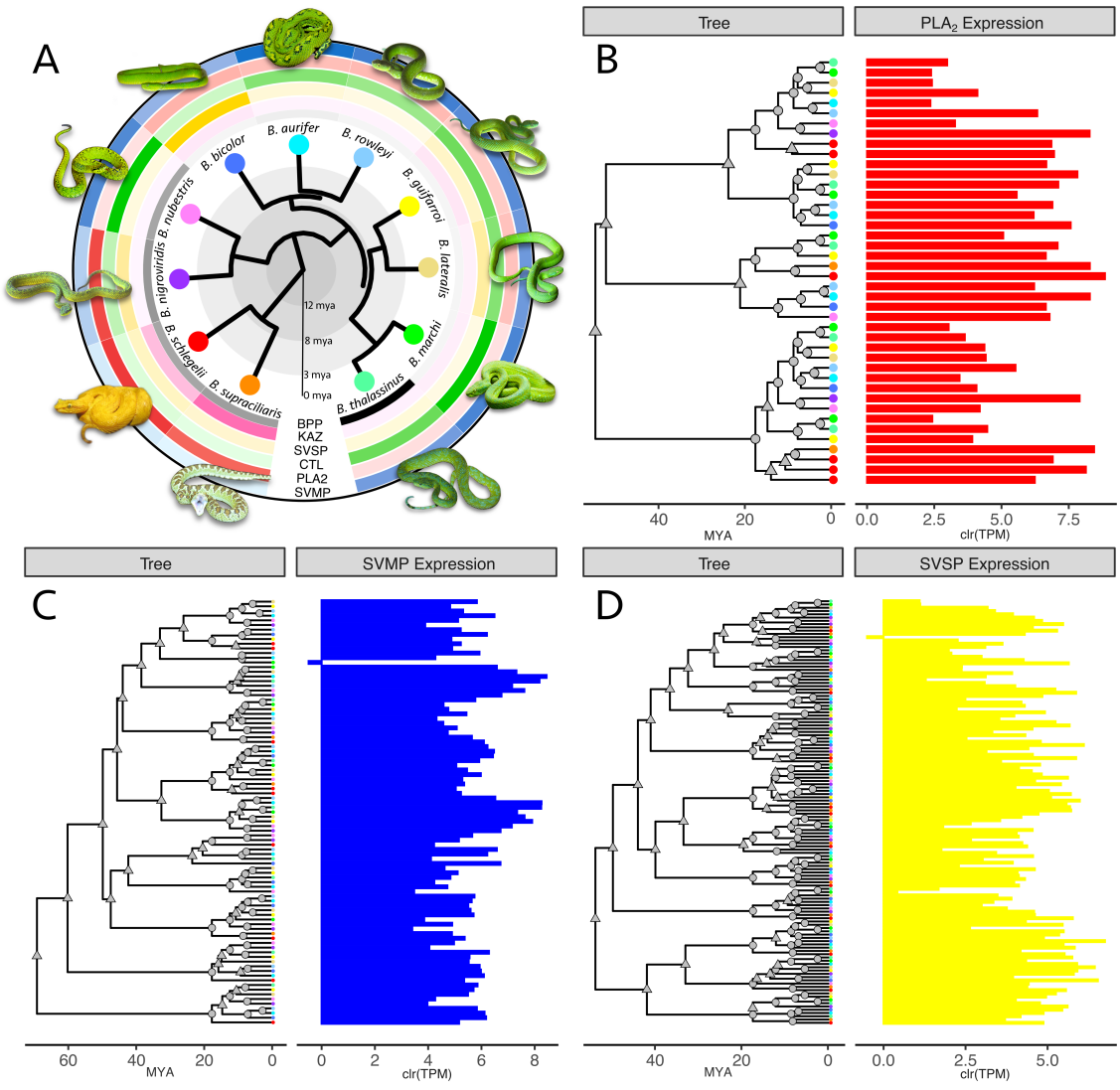


Figure 4.4.1: A) Toxin family expression for each species of palm-pitviper. Gene specific toxin expression of $PLA_2$s (B), SVMPs (C), and SVSPs (D) in centered log-ratio transformed TPM (negative values indicate expression below the geometric mean of transcript expression). Terminal colors correspond to tip labels in A. Node shapes indicate whether divergence was the result of a gene duplication (triangle) or speciation (circle) event. Variation in expression was apparent among and within toxin families.

$A_2$s ($PLA_2$s), snake venom metalloproteinases (SVMPs), snake venom serine proteinases (SVSPs), and CTLs accounted for large proportions of toxin expression for several species. In particular, emphasis on expression of SVMPs and CTLs was particularly common (e.g., *B. nubestris*, *B.aurifer*, *B. rowleyi*, *B. guifarroi. B. lateralis*, *B. marchi*, and *B. thalassinus*). In contrast, *B. nigroviridis*, *B. schlegelii*, and *B. supraciliaris* exhibited relatively higher expression of $PLA_2$s. In the case of *B. nigroviridis*, this pattern reflect the abundance of the two components of nigroviriditoxin, a heterodimeric neurotoxic $PLA_2$ complex. In *B. schlegelii* and *B. supraciliaris*, the high proportion of expression was achieved through expression of two myotoxic $PLA_2$s previously identified in the venom of *B. schlegelii*.

### 4.4.3 Phylogenetic Patterns in Toxins & Nontoxins

We utilized a comparative phylogenetics approach based on methods used by Dunn et al. (2018) to examine characteristics of expression evolution among toxin gene families compared to their nontoxin counterparts. We successfully calibrated 1352 gene family trees against the palm-pitviper species tree, each of which included gene representatives from at least 9 palm-pitviper species (>72%). We fit Brownian motion models of evolution to each tree to estimate phylogenetic signal (Blomberg's K and Pagel's $\lambda$) and estimates of expression variance ($\sigma^2$). Our use of gene trees rather than a species tree means that these metrics do not necessarily reflect phylogenetic signal of the species tree, but rather how much variance can be attributed to gene and species effects. In orthogroups with duplications, where the majority of terminal edges in the data set descended from speciation events, low support for phylogenetic signal (i.e., low/non-significant values of $\lambda$ and K) would suggest the majority of variation in expression can be attributed to species-specific effects. Toxins varied substantially in estimates and significance of K and $\lambda$ (Table 4.4.1).

We found no significant difference in phylogenetic signal between toxins and nontoxins based on K ($p = 0.15$, Fig. 4.4.2A) and while we initially found a significantly higher estimate of $\lambda$ in toxins ($p = 0.02$, Fig. 4.4.2B), this was largely attributed to a large proportion of nontoxin transcripts with extremely low estimates of $\lambda$. Removing these transcripts resulted in no significant differences being detected between toxins and nontoxins ($p = 1$, Fig. 4.4.2C).

Similar to estimates of lambda and K, $\sigma^2$ was highly variable across toxin families (Fig. 4.4.3). However, toxin families were determined to have significantly higher estimates of $\sigma^2$ compared

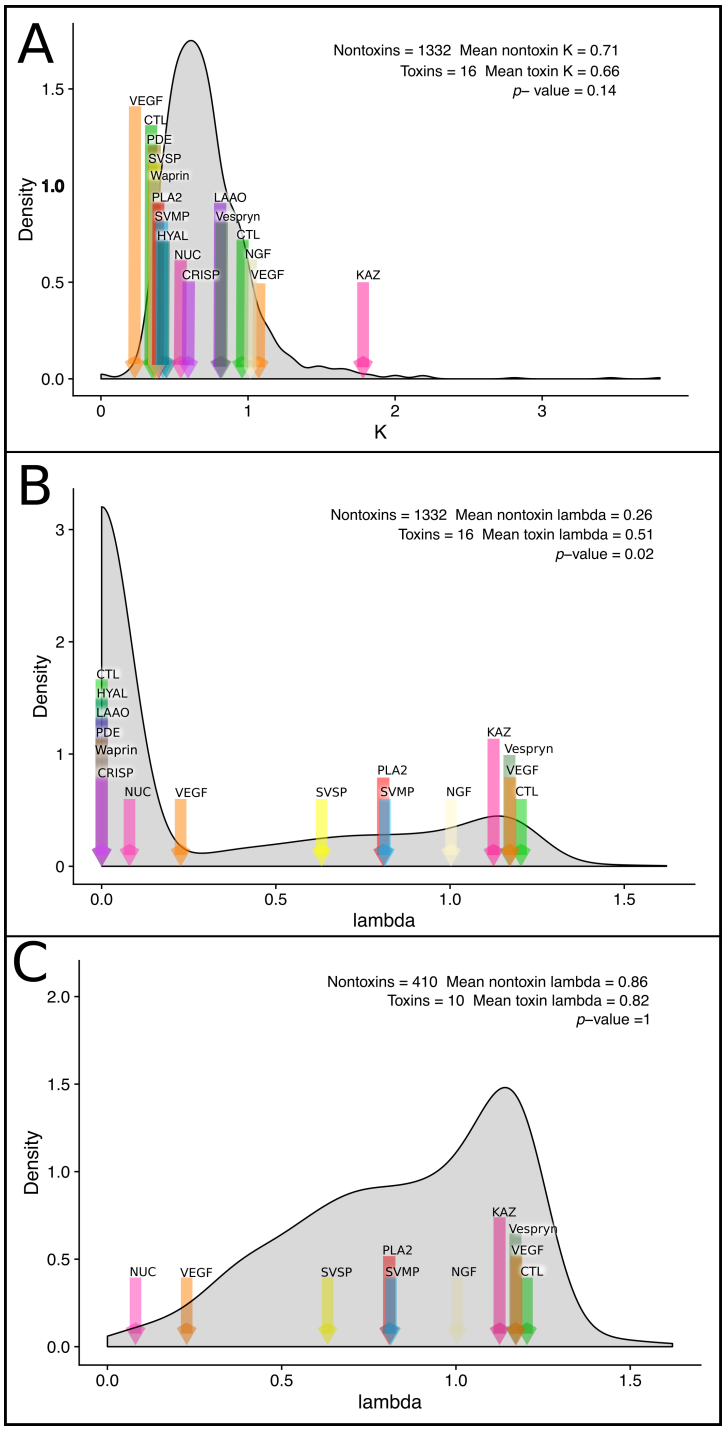


Figure 4.4.2: Estimates of phylogenetic signal for toxins shown against a nontoxin null distribution. Phylogenetic signal was not found to be significantly different between toxins and nontoxins based on Blomberg's K (A). Toxins were found to have significantly higher estimates of Pagel's $\lambda$ (B), but this was largely driven by a high proportion of nontoxins with very small estimates of Pagel's $\lambda$. Removing trees with estimates of Pagel's $\lambda$ <0.0001 resulted in no significant differences in estimates of Pagel's $\lambda$ between toxins and nontoxins (C).

| Orthogroup | Toxin family | K | $p$-value | $\lambda$ | $p$-value |
|---|---|---|---|---|---|
| OG0000000 | SVSP | 0.37 | 0.001 | 0.63 | <0.001 |
| OG0000001 | SVMP | 0.42 | 0.001 | 0.81 | <0.001 |
| OG0000009 | PLA2 | 0.39 | 0.001 | 0.81 | 0.001 |
| OG0000012 | CTL | 0.35 | 0.042 | 0.00 | 1.000 |
| OG0000021 | VEGF | 0.23 | 0.412 | 0.23 | 0.107 |
| OG0000186 | CTL | 0.96 | 0.056 | 1.20 | 0.070 |
| OG0000204 | KAZ | 1.78 | 0.001 | 1.12 | 0.001 |
| OG0000249 | VEGF | 1.07 | 0.088 | 1.17 | 0.065 |
| OG0000618 | HYAL | 0.43 | 0.846 | 0.00 | 1.000 |
| OG0000651 | LAAO | 0.81 | 0.268 | 0.00 | 1.000 |
| OG0000724 | NGF | 1.02 | 0.033 | 1.00 | 0.186 |
| OG0000733 | NUC | 0.54 | 0.586 | 0.08 | 0.926 |
| OG0000761 | PDE | 0.37 | 0.938 | 0.00 | 1.000 |
| OG0001172 | Waprin | 0.38 | 0.956 | 0.00 | 1.000 |
| OG0001333 | CRISP | 0.59 | 0.480 | 0.00 | 1.000 |
| OG0001592 | Vespryn | 0.82 | 0.142 | 1.17 | 0.310 |

Table 4.4.1: Estimates of Blomberg's K and Pagel's $\lambda$ for calibrated toxin trees with $p$-values testing the null hypothesis of no phylogenetic signal.

to nontoxin families ($p$ <0.001). While overall variation in expression was higher for toxins, there was no evidence for higher variation occurring as a result of duplications rather than speciation events (i.e., the ortholog conjecture) in toxins ($p$-value = 0.99) or nontoxins ($p$-value = 1, Fig. 4.4.4). This pattern remained for the largest toxin families despite the presumed opportunity for diversification in expression afforded by high duplication rates (Fig. 4.4.4).

### 4.4.4 Expression Regimes in Toxin Families

We used the multiple optima Reversible Jump Markov Chain Monte Carlo (RJMCMC) algorithm of the R package bayou to infer differential regimes in expression in three toxin families: $PLA_2$s, SVMPs, and SVSPs. At least one shift in expression optima was inferred for each family, and multiple shifts were detected in $PLA_2$s and SVMPs (Fig. 4.4.5). Of the five shifts detected in $PLA_2$s, two corresponded to decreased expression of $PLA_2$s homologous with the two subunits of nigroviriditoxin in the "montane" palm-pitvipers (*B. nigroviridis*, *B. nubestris*, *B. lateralis*, *B. guifarroi*, *B. marchi*, *B. thalassinus*, *B. aurifer*, *B. bicolor*, and *B. rowleyi*). Two additional shifts led to the dramatic increase in expression of nigroviriditoxin subunits observed in *B. nigroviridis*. Similarly, a third led to moderate expression of a nigroviriditoxin-like subunit in *B. rowleyi*. Three

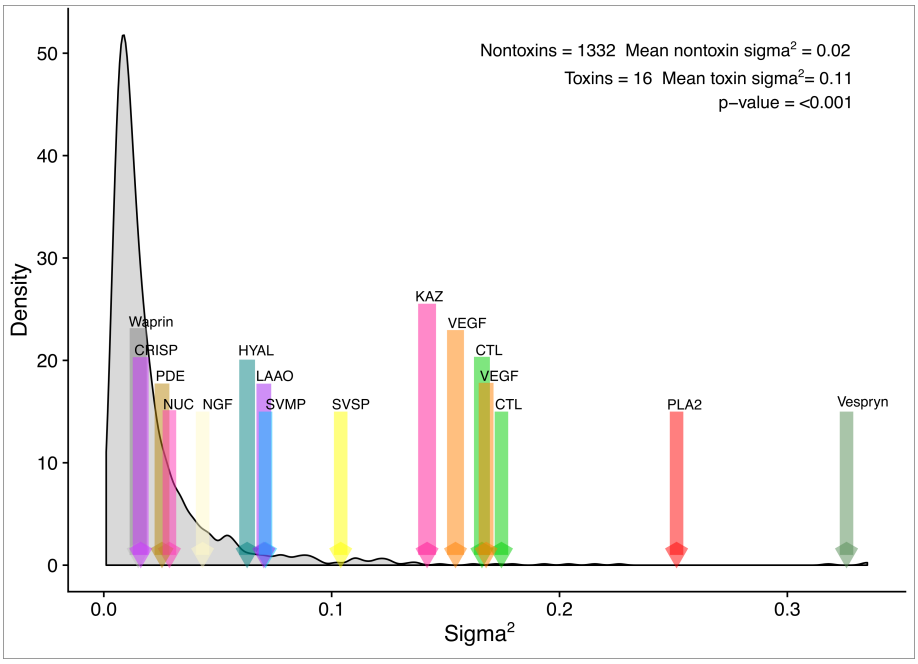


Figure 4.4.3: Distribution of sigma estimates under a Brownian motion model for nontoxins with estimates of sigma for toxins shown as colored arrows. Estimates of sigma were significantly higher for toxins than nontoxins.

rate shifts were inferred for SVMPs. As in $PLA_2$s, two shifts in expression optima were identified in homologous clades of SVMPs transcripts in the "montane" palm-pitvipers. However, in SVMPs these shifts led to increased expression. Only one rate shift was inferred for SVSPs and it was comparatively less supported than shifts in $PLA_2$s and SVMPs (posterior probability of $<0.35$ compared to $>0.7$ for $PLA_2$ and SVMP shifts).

## 4.5 Discussion

We used a comparative phylogenetic context to examine how toxin expression evolves among toxin gene families to produce diverse venom phenotypes. We showed that patterns of expression are the result of gene and lineage specific patterns of expression which contribute to high evolutionary lability of venoms. The contrasting patterns of selection regimes observed in SVSPs versus PLA2s and SVMPs, as well as the broad variation in estimated rate parameters among toxin families demonstrate that toxin families experience differential selection pressures that may act uniformly or differentially across genes and species. Moreover, shifts in expression optima observed in $PLA_2$s

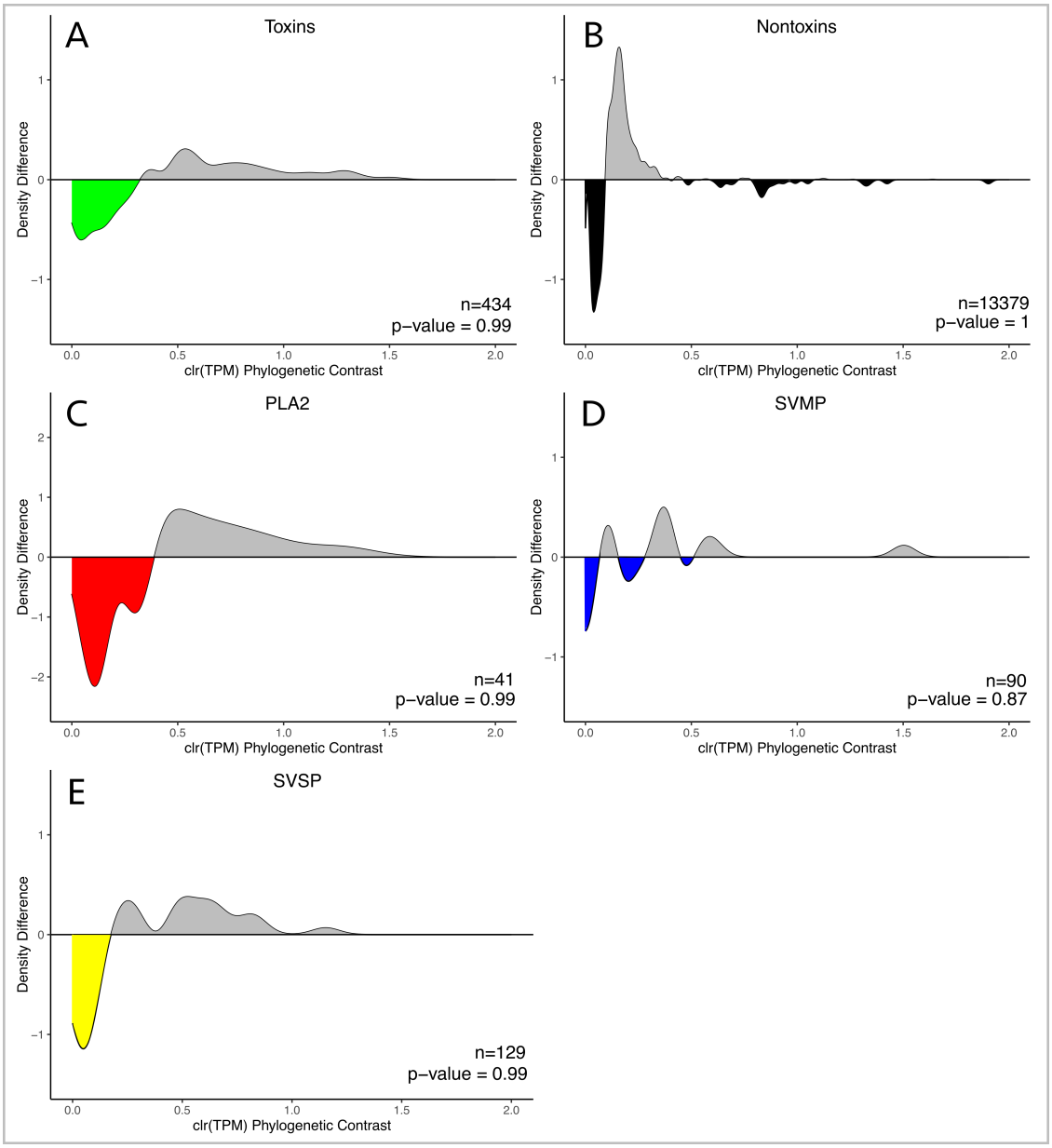


Figure 4.4.4: Differences in the density of duplication events (colors) and speciation events (grey) for toxins (A), nontoxins (B), and three major snake toxin families: $PLA_2$s (C), SVMPs (D), and SVSPs (E). Under the ortholog conjecture, the density of duplication events is expected to be higher as phylogentic independent contrast values increase. We found no support for the ortholog conjecture in expression of toxins, nontoxins, or major toxin families.

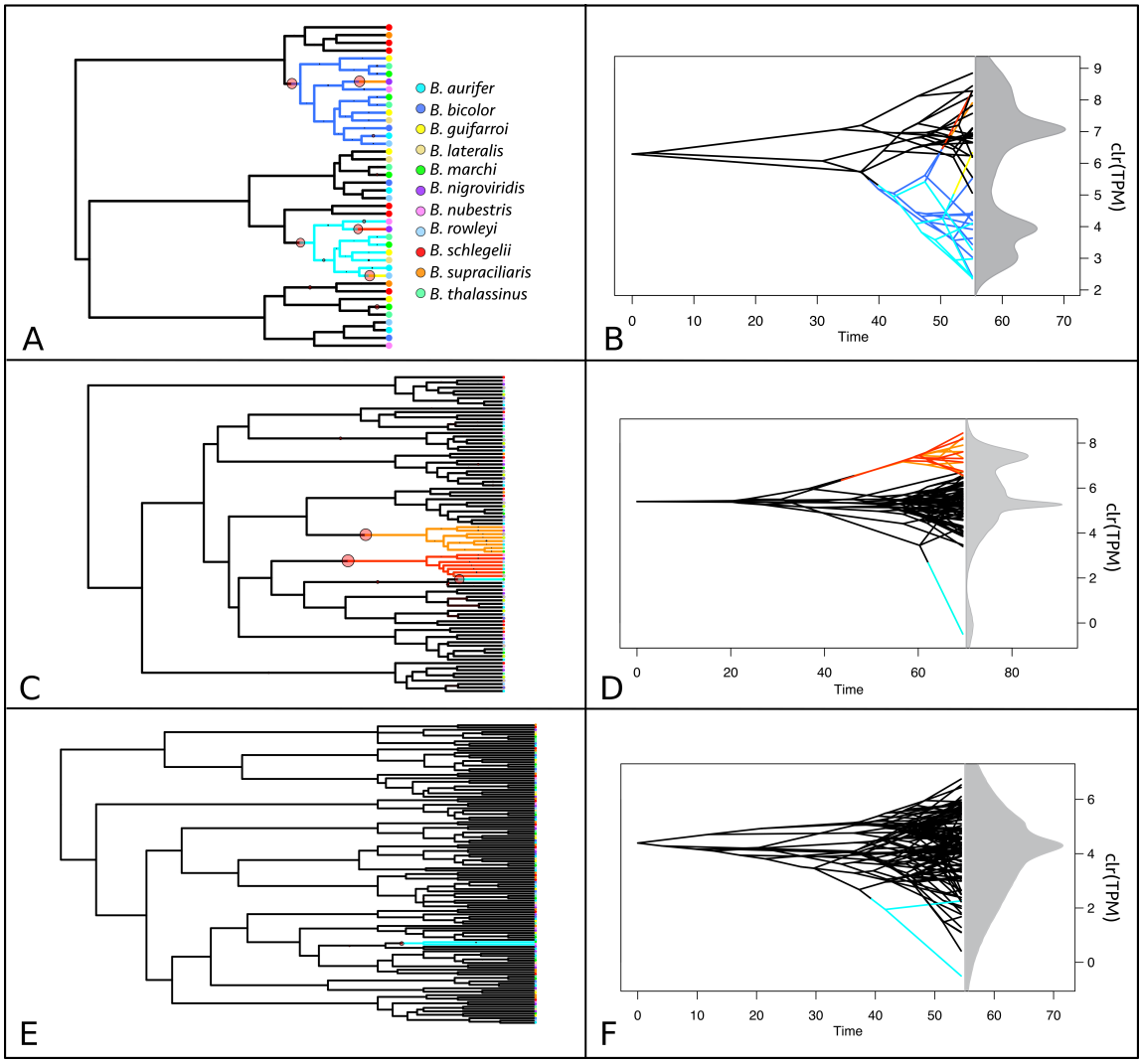


Figure 4.4.5: Gene family phylogenies (A, C, E) and density-phenograms (B, D, F) displaying evolutionary regimes and phenotypic variation identified with bayou. Rows correspond to the three toxin families investigated: $PLA_2$s (A, B), SVMPs (C,D), and SVSPs (E, F). Tip colors indicate transcript species and correspond to labels in (A). Lineage colors denote unique evolutionary regimes and correspond between phylogenies and phenograms. Red circles on phylogenies denote identified rate shifts with circle size corresponding to posterior probability of a shift occurring. Grey distributions to the right of phenograms show density of phenotypes.

and SVMPs suggest that strong gene + lineage effects have a role in shaping venom compositions. Thus, our findings provide empirical evidence that while venom composition can vary widely among species, much of the putatively 'adaptive' variation may be due to the inherent variability in venom gene expression with relatively few adaptive shifts in expression.

### 4.5.1 Adaptive Shifts in Toxin Expression

We identified shifts in expression for three diverse and highly expressed toxin families, but each family varied in the number of optima and terminals that were effected (Fig. 4.4.5). Multiple regime shifts were detected in $PLA_2$s and SVMPs, including clade-specific shifts. In contrast, only one rate shift was identified in SVSPs and with a lower posterior probability than any rate shift identified in $PLA_2$s and SVMPs. The differences in the patterns of recovered rate shifts indicate selection acts differentially among gene families and with clade-specific effects.

Notably, two of the rate shifts identified in PLA2s and SVMPs occurred in effectively the same clade of species – the montane palm-pitvipers – which suggests a shift to a specific phenotypic optima in their common ancestor that has been broadly retained (Fig. 4.4.5). The observed pattern of increased SVMP expression and decreased $PLA_2$ expression is consistent with a venom phenotype dichotomy observed in other pitvipers. For example, many rattlesnake venoms are characterized by having venoms with either a high proportion of SVMPs (Type I/Type B) or a high proportion of $PLA_2$s (Type II/Type A) (Soto et al., 1988; Mackessy, 2008), particularly $PLA_2$s making up the neurotoxic $PLA_2$ complex identified as crotoxin, mojave toxin, canebrake toxin, or sistruxin (Doley et al., 2010; Gutiérrez and Lomonte, 2013). The expression regime identified in montane palm-pitvipers suggests a shift to the Type I/Type B venom phenotype, especially given that the two $PLA_2$s clades identified as decreasing expression optima are homologous to nigroviriditoxin which functions similarly to crotoxin (Lomonte et al., 2015). The shifts in increased $PLA_2$ expression in *B. nigroviridis* are consistent with its unique shift to a Type II/Type A venom phenotype (Fernández et al., 2010). Moreover, the multiple regime shifts observed in the montane *Bothriechis* and their consistency with other venom phenotypes suggests coordinated changes in expression among these toxins.

Recently, the incorporation of high resolution sequence and proteomic data have provided evidence that venoms evolve as integrated systems and several mechanisms have been proposed

that would facilitate coordinated evolution of expression (Aird et al., 2015). For example, systems analysis of transcriptome data suggest that venoms operate as modular systems wherein groups of toxins are affected by common regulatory elements like transcription factors (Mason et al., 2020). Variation in one or a few local transcription factors that affect several loci could result in rapid and coordinated evolution as seen in our analyses. Alternatively, microRNAs that simultaneously affect multiple toxin transcripts have been suggested as an alternative form of regulation (Durban et al., 2017). Observed shifts in expression optima could also be associated with other sources of variation such as ontogenetic shift that have been documented in the *Bothriechis* and in Type I/Type II venom dichotomy (Pla et al., 2017; Mackessy et al., 2003; Calvete et al., 2010). As such, empirical tests of whether ontogenetic variation is broadly observed in palm-pitvipers and whether toxins involved in ontogenetic shifts are the same as those experiencing shifts in expression regime would be highly beneficial.

### 4.5.2 Characteristics of Toxin Family Evolution

We examined differences in phylogenetic signal and variation among toxins and nontoxins to identify characteristics promoting the diversification of venoms. Toxins and nontoxins showed little difference in phylogenetic signal (Fig. 4.4.2). Because toxins are presumably more labile and should respond rapidly to local adaptation we expected them to exhibit little phylogenetic signal and generally lower signal than nontoxins that we expect to be constrained by cellular processes and house-keeping functions. Toxins and nontoxins were highly variable in phylogenetic signal, including a large number of orthogroups ( 70%) with estimates of $\lambda$ near zero (<0.0001) (Fig. 4.4.2). In contrast, there was no difference in phylogenetic signal in Blomberg's K or lambda once extremely small estimates had been removed. In the case of large gene families where most duplications took place prior to speciation events, detecting significant phylogenetic signal indicates that phylogenetic inertia can be attributed to gene-specific effects in addition to any species effects.

Variation among toxin genes could also not be attributed primarily to gene specific effects. Had this been the case, we expected to find evidence that higher variance in expression was associated with gene duplications (i.e., the ortholog conjecture). Instead, we found that large variation in expression more often occurred following speciation events than following duplications for toxins and nontoxins (Fig. 4.4.4). However, although toxins did not appear to have more variance attributed

to duplication effects, they were substantially more variable than nontoxins (Fig. 4.4.3). This contrasting pattern suggests that toxins are not uniformly more responsive to selection, but are generally more variable; a finding which is consistent with previous work examining selection within other snake lineages (Rautsaw et al., 2019). Taken together, these findings provide evidence for an intuitive model of expression evolution in toxin genes; gene-specific expression regimes are heritable and establish initial expression that is detectable as phylogenetic inertia. However, toxins expression remains labile and thus, high variation occurs among species, though the extent to which variation among individual species is actually adaptive remains unclear.

### 4.5.3 The Utility of Comparative Approaches

As diverse functional genomic datasets become more common, innovative approaches for comparative analyses are needed to draw informative conclusions. Genome scale data introduce a number of challenges to traditional analyses (Dunn et al., 2013), especially when resources like reliable references are limited, as is the case here. Our approach, based on that of Dunn et al., 2018, offered a number of advantages that facilitated informative comparisons. First, this approach explicitly incorporates phylogenetic information, the lack of which can result in incorrect or misleading conclusions (Dunn et al., 2018). Second, our approach can utilize the wide body of literature and methodologies developed for comparative phylogenetic analyses, although interpretations must be considered carefully. For example, although we had limited intraspecific (i.e., replicates) sampling, there are several approaches that can accommodate replication and utilize estimates of intraspecific variance for robust inference (Goolsby and Harmon, 2015; Goolsby et al., 2017). Third, although we identified and incorporated duplication information for explicit hypothesis tests, a gene tree based approach is free of assumptions based on orthology and paralogy. Despite recent advancements in the ability to identify orthologs (Kuzniar et al., 2008; Emms and Kelly, 2019), determining orthology and paralogy remains challenging, especially for systems experiencing high gene turnover like venoms and transcriptome data where true orthologs may be absent due to gene silencing. Improving methods for determining orthology in these cases would be a promising avenue for future development, but until that time, methods relying on as few assumptions as possible should be preferred. While imperfect, our gene-tree based approach nonetheless provided an effective means of evolutionary inference with demonstrated utility for identifying adaptive regimes and characteristics

affecting phenotypic evolution.

## 4.6 Conclusions

Snake venoms are complex phenotypes that exhibit broad interspecific diversity, though many of the mechanisms underlying differentiation remain unclear. Through a gene tree based comparative approach, we have shown that toxin expression is mediated by selection acting on genes within specific clades and the inherent variability of toxin genes. As genomic resources become increasingly available for different species and novel analytical approaches are developed, our ability to identify the proximate causes of lineage specific selection and the molecular mechanisms underlying diversification will continue to improve. The approaches utilized here represent our contributions to analyses of venom diversification and complex phenotypes more broadly. Although we implement our comparison in the limited context of a single pitviper group, we demonstrate the power of comparative approaches with genomic data to elucidate evolutionary processes affecting phenotypic diversification.

## 4.7 Acknowledgments

We would like to thank Fabian Bonilla, the Sandi Harmon and Chacón families, Alex Robertson, Josiah H. Townsend, Erich Hofmann, Emmanuel O. Murillo, Jocelyn A. Castro, Christopher Grünwald, Jason Jones, Ricardo Ramírez Chaparro, and Héctor Franz for assistance with collecting specimens used in this work. Funding was provided by the National Science Foundation grants DUE 1161228, DEB 1638879, and DEB 1822417 to C.L.P. and the Southwestern Association of Naturalists McCarley Research Grant, the Theodore Roosevelt Memorial Fund through the American Museum of Natural History, and The Explorers Club Exploration Fund and Mamont Scholars program to A.J.M. We thank the University of Central Florida and Clemson University Animal Care and Use Committees for reviewing and approving animal-based protocols (16-17W: University of Central Florida and 2017-067: Clemson University). Parallel computing resources were provided by the Clemson Palmetto High-Performance Computing Cluster and supplemented with computing resources from the Clemson University Bioinformatics and Genomics Facility.

# References


Albalat, R. and Cañestro, C. (2016). Evolution by gene loss. *Nature Reviews Genetics*, 17(7):379–391.

Alencar, L. R. V., Martins, M., Burin, G., and Quental, T. B. (2017). Arboreality constrains morphological evolution but not species diversification in vipers. *Proceedings of the Royal Society B: Biological Sciences*, 284(1869):20171775.

Altenhoff, A. M., Studer, R. A., Robinson-Rechavi, M., and Dessimoz, C. (2012). Resolving the ortholog conjecture: Orthologs tend to be weakly, but significantly, more similar in function than paralogs. *PLoS Computational Biology*, 8(5).

Arnold, S. J. (1992). Constraints on phenotypic evolution. *American Society of Naturalists*, 140:S85–S107.

Blomberg, S. P. and Garland Jr, T. (2002). Tempo and mode in evolution: phylogenetic inertia, adaptation and comparative methods. *Journal of Evolutionary Biology*, 15(6):899–910.

Carroll, S. B. (2008). Evo-Devo and an Expanding Evolutionary Synthesis: A Genetic Theory of Morphological Evolution. *Cell*, 134(1):25–36.

Casewell, N. R., Huttley, G. A., and Wüster, W. (2012). Dynamic evolution of venom proteins in squamate reptiles. *Nature Communications*, 3(1066):1–10.

Casewell, N. R., Wagstaff, S. C., Wüster, W., Cook, D. a. N., Bolton, F. M. S., King, S. I., Pla, D., Sanz, L., Calvete, J. J., and Harrison, R. a. (2014). Medically important differences in snake venom composition are dictated by distinct postgenomic mechanisms. *Proceedings of the National Academy of Sciences of the United States of America*, 111(25):9205–10.

Chang, D. and Duda, T. F. (2012). Extensive and Continuous Duplication Facilitates Rapid Evolution and Diversification of Gene Families. *Molecular Biology and Evolution*, 29(8):2019–2029.

Chen, X. and Zhang, J. (2012). The Ortholog Conjecture Is Untestable by the Current Gene Ontology but Is Supported by RNA Sequencing Data. *PLoS Computational Biology*, 8(11).

Duncan, E. J. and Dearden, P. K. (2010). Evolution of a genomic regulatory domain: the role of gene co-option and gene duplication in the Enhancer of split complex. *Genome Research*, 20(7):917–28.

Dunn, C. W., Luo, X., and Wu, Z. (2013). Phylogenetic analysis of gene expression. *Integrative and Comparative Biology*, 53(5):847–856.

Dunn, C. W., Zapata, F., Munro, C., Siebert, S., and Hejnol, A. (2018). Pairwise comparisons across species are problematic when analyzing functional genomic data. *Proceedings of the National Academy of Sciences of the United States of America*, 115(3):E409–E417.

Emms, D. M. and Kelly, S. (2019). Orthofinder: phylogenetic orthology inference for comparative genomics. *Genome biology*, 20(1):1–14.

Fernández, R. and Gabaldón, T. (2020). Gene gain and loss across the metazoan tree of life. *Nature Ecology & Evolution*, pages 1–10.

Fry, B. G. (2005). From genome to "venome": molecular origin and evolution of the snake venom proteome inferred from phylogenetic analysis of toxin sequences and related body proteins. *Genome research*, 15(3):403–20.

Fu, L., Niu, B., Zhu, Z., Wu, S., and Li, W. (2012). CD-HIT: accelerated for clustering the next-generation sequencing data. *Bioinformatics*, 28(23):3150–3152.

Futuyma, D. J. (2010). Evolutionary constraint and ecological consequences. *Evolution: International Journal of Organic Evolution*, 64(7):1865–1884.

Gibbs, H. L. and Rossiter, W. (2008). Rapid Evolution by Positive Selection and Gene Gain and Loss: $PLA_2$ Venom Genes in Closely Related *Sistrurus* Rattlesnakes with Divergent Diets. *Journal of Molecular Evolution*, 66(2):151–166.

Goolsby, E. W., Bruggeman, J., and Ané, C. (2017). Rphylopars: fast multivariate phylogenetic comparative methods for missing data and within-species variation. *Methods in Ecology and Evolution*, 8(1):22–27.

Goolsby, E. W. and Harmon, L. (2015). Phylogenetic Comparative Methods for Evaluating the Evolutionary History of Function-Valued Traits. *Systematic Biology*, 64(4):568–578.

Haney, R. A., Clarke, T. H., Gadgil, R., Fitzpatrick, R., Hayashi, C. Y., Ayoub, N. A., and Garb, J. E. (2016). Effects of Gene Duplication, Positive Selection, and Shifts in Gene Expression on the Evolution of the Venom Gland Transcriptome in Widow Spiders. *Genome Biology and Evolution*, 8(1):228–242.

Harmon, L. J., Weir, J. T., Brock, C. D., Glor, R. E., and Challenger, W. (2008). GEIGER: investigating evolutionary radiations. *Bioinformatics*, 24(1):129–131.

Hoekstra, H. E. and Coyne, J. A. (2007). The locus of evolution: Evo devo and the genetics of adaptation. *Evolution*, 61(5):995–1016.

Holding, M. L., Biardi, J. E., and Gibbs, H. L. (2016). Coevolution of venom function and venom resistance in a rattlesnake predator and its squirrel prey. *Proceedings of the Royal Society B: Biological Sciences*, 283(1829):20152841.

Holland, P. W., Garcia-Fernàndez, J., Williams, N. A., and Sidow, A. (1994). Gene duplications and the origins of vertebrate development. *Development*, 1994(Supplement):125–133.

Kalyaanamoorthy, S., Minh, B. Q., Wong, T. K., Von Haeseler, A., and Jermiin, L. S. (2017). ModelFinder: Fast model selection for accurate phylogenetic estimates. *Nature Methods*, 14(6):587–589.

Koonin, E. V. (2005). Orthologs, Paralogs, and Evolutionary Genomics. *Annual Review of Genetics*, 39(1):309–338.

Kordis, D. and Gubensek, F. (2000). Adaptive evolution of animal toxin multigene families. *Gene*, 261:43–52.

Kryuchkova-Mostacci, N. and Robinson-Rechavi, M. (2016). Tissue-Specificity of Gene Expression Diverges Slowly between Orthologs, and Rapidly between Paralogs. *PLoS Computational Biology*, 12(12).

Kuzniar, A., van Ham, R. C. H. J., Pongor, S., and Leunissen, J. A. M. (2008). The quest for orthologs: finding the corresponding gene across genomes. *Trends in Genetics*, 24(11):539–551.

Langmead, B. and Salzberg, S. L. (2012). Fast gapped-read alignment with Bowtie 2. *Nat Methods*, 9(4):357–359.

Li, Q., Barghi, N., Lu, A., Fedosov, A. E., Bandyopadhyay, P. K., Lluisma, A. O., Concepcion, G. P., Yandell, M., Olivera, B. M., and Safavi-Hemami, H. (2017). Divergence of the Venom Exogene Repertoire in Two Sister Species of *Turriconus*. *Genome Biology and Evolution*, 9(9):2211–2225.

Lomonte, B., Mora-Obando, D., Fernández, J., Sanz, L., Pla, D., María Gutiérrez, J., and Calvete, J. J. (2015). First crotoxin-like phospholipase $A_2$ complex from a New World non-rattlesnake species: Nigroviriditoxin, from the arboreal Neotropical snake *Bothriechis nigroviridis*. *Toxicon*, 93:144–54.

Lomonte, B., Tsai, W. C., Bonilla, F., Solórzano, A., Solano, G., Angulo, Y., Gutiérrez, J. M., and Calvete, J. J. (2012). Snake venomics and toxicological profiling of the arboreal pitviper *Bothriechis supraciliaris* from Costa Rica. *Toxicon*, 59(5):592–599.

Losos, J. B. (2011). Convergence, adaptation, and constraint. *Evolution*, 65(7):1827–1840.

Margres, M. J., McGivern, J. J., Seavy, M., Wray, K. P., Facente, J., and Rokyta, D. R. (2015). Contrasting modes and tempos of venom expression evolution in two snake species. *Genetics*, 199(1):165–76.

Margres, M. J., McGivern, J. J., Wray, K. P., Seavy, M., Calvin, K., and Rokyta, D. R. (2014). Linking the transcriptome and proteome to characterize the venom of the eastern diamondback rattlesnake (*Crotalus adamanteus*). *Journal of Proteomics*, 96:145–158.

Mason, A. J., Margres, M. J., Strickland, J. L., Rokyta, D. R., Sasa, M., and Parkinson, C. L. (2020). Trait differentiation and modular toxin expression in palm-pitvipers. *BMC Genomics*, 21(1):147.

Moczek, A. P. (2005). The Evolution and Development of Novel Traits, or How Beetles Got Their Horns. *BioScience*, 55(11):937.

Morel, B., Kozlov, A. M., Stamatakis, A., and Szöllösi, G. J. (2020). GeneRax: A tool for species tree-aware maximum likelihood based gene family tree inference under gene duplication, transfer, and loss. *bioRxiv*.

Nehrt, N. L., Clark, W. T., Radivojac, P., and Hahn, M. W. (2011). Testing the ortholog conjecture with comparative functional genomic data from mammals. *PLoS Computational Biology*, 7(6).

Nei, M., Gu, X., and Sitnikova, T. (1997). Evolution by the birth-and-death process in multigene families of the vertebrate immune system. *Proceedings of the National Academy of Sciences of the United States of America*, 94(15):7799–806.

Nguyen, L.-T., Schmidt, H. A., von Haeseler, A., and Minh, B. Q. (2015). IQ-TREE: A Fast and Effective Stochastic Algorithm for Estimating Maximum-Likelihood Phylogenies. *Molecular Biology and Evolution*, 32(1):268–274.

Ohno, S. (2013). *Evolution by gene duplication*. Springer Science & Business Media.

Prasad, K. V., Song, B. H., Olson-Manning, C., Anderson, J. T., Lee, C. R., Schranz, M. E., Windsor, A. J., Clauss, M. J., Manzaneda, A. J., Naqvi, I., Reichelt, M., Gershenzon, J., Rupasinghe, S. G., Schuler, M. A., and Mitchell-Olds, T. (2012). A gain-of-function polymorphism controlling complex traits and fitness in nature. *Science*, 337(6098):1081–1084.

Rautsaw, R. M., Hofmann, E. P., Margres, M. J., Holding, M. L., Strickland, J. L., Mason, A. J., Rokyta, D. R., and Parkinson, C. L. (2019). Intraspecific sequence and gene expression variation contribute little to venom diversity in sidewinder rattlesnakes (Crotalus cerastes). *Proceedings of the Royal Society B*, 286(1906):20190810.

Richter, D. J., Fozouni, P., Eisen, M. B., and King, N. (2018). Gene family innovation, conservation and loss on the animal stem lineage. *eLife*, 7:e34226.

Rogozin, I. B., Managadze, D., Shabalina, S. A., and Koonin, E. V. (2014). Gene Family Level Comparative Analysis of Gene Expression in Mammals Validates the Ortholog Conjecture. *Genome Biology and Evolution*, 6(4):754–762.

Rokyta, D. R., Margres, M. J., and Calvin, K. (2015). Post-transcriptional mechanisms contribute little to phenotypic variation in snake venoms. *G3: Genes, Genomes, Genetics*, 5(11):2375–2382.

Rotenberg, D., Bamberger, E. S., and Kochva, E. (1971). Studies on Ribonucleic Acid Synthesis in the Venom Glands of *Vipera palaestinae* (Ophidia, Reptilia). Technical report.

Sunagar, K. and Moran, Y. (2015). The Rise and Fall of an Evolutionary Innovation: Contrasting Strategies of Venom Evolution in Ancient and Young Animals. *PLoS Genetics*, 11(10):e1005596.

Taylor, M. B. and Ehrenreich, I. M. (2015). Higher-order genetic interactions and their contribution to complex traits.

Townsend, J. H., Medina-Flores, M., Wilson, L. D., Jadin, R. C., and Austin, J. D. (2013). A relict lineage and new species of green palm-pitviper (Squamata, Viperidae, *Bothriechis*) from the Chortís Highlands of Mesoamerica. *ZooKeys*, 298:77–106.

Townsend, J. P., López-Giráldez, F., and Friedman, R. (2008). The phylogenetic informativeness of nucleotide and amino acid sequences for reconstructing the vertebrate tree. *Journal of Molecular Evolution*, 67(5):437–447.

True, J. R. and Carroll, S. B. (2002). Gene co-option in physiological and morphological evolution. *Annual Review of Cell and Developmental Biology*, 18(1):53–80.

Uyeda, J. C. and Harmon, L. J. (2014). A Novel Bayesian Method for Inferring and Interpreting the Dynamics of Adaptive Landscapes from Phylogenetic Comparative Data. *Systematic Biology*, 63(6):902–918.

Wang, L.-G., Tsan, T., Lam, Y., Xu, S., Dai, Z., Zhou, L., Feng, T., Guo, P., Dunn, C. W., Jones, B. R., Bradley, T., Zhu, H., Guan, Y., Jiang, Y., and Yu, G. (2019). Treeio: An R Package for Phylogenetic Tree Input and Output with Richly Annotated and Associated Data. *Molecular Biology and Evolution*, 37(2):599–603.

Whittington, A. C., Mason, A. J., and Rokyta, D. R. (2018). A Single Mutation Unlocks Cascading Exaptations in the Origin of a Potent Pitviper Neurotoxin. *Molecular Biology and Evolution*, 35(4):887–898.

# Chapter 5

# Conclusions

Biological diversification is a complex process that is a result of speciation and phenotypic adaptation; two processes which are shaped by a variety of factors that may alternatively promote or inhibit divergence. Phylogenetic inference can facilitate understanding the progression and context of many speciation events, but decades of molecular phylogenetic studies have shown the challenges to recovering robust species trees (Doyle, 1992; Maddison, 1997; Jeffroy et al., 2006). Rapid radiations, incomplete lineage sorting, and introgression through secondary contact and hybridization can generate conflicting genetic signatures that complicate species tree inference if unaccounted for, but they also inform our understanding of how speciation progresses (Dávalos et al., 2012; Kutschera et al., 2014; Copetti et al., 2017). Introgression, in particular, is now widely recognized as a ubiquitous occurrence that is increasingly appreciated for its role in establishing or increasing genetic variation that can shape evolutionary trajectories (Wolf and Mort, 1986; Dowling and Secor, 1997; Salzburger et al., 2002; Leducq et al., 2016; Hvala et al., 2018). Testing for introgression in phylogenetic datasets can lend special insight into speciation processes especially when used in combination with high-resolution genomic data.

I demonstrated the utility and importance of considering reticulate evolution through phylogenomic analyses of palm-pitvipers. Using several gene tree and allele frequency approaches of phylogenetic network inference, I found strong evidence for reticulate evolution in the phylogeny of palm-pitvipers (Mason et al., 2019). In addition to providing statistical support for a role of introgression, the three methods tested implicated similar lineages. Ancestral state reconstruction of the biogeographic history of palm-pitvipers placed reticulating lineages in the same or adjacent biogeo-

graphic regions during the time-frame reticulation likely occurred (Mason et al., 2019); a time-frame that also coincided with a time of geologic upheaval in Middle America. Together, these concordant results showcase the advantages of using multiple lines of evidence and several statistical approaches to generate evidence for robust hypothesis testing. Importantly, reticulation also resolved historical incongruence among palm-pitviper phylogenies which show the capability of genomic data to provide biological insight while giving additional context for previous work.

A resolved, well-understood phylogeny provides a powerful tool for comparative analyses, especially with regard to investigations of diversification which depend on species' evolutionary histories. Unfortunately, the field of venom research has been slow to incorporate phylogenetic perspectives into investigations of venom variation (Gibbs et al., 2013; Arbuckle, 2018; Barua and Mikheyev, 2019) and mechanistic inference have been similarly limited. To address these limitations, I took two alternative approaches to infer modes and mechanisms of evolution of snake venom phenotypes. In the first case, I focused on one pair of sister taxa (*Bothriechis nigroviridis* and *B. nubestris* that I showed had strongly divergent patterns of toxin expression (Mason et al., 2020). Using these two taxa and a novel approach in snake venoms, I demonstrated that broad shifts in venom composition occur through modular regulation of expression (Mason et al., 2020). Modular regulation has been critical to the evolution of biological complexity and can facilitate extremely rapid phenotypic evolution (Dynan, 1989; von Dassow and Munro, 1999; Fraser, 2005). In snake venoms, modular regulation of expression likely explains an array of extreme variations observed in snake venoms and other phenotypes (Yang, 2001; Ferguson et al., 2011; Van Belleghem et al., 2017). My work also highlighted the potential of systems-based approaches to analyzing gene expression in non-model systems like venom. As genomic resources become more widely available, their expanding implementation of systems-based approaches will lead to improved insights on the genomics of phenotypic diversification.

A major challenge to understanding the diversification of venom phenotypes has been the complications derived from differing homology relationships of genes within a venom gene family. Toxin families evolve through birth-death processes (Duda and Palumbi, 1999; Chang and Duda, 2012; Casewell et al., 2013) with high rates of duplication and loss. This high rate of gene turnover creates an issue for most comparative analyses of RNAseq data which assume a single reference or at least orthology of transcripts across treatments (Love et al., 2014; Russo et al., 2018). To overcome this complication, I utilized a gene tree based approach to investigate how expression

evolves within and among toxin gene families as well as what characteristics differentiate toxins from nontoxins. Through these methods, I showed patterns of expression evolution are not uniform across toxin families; two of the three largest toxin families in palm-pitvipers showed evidence of multiple shifts in expression optima. Toxins showed greater variation in expression than nontoxins, suggesting they are more labile than their nontoxin counterparts. More broadly, the gene-tree based approach I utilized allowed me to leverage a substantial amount of data to test our hypotheses while explicitly incorporating phylogenetic information. This approach can be implemented in a variety of systems to give phylogenetic context to functional genomic comparisons and accelerate insights on phenotypic diversification (Dunn et al., 2018).

Cumulatively, I have utilized multiple genomic approaches to discern patterns of diversification affecting speciation and venom evolution in palm-pitvipers, which provided an ideal model system for investigating speciation and adaptation. Although many of the questions I addressed are specific to palm-pitvipers, they are derived from general hypotheses with wide applicability in other systems. Furthermore, in each case I have advanced the field by using recently developed methods in novel contexts or using multiple methods together for robust inference. As sequencing technologies continue to develop and the cost of generating molecular data decreases, these types of data will cease to be limiting factors for research questions. Instead, it will become increasingly important to consider and integrate complimentary data types such as ecology and life-history with novel models and methods to comprehensively identify the proximate drivers of diversification.

### 5.0.1 Significance

Palm-pitvipers are a unique but advantageous taxonomic group for examining how diversification occurs through speciation, adaptation, and the mechanisms that promote diversification. Using this group as a model system, I have established robust methodologies for testing for reticulate evolution and identified reticulation as a source of discordance in the phylogeny of palm-pitvipers. Palm-pitviper venom phenotypes evolve rapidly through coordinated shifts in toxin expression among multi-gene toxin families, likely through modular genetic architecture. The modes of diversification identified in palm-pitvipers certainly apply to other snakes (Mackessy, 2010; Burbrink and Gehara, 2018), and are similarly relevant to other taxonomic groups. Further tests of the forces of evolution and mechanisms of adaptation implicated as key players in the evolution of palm-pitvipers will lend greater understanding to the processes of speciation and adaptation across the tree of life.

# References


Arbuckle, K. (2018). Phylogenetic comparative methods can provide important insights into the evolution of toxic weaponry. 10(12).

Copetti, D., Búrquez, A., Bustamante, E., Charboneau, J. L. M., Childs, K. L., Eguiarte, L. E., Lee, S., Liu, T. L., McMahon, M. M., Whiteman, N. K., Wing, R. A., Wojciechowski, M. F., and Sanderson, M. J. (2017). Extensive gene tree discordance and hemiplasy shaped the genomes of North American columnar cacti. *Proceedings of the National Academy of Sciences of the United States of America*, 114(45):12003–12008.

Dávalos, L. M., Cirranello, A. L., Geisler, J. H., and Simmons, N. B. (2012). Understanding phylogenetic incongruence: lessons from phyllostomid bats. *Biological Reviews*, 87(4):991–1024.

Dowling, T. E. and Secor, C. L. (1997). The role of hybridization and introgression in the diversification of animals. *Annual review of Ecology and Systematics*, 28(1):593–619.

Doyle, J. J. (1992). Gene Trees and Species Trees: Molecular Systematics as One-Character Taxonomy. *Systematic Botany*, 17(1):144–163.

Duda, T. F. and Palumbi, S. R. (1999). Molecular genetics of ecological diversification: duplication and rapid evolution of toxin genes of the venomous gastropod *Conus*. *Proceedings of the National Academy of Sciences of the United States of America*, 96(12):6820–3.

Dynan, W. S. (1989). Modularity in promoters and enhancers. *Cell*, 58(1):1–4.

Fraser, H. B. (2005). Modularity and evolutionary constraint on proteins. *Nature Genetics*, 37(4):351–352.

Gibbs, H. L., Sanz, L., Sovic, M. G., and Calvete, J. J. (2013). Phylogeny-Based Comparative Analysis of Venom Proteome Variation in a Clade of Rattlesnakes (*Sistrurus* sp.). *PLoS ONE*, 8(6).

Hvala, J. A., Frayer, M. E., and Payseur, B. A. (2018). Signatures of hybridization and speciation in genomic patterns of ancestry. *Evolution*, 72(8):1540–1552.

Jeffroy, O., Brinkmann, H., Delsuc, F., and Philippe, H. (2006). Phylogenomics: the beginning of incongruence? *Trends in Genetics*, 22(4):225–231.

Kutschera, V. E., Bidon, T., Hailer, F., Rodi, J. L., Fain, S. R., and Janke, A. (2014). Bears in a forest of gene trees: phylogenetic inference is complicated by incomplete lineage sorting and gene flow. *Molecular Biology and Evolution*, 31(8):2004–2017.

Leducq, J.-B., Nielly-Thibault, L., Charron, G., Eberlein, C., Verta, J.-P., Samani, P., Sylvester, K., Hittinger, C. T., Bell, G., and Landry, C. R. (2016). Speciation driven by hybridization and chromosomal plasticity in a wild yeast. *Nature Microbiology*, 1(1):15003.

Maddison, W. P. (1997). Gene Trees in Species Trees. *Systematic Biology*, 46(3):523–536.

Salzburger, W., Baric, S., and Sturmbauer, C. (2002). Speciation via introgressive hybridization in East African cichlids? *Molecular Ecology*, 11(3):619–625.

Wolf, H. G. and Mort, M. A. (1986). Inter-specific hybridization underlies phenotypic variability in Daphnia populations. *Oecologia*, 68(4):507–511.

# Appendices

# Appendix A Supporting Information for Chapter 2: Reticulate evolution in Nuclear Middle America causes discordance in the phylogeny of palm-pitvipers (Viperidae: *Bothriechis*)

## A.1 Data Availability

| Species | Specimen | Museum or Specimen ID | Locality | Fastq accession | 12S | 16S | ATP6 | ATP8 | COX1 | COX2 | COX3 | CYTB | ND1 | ND2 | ND3 | ND4 | ND4L | ND5 | ND6 |
|---|---|---|---|---|---|---|---|---|---|---|---|---|---|---|---|---|---|---|---|
| *Agkistrodon contortrix* | S2093 | FTB 1712 | "Dearborn, Indiana, USA" | SRR8362566 | MK313326 | MK313353 | MK313375 | MK313399 | MK313425 | MK313532 | MK313674 | MK313557 | MK313581 | MK313477 | MK313505 | MK313438 | MK313608 | MK313662 | MK313637 |
| *Atropoides nummifer* | S1984 | CLP168 | "San Jose, Costa Rica" | SRR8362565 | MK313308 | MK313348 | MK313373 | MK313397 | MK313427 | MK313530 | MK313672 | MK313555 | MK313583 | MK313479 | MK313503 | MK313454 | MK313606 | MK313644 | MK313619 |
| *Bitis nasicornis* | S2012 | CAS 207875 | "Bioko Sur Prov., Equatorial Guinea " | SRR8362564 | - | - | - | - | - | - | - | - | - | - | - | - | - | - | - |
| *Bitis nasicornis* | S1931 | CAS 207874 | "Bioko Sur Prov., Equatorial Guinea " | SRR8362563 | - | - | - | - | - | - | - | - | - | - | - | - | - | - | - |
| *Bothriechis aurifer* | S17967 | UTA R-46661 | "Union Barrios, Baja Verapaz, Guatemala" | SRR8362562 | MK313319 | MK313339 | MK313365 | MK313392 | MK313417 | MK313523 | MK313682 | MK313548 | MK313573 | MK313470 | MK313495 | MK313447 | MK313599 | MK313655 | MK313631 |
| *Bothriechis aurifer* | S2070 | UTA-R35031 | Guatemala | SRR8362561 | MK313320 | MK313340 | MK313366 | MK313393 | MK313418 | MK313524 | MK313683 | MK313549 | MK313574 | MK313471 | MK313496 | MK313448 | MK313600 | MK313654 | MK313630 |
| *Bothriechis bicolor* | S17968 | UTA R-39413 | "Municipio San Rafael Pie De la Cuesta, San Marcos, Guatemala" | SRR8362560 | MK313317 | MK313338 | MK313364 | MK313390 | MK313416 | MK313520 | MK313681 | MK313546 | MK313572 | MK313468 | MK313494 | MK313446 | MK313596 | MK313653 | MK313628 |
| *Bothriechis bicolor* | S1990 | DPL 2899 | - | SRR8362559 | MK313316 | MK313337 | MK313363 | MK313389 | MK313415 | MK313519 | MK313680 | MK313545 | MK313571 | MK313467 | MK313493 | MK313445 | MK313595 | MK313652 | MK313627 |
| *Bothriechis guifarroi* | S17970 | USNM 579874 | "Reserva de Vida Silvestre Texiguat, Atlantida Department, Honduras" | SRR8362568 | MK313315 | MK313336 | MK313362 | MK313384 | MK313414 | MK313518 | MK313679 | MK313544 | MK313570 | MK313466 | MK313491 | MK313441 | MK313594 | MK313651 | MK313626 |
| *Bothriechis lateralis* | S1968 | MH 105 | - | SRR8362567 | MK313313 | MK313334 | MK313360 | MK313382 | MK313412 | MK313516 | MK313677 | MK313542 | MK313568 | MK313464 | MK313490 | MK313439 | MK313592 | MK313649 | MK313624 |
| *Bothriechis lateralis* | S2079 | MH 106 | - | SRR8362591 | MK313314 | MK313335 | MK313361 | MK313383 | MK313413 | MK313517 | MK313678 | MK313543 | MK313569 | MK313465 | MK313492 | MK313440 | MK313593 | MK313650 | MK313625 |
| *Bothriechis marchi* | S17971 | JAC 15079 | Honduras | SRR8362590 | MK313322 | MK313343 | MK313369 | MK313388 | MK313421 | MK313522 | MK313685 | MK313551 | MK313577 | MK313473 | MK313498 | MK313451 | MK313598 | MK313657 | MK313633 |
| *Bothriechis nigroviridis* | S1981 | CAS178120 | "Las Tablas, Puntarenas, Costa Rica" | SRR8362593 | MK313325 | MK313346 | MK313372 | MK313387 | MK313424 | MK313526 | MK313689 | MK313554 | MK313580 | MK313476 | MK313502 | MK313444 | MK313604 | MK313661 | MK313636 |
| *Bothriechis nubestris* | S17975 | MZUCR 11151 | "San Gerardo de Dota, San Jose, Costa Rica" | SRR8362592 | MK313324 | MK313345 | MK313371 | MK313386 | MK313423 | MK313528 | MK313688 | MK313553 | MK313579 | MK313475 | MK313501 | MK313443 | MK313603 | MK313660 | MK313635 |
| *Bothriechis nubestris* | S1980 | FHSM 8090 | Captive Animal (Houston Zoo) | SRR8362587 | MK313323 | MK313344 | MK313370 | MK313385 | MK313422 | MK313527 | MK313687 | MK313552 | MK313578 | MK313474 | MK313500 | MK313442 | MK313602 | MK313659 | MK313634 |
| *Bothriechis rowleyi* | S17979 | San Antonio Zoo 2 | Captive Animal (San Antonio Zoo) | SRR8362586 | MK313321 | MK313341 | MK313367 | MK313391 | MK313419 | MK313525 | MK313686 | MK313547 | MK313575 | MK313469 | MK313499 | MK313449 | MK313601 | MK313658 | MK313629 |
| *Bothriechis schlegelii* | S1959 | USNM 319276 | Panama | SRR8362589 | MK313304 | MK313330 | MK313356 | MK313401 | MK313408 | MK313512 | MK313668 | MK313538 | MK313564 | MK313460 | MK313486 | MK313434 | MK313590 | MK313645 | MK313620 |
| *Bothriechis schlegelii* | S2058 | USNM 347536 | Panama | SRR8362588 | MK313305 | MK313331 | MK313357 | MK313402 | MK313409 | MK313513 | MK313669 | MK313539 | MK313565 | MK313461 | MK313487 | MK313435 | MK313591 | MK313646 | MK313621 |
| *Bothriechis supraciliaris* | S17980 | San Vito 5 | Costa Rica | SRR8362585 | MK313307 | MK313333 | MK313359 | MK313404 | MK313411 | MK313515 | MK313671 | MK313541 | MK313567 | MK313463 | MK313489 | MK313437 | MK313611 | MK313648 | MK313623 |
| *Bothriechis supraciliaris* | S1992 | MSU 1069 | - | SRR8362584 | MK313306 | MK313332 | MK313358 | MK313403 | MK313410 | MK313514 | MK313670 | MK313540 | MK313566 | MK313462 | MK313488 | MK313436 | MK313610 | MK313647 | MK313622 |
| *Bothriechis thalassinus* | S2077 | UTA R-46526 | "Sierra de Caral, Izabal, Guatemala" | SRR8362574 | MK313318 | MK313342 | MK313368 | MK313394 | MK313420 | MK313521 | MK313684 | MK313550 | MK313576 | MK313472 | MK313497 | MK313450 | MK313597 | MK313656 | MK313632 |
| *Bothrocophias hyoprora* | S2048 | KU 222208 | "San Jacinto, Loreto, Peru" | SRR8362575 | - | - | - | - | - | - | - | - | - | - | - | - | - | - | - |
| *Bothrops atrox* | S1951 | KU 214909 | "Madre de Dios, Cuzco Amazonico, Peru" | SRR8362576 | MK313303 | MK313329 | MK313355 | MK313381 | MK313407 | MK313511 | MK313667 | MK313537 | MK313563 | MK313459 | MK313485 | MK313433 | MK313589 | MK313664 | MK313638 |
| *Bothrops atrox* | S1957 | WED 59917 | "Andoas, Peru" | SRR8362577 | - | - | - | - | - | - | - | - | - | - | - | - | - | - | - |
| *Bothrops brazili* | S1967 | USNM 562703 | "Amazonas, Venezuela" | SRR8362578 | - | - | - | - | - | - | - | - | - | - | - | - | - | - | - |
| *Bothrops brazili* | S2055 | RWM 17832 | "Amazonas, Venezuela" | SRR8362579 | - | - | - | - | - | - | - | - | - | - | - | - | - | - | - |
| *Bothrops diporus* | S7372 | CTMZ-15852 | "Santa Maria, Córdoba, Argentina" | SRR8362580 | - | - | - | - | - | - | - | - | - | - | - | - | - | - | - |
| *Bothrops fonsecai* | S7400 | CTMZ-00301 | "Bananal, São Paulo, Brazil" | SRR8362581 | - | - | - | - | - | - | - | - | - | - | - | - | - | - | - |
| *Bungarus multicinctus* | S12224 | CTMZ-04086 | "Ninh Binh, Vietnam" | SRR8362582 | - | - | - | - | - | - | - | - | - | - | - | - | - | - | - |
| *Causus maculatus* | S2001 | AMNH 117677 | "Southwestern Province, Cameroon" | SRR8362583 | - | - | - | - | - | - | - | - | - | - | - | - | - | - | - |
| *Causus maculatus* | S0786 | KU291882 | "Moyenne Guinee, Guinea" | SRR8362556 | - | - | - | - | - | - | - | - | - | - | - | - | - | - | - |
| *Cerrophidion godmani* | S1952 | KU 291242 | "Cerro El Pital, Chalatenango, El Salvador" | SRR8362555 | - | - | - | - | - | - | - | - | - | - | - | - | - | - | - |
| *Cerrophidion godmani* | S1958 | KU 289801 | "Parque Nacional Montecristo, Santa Ana, El Salvador" | SRR8362554 | MK313309 | MK313349 | MK313374 | MK313398 | MK313428 | MK313531 | MK313673 | MK313556 | MK313584 | MK313480 | MK313504 | MK313455 | MK313607 | MK313643 | MK313618 |
| *Crotalus cerastes* | S1948 | FHSM 11278 | "Clark County, Nevada, USA" | SRR8362553 | - | - | - | - | - | - | - | - | - | - | - | - | - | - | - |
| *Crotalus cerastes* | S2043 | FHSM 11279 | "San Diego, California, USA" | SRR8362552 | MK313328 | MK313354 | MK313380 | MK313406 | MK313432 | MK313536 | MK313692 | MK313562 | MK313588 | MK313484 | MK313510 | MK313458 | MK313614 | MK313666 | MK313639 |
| *Lachesis muta* | S1956 | WED 57798 | - | SRR8362551 | - | - | - | - | - | - | - | - | - | - | - | - | - | - | - |
| *Lachesis muta* | S1969 | MH 111 | - | SRR8362550 | MK313327 | MK313347 | MK313377 | MK313405 | MK313426 | MK313529 | MK313691 | MK313561 | MK313582 | MK313483 | MK313507 | MK313453 | MK313613 | MK313663 | MK313640 |
| *Mixcoatlus melanurus* | S2078 | UTA-R34605 | Mexico | SRR8362549 | MK313311 | MK313351 | MK313378 | MK313395 | MK313431 | MK313535 | MK313675 | MK313559 | MK313585 | MK313482 | MK313508 | MK313457 | MK313609 | MK313665 | MK313616 |
| *Ophryacus smaragdinus* | S2065 | CLP 1094 | Mexico | SRR8362558 | - | - | - | - | - | - | - | - | - | - | - | - | - | - | - |
| *Ophryacus undulatus* | S1923 | AMNH 118187 | "Puebla, Mexico" | SRR8362557 | MK313312 | MK313352 | MK313379 | MK313396 | MK313430 | MK313534 | MK313676 | MK313560 | MK313586 | MK313478 | MK313509 | MK313452 | MK313605 | MK313641 | MK313615 |
| *Ophryacus undulatus* | S2035 | CLP 73 | Mexico | SRR8362571 | - | - | - | - | - | - | - | - | - | - | - | - | - | - | - |
| *Oxybelis aeneus* | S12205 | CTMZ-00806 | "Peixe, Tocantins, Brazil" | SRR8362572 | - | - | - | - | - | - | - | - | - | - | - | - | - | - | - |
| *Pareas vindumi* | S8103 | CAS248147 | "Myitkyina Dist., Kachin, Myanmar" | SRR8362569 | - | - | - | - | - | - | - | - | - | - | - | - | - | - | - |
| *Porthidium dunni* | S1925 | AMNH 118314 | "Oaxaca, Mexico" | SRR8362570 | MK313310 | MK313350 | MK313376 | MK313400 | MK313429 | MK313533 | MK313690 | MK313558 | MK313587 | MK313481 | MK313506 | MK313456 | MK313612 | MK313642 | MK313617 |
| *Porthidium dunni* | S2040 | ENS 9705 | "Oaxaca, Mexico" | SRR8362573 | - | - | - | - | - | - | - | - | - | - | - | - | - | - | - |

Table A.1: Data availability for samples used in phylogenetic analyses

## A.2 Supplementary Methods

### A.2.1 Sampling & Sequence Generation

We used the Anchored Hybrid Enrichment method described in Lemmon et al. (2012) to generate genomic sequences for phylogenomic analyses. Whole genomic DNA was extracted from tissue using the Qiagen DNeasy kit following manufacturer's protocols at the Center for Anchored Phylogeneomics at Florida State University. Isolated genomic DNA was fragmented to a size range of approximately 150-300 bp via a Covaris E220 focused-ultrasonicator with Covaris microTUBES. Genomic libraries were prepared with a Beckman-Coulter Bimex FXp Automation Workstation following a modified protocol of Meyer and Kircher (2010) with a size selection step using SPRIselect beads with 0.9x beads to sample volume after blunt-end repair. Libraries were pooled in groups of 17 before enrichment with the Agilent Custom Sure Select kit and the original probe set described in Lemmon et al. (2012) and improved for Squamate taxa in Ruane et al. (2015) and Tucker et al. (2016). Libraries were sequenced on a HiSeq 2500 at the FSU College of Medicine's Translational Science Laboratory and approximately 1Gb of 150 pair-end sequence data were collected per sample. Following sequencing reads were demultiplexed and assigned to samples based on unique 8 bp barcode indices.

### A.2.2 Data Processing

Briefly, we cleaned raw reads using TrimGalore! v.0.4.4 (Krueger, 2015) with a minimum quality score of twenty and minimum length of 30 bp. Anchored loci were assembled using the IBA.py script, which performs an iterative baited assembly using USEARCH 10.0.240 (Edgar, 2010) and Bridger 2014-12-01 (Chang et al., 2015) to select and assemble reads with high similarity to the probe region. We implemented IBA with three iterations, a kmer size of 25, and a minimum coverage of 10x, using the *Anolis* probe sequence as the reference. Assembled sequences for each individual were reorganized by loci and aligned to the probe region with MAFFT v.7.035b (Katoh and Standley, 2013). To determine orthology of trimmed probe regions, we mapped sequences to the Burmese python genome with NCBI BLASTN allowing up to three target hits and three hits per target with the –max_target_seqs 3 and –max_hsps 2 options, respectively. We then filtered BLAST results by bit score, removing those sequences with bit scores $\geq$ 90% of the best bit-score and re-blasted remaining sequences to the python genome to determine their position. To determine

orthology we used ortholog_filter.py, which selects single hit sequences that map to the same region of the python genome.

Once orthologous copies for each taxon had been selected, we performed locus-specific alignments with MAFFT and processed by locus in FASconCAT-G (Kück and Longo, 2014) to generate strict consensuses. We used the remove_duplicates.py script to identify and remove duplicate sequences within each locus for each taxon as these sequences that represent contamination or duplications. The remaining sequences were then aligned by locus a final time using MAFFT, to generate the final alignment set for each locus. Alignments were trimmed by density and entropy using the Python script Trim_DE.py to remove sites with a density of less than 0.6% or entropy >1.5. Final alignments were checked manually in Geneious 10.2.3 (Kearse et al., 2012).

### A.2.3 Data Processing

We tested the hypothesis that recent and/or historic gene flow has led to conflicting phylogenetic signals in *Bothriechis* using three methods (PhyloNet, SNaQ, and TreeMix) to infer migration (gene flow) or reticulation and model comparison to inferred species trees. These analyses were conducted using a reduced dataset of only *Bothriechis*. The first two methods, PhyloNet and SNaQ infer phylogenetic networks using sequence data, gene trees, or 4-taxon concordance factors. Both methods can infer networks using a heuristic search of network space with maximum pseudo-likelihood criterion for computational efficiency (Yu and Nakhleh, 2015; Solís-Lemus and Ané, 2016). Due to the heuristic nature of these methods, accurate network inference is contingent on performing a sufficient number of searches to identify the best network. The primary differences between these two networks is the use of rooted taxon triplets (PhyloNet) versus unrooted 4-taxon quartets (SNaQ) and differing methods of network identifiability. The observed tradeoff is that SNaQ should converge on an optimal network more quickly than PhyloNet, but at the cost of making restrictive assumptions about the network structure Solís-Lemus and Ané (2016). In contrast to network inference methods, TreeMix uses a statistical algorithm incorporating allele frequency data to determine the most likely relationship among populations allowing specified number of migration events (i.e., gene flow) (Pickrell and Pritchard, 2012). TreeMix's algorithmic approach means that it can rapidly arrive and consistently arrive at a single answer. However, its design for modeling population processes (as opposed to species) and use of allele frequencies may make it less reliable for our datasets than network inference methods.

To evaluate the relative contribution of varying numbers of reticulations, we inferred networks and trees with between zero and nine reticulations for each method. As the methods used here all account for ILS, comparisons against models with zero reticulations also serve as explicit tests of whether ILS alone sufficiently explains gene tree discordance. We calculated AIC for each model based on log likelihood or log pseudo-likelihood score treating each reticulation as a free parameter in the model. We then determined the optimal number of reticulations based on the relative change in AIC, which is expected to decrease rapidly as model performance improves and level off due to diminishing returns with extraneous numbers of reticulations. Where models with one or more reticulations performed better, we concluded that ILS alone insufficiently explained observed gene tree discordance.

All PhyloNet analyses were conducted in PhyloNet v. 3.6.2 (Than et al., 2008) using gene trees inferred for each anchored locus in RAxML as in the species tree estimation analyses (above). PhyloNet can infer rooted phylogenetic networks using a full likelihood optimality criterion Yu et al. (2014), but at a high run time cost per terminal which was prohibitive for our dataset. Instead, we used the maximum pseudo-likelihood criterion for computational efficiency (Yu and Nakhleh, 2015). Because preliminary analysis of network estimation in PhyloNet indicated high variability in the "best" network discovered by PhyloNet's heuristic search, we performed 25 iterations of 500 independent searches of network space. We retained the top five models for each iteration of searches and selected the top five models across all iterations for evaluation.

For SNaQ analyses we similarly used gene trees recovered in RAxML as in PhyloNet and species tree estimation analyses (above) and implemented SNaQ in the Julia package PhyloNetworks Solís-Lemus and Ané (2016). To determine the most likely network, we conducted 100 searches of network space and retained the network with the highest pseudolikelihood. To infer networks with 0-9 reticulation edges we used the ASTRAL topology as the starting tree for the first network search, with the best networks as starting networks for subsequent searches with additional reticulation edges.

We used TreeMix v 1.13 (Pickrell and Pritchard, 2012) to infer a most likely tree with migration edges representing gene flow between populations (here *Bothriechis* species). To implement TreeMix, we phased alleles for each sample using bash and python wrappers for bwa (Li and Durbin, 2009) and GATK (McKenna et al., 2010) based on scripts from (Alexander, 2015) and extracted independent SNPs from each locus. TreeMix was run with each *Bothriechis* species defining

a population and specifying 0-9 migration edges. We additionally used the three-population and four-popuation tests to calculate the f3 and f4 statistics for all possible population combinations.

## A.3 Description of calibration points used in dated phylogeny and description of biogeographic regions used in ancestral area reconstruction

### A.3.1 Description of calibration points used in dated phylogeny

1. Stem Colubroides – Constrained to a maximum age of 93 Mya (Fig S3). Calibration point based on *Haasiophis terrasanctus* Tchernov et al. (2000), which is considered a basal Alethinophidia (Tchernov et al., 2000; Hsiang et al., 2015). We set the calibration for the node represented in our sampling by the most recent common ancestor between *Oxybelis aenus* and *Pareas margaritophorus*. The reasoning for such constraint is based on the relative time of cladogenic events, where the most recent common ancestor (MRCA) of Colubroides cannot be older than the basal nodes of Alethinophidia.

2. Stem Colubroidea – Constrained to a minimum age of 35.2 Mya and a maximum age of 54 mya (Fig S3). The ages for this calibration point are based on Colubrid indet. Smith (2013) and on *Procerophis sahnii* Rage et al. (2008), respectively. Smith (2013) described Colubrid indet. as a Colubridae (sensu Lawson et al. (2005), but Colubroidea sensu Zaher et al. (2009)) based on some few vertebrae characteristics, mainly based on the lack of hypapophyses and on the presence of a narrow hemal keel. *Procerophis sahnii* was described as being a Colubroidea (Colubroides sensu Zaher et al. (2009)), and Rage et al. (2008) sustained that the fossil could not be referred to any extant colubroid family. Head et al (2016) supported such interpretation indicating that *Procerophis sahnii* represents a basal Colubroides. We calibrate using these constraints the clade represented by the MRCAbetween *Oxybelis aenus* and *Bungarus multicinctus*.

3. Stem Viperidae – Constrained to a minimum age of 22.1 Mya and a maximum age of 93 Mya (Fig S3). Constraints were based on *Vipera* cf. *V. antiqua* Szyndlar and Böhme, 1993 and *Haasiophis terrasanctus*, respectively. Szyndlar and Böhme (1993) described *Vipera* cf. *V. antiqua* by using cervical vertebrae that clearly present the main features of an extant Viperi-

dae (long and straight hypapophysis, and a large and characteristic condyle). However, the positioning of this fossil within the genus *Vipera* can be questionable, because some species of *Causus* can also present the characters used by Szyndlar and Böhme (1993) and by Szyndlar and Rage (1999) to assign the fossil to *Vipera*. We are using here a more conservative phylogenetic position for this fossil, thus we are considering *Vipera* cf. *V. antiqua* as a basal Viperidae, without associating it to any of the extant subfamilies or genera. *Haasiophis terrasanctus* was used to define an upper bound to the age of this clade, since the MRCA of all Viperidae cannot be older than the basal split of Alethinophidia. We set this calibration point on the node that includes the MRCA of *Bitis nasicornis* and *Bungarus multicinctus*.

4. Stem Crotalinae – Constrained to a minimum of 11.2 Mya and a maximum of 54 Mya (Fig S3). We based these constraints on Crotalinae gen. & sp. indet. A Ivanov, 1999 and on *Procerophis sahnii*, respectively. Crotalinae gen. sp. indet. A can be unequivocally associate to the subfamily Crotalinae, since the fossil was described based on a maxilla with an almost complete preserved fang, and the maxilla presents the characteristic depression that accommodates the pit organ in crotalines. However, the assignment of such fossil to any of the current extant genera is questionable (Ivanov, 1999). We used *Procerophis sahnii* to constrain the maximum age of the stem Crotalinae, which cannot be older than the initial split within Colubroides. We set the age constraints to the node represented by the MRCA of *Agkistrodon contortrix* and *Causus maculatus*.

### A.3.2 Biogeographic Regions

1. South America, defined as any region south of the Isthmus of Panama
2. The southern Middle American Isthmus stretching from the Isthmus of Panama to the Nicaraguan Depression.
3. The Chortís Block, occupying the region between the Nicaraguan depression and the Motagua-Paolochic fault.
4. The Mayan Block defined as the region north of the Motagua-Paolochic fault.

## A.4 Sequence Information

| Species | Specimen | Museum or Specimen ID | Locality | Read Count | Percent High-Quality Mitogenome Coverage | Sequence length (bp) | | | | | | | | | | | | | | |
|---|---|---|---|---|---|---|---|---|---|---|---|---|---|---|---|---|---|---|---|---|
| | | | | | | 12S | 16S | ATP6 | ATP8 | COX1 | COX2 | COX3 | CYTB | ND1 | ND2 | ND3 | ND4 | ND4L | ND5 | ND6 |
| *Agkistrodon contortrix* | S2093 | FTB 1712 | "Dearborn, Indiana, USA" | 2140413 | 95.8 | 911 | 1481 | 681 | 165 | 1602 | 685 | 784 | 1114 | 961 | 1030 | 343 | 1338 | 291 | 1785 | 522 |
| *Atropoides nummifer* | S1984 | CLP168 | "San Jose, Costa Rica" | 711555 | 98.1 | 914 | 1479 | 681 | 165 | 1602 | 685 | 784 | 1114 | 961 | 1030 | 343 | 1338 | 291 | 1788 | 522 |
| *Bitis nasicornis* | S2012 | CAS 207875 | "Bioko Sur Prov., Equatorial Guinea " | 2459375 | - | - | - | - | - | - | - | - | - | - | - | - | - | - | - | - |
| *Bitis nasicornis* | S1931 | CAS 207874 | "Bioko Sur Prov., Equatorial Guinea " | 3532801 | - | - | - | - | - | - | - | - | - | - | - | - | - | - | - | - |
| *Bothriechis aurifer* | S17967 | UTA R-46661 | "Union Barrios, Baja Verapaz, Guatemala" | 2300244 | 96.5 | 914 | 1491 | 681 | 165 | 1602 | 685 | 784 | 1114 | 961 | 1030 | 343 | 1338 | 291 | 1787 | 521 |
| *Bothriechis aurifer* | S2070 | UTA-R35031 | Guatemala | 5738775 | 96.7 | 914 | 1490 | 681 | 165 | 1602 | 685 | 784 | 1114 | 961 | 1030 | 343 | 1338 | 291 | 1787 | 521 |
| *Bothriechis bicolor* | S17968 | UTA R-39413 | "Municipio San Rafael Pie De la Cuesta, San Marcos, Guatemala" | 2418021 | 96.5 | 916 | 1487 | 681 | 165 | 1602 | 685 | 784 | 1114 | 961 | 1030 | 343 | 1338 | 291 | 1787 | 515 |
| *Bothriechis bicolor* | S1990 | DPL 2899 | - | 3797836 | 97.9 | 916 | 1486 | 681 | 165 | 1602 | 685 | 784 | 1114 | 961 | 1030 | 343 | 1338 | 291 | 1787 | 516 |
| *Bothriechis guifarroi* | S17970 | USNM 579874 | "Reserva de Vida Silvestre Texiguat, Atlantida Department, Honduras" | 2052777 | 97.7 | 912 | 1483 | 681 | 165 | 1602 | 685 | 784 | 1114 | 961 | 1030 | 343 | 1339 | 291 | 1785 | 522 |
| *Bothriechis lateralis* | S1968 | MH 105 | - | 3621118 | 90.0 | 909 | 1177 | 681 | 155 | 1603 | 685 | 647 | 994 | 849 | 1017 | 317 | 518 | 287 | 1586 | 522 |
| *Bothriechis lateralis* | S2079 | MH 106 | - | 2100983 | 91 | 909 | 1385 | 657 | 165 | 1588 | 685 | 784 | 1114 | 960 | 1030 | 307 | 1158 | 291 | 1731 | 522 |
| *Bothriechis marchi* | S17971 | JAC 15079 | Honduras | 952773 | 85.8 | 504 | 283 | 590 | 152 | 900 | 667 | 633 | 767 | 643 | 2762 | 77 | 705 | 61 | 933 | 521 |
| *Bothriechis nigroviridis* | S1981 | CAS178120 | "Las Tablas, Puntarenas, Costa Rica" | 3048403 | 93.4 | 909 | 1422 | 681 | 165 | 1602 | 685 | 784 | 1111 | 961 | 1030 | 343 | 1338 | 291 | 1787 | 522 |
| *Bothriechis nubestris* | S17975 | MZUCR 11151 | "San Gerardo de Dota, San Jose, Costa Rica" | 2178176 | 97.7 | 910 | 1484 | 681 | 165 | 1602 | 685 | 784 | 1111 | 961 | 1030 | 343 | 1338 | 291 | 1787 | 522 |
| *Bothriechis nubestris* | S1980 | FHSM 8090 | Captive Animal (Houston Zoo) | 3153990 | 97.2 | 911 | 1484 | 681 | 165 | 1602 | 685 | 784 | 1111 | 961 | 1030 | 343 | 1338 | 291 | 1787 | 522 |
| *Bothriechis rowleyi* | S17979 | San Antonio Zoo 2 | Captive Animal (San Antonio Zoo) | 2208248 | 92.3 | 914 | 1489 | 678 | 165 | 1600 | 685 | 784 | 1114 | 961 | 1030 | 342 | 1338 | 291 | 1784 | 515 |
| *Bothriechis schlegelii* | S1959 | USNM 319276 | Panama | 5991705 | 98.0 | 911 | 1478 | 681 | 162 | 1602 | 685 | 784 | 1114 | 961 | 1030 | 343 | 1338 | 291 | 1775 | 521 |
| *Bothriechis schlegelii* | S2058 | USNM 347536 | Panama | 3123972 | 97.1 | 911 | 1478 | 681 | 162 | 1602 | 685 | 784 | 1114 | 961 | 1030 | 343 | 1338 | 291 | 1775 | 521 |
| *Bothriechis supraciliaris* | S17980 | San Vito 5 | "San Vito, Puntarenas, Costa Rica" | 2196930 | 91.9 | 913 | 1338 | 681 | 165 | 1594 | 685 | 784 | 1114 | 961 | 1030 | 343 | 1338 | 291 | 1775 | 522 |
| *Bothriechis supraciliaris* | S1992 | MSU 1069 | - | 3207619 | 97.5 | 913 | 1485 | 681 | 165 | 1602 | 685 | 784 | 1114 | 961 | 1030 | 343 | 1338 | 291 | 1775 | 522 |
| *Bothriechis thalassinus* | S2077 | UTA R-46526 | "Sierra de Caral, Izabal, Guatemala" | 6178333 | 95.2 | 914 | 1488 | 681 | 165 | 1602 | 685 | 784 | 1114 | 961 | 1030 | 343 | 1338 | 291 | 1783 | 522 |
| *Bothrocophias hyoprora* | S2048 | KU 222208 | "San Jacinto, Loreto, Peru" | 4029527 | - | - | - | - | - | - | - | - | - | - | - | - | - | - | - | - |
| *Bothrops atrox* | S1951 | KU 214909 | "Madre de Dios, Cuzco Amazonico, Peru" | 5173201 | 98.7 | 910 | 1482 | 681 | 165 | 1602 | 685 | 784 | 1114 | 961 | 1030 | 343 | 1338 | 291 | 1781 | 522 |
| *Bothrops atrox* | S1957 | WED 59917 | "Andoas, Peru" | 3544295 | - | - | - | - | - | - | - | - | - | - | - | - | - | - | - | - |
| *Bothrops brazili* | S1967 | USNM 562703 | "Amazonas, Venezuela" | 4064730 | - | - | - | - | - | - | - | - | - | - | - | - | - | - | - | - |
| *Bothrops brazili* | S2055 | RWM 17832 | "Amazonas, Venezuela" | 3562051 | - | - | - | - | - | - | - | - | - | - | - | - | - | - | - | - |
| *Bothrops diporus* | S7372 | CTMZ-15852 | "Santa Maria, Córdoba, Argentina" | 1346438 | - | - | - | - | - | - | - | - | - | - | - | - | - | - | - | - |
| *Bothrops fonsecai* | S7400 | CTMZ-00301 | "Bananal, São Paulo, Brazil" | 1189054 | - | - | - | - | - | - | - | - | - | - | - | - | - | - | - | - |
| *Bungarus multicinctus* | S12224 | CTMZ-04086 | "Ninh Binh, Vietnam" | 1938090 | - | - | - | - | - | - | - | - | - | - | - | - | - | - | - | - |
| *Causus maculatus* | S2001 | AMNH 117677 | "Southwestern Province, Cameroon" | 4434646 | - | - | - | - | - | - | - | - | - | - | - | - | - | - | - | - |
| *Causus maculatus* | S0786 | KU291882 | "Moyenne Guinee, Guinea" | 3364507 | - | - | - | - | - | - | - | - | - | - | - | - | - | - | - | - |
| *Cerrophidion godmani* | S1952 | KU 291242 | "Cerro El Pital, Chalatenango, El Salvador" | 4079397 | - | - | - | - | - | - | - | - | - | - | - | - | - | - | - | - |
| *Cerrophidion godmani* | S1958 | KU 289801 | "Parque Nacional Montecristo, Santa Ana, El Salvador" | 4079397 | 96.7 | 918 | 1484 | 681 | 165 | 1602 | 685 | 784 | 1114 | 961 | 1030 | 343 | 1338 | 291 | 1787 | 522 |
| *Crotalus cerastes* | S1948 | FHSM 11278 | "Clark County, Nevada, USA" | 3428746 | - | - | - | - | - | - | - | - | - | - | - | - | - | - | - | - |
| *Crotalus cerastes* | S2043 | FHSM 11279 | "San Diego, California, USA" | 3793158 | 96 | 917 | 1476 | 681 | 165 | 1602 | 685 | 784 | 1114 | 961 | 1030 | 343 | 1338 | 291 | 1785 | 522 |
| *Lachesis muta* | S1956 | WED 57798 | - | 5347464 | - | - | - | - | - | - | - | - | - | - | - | - | - | - | - | - |
| *Lachesis muta* | S1969 | MH 111 | - | 2892171 | 98.3 | 908 | 1480 | 681 | 165 | 1602 | 685 | 784 | 1114 | 961 | 1030 | 343 | 1338 | 291 | 1789 | 522 |
| *Mixcoatlus melanurus* | S2078 | UTA-R34605 | Mexico | 3715746 | 96.2 | 913 | 1483 | 681 | 165 | 1602 | 685 | 784 | 1111 | 961 | 1030 | 343 | 1338 | 291 | 1750 | 451 |
| *Ophryacus smaragdinus* | S2065 | CLP 1094 | Mexico | 3479835 | - | - | - | - | - | - | - | - | - | - | - | - | - | - | - | - |
| *Ophryacus undulatus* | S1923 | AMNH 118187 | "Puebla, Mexico" | 3304811 | 94.5 | 912 | 1486 | 681 | 165 | 1602 | 685 | 784 | 1111 | 961 | 1030 | 343 | 1338 | 291 | 1782 | 526 |
| *Ophryacus undulatus* | S2035 | CLP 73 | Mexico | 1098042 | - | - | - | - | - | - | - | - | - | - | - | - | - | - | - | - |
| *Ozybelis aeneus* | S12205 | CTMZ-00806 | "Peixe, Tocantins, Brazil" | 1737812 | - | - | - | - | - | - | - | - | - | - | - | - | - | - | - | - |
| *Pareas vindumi* | S8103 | CAS248147 | "Myitkyina Dist., Kachin, Myanmar" | 2211209 | - | - | - | - | - | - | - | - | - | - | - | - | - | - | - | - |
| *Porthidium dunni* | S1925 | AMNH 118314 | "Oaxaca, Mexico" | 3592027 | 96.0 | 912 | 1482 | 681 | 165 | 1602 | 685 | 784 | 1114 | 961 | 1030 | 343 | 1337 | 291 | 1710 | 522 |
| *Porthidium dunni* | S2040 | ENS 9705 | "Oaxaca, Mexico" | 316456 | - | - | - | - | - | - | - | - | - | - | - | - | - | - | - | - |

Table A.2: Sequence information for samples used in phylogenetic analyses

## A.5 *BEAST2 and ASTRALIII phylogeny of New World pitviper genera and *Bothriechis* species, phylogenies of New World pitviper genera and *Bothriechis* species for protein coding mitochondrial loci and ribosomal RNA, time-calibrated phylogenetic tree of snakes based on anchored phylogenetic loci and four fossil constraints, Change in AIC associated with additional reticulations in PhyloNet, SNaQ, and TreeMix, top five networks with two reticulations recovered by PhyloNet, and model evaluation statistics for ancestral area reconstruction in BioGeoBEARS

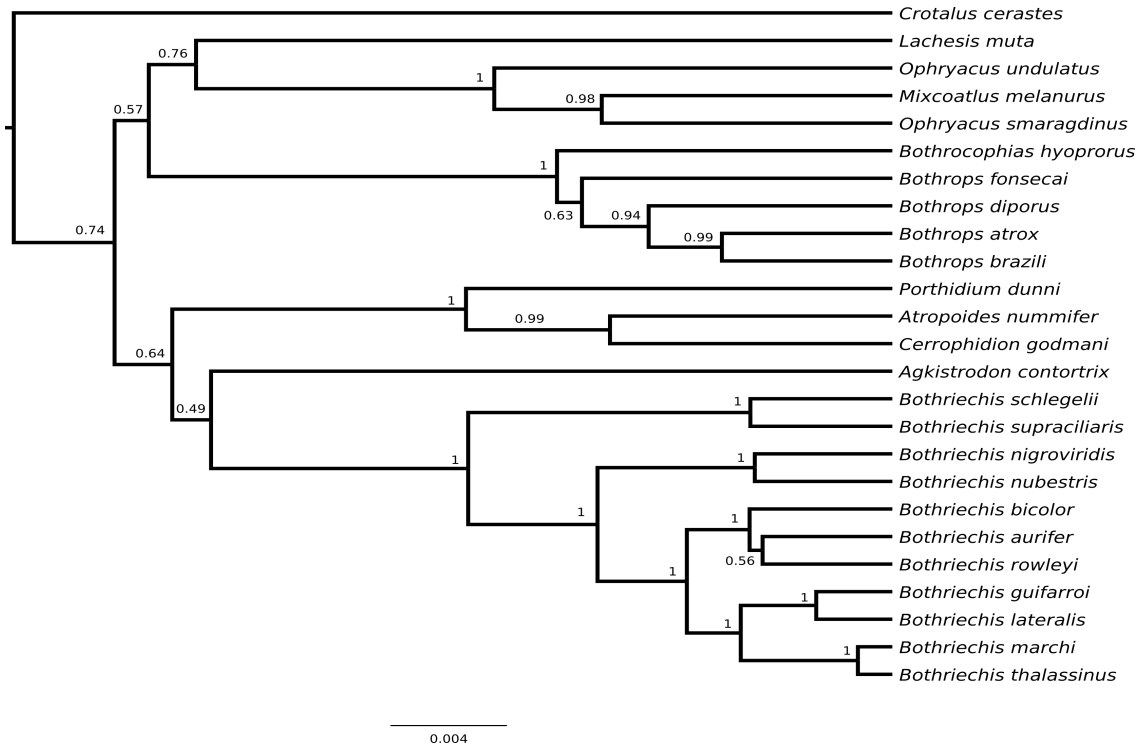


Figure A.1: *BEAST2 phylogeny of New World pitviper genera and *Bothriechis* species. Bayesian posterior probabilities are shown by nodes.

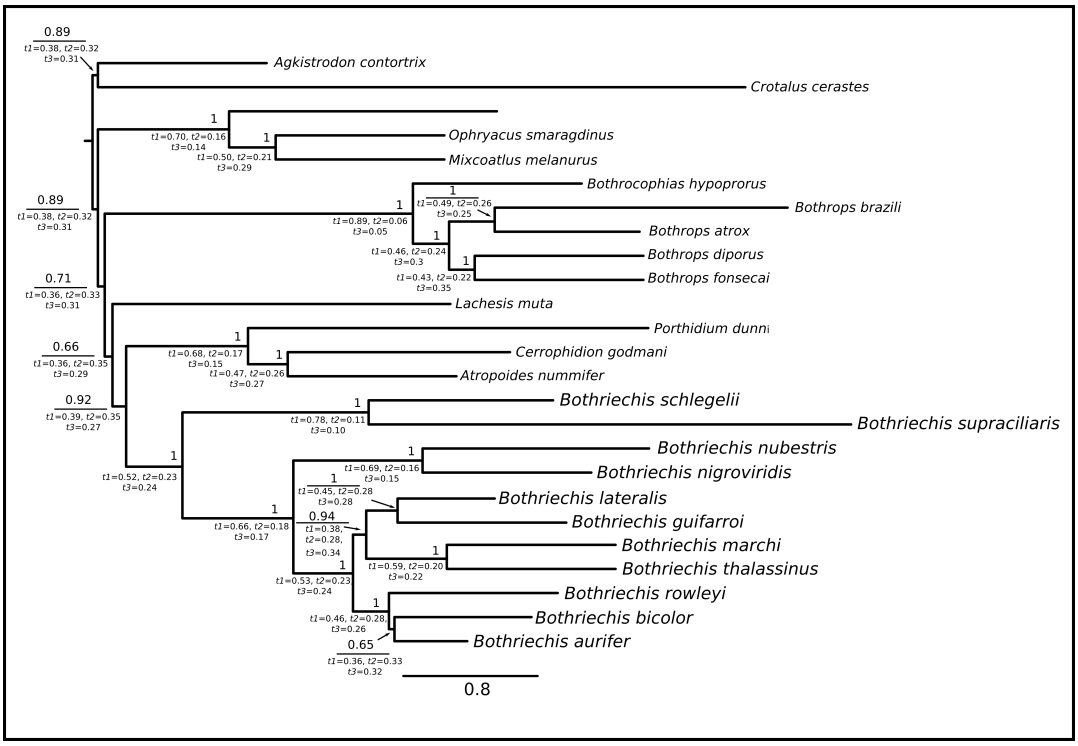


Figure A.2: ASTRALIII phylogeny of New World pitviper genera and *Bothriechis* species. Bayesian posterior probabilities (top values) and topology scores (bottom values) are shown by nodes.

| Model | LnL | DF null | AIC | AICwt |
|---|---|---|---|---|
| DEC | -16.50 | 2 | 37.00 | 0.52 |
| DIVALIKE | -16.57 | 2 | 37.13 | 0.48 |
| BAYAREALIKE | -23.47 | 2 | 50.94 | 0.00 |

Table A.3: Model evaluation statistics for ancestral area reconstruction in 'BioGeoBEARS'

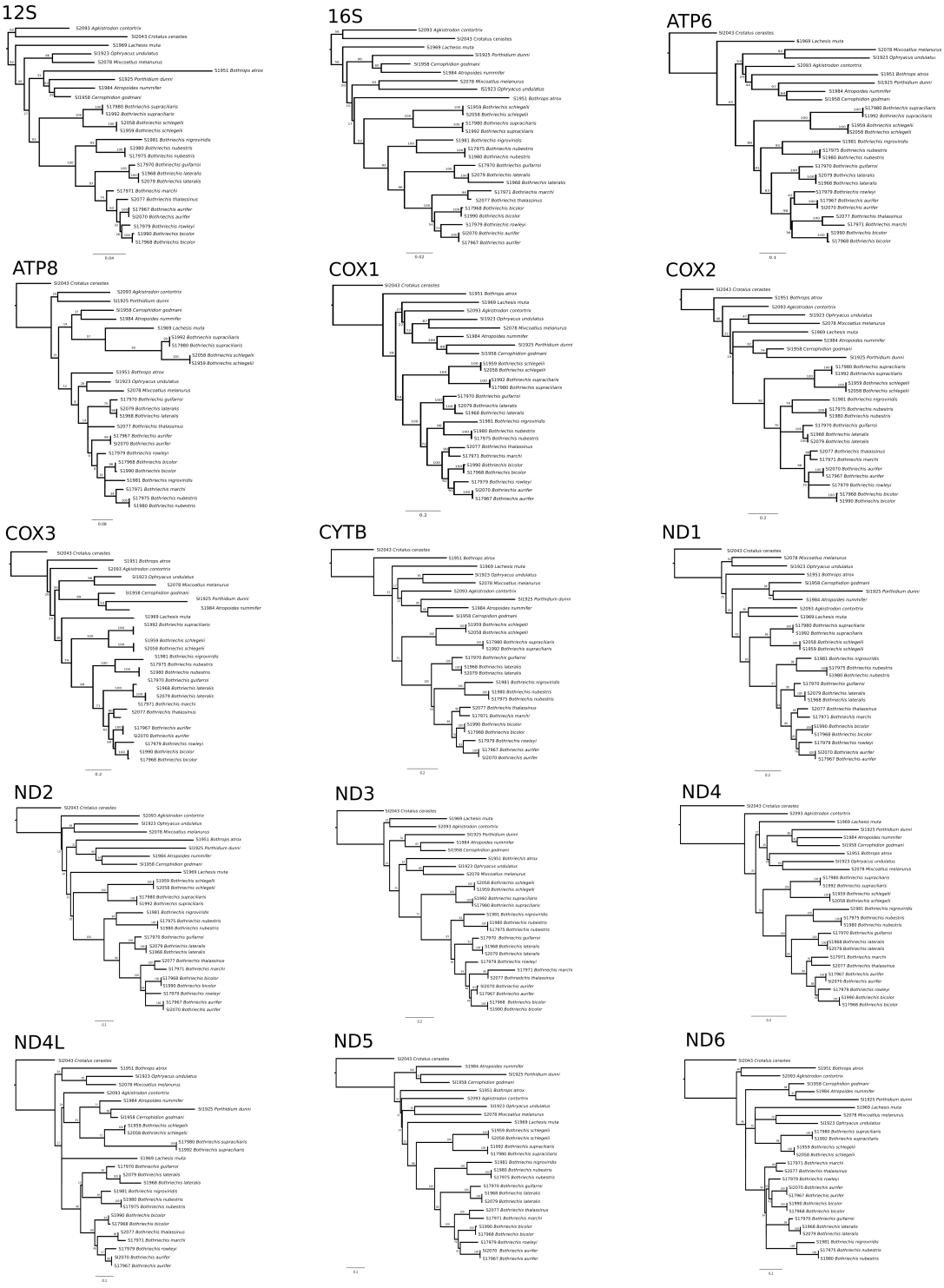


Figure A.3: Phylogenies of New World pitviper genera and *Bothriechis* species for protein coding mitochondrial loci and ribosomal RNA inferred in RAXML. Bootstrap support values are shown adjacent to nodes.

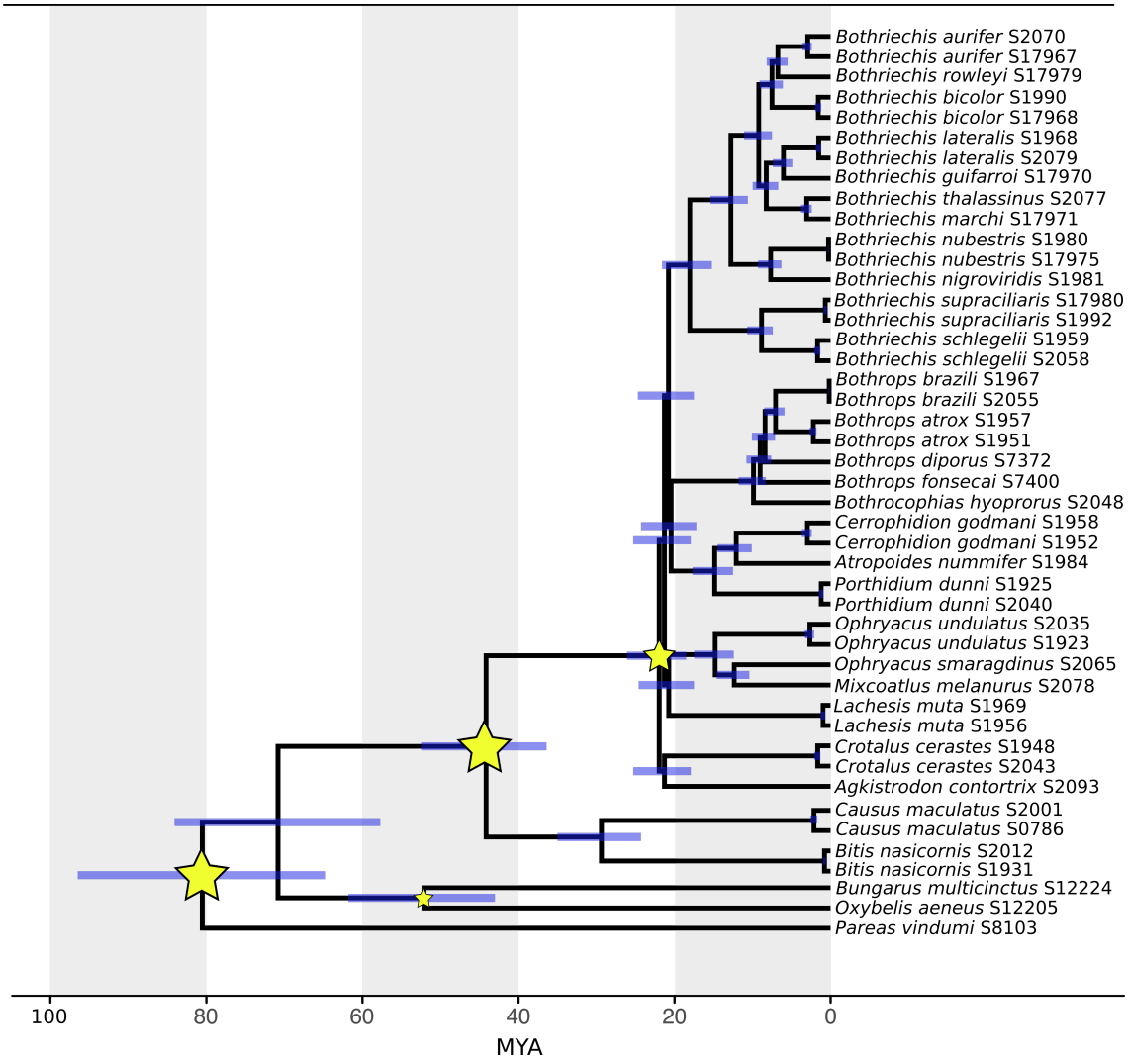


Figure A.4: Time-calibrated phylogenetic tree of snakes based on anchored phylogenetic loci and four fossil constraints indicated by stars. Blue node bars indicated the 95% confidence interval for of the node age estimate.

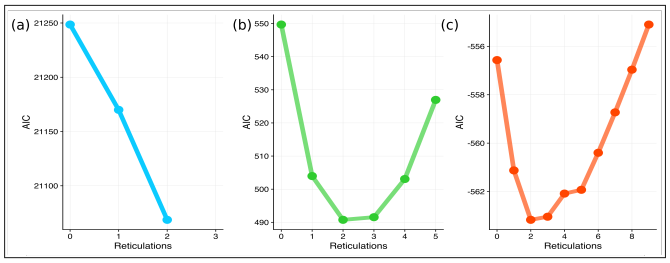


Figure A.5: Change in AIC associated with additional reticulations in (a) PhyloNet, (b) SNaQ, and (c) TreeMix. Models with two reticulations are optimal across the methods and are significantly better than models without reticulations (i.e., the species tree), indicating a role of gene flow/migration in the phylogeny.

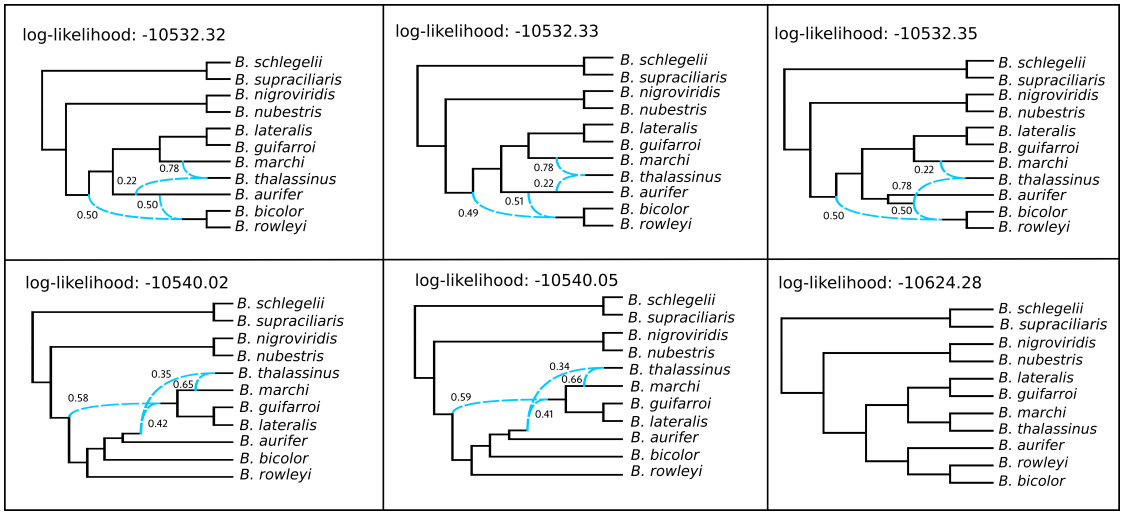


Figure A.6: Top five phylogenetic networks inferred using the maximum pseudolikelihood approach of PhyloNet allowing up to 2 reticulation events. Blue edges represent reticulation among lineages and the loglikelihood of each network is displayed.

## A.6 Supplementary tables for three-population tests, and four-population tests, and D-statistics

Table A.4: Results of the three-population tests implemented in TreeMix, using 368 putatively independent SNPs.

| Pop 1 | Pop 2 | Pop 3 | f3 | SE | Z-score |
|---|---|---|---|---|---|
| Baurifer | Bbicolor | Bguifarroi | 0.03 | 0.009 | 3.413 |
| Bbicolor | Baurifer | Bguifarroi | 0.041 | 0.01 | 4.214 |
| Bguifarroi | Baurifer | Bbicolor | 0.078 | 0.014 | 5.645 |
| Baurifer | Bbicolor | Bmarchi | 0.027 | 0.008 | 3.276 |
| Bbicolor | Baurifer | Bmarchi | 0.045 | 0.01 | 4.344 |
| Bmarchi | Baurifer | Bbicolor | 0.092 | 0.015 | 6.18 |
| Baurifer | Bbicolor | Bnubestris | 0.031 | 0.009 | 3.483 |
| Bbicolor | Baurifer | Bnubestris | 0.041 | 0.01 | 4.136 |
| Bnubestris | Baurifer | Bbicolor | 0.191 | 0.02 | 9.462 |
| Baurifer | Bbicolor | Browleyi | 0.022 | 0.008 | 2.906 |
| Bbicolor | Baurifer | Browleyi | 0.049 | 0.011 | 4.646 |
| Browleyi | Baurifer | Bbicolor | 0.067 | 0.013 | 5.138 |
| Baurifer | Bbicolor | Bsupraciliaris | 0.036 | 0.01 | 3.803 |
| Bbicolor | Baurifer | Bsupraciliaris | 0.035 | 0.009 | 3.872 |
| Bsupraciliaris | Baurifer | Bbicolor | 0.25 | 0.022 | 11.281 |
| Baurifer | Bbicolor | Bthalassinus | 0.031 | 0.009 | 3.603 |
| Bbicolor | Baurifer | Bthalassinus | 0.04 | 0.01 | 4.163 |
| Bthalassinus | Baurifer | Bbicolor | 0.094 | 0.015 | 6.157 |
| Baurifer | Bbicolor | Bschlegelii | 0.037 | 0.01 | 3.801 |
| Bbicolor | Baurifer | Bschlegelii | 0.035 | 0.009 | 3.848 |
| Bschlegelii | Baurifer | Bbicolor | 0.224 | 0.021 | 10.539 |
| Baurifer | Bbicolor | Blateralis | 0.034 | 0.01 | 3.493 |
| Bbicolor | Baurifer | Blateralis | 0.038 | 0.009 | 4.095 |
| Blateralis | Baurifer | Bbicolor | 0.092 | 0.015 | 6.313 |

| Pop 1 | Pop 2 | Pop 3 | f3 | SE | Z-score |
|---|---|---|---|---|---|
| Baurifer | Bbicolor | Bnigroviridis | 0.03 | 0.009 | 3.281 |
| Bbicolor | Baurifer | Bnigroviridis | 0.041 | 0.01 | 4.239 |
| Bnigroviridis | Baurifer | Bbicolor | 0.181 | 0.02 | 9.145 |
| Baurifer | Bguifarroi | Bmarchi | 0.062 | 0.012 | 5.065 |
| Bguifarroi | Baurifer | Bmarchi | 0.046 | 0.011 | 4.048 |
| Bmarchi | Baurifer | Bguifarroi | 0.057 | 0.012 | 4.868 |
| Baurifer | Bguifarroi | Bnubestris | 0.064 | 0.012 | 5.215 |
| Bguifarroi | Baurifer | Bnubestris | 0.044 | 0.011 | 4.013 |
| Bnubestris | Baurifer | Bguifarroi | 0.158 | 0.019 | 8.392 |
| Baurifer | Bguifarroi | Browleyi | 0.04 | 0.01 | 3.845 |
| Bguifarroi | Baurifer | Browleyi | 0.069 | 0.013 | 5.304 |
| Browleyi | Baurifer | Bguifarroi | 0.05 | 0.011 | 4.406 |
| Baurifer | Bguifarroi | Bsupraciliaris | 0.071 | 0.013 | 5.417 |
| Bguifarroi | Baurifer | Bsupraciliaris | 0.038 | 0.01 | 3.733 |
| Bsupraciliaris | Baurifer | Bguifarroi | 0.216 | 0.021 | 10.247 |
| Baurifer | Bguifarroi | Bthalassinus | 0.066 | 0.013 | 5.247 |
| Bguifarroi | Baurifer | Bthalassinus | 0.042 | 0.011 | 3.9 |
| Bthalassinus | Baurifer | Bguifarroi | 0.059 | 0.012 | 4.872 |
| Baurifer | Bguifarroi | Bschlegelii | 0.072 | 0.013 | 5.484 |
| Bguifarroi | Baurifer | Bschlegelii | 0.037 | 0.01 | 3.63 |
| Bschlegelii | Baurifer | Bguifarroi | 0.189 | 0.02 | 9.448 |
| Baurifer | Bguifarroi | Blateralis | 0.084 | 0.014 | 6.067 |
| Bguifarroi | Baurifer | Blateralis | 0.024 | 0.009 | 2.649 |
| Blateralis | Baurifer | Bguifarroi | 0.041 | 0.01 | 4.284 |
| Baurifer | Bguifarroi | Bnigroviridis | 0.062 | 0.012 | 5.08 |
| Bguifarroi | Baurifer | Bnigroviridis | 0.046 | 0.011 | 4.127 |
| Bnigroviridis | Baurifer | Bguifarroi | 0.148 | 0.018 | 8.064 |
| Baurifer | Bmarchi | Bnubestris | 0.052 | 0.012 | 4.485 |
| Bmarchi | Baurifer | Bnubestris | 0.067 | 0.013 | 5.24 |

| Pop 1 | Pop 2 | Pop 3 | f3 | SE | Z-score |
|---|---|---|---|---|---|
| Bnubestris | Baurifer | Bmarchi | 0.17 | 0.019 | 8.813 |
| Baurifer | Bmarchi | Browleyi | 0.031 | 0.009 | 3.628 |
| Bmarchi | Baurifer | Browleyi | 0.088 | 0.015 | 5.997 |
| Browleyi | Baurifer | Bmarchi | 0.058 | 0.012 | 4.701 |
| Baurifer | Bmarchi | Bsupraciliaris | 0.061 | 0.012 | 5.015 |
| Bmarchi | Baurifer | Bsupraciliaris | 0.058 | 0.012 | 4.81 |
| Bsupraciliaris | Baurifer | Bmarchi | 0.225 | 0.021 | 10.499 |
| Baurifer | Bmarchi | Bthalassinus | 0.097 | 0.014 | 6.695 |
| Bmarchi | Baurifer | Bthalassinus | 0.022 | 0.008 | 2.882 |
| Bthalassinus | Baurifer | Bmarchi | 0.028 | 0.01 | 2.856 |
| Baurifer | Bmarchi | Bschlegelii | 0.06 | 0.012 | 4.995 |
| Bmarchi | Baurifer | Bschlegelii | 0.059 | 0.012 | 4.814 |
| Bschlegelii | Baurifer | Bmarchi | 0.2 | 0.02 | 9.768 |
| Baurifer | Bmarchi | Blateralis | 0.064 | 0.013 | 5.054 |
| Blateralis | Baurifer | Bmarchi | 0.061 | 0.012 | 5.15 |
| Bmarchi | Baurifer | Blateralis | 0.055 | 0.012 | 4.658 |
| Baurifer | Bmarchi | Bnigroviridis | 0.056 | 0.012 | 4.678 |
| Bmarchi | Baurifer | Bnigroviridis | 0.063 | 0.012 | 5.048 |
| Bnigroviridis | Baurifer | Bmarchi | 0.155 | 0.019 | 8.276 |
| Baurifer | Bnubestris | Browleyi | 0.043 | 0.011 | 4.002 |
| Bnubestris | Baurifer | Browleyi | 0.18 | 0.02 | 9.119 |
| Browleyi | Baurifer | Bnubestris | 0.047 | 0.011 | 4.262 |
| Baurifer | Bnubestris | Bsupraciliaris | 0.092 | 0.015 | 6.181 |
| Bnubestris | Baurifer | Bsupraciliaris | 0.13 | 0.017 | 7.509 |
| Bsupraciliaris | Baurifer | Bnubestris | 0.194 | 0.02 | 9.603 |
| Baurifer | Bnubestris | Bthalassinus | 0.057 | 0.012 | 4.827 |
| Bnubestris | Baurifer | Bthalassinus | 0.165 | 0.019 | 8.673 |
| Bthalassinus | Baurifer | Bnubestris | 0.068 | 0.013 | 5.093 |
| Baurifer | Bnubestris | Bschlegelii | 0.095 | 0.015 | 6.303 |

| Pop 1 | Pop 2 | Pop 3 | f3 | SE | Z-score |
|---|---|---|---|---|---|
| Bnubestris | Baurifer | Bschlegelii | 0.127 | 0.017 | 7.428 |
| Bschlegelii | Baurifer | Bnubestris | 0.165 | 0.019 | 8.685 |
| Baurifer | Bnubestris | Blateralis | 0.063 | 0.012 | 5.064 |
| Blateralis | Baurifer | Bnubestris | 0.063 | 0.013 | 5.018 |
| Bnubestris | Baurifer | Blateralis | 0.159 | 0.019 | 8.5 |
| Baurifer | Bnubestris | Bnigroviridis | 0.14 | 0.018 | 7.853 |
| Bnigroviridis | Baurifer | Bnubestris | 0.071 | 0.013 | 5.292 |
| Bnubestris | Baurifer | Bnigroviridis | 0.082 | 0.014 | 5.828 |
| Baurifer | Browleyi | Bsupraciliaris | 0.047 | 0.011 | 4.323 |
| Browleyi | Baurifer | Bsupraciliaris | 0.042 | 0.011 | 4.025 |
| Bsupraciliaris | Baurifer | Browleyi | 0.239 | 0.022 | 10.96 |
| Baurifer | Browleyi | Bthalassinus | 0.036 | 0.009 | 3.932 |
| Browleyi | Baurifer | Bthalassinus | 0.053 | 0.012 | 4.592 |
| Bthalassinus | Baurifer | Browleyi | 0.089 | 0.015 | 5.918 |
| Baurifer | Browleyi | Bschlegelii | 0.048 | 0.011 | 4.401 |
| Browleyi | Baurifer | Bschlegelii | 0.041 | 0.011 | 3.927 |
| Bschlegelii | Baurifer | Browleyi | 0.212 | 0.021 | 10.167 |
| Baurifer | Browleyi | Blateralis | 0.043 | 0.011 | 4.002 |
| Blateralis | Baurifer | Browleyi | 0.083 | 0.014 | 5.986 |
| Browleyi | Baurifer | Blateralis | 0.047 | 0.011 | 4.262 |
| Baurifer | Browleyi | Bnigroviridis | 0.039 | 0.01 | 3.774 |
| Bnigroviridis | Baurifer | Browleyi | 0.172 | 0.019 | 8.861 |
| Browleyi | Baurifer | Bnigroviridis | 0.051 | 0.011 | 4.455 |
| Baurifer | Bsupraciliaris | Bthalassinus | 0.063 | 0.012 | 5.202 |
| Bsupraciliaris | Baurifer | Bthalassinus | 0.223 | 0.021 | 10.506 |
| Bthalassinus | Baurifer | Bsupraciliaris | 0.062 | 0.013 | 4.78 |
| Baurifer | Bsupraciliaris | Bschlegelii | 0.217 | 0.021 | 10.373 |
| Bschlegelii | Baurifer | Bsupraciliaris | 0.043 | 0.01 | 4.248 |
| Bsupraciliaris | Baurifer | Bschlegelii | 0.069 | 0.013 | 5.31 |

| Pop 1 | Pop 2 | Pop 3 | f3 | SE | Z-score |
|---|---|---|---|---|---|
| Baurifer | Bsupraciliaris | Blateralis | 0.075 | 0.013 | 5.636 |
| Blateralis | Baurifer | Bsupraciliaris | 0.05 | 0.011 | 4.463 |
| Bsupraciliaris | Baurifer | Blateralis | 0.211 | 0.021 | 10.128 |
| Baurifer | Bsupraciliaris | Bnigroviridis | 0.105 | 0.016 | 6.705 |
| Bnigroviridis | Baurifer | Bsupraciliaris | 0.106 | 0.016 | 6.595 |
| Bsupraciliaris | Baurifer | Bnigroviridis | 0.181 | 0.02 | 9.179 |
| Baurifer | Bthalassinus | Bschlegelii | 0.065 | 0.012 | 5.295 |
| Bschlegelii | Baurifer | Bthalassinus | 0.196 | 0.02 | 9.694 |
| Bthalassinus | Baurifer | Bschlegelii | 0.061 | 0.013 | 4.671 |
| Baurifer | Bthalassinus | Blateralis | 0.067 | 0.013 | 5.2 |
| Blateralis | Baurifer | Bthalassinus | 0.058 | 0.012 | 5.014 |
| Bthalassinus | Baurifer | Blateralis | 0.058 | 0.012 | 4.738 |
| Baurifer | Bthalassinus | Bnigroviridis | 0.059 | 0.012 | 4.892 |
| Bnigroviridis | Baurifer | Bthalassinus | 0.151 | 0.018 | 8.216 |
| Bthalassinus | Baurifer | Bnigroviridis | 0.066 | 0.013 | 5.013 |
| Baurifer | Bschlegelii | Blateralis | 0.077 | 0.013 | 5.749 |
| Blateralis | Baurifer | Bschlegelii | 0.049 | 0.011 | 4.364 |
| Bschlegelii | Baurifer | Blateralis | 0.183 | 0.02 | 9.281 |
| Baurifer | Bschlegelii | Bnigroviridis | 0.102 | 0.015 | 6.609 |
| Bnigroviridis | Baurifer | Bschlegelii | 0.109 | 0.016 | 6.754 |
| Bschlegelii | Baurifer | Bnigroviridis | 0.158 | 0.019 | 8.433 |
| Baurifer | Blateralis | Bnigroviridis | 0.067 | 0.013 | 5.294 |
| Blateralis | Baurifer | Bnigroviridis | 0.059 | 0.012 | 4.814 |
| Bnigroviridis | Baurifer | Blateralis | 0.144 | 0.018 | 7.946 |
| Bbicolor | Bguifarroi | Bmarchi | 0.077 | 0.014 | 5.663 |
| Bguifarroi | Bbicolor | Bmarchi | 0.043 | 0.011 | 3.797 |
| Bmarchi | Bbicolor | Bguifarroi | 0.06 | 0.012 | 4.882 |
| Bbicolor | Bguifarroi | Bnubestris | 0.074 | 0.013 | 5.539 |
| Bguifarroi | Bbicolor | Bnubestris | 0.045 | 0.011 | 4.025 |

| Pop 1 | Pop 2 | Pop 3 | f3 | SE | Z-score |
|---|---|---|---|---|---|
| Bnubestris | Bbicolor | Bguifarroi | 0.157 | 0.019 | 8.354 |
| Bbicolor | Bguifarroi | Browleyi | 0.059 | 0.012 | 4.922 |
| Bguifarroi | Bbicolor | Browleyi | 0.061 | 0.013 | 4.837 |
| Browleyi | Bbicolor | Bguifarroi | 0.057 | 0.012 | 4.604 |
| Bbicolor | Bguifarroi | Bsupraciliaris | 0.076 | 0.014 | 5.548 |
| Bguifarroi | Bbicolor | Bsupraciliaris | 0.044 | 0.011 | 4.005 |
| Bsupraciliaris | Bbicolor | Bguifarroi | 0.21 | 0.021 | 10.046 |
| Bbicolor | Bguifarroi | Bthalassinus | 0.076 | 0.014 | 5.615 |
| Bguifarroi | Bbicolor | Bthalassinus | 0.043 | 0.011 | 3.853 |
| Bthalassinus | Bbicolor | Bguifarroi | 0.058 | 0.012 | 4.791 |
| Bbicolor | Bguifarroi | Bschlegelii | 0.077 | 0.014 | 5.608 |
| Bguifarroi | Bbicolor | Bschlegelii | 0.043 | 0.011 | 3.931 |
| Bschlegelii | Bbicolor | Bguifarroi | 0.182 | 0.02 | 9.224 |
| Bbicolor | Bguifarroi | Blateralis | 0.092 | 0.015 | 6.287 |
| Bguifarroi | Bbicolor | Blateralis | 0.027 | 0.01 | 2.846 |
| Blateralis | Bbicolor | Bguifarroi | 0.038 | 0.009 | 4.003 |
| Bbicolor | Bguifarroi | Bnigroviridis | 0.073 | 0.013 | 5.477 |
| Bguifarroi | Bbicolor | Bnigroviridis | 0.046 | 0.011 | 4.096 |
| Bnigroviridis | Bbicolor | Bguifarroi | 0.148 | 0.019 | 8.01 |
| Bbicolor | Bmarchi | Bnubestris | 0.066 | 0.013 | 5.076 |
| Bmarchi | Bbicolor | Bnubestris | 0.072 | 0.013 | 5.307 |
| Bnubestris | Bbicolor | Bmarchi | 0.166 | 0.019 | 8.644 |
| Bbicolor | Bmarchi | Browleyi | 0.054 | 0.012 | 4.627 |
| Bmarchi | Bbicolor | Browleyi | 0.083 | 0.014 | 5.78 |
| Browleyi | Bbicolor | Bmarchi | 0.062 | 0.013 | 4.862 |
| Bbicolor | Bmarchi | Bsupraciliaris | 0.07 | 0.013 | 5.224 |
| Bmarchi | Bbicolor | Bsupraciliaris | 0.067 | 0.013 | 5.159 |
| Bsupraciliaris | Bbicolor | Bmarchi | 0.216 | 0.021 | 10.229 |
| Bbicolor | Bmarchi | Bthalassinus | 0.111 | 0.016 | 6.989 |

| Pop 1 | Pop 2 | Pop 3 | f3 | SE | Z-score |
|---|---|---|---|---|---|
| Bmarchi | Bbicolor | Bthalassinus | 0.026 | 0.008 | 3.212 |
| Bthalassinus | Bbicolor | Bmarchi | 0.024 | 0.01 | 2.489 |
| Bbicolor | Bmarchi | Bschlegelii | 0.068 | 0.013 | 5.2 |
| Bmarchi | Bbicolor | Bschlegelii | 0.069 | 0.013 | 5.186 |
| Bschlegelii | Bbicolor | Bmarchi | 0.19 | 0.02 | 9.471 |
| Bbicolor | Bmarchi | Blateralis | 0.075 | 0.014 | 5.493 |
| Blateralis | Bbicolor | Bmarchi | 0.055 | 0.012 | 4.746 |
| Bmarchi | Bbicolor | Blateralis | 0.062 | 0.013 | 4.859 |
| Bbicolor | Bmarchi | Bnigroviridis | 0.071 | 0.013 | 5.285 |
| Bmarchi | Bbicolor | Bnigroviridis | 0.066 | 0.013 | 5.096 |
| Bnigroviridis | Bbicolor | Bmarchi | 0.151 | 0.019 | 8.097 |
| Bbicolor | Bnubestris | Browleyi | 0.061 | 0.012 | 4.988 |
| Bnubestris | Bbicolor | Browleyi | 0.171 | 0.019 | 8.775 |
| Browleyi | Bbicolor | Bnubestris | 0.055 | 0.012 | 4.519 |
| Bbicolor | Bnubestris | Bsupraciliaris | 0.097 | 0.015 | 6.394 |
| Bnubestris | Bbicolor | Bsupraciliaris | 0.135 | 0.018 | 7.652 |
| Bsupraciliaris | Bbicolor | Bnubestris | 0.189 | 0.02 | 9.323 |
| Bbicolor | Bnubestris | Bthalassinus | 0.067 | 0.013 | 5.161 |
| Bnubestris | Bbicolor | Bthalassinus | 0.165 | 0.019 | 8.624 |
| Bthalassinus | Bbicolor | Bnubestris | 0.067 | 0.013 | 5.067 |
| Bbicolor | Bnubestris | Bschlegelii | 0.099 | 0.015 | 6.511 |
| Bnubestris | Bbicolor | Bschlegelii | 0.133 | 0.018 | 7.536 |
| Bschlegelii | Bbicolor | Bnubestris | 0.16 | 0.019 | 8.429 |
| Bbicolor | Bnubestris | Blateralis | 0.07 | 0.013 | 5.381 |
| Blateralis | Bbicolor | Bnubestris | 0.06 | 0.012 | 4.806 |
| Bnubestris | Bbicolor | Blateralis | 0.162 | 0.019 | 8.516 |
| Bbicolor | Bnubestris | Bnigroviridis | 0.15 | 0.018 | 8.163 |
| Bnigroviridis | Bbicolor | Bnubestris | 0.072 | 0.014 | 5.234 |
| Bnubestris | Bbicolor | Bnigroviridis | 0.081 | 0.014 | 5.755 |

| Pop 1 | Pop 2 | Pop 3 | f3 | SE | Z-score |
|---|---|---|---|---|---|
| Bbicolor | Browleyi | Bsupraciliaris | 0.06 | 0.012 | 4.912 |
| Browleyi | Bbicolor | Bsupraciliaris | 0.056 | 0.012 | 4.599 |
| Bsupraciliaris | Bbicolor | Browleyi | 0.226 | 0.021 | 10.513 |
| Bbicolor | Browleyi | Bthalassinus | 0.054 | 0.011 | 4.692 |
| Browleyi | Bbicolor | Bthalassinus | 0.062 | 0.013 | 4.918 |
| Bthalassinus | Bbicolor | Browleyi | 0.081 | 0.014 | 5.561 |
| Bbicolor | Browleyi | Bschlegelii | 0.061 | 0.012 | 4.979 |
| Browleyi | Bbicolor | Bschlegelii | 0.055 | 0.012 | 4.532 |
| Bschlegelii | Bbicolor | Browleyi | 0.198 | 0.02 | 9.697 |
| Bbicolor | Browleyi | Blateralis | 0.058 | 0.012 | 4.878 |
| Blateralis | Bbicolor | Browleyi | 0.072 | 0.013 | 5.399 |
| Browleyi | Bbicolor | Blateralis | 0.058 | 0.012 | 4.646 |
| Bbicolor | Browleyi | Bnigroviridis | 0.058 | 0.012 | 4.835 |
| Bnigroviridis | Bbicolor | Browleyi | 0.164 | 0.019 | 8.507 |
| Browleyi | Bbicolor | Bnigroviridis | 0.058 | 0.012 | 4.679 |
| Bbicolor | Bsupraciliaris | Bthalassinus | 0.067 | 0.013 | 5.168 |
| Bsupraciliaris | Bbicolor | Bthalassinus | 0.218 | 0.021 | 10.353 |
| Bthalassinus | Bbicolor | Bsupraciliaris | 0.067 | 0.013 | 5.031 |
| Bbicolor | Bsupraciliaris | Bschlegelii | 0.216 | 0.021 | 10.191 |
| Bschlegelii | Bbicolor | Bsupraciliaris | 0.043 | 0.01 | 4.231 |
| Bsupraciliaris | Bbicolor | Bschlegelii | 0.069 | 0.013 | 5.334 |
| Bbicolor | Bsupraciliaris | Blateralis | 0.077 | 0.014 | 5.63 |
| Blateralis | Bbicolor | Bsupraciliaris | 0.053 | 0.012 | 4.525 |
| Bsupraciliaris | Bbicolor | Blateralis | 0.209 | 0.021 | 10.02 |
| Bbicolor | Bsupraciliaris | Bnigroviridis | 0.11 | 0.016 | 6.857 |
| Bnigroviridis | Bbicolor | Bsupraciliaris | 0.112 | 0.016 | 6.778 |
| Bsupraciliaris | Bbicolor | Bnigroviridis | 0.175 | 0.02 | 8.92 |
| Bbicolor | Bthalassinus | Bschlegelii | 0.068 | 0.013 | 5.257 |
| Bschlegelii | Bbicolor | Bthalassinus | 0.19 | 0.02 | 9.515 |

| Pop 1 | Pop 2 | Pop 3 | f3 | SE | Z-score |
|---|---|---|---|---|---|
| Bthalassinus | Bbicolor | Bschlegelii | 0.066 | 0.013 | 4.947 |
| Bbicolor | Bthalassinus | Blateralis | 0.074 | 0.014 | 5.412 |
| Blateralis | Bbicolor | Bthalassinus | 0.056 | 0.012 | 4.772 |
| Bthalassinus | Bbicolor | Blateralis | 0.061 | 0.013 | 4.834 |
| Bbicolor | Bthalassinus | Bnigroviridis | 0.069 | 0.013 | 5.258 |
| Bnigroviridis | Bbicolor | Bthalassinus | 0.153 | 0.019 | 8.162 |
| Bthalassinus | Bbicolor | Bnigroviridis | 0.065 | 0.013 | 4.964 |
| Bbicolor | Bschlegelii | Blateralis | 0.078 | 0.014 | 5.738 |
| Blateralis | Bbicolor | Bschlegelii | 0.051 | 0.012 | 4.448 |
| Bschlegelii | Bbicolor | Blateralis | 0.181 | 0.02 | 9.152 |
| Bbicolor | Bschlegelii | Bnigroviridis | 0.107 | 0.016 | 6.764 |
| Bnigroviridis | Bbicolor | Bschlegelii | 0.115 | 0.017 | 6.901 |
| Bschlegelii | Bbicolor | Bnigroviridis | 0.152 | 0.019 | 8.192 |
| Bbicolor | Blateralis | Bnigroviridis | 0.074 | 0.013 | 5.547 |
| Blateralis | Bbicolor | Bnigroviridis | 0.055 | 0.012 | 4.619 |
| Bnigroviridis | Bbicolor | Blateralis | 0.148 | 0.018 | 7.992 |
| Bguifarroi | Bmarchi | Bnubestris | 0.034 | 0.01 | 3.316 |
| Bmarchi | Bguifarroi | Bnubestris | 0.069 | 0.013 | 5.218 |
| Bnubestris | Bguifarroi | Bmarchi | 0.168 | 0.019 | 8.723 |
| Bguifarroi | Bmarchi | Browleyi | 0.038 | 0.011 | 3.492 |
| Bmarchi | Bguifarroi | Browleyi | 0.065 | 0.013 | 5.077 |
| Browleyi | Bguifarroi | Bmarchi | 0.08 | 0.014 | 5.713 |
| Bguifarroi | Bmarchi | Bsupraciliaris | 0.037 | 0.011 | 3.503 |
| Bmarchi | Bguifarroi | Bsupraciliaris | 0.066 | 0.013 | 5.083 |
| Bsupraciliaris | Bguifarroi | Bmarchi | 0.216 | 0.021 | 10.293 |
| Bguifarroi | Bmarchi | Bthalassinus | 0.077 | 0.014 | 5.647 |
| Bmarchi | Bguifarroi | Bthalassinus | 0.026 | 0.008 | 3.138 |
| Bthalassinus | Bguifarroi | Bmarchi | 0.024 | 0.01 | 2.555 |
| Bguifarroi | Bmarchi | Bschlegelii | 0.035 | 0.01 | 3.377 |

| Pop 1 | Pop 2 | Pop 3 | f3 | SE | Z-score |
|---|---|---|---|---|---|
| Bmarchi | Bguifarroi | Bschlegelii | 0.069 | 0.013 | 5.169 |
| Bschlegelii | Bguifarroi | Bmarchi | 0.19 | 0.02 | 9.494 |
| Bguifarroi | Bmarchi | Blateralis | 0.026 | 0.009 | 2.807 |
| Blateralis | Bguifarroi | Bmarchi | 0.039 | 0.01 | 4.069 |
| Bmarchi | Bguifarroi | Blateralis | 0.077 | 0.014 | 5.545 |
| Bguifarroi | Bmarchi | Bnigroviridis | 0.04 | 0.011 | 3.68 |
| Bmarchi | Bguifarroi | Bnigroviridis | 0.063 | 0.013 | 4.941 |
| Bnigroviridis | Bguifarroi | Bmarchi | 0.154 | 0.019 | 8.223 |
| Bguifarroi | Bnubestris | Browleyi | 0.047 | 0.011 | 4.119 |
| Bnubestris | Bguifarroi | Browleyi | 0.155 | 0.019 | 8.263 |
| Browleyi | Bguifarroi | Bnubestris | 0.071 | 0.013 | 5.267 |
| Bguifarroi | Bnubestris | Bsupraciliaris | 0.066 | 0.013 | 5.071 |
| Bnubestris | Bguifarroi | Bsupraciliaris | 0.136 | 0.018 | 7.658 |
| Bsupraciliaris | Bguifarroi | Bnubestris | 0.187 | 0.02 | 9.318 |
| Bguifarroi | Bnubestris | Bthalassinus | 0.036 | 0.01 | 3.485 |
| Bnubestris | Bguifarroi | Bthalassinus | 0.166 | 0.019 | 8.666 |
| Bthalassinus | Bguifarroi | Bnubestris | 0.066 | 0.013 | 5.023 |
| Bguifarroi | Bnubestris | Bschlegelii | 0.068 | 0.013 | 5.142 |
| Bnubestris | Bguifarroi | Bschlegelii | 0.135 | 0.018 | 7.592 |
| Bschlegelii | Bguifarroi | Bnubestris | 0.157 | 0.019 | 8.375 |
| Bguifarroi | Bnubestris | Blateralis | 0.023 | 0.009 | 2.494 |
| Blateralis | Bguifarroi | Bnubestris | 0.042 | 0.01 | 4.15 |
| Bnubestris | Bguifarroi | Blateralis | 0.18 | 0.02 | 9.158 |
| Bguifarroi | Bnubestris | Bnigroviridis | 0.122 | 0.017 | 7.134 |
| Bnigroviridis | Bguifarroi | Bnubestris | 0.072 | 0.014 | 5.293 |
| Bnubestris | Bguifarroi | Bnigroviridis | 0.081 | 0.014 | 5.696 |
| Bguifarroi | Browleyi | Bsupraciliaris | 0.045 | 0.011 | 4.009 |
| Browleyi | Bguifarroi | Bsupraciliaris | 0.073 | 0.014 | 5.352 |
| Bsupraciliaris | Bguifarroi | Browleyi | 0.209 | 0.021 | 10.017 |

| Pop 1 | Pop 2 | Pop 3 | f3 | SE | Z-score |
|---|---|---|---|---|---|
| Bguifarroi | Browleyi | Bthalassinus | 0.039 | 0.011 | 3.606 |
| Browleyi | Bguifarroi | Bthalassinus | 0.079 | 0.014 | 5.721 |
| Bthalassinus | Bguifarroi | Browleyi | 0.063 | 0.013 | 4.879 |
| Bguifarroi | Browleyi | Bschlegelii | 0.045 | 0.011 | 4.009 |
| Browleyi | Bguifarroi | Bschlegelii | 0.073 | 0.014 | 5.352 |
| Bschlegelii | Bguifarroi | Browleyi | 0.18 | 0.02 | 9.147 |
| Bguifarroi | Browleyi | Blateralis | 0.027 | 0.01 | 2.792 |
| Blateralis | Bguifarroi | Browleyi | 0.038 | 0.009 | 4.05 |
| Browleyi | Bguifarroi | Blateralis | 0.091 | 0.015 | 6.134 |
| Bguifarroi | Browleyi | Bnigroviridis | 0.045 | 0.011 | 4.009 |
| Bnigroviridis | Bguifarroi | Browleyi | 0.149 | 0.019 | 8.033 |
| Browleyi | Bguifarroi | Bnigroviridis | 0.073 | 0.014 | 5.352 |
| Bguifarroi | Bsupraciliaris | Bthalassinus | 0.035 | 0.01 | 3.471 |
| Bsupraciliaris | Bguifarroi | Bthalassinus | 0.218 | 0.021 | 10.381 |
| Bthalassinus | Bguifarroi | Bsupraciliaris | 0.067 | 0.013 | 5.005 |
| Bguifarroi | Bsupraciliaris | Bschlegelii | 0.183 | 0.02 | 9.16 |
| Bschlegelii | Bguifarroi | Bsupraciliaris | 0.042 | 0.01 | 4.146 |
| Bsupraciliaris | Bguifarroi | Bschlegelii | 0.07 | 0.013 | 5.402 |
| Bguifarroi | Bsupraciliaris | Blateralis | 0.028 | 0.01 | 2.898 |
| Blateralis | Bguifarroi | Bsupraciliaris | 0.037 | 0.01 | 3.841 |
| Bsupraciliaris | Bguifarroi | Blateralis | 0.225 | 0.021 | 10.642 |
| Bguifarroi | Bsupraciliaris | Bnigroviridis | 0.081 | 0.014 | 5.672 |
| Bnigroviridis | Bguifarroi | Bsupraciliaris | 0.114 | 0.017 | 6.842 |
| Bsupraciliaris | Bguifarroi | Bnigroviridis | 0.173 | 0.02 | 8.862 |
| Bguifarroi | Bthalassinus | Bschlegelii | 0.035 | 0.01 | 3.501 |
| Bschlegelii | Bguifarroi | Bthalassinus | 0.19 | 0.02 | 9.501 |
| Bthalassinus | Bguifarroi | Bschlegelii | 0.067 | 0.013 | 4.979 |
| Bguifarroi | Bthalassinus | Blateralis | 0.025 | 0.009 | 2.723 |
| Blateralis | Bguifarroi | Bthalassinus | 0.04 | 0.01 | 4.112 |

| Pop 1 | Pop 2 | Pop 3 | f3 | SE | Z-score |
|---|---|---|---|---|---|
| Bthalassinus | Bguifarroi | Blateralis | 0.077 | 0.014 | 5.55 |
| Bguifarroi | Bthalassinus | Bnigroviridis | 0.039 | 0.011 | 3.695 |
| Bnigroviridis | Bguifarroi | Bthalassinus | 0.155 | 0.019 | 8.25 |
| Bthalassinus | Bguifarroi | Bnigroviridis | 0.063 | 0.013 | 4.857 |
| Bguifarroi | Bschlegelii | Blateralis | 0.029 | 0.01 | 2.963 |
| Blateralis | Bguifarroi | Bschlegelii | 0.036 | 0.009 | 3.836 |
| Bschlegelii | Bguifarroi | Blateralis | 0.196 | 0.02 | 9.736 |
| Bguifarroi | Bschlegelii | Bnigroviridis | 0.076 | 0.014 | 5.498 |
| Bnigroviridis | Bguifarroi | Bschlegelii | 0.118 | 0.017 | 7.013 |
| Bschlegelii | Bguifarroi | Bnigroviridis | 0.149 | 0.018 | 8.089 |
| Bguifarroi | Blateralis | Bnigroviridis | 0.028 | 0.01 | 2.881 |
| Blateralis | Bguifarroi | Bnigroviridis | 0.037 | 0.01 | 3.859 |
| Bnigroviridis | Bguifarroi | Blateralis | 0.166 | 0.019 | 8.699 |
| Bmarchi | Bnubestris | Browleyi | 0.078 | 0.014 | 5.564 |
| Bnubestris | Bmarchi | Browleyi | 0.159 | 0.019 | 8.369 |
| Browleyi | Bmarchi | Bnubestris | 0.067 | 0.013 | 5.071 |
| Bmarchi | Bnubestris | Bsupraciliaris | 0.099 | 0.016 | 6.332 |
| Bnubestris | Bmarchi | Bsupraciliaris | 0.139 | 0.018 | 7.766 |
| Bsupraciliaris | Bmarchi | Bnubestris | 0.184 | 0.02 | 9.214 |
| Bmarchi | Bnubestris | Bthalassinus | 0.028 | 0.008 | 3.338 |
| Bnubestris | Bmarchi | Bthalassinus | 0.21 | 0.021 | 10.075 |
| Bthalassinus | Bmarchi | Bnubestris | 0.022 | 0.01 | 2.344 |
| Bmarchi | Bnubestris | Bschlegelii | 0.102 | 0.016 | 6.468 |
| Bnubestris | Bmarchi | Bschlegelii | 0.136 | 0.018 | 7.631 |
| Bschlegelii | Bmarchi | Bnubestris | 0.157 | 0.019 | 8.337 |
| Blateralis | Bmarchi | Bnubestris | 0.051 | 0.011 | 4.403 |
| Bmarchi | Bnubestris | Blateralis | 0.066 | 0.013 | 5.056 |
| Bnubestris | Bmarchi | Blateralis | 0.172 | 0.019 | 8.822 |
| Bmarchi | Bnubestris | Bnigroviridis | 0.151 | 0.019 | 8.071 |

| Pop 1 | Pop 2 | Pop 3 | f3 | SE | Z-score |
|---|---|---|---|---|---|
| Bnigroviridis | Bmarchi | Bnubestris | 0.066 | 0.013 | 5.02 |
| Bnubestris | Bmarchi | Bnigroviridis | 0.087 | 0.015 | 5.946 |
| Bmarchi | Browleyi | Bsupraciliaris | 0.073 | 0.014 | 5.348 |
| Browleyi | Bmarchi | Bsupraciliaris | 0.072 | 0.014 | 5.296 |
| Bsupraciliaris | Bmarchi | Browleyi | 0.21 | 0.021 | 10.016 |
| Bmarchi | Browleyi | Bthalassinus | 0.026 | 0.008 | 3.212 |
| Browleyi | Bmarchi | Bthalassinus | 0.119 | 0.017 | 7.171 |
| Bthalassinus | Bmarchi | Browleyi | 0.024 | 0.01 | 2.489 |
| Bmarchi | Browleyi | Bschlegelii | 0.075 | 0.014 | 5.431 |
| Browleyi | Bmarchi | Bschlegelii | 0.07 | 0.013 | 5.207 |
| Bschlegelii | Bmarchi | Browleyi | 0.184 | 0.02 | 9.212 |
| Blateralis | Bmarchi | Browleyi | 0.05 | 0.011 | 4.515 |
| Bmarchi | Browleyi | Blateralis | 0.066 | 0.013 | 5.015 |
| Browleyi | Bmarchi | Blateralis | 0.079 | 0.014 | 5.593 |
| Bmarchi | Browleyi | Bnigroviridis | 0.07 | 0.013 | 5.212 |
| Bnigroviridis | Bmarchi | Browleyi | 0.147 | 0.019 | 7.93 |
| Browleyi | Bmarchi | Bnigroviridis | 0.075 | 0.014 | 5.427 |
| Bmarchi | Bsupraciliaris | Bthalassinus | 0.024 | 0.008 | 3.043 |
| Bsupraciliaris | Bmarchi | Bthalassinus | 0.259 | 0.022 | 11.631 |
| Bthalassinus | Bmarchi | Bsupraciliaris | 0.026 | 0.01 | 2.674 |
| Bmarchi | Bsupraciliaris | Bschlegelii | 0.215 | 0.021 | 10.069 |
| Bschlegelii | Bmarchi | Bsupraciliaris | 0.044 | 0.01 | 4.249 |
| Bsupraciliaris | Bmarchi | Bschlegelii | 0.068 | 0.013 | 5.314 |
| Blateralis | Bmarchi | Bsupraciliaris | 0.048 | 0.011 | 4.273 |
| Bmarchi | Bsupraciliaris | Blateralis | 0.069 | 0.013 | 5.172 |
| Bsupraciliaris | Bmarchi | Blateralis | 0.214 | 0.021 | 10.211 |
| Bmarchi | Bsupraciliaris | Bnigroviridis | 0.107 | 0.016 | 6.619 |
| Bnigroviridis | Bmarchi | Bsupraciliaris | 0.111 | 0.016 | 6.726 |
| Bsupraciliaris | Bmarchi | Bnigroviridis | 0.176 | 0.02 | 8.967 |

| Pop 1 | Pop 2 | Pop 3 | f3 | SE | Z-score |
|---|---|---|---|---|---|
| Bmarchi | Bthalassinus | Bschlegelii | 0.026 | 0.008 | 3.212 |
| Bschlegelii | Bmarchi | Bthalassinus | 0.233 | 0.021 | 10.818 |
| Bthalassinus | Bmarchi | Bschlegelii | 0.024 | 0.01 | 2.489 |
| Blateralis | Bmarchi | Bthalassinus | 0.091 | 0.014 | 6.358 |
| Bmarchi | Bthalassinus | Blateralis | 0.025 | 0.008 | 3.042 |
| Bthalassinus | Bmarchi | Blateralis | 0.025 | 0.01 | 2.608 |
| Bmarchi | Bthalassinus | Bnigroviridis | 0.025 | 0.008 | 3.174 |
| Bnigroviridis | Bmarchi | Bthalassinus | 0.192 | 0.02 | 9.489 |
| Bthalassinus | Bmarchi | Bnigroviridis | 0.025 | 0.01 | 2.534 |
| Blateralis | Bmarchi | Bschlegelii | 0.045 | 0.011 | 4.161 |
| Bmarchi | Bschlegelii | Blateralis | 0.072 | 0.014 | 5.306 |
| Bschlegelii | Bmarchi | Blateralis | 0.187 | 0.02 | 9.366 |
| Bmarchi | Bschlegelii | Bnigroviridis | 0.105 | 0.016 | 6.542 |
| Bnigroviridis | Bmarchi | Bschlegelii | 0.113 | 0.017 | 6.826 |
| Bschlegelii | Bmarchi | Bnigroviridis | 0.154 | 0.019 | 8.261 |
| Blateralis | Bmarchi | Bnigroviridis | 0.051 | 0.011 | 4.442 |
| Bmarchi | Blateralis | Bnigroviridis | 0.066 | 0.013 | 5.02 |
| Bnigroviridis | Bmarchi | Blateralis | 0.152 | 0.019 | 8.146 |
| Bnubestris | Browleyi | Bsupraciliaris | 0.134 | 0.018 | 7.592 |
| Browleyi | Bnubestris | Bsupraciliaris | 0.092 | 0.015 | 6.086 |
| Bsupraciliaris | Bnubestris | Browleyi | 0.19 | 0.02 | 9.381 |
| Bnubestris | Browleyi | Bthalassinus | 0.158 | 0.019 | 8.348 |
| Browleyi | Bnubestris | Bthalassinus | 0.068 | 0.013 | 5.155 |
| Bthalassinus | Bnubestris | Browleyi | 0.074 | 0.014 | 5.335 |
| Bnubestris | Browleyi | Bschlegelii | 0.132 | 0.018 | 7.526 |
| Browleyi | Bnubestris | Bschlegelii | 0.094 | 0.015 | 6.148 |
| Bschlegelii | Bnubestris | Browleyi | 0.16 | 0.019 | 8.44 |
| Blateralis | Bnubestris | Browleyi | 0.063 | 0.013 | 4.917 |
| Bnubestris | Browleyi | Blateralis | 0.159 | 0.019 | 8.423 |

| Pop 1 | Pop 2 | Pop 3 | f3 | SE | Z-score |
|---|---|---|---|---|---|
| Browleyi | Bnubestris | Blateralis | 0.067 | 0.013 | 5.113 |
| Bnigroviridis | Bnubestris | Browleyi | 0.075 | 0.014 | 5.378 |
| Bnubestris | Browleyi | Bnigroviridis | 0.078 | 0.014 | 5.617 |
| Browleyi | Bnubestris | Bnigroviridis | 0.148 | 0.019 | 7.967 |
| Bnubestris | Bsupraciliaris | Bthalassinus | 0.135 | 0.018 | 7.658 |
| Bsupraciliaris | Bnubestris | Bthalassinus | 0.188 | 0.02 | 9.36 |
| Bthalassinus | Bnubestris | Bsupraciliaris | 0.097 | 0.016 | 6.229 |
| Bnubestris | Bsupraciliaris | Bschlegelii | 0.252 | 0.022 | 11.192 |
| Bschlegelii | Bnubestris | Bsupraciliaris | 0.041 | 0.01 | 4.132 |
| Bsupraciliaris | Bnubestris | Bschlegelii | 0.072 | 0.013 | 5.398 |
| Blateralis | Bnubestris | Bsupraciliaris | 0.08 | 0.014 | 5.752 |
| Bnubestris | Bsupraciliaris | Blateralis | 0.142 | 0.018 | 7.855 |
| Bsupraciliaris | Bnubestris | Blateralis | 0.181 | 0.02 | 9.133 |
| Bnigroviridis | Bnubestris | Bsupraciliaris | 0.058 | 0.012 | 4.665 |
| Bnubestris | Bsupraciliaris | Bnigroviridis | 0.095 | 0.015 | 6.249 |
| Bsupraciliaris | Bnubestris | Bnigroviridis | 0.229 | 0.022 | 10.583 |
| Bnubestris | Bthalassinus | Bschlegelii | 0.134 | 0.018 | 7.609 |
| Bschlegelii | Bnubestris | Bthalassinus | 0.158 | 0.019 | 8.402 |
| Bthalassinus | Bnubestris | Bschlegelii | 0.098 | 0.016 | 6.267 |
| Blateralis | Bnubestris | Bthalassinus | 0.053 | 0.012 | 4.528 |
| Bnubestris | Bthalassinus | Blateralis | 0.169 | 0.019 | 8.739 |
| Bthalassinus | Bnubestris | Blateralis | 0.063 | 0.013 | 4.92 |
| Bnigroviridis | Bnubestris | Bthalassinus | 0.069 | 0.013 | 5.134 |
| Bnubestris | Bthalassinus | Bnigroviridis | 0.084 | 0.014 | 5.844 |
| Bthalassinus | Bnubestris | Bnigroviridis | 0.148 | 0.019 | 7.994 |
| Blateralis | Bnubestris | Bschlegelii | 0.081 | 0.014 | 5.812 |
| Bnubestris | Bschlegelii | Blateralis | 0.141 | 0.018 | 7.828 |
| Bschlegelii | Bnubestris | Blateralis | 0.151 | 0.019 | 8.137 |
| Bnigroviridis | Bnubestris | Bschlegelii | 0.064 | 0.013 | 4.968 |

| Pop 1 | Pop 2 | Pop 3 | f3 | SE | Z-score |
|---|---|---|---|---|---|
| Bnubestris | Bschlegelii | Bnigroviridis | 0.089 | 0.015 | 6.028 |
| Bschlegelii | Bnubestris | Bnigroviridis | 0.203 | 0.021 | 9.768 |
| Blateralis | Bnubestris | Bnigroviridis | 0.136 | 0.018 | 7.675 |
| Bnigroviridis | Bnubestris | Blateralis | 0.067 | 0.013 | 5.056 |
| Bnubestris | Blateralis | Bnigroviridis | 0.086 | 0.015 | 5.914 |
| Browleyi | Bsupraciliaris | Bthalassinus | 0.07 | 0.013 | 5.238 |
| Bsupraciliaris | Browleyi | Bthalassinus | 0.212 | 0.021 | 10.139 |
| Bthalassinus | Browleyi | Bsupraciliaris | 0.073 | 0.014 | 5.229 |
| Browleyi | Bsupraciliaris | Bschlegelii | 0.212 | 0.021 | 9.976 |
| Bschlegelii | Browleyi | Bsupraciliaris | 0.042 | 0.01 | 4.146 |
| Bsupraciliaris | Browleyi | Bschlegelii | 0.07 | 0.013 | 5.402 |
| Blateralis | Browleyi | Bsupraciliaris | 0.055 | 0.012 | 4.56 |
| Browleyi | Bsupraciliaris | Blateralis | 0.075 | 0.014 | 5.446 |
| Bsupraciliaris | Browleyi | Blateralis | 0.207 | 0.021 | 9.988 |
| Bnigroviridis | Browleyi | Bsupraciliaris | 0.114 | 0.017 | 6.842 |
| Browleyi | Bsupraciliaris | Bnigroviridis | 0.109 | 0.016 | 6.694 |
| Bsupraciliaris | Browleyi | Bnigroviridis | 0.173 | 0.02 | 8.862 |
| Browleyi | Bthalassinus | Bschlegelii | 0.07 | 0.013 | 5.261 |
| Bschlegelii | Browleyi | Bthalassinus | 0.184 | 0.02 | 9.256 |
| Bthalassinus | Browleyi | Bschlegelii | 0.073 | 0.014 | 5.204 |
| Blateralis | Browleyi | Bthalassinus | 0.052 | 0.011 | 4.61 |
| Browleyi | Bthalassinus | Blateralis | 0.078 | 0.014 | 5.565 |
| Bthalassinus | Browleyi | Blateralis | 0.065 | 0.013 | 4.886 |
| Bnigroviridis | Browleyi | Bthalassinus | 0.149 | 0.019 | 7.995 |
| Browleyi | Bthalassinus | Bnigroviridis | 0.074 | 0.014 | 5.399 |
| Bthalassinus | Browleyi | Bnigroviridis | 0.069 | 0.013 | 5.085 |
| Blateralis | Browleyi | Bschlegelii | 0.054 | 0.012 | 4.551 |
| Browleyi | Bschlegelii | Blateralis | 0.076 | 0.014 | 5.493 |
| Bschlegelii | Browleyi | Blateralis | 0.178 | 0.02 | 9.072 |

| Pop 1 | Pop 2 | Pop 3 | f3 | SE | Z-score |
|---|---|---|---|---|---|
| Bnigroviridis | Browleyi | Bschlegelii | 0.118 | 0.017 | 7.013 |
| Browleyi | Bschlegelii | Bnigroviridis | 0.105 | 0.016 | 6.54 |
| Bschlegelii | Browleyi | Bnigroviridis | 0.149 | 0.018 | 8.089 |
| Blateralis | Browleyi | Bnigroviridis | 0.055 | 0.012 | 4.574 |
| Bnigroviridis | Browleyi | Blateralis | 0.148 | 0.018 | 8.011 |
| Browleyi | Blateralis | Bnigroviridis | 0.075 | 0.014 | 5.433 |
| Bschlegelii | Bsupraciliaris | Bthalassinus | 0.042 | 0.01 | 4.117 |
| Bsupraciliaris | Bthalassinus | Bschlegelii | 0.071 | 0.013 | 5.423 |
| Bthalassinus | Bsupraciliaris | Bschlegelii | 0.215 | 0.021 | 10.097 |
| Blateralis | Bsupraciliaris | Bthalassinus | 0.046 | 0.011 | 4.241 |
| Bsupraciliaris | Bthalassinus | Blateralis | 0.215 | 0.021 | 10.273 |
| Bthalassinus | Bsupraciliaris | Blateralis | 0.07 | 0.014 | 5.158 |
| Bnigroviridis | Bsupraciliaris | Bthalassinus | 0.109 | 0.016 | 6.701 |
| Bsupraciliaris | Bthalassinus | Bnigroviridis | 0.177 | 0.02 | 9.03 |
| Bthalassinus | Bsupraciliaris | Bnigroviridis | 0.108 | 0.016 | 6.618 |
| Blateralis | Bsupraciliaris | Bschlegelii | 0.191 | 0.02 | 9.43 |
| Bschlegelii | Bsupraciliaris | Blateralis | 0.041 | 0.01 | 4.071 |
| Bsupraciliaris | Bschlegelii | Blateralis | 0.071 | 0.013 | 5.451 |
| Bnigroviridis | Bsupraciliaris | Bschlegelii | 0.221 | 0.021 | 10.27 |
| Bschlegelii | Bsupraciliaris | Bnigroviridis | 0.046 | 0.011 | 4.408 |
| Bsupraciliaris | Bschlegelii | Bnigroviridis | 0.066 | 0.013 | 5.15 |
| Blateralis | Bsupraciliaris | Bnigroviridis | 0.089 | 0.015 | 6.093 |
| Bnigroviridis | Bsupraciliaris | Blateralis | 0.114 | 0.017 | 6.853 |
| Bsupraciliaris | Blateralis | Bnigroviridis | 0.173 | 0.02 | 8.852 |
| Blateralis | Bthalassinus | Bschlegelii | 0.046 | 0.011 | 4.26 |
| Bschlegelii | Bthalassinus | Blateralis | 0.186 | 0.02 | 9.346 |
| Bthalassinus | Bschlegelii | Blateralis | 0.07 | 0.014 | 5.18 |
| Bnigroviridis | Bthalassinus | Bschlegelii | 0.114 | 0.017 | 6.896 |
| Bschlegelii | Bthalassinus | Bnigroviridis | 0.153 | 0.019 | 8.24 |

| Pop 1 | Pop 2 | Pop 3 | f3 | SE | Z-score |
|---|---|---|---|---|---|
| Bthalassinus | Bschlegelii | Bnigroviridis | 0.103 | 0.016 | 6.442 |
| Blateralis | Bthalassinus | Bnigroviridis | 0.051 | 0.011 | 4.442 |
| Bnigroviridis | Bthalassinus | Blateralis | 0.152 | 0.019 | 8.146 |
| Bthalassinus | Blateralis | Bnigroviridis | 0.066 | 0.013 | 5 |
| Blateralis | Bschlegelii | Bnigroviridis | 0.084 | 0.014 | 5.886 |
| Bnigroviridis | Bschlegelii | Blateralis | 0.119 | 0.017 | 7.03 |
| Bschlegelii | Blateralis | Bnigroviridis | 0.148 | 0.018 | 8.099 |

Table A.5: Results of the four-population tests implemented in TreeMix, using 368 putatively independent SNPs.

| Pop 1 | Pop 2 | Pop 3 | Pop 4 | f4 | SE f4 | Z-score |
|---|---|---|---|---|---|---|
| Baurifer | Bbicolor | Bguifarroi | Bmarchi | -0.003 | 0.005 | -0.7 |
| Baurifer | Bguifarroi | Bbicolor | Bmarchi | 0.032 | 0.011 | 2.999 |
| Baurifer | Bmarchi | Bbicolor | Bguifarroi | 0.035 | 0.01 | 3.5 |
| Baurifer | Bbicolor | Bguifarroi | Bnubestris | 0.001 | 0.005 | 0.14 |
| Baurifer | Bguifarroi | Bbicolor | Bnubestris | 0.034 | 0.01 | 3.299 |
| Baurifer | Bnubestris | Bbicolor | Bguifarroi | 0.033 | 0.01 | 3.223 |
| Baurifer | Bbicolor | Bguifarroi | Browleyi | -0.008 | 0.007 | -1.121 |
| Baurifer | Bguifarroi | Bbicolor | Browleyi | 0.009 | 0.01 | 0.954 |
| Baurifer | Browleyi | Bbicolor | Bguifarroi | 0.017 | 0.009 | 1.984 |
| Baurifer | Bbicolor | Bguifarroi | Bsupraciliaris | 0.006 | 0.004 | 1.323 |
| Baurifer | Bguifarroi | Bbicolor | Bsupraciliaris | 0.04 | 0.01 | 3.887 |
| Baurifer | Bsupraciliaris | Bbicolor | Bguifarroi | 0.034 | 0.011 | 3.094 |
| Baurifer | Bbicolor | Bguifarroi | Bthalassinus | 0.001 | 0.005 | 0.203 |
| Baurifer | Bguifarroi | Bbicolor | Bthalassinus | 0.035 | 0.011 | 3.346 |
| Baurifer | Bthalassinus | Bbicolor | Bguifarroi | 0.034 | 0.011 | 3.21 |
| Baurifer | Bbicolor | Bguifarroi | Bschlegelii | 0.006 | 0.004 | 1.446 |
| Baurifer | Bguifarroi | Bbicolor | Bschlegelii | 0.041 | 0.01 | 4.025 |
| Baurifer | Bschlegelii | Bbicolor | Bguifarroi | 0.035 | 0.011 | 3.176 |
| Baurifer | Bbicolor | Bguifarroi | Blateralis | 0.003 | 0.004 | 0.786 |
| Baurifer | Bguifarroi | Bbicolor | Blateralis | 0.054 | 0.012 | 4.661 |
| Baurifer | Blateralis | Bbicolor | Bguifarroi | 0.051 | 0.012 | 4.182 |
| Baurifer | Bbicolor | Bguifarroi | Bnigroviridis | 0 | 0.005 | 0 |
| Baurifer | Bguifarroi | Bbicolor | Bnigroviridis | 0.032 | 0.01 | 3.103 |
| Baurifer | Bnigroviridis | Bbicolor | Bguifarroi | 0.032 | 0.01 | 3.076 |
| Baurifer | Bbicolor | Bmarchi | Bnubestris | 0.004 | 0.006 | 0.654 |
| Baurifer | Bmarchi | Bbicolor | Bnubestris | 0.025 | 0.01 | 2.524 |

| Pop 1 | Pop 2 | Pop 3 | Pop 4 | f4 | SE f4 | Z-score |
|---|---|---|---|---|---|---|
| Baurifer | Bnubestris | Bbicolor | Bmarchi | 0.021 | 0.01 | 1.992 |
| Baurifer | Bbicolor | Bmarchi | Browleyi | -0.004 | 0.006 | -0.691 |
| Baurifer | Bmarchi | Bbicolor | Browleyi | 0.005 | 0.008 | 0.577 |
| Baurifer | Browleyi | Bbicolor | Bmarchi | 0.009 | 0.007 | 1.235 |
| Baurifer | Bbicolor | Bmarchi | Bsupraciliaris | 0.009 | 0.006 | 1.562 |
| Baurifer | Bmarchi | Bbicolor | Bsupraciliaris | 0.034 | 0.01 | 3.397 |
| Baurifer | Bsupraciliaris | Bbicolor | Bmarchi | 0.025 | 0.011 | 2.206 |
| Baurifer | Bbicolor | Bmarchi | Bthalassinus | 0.004 | 0.005 | 0.899 |
| Baurifer | Bmarchi | Bbicolor | Bthalassinus | 0.07 | 0.013 | 5.285 |
| Baurifer | Bthalassinus | Bbicolor | Bmarchi | 0.066 | 0.014 | 4.814 |
| Baurifer | Bbicolor | Bmarchi | Bschlegelii | 0.01 | 0.006 | 1.638 |
| Baurifer | Bmarchi | Bbicolor | Bschlegelii | 0.033 | 0.01 | 3.404 |
| Baurifer | Bschlegelii | Bbicolor | Bmarchi | 0.024 | 0.011 | 2.129 |
| Baurifer | Bbicolor | Bmarchi | Blateralis | 0.007 | 0.006 | 1.095 |
| Baurifer | Blateralis | Bbicolor | Bmarchi | 0.03 | 0.012 | 2.573 |
| Baurifer | Bmarchi | Bbicolor | Blateralis | 0.037 | 0.011 | 3.455 |
| Baurifer | Bbicolor | Bmarchi | Bnigroviridis | 0.003 | 0.007 | 0.487 |
| Baurifer | Bmarchi | Bbicolor | Bnigroviridis | 0.029 | 0.011 | 2.72 |
| Baurifer | Bnigroviridis | Bbicolor | Bmarchi | 0.026 | 0.011 | 2.281 |
| Baurifer | Bbicolor | Bnubestris | Browleyi | -0.008 | 0.007 | -1.213 |
| Baurifer | Bnubestris | Bbicolor | Browleyi | 0.012 | 0.01 | 1.135 |
| Baurifer | Browleyi | Bbicolor | Bnubestris | 0.02 | 0.009 | 2.215 |
| Baurifer | Bbicolor | Bnubestris | Bsupraciliaris | 0.005 | 0.006 | 0.846 |
| Baurifer | Bnubestris | Bbicolor | Bsupraciliaris | 0.061 | 0.013 | 4.576 |
| Baurifer | Bsupraciliaris | Bbicolor | Bnubestris | 0.056 | 0.014 | 4.042 |
| Baurifer | Bbicolor | Bnubestris | Bthalassinus | 0 | 0.006 | 0.053 |
| Baurifer | Bnubestris | Bbicolor | Bthalassinus | 0.026 | 0.011 | 2.517 |
| Baurifer | Bthalassinus | Bbicolor | Bnubestris | 0.026 | 0.011 | 2.46 |
| Baurifer | Bbicolor | Bnubestris | Bschlegelii | 0.006 | 0.006 | 0.869 |

| Pop 1 | Pop 2 | Pop 3 | Pop 4 | f4 | SE f4 | Z-score |
|---|---|---|---|---|---|---|
| Baurifer | Bnubestris | Bbicolor | Bschlegelii | 0.064 | 0.014 | 4.718 |
| Baurifer | Bschlegelii | Bbicolor | Bnubestris | 0.058 | 0.014 | 4.123 |
| Baurifer | Bbicolor | Bnubestris | Blateralis | 0.003 | 0.006 | 0.42 |
| Baurifer | Blateralis | Bbicolor | Bnubestris | 0.029 | 0.011 | 2.629 |
| Baurifer | Bnubestris | Bbicolor | Blateralis | 0.032 | 0.01 | 3.033 |
| Baurifer | Bbicolor | Bnubestris | Bnigroviridis | -0.001 | 0.005 | -0.126 |
| Baurifer | Bnigroviridis | Bbicolor | Bnubestris | 0.11 | 0.017 | 6.465 |
| Baurifer | Bnubestris | Bbicolor | Bnigroviridis | 0.109 | 0.017 | 6.436 |
| Baurifer | Bbicolor | Browleyi | Bsupraciliaris | 0.014 | 0.007 | 2.023 |
| Baurifer | Browleyi | Bbicolor | Bsupraciliaris | 0.024 | 0.009 | 2.806 |
| Baurifer | Bsupraciliaris | Bbicolor | Browleyi | 0.011 | 0.011 | 0.999 |
| Baurifer | Bbicolor | Browleyi | Bthalassinus | 0.009 | 0.007 | 1.353 |
| Baurifer | Browleyi | Bbicolor | Bthalassinus | 0.013 | 0.007 | 1.835 |
| Baurifer | Bthalassinus | Bbicolor | Browleyi | 0.005 | 0.009 | 0.526 |
| Baurifer | Bbicolor | Browleyi | Bschlegelii | 0.014 | 0.007 | 2.102 |
| Baurifer | Browleyi | Bbicolor | Bschlegelii | 0.025 | 0.009 | 2.967 |
| Baurifer | Bschlegelii | Bbicolor | Browleyi | 0.011 | 0.011 | 1.081 |
| Baurifer | Bbicolor | Browleyi | Blateralis | 0.011 | 0.007 | 1.609 |
| Baurifer | Blateralis | Bbicolor | Browleyi | 0.009 | 0.01 | 0.869 |
| Baurifer | Browleyi | Bbicolor | Blateralis | 0.02 | 0.008 | 2.383 |
| Baurifer | Bbicolor | Browleyi | Bnigroviridis | 0.008 | 0.008 | 1.012 |
| Baurifer | Bnigroviridis | Bbicolor | Browleyi | 0.008 | 0.01 | 0.815 |
| Baurifer | Browleyi | Bbicolor | Bnigroviridis | 0.016 | 0.009 | 1.789 |
| Baurifer | Bbicolor | Bsupraciliaris | Bthalassinus | -0.005 | 0.006 | -0.805 |
| Baurifer | Bsupraciliaris | Bbicolor | Bthalassinus | 0.027 | 0.011 | 2.449 |
| Baurifer | Bthalassinus | Bbicolor | Bsupraciliaris | 0.032 | 0.01 | 3.068 |
| Baurifer | Bbicolor | Bsupraciliaris | Bschlegelii | 0 | 0.001 | 0.308 |
| Baurifer | Bschlegelii | Bbicolor | Bsupraciliaris | 0.181 | 0.02 | 9.095 |
| Baurifer | Bsupraciliaris | Bbicolor | Bschlegelii | 0.181 | 0.02 | 9.126 |

| Pop 1 | Pop 2 | Pop 3 | Pop 4 | f4 | SE f4 | Z-score |
|---|---|---|---|---|---|---|
| Baurifer | Bbicolor | Bsupraciliaris | Blateralis | -0.003 | 0.004 | -0.571 |
| Baurifer | Blateralis | Bbicolor | Bsupraciliaris | 0.041 | 0.011 | 3.841 |
| Baurifer | Bsupraciliaris | Bbicolor | Blateralis | 0.039 | 0.011 | 3.56 |
| Baurifer | Bbicolor | Bsupraciliaris | Bnigroviridis | -0.006 | 0.005 | -1.172 |
| Baurifer | Bnigroviridis | Bbicolor | Bsupraciliaris | 0.075 | 0.014 | 5.375 |
| Baurifer | Bsupraciliaris | Bbicolor | Bnigroviridis | 0.069 | 0.014 | 4.798 |
| Baurifer | Bbicolor | Bthalassinus | Bschlegelii | 0.005 | 0.006 | 0.87 |
| Baurifer | Bschlegelii | Bbicolor | Bthalassinus | 0.028 | 0.011 | 2.556 |
| Baurifer | Bthalassinus | Bbicolor | Bschlegelii | 0.033 | 0.01 | 3.222 |
| Baurifer | Bbicolor | Bthalassinus | Blateralis | 0.002 | 0.006 | 0.376 |
| Baurifer | Blateralis | Bbicolor | Bthalassinus | 0.033 | 0.012 | 2.843 |
| Baurifer | Bthalassinus | Bbicolor | Blateralis | 0.036 | 0.011 | 3.151 |
| Baurifer | Bbicolor | Bthalassinus | Bnigroviridis | -0.001 | 0.006 | -0.172 |
| Baurifer | Bnigroviridis | Bbicolor | Bthalassinus | 0.029 | 0.011 | 2.764 |
| Baurifer | Bthalassinus | Bbicolor | Bnigroviridis | 0.028 | 0.011 | 2.655 |
| Baurifer | Bbicolor | Bschlegelii | Blateralis | -0.003 | 0.004 | -0.668 |
| Baurifer | Blateralis | Bbicolor | Bschlegelii | 0.043 | 0.011 | 4.03 |
| Baurifer | Bschlegelii | Bbicolor | Blateralis | 0.04 | 0.011 | 3.702 |
| Baurifer | Bbicolor | Bschlegelii | Bnigroviridis | -0.006 | 0.005 | -1.165 |
| Baurifer | Bnigroviridis | Bbicolor | Bschlegelii | 0.072 | 0.014 | 5.262 |
| Baurifer | Bschlegelii | Bbicolor | Bnigroviridis | 0.065 | 0.014 | 4.609 |
| Baurifer | Bbicolor | Blateralis | Bnigroviridis | -0.003 | 0.007 | -0.511 |
| Baurifer | Blateralis | Bbicolor | Bnigroviridis | 0.033 | 0.011 | 2.888 |
| Baurifer | Bnigroviridis | Bbicolor | Blateralis | 0.036 | 0.011 | 3.33 |
| Baurifer | Bguifarroi | Bmarchi | Bnubestris | 0.002 | 0.009 | 0.208 |
| Baurifer | Bmarchi | Bguifarroi | Bnubestris | -0.01 | 0.007 | -1.449 |
| Baurifer | Bnubestris | Bguifarroi | Bmarchi | -0.012 | 0.007 | -1.633 |
| Baurifer | Bguifarroi | Bmarchi | Browleyi | -0.022 | 0.011 | -1.985 |
| Baurifer | Bmarchi | Bguifarroi | Browleyi | -0.031 | 0.01 | -3.065 |

| Pop 1 | Pop 2 | Pop 3 | Pop 4 | f4 | SE f4 | Z-score |
|---|---|---|---|---|---|---|
| Baurifer | Browleyi | Bguifarroi | Bmarchi | -0.008 | 0.007 | -1.145 |
| Baurifer | Bguifarroi | Bmarchi | Bsupraciliaris | 0.008 | 0.008 | 1.036 |
| Baurifer | Bmarchi | Bguifarroi | Bsupraciliaris | -0.001 | 0.006 | -0.106 |
| Baurifer | Bsupraciliaris | Bguifarroi | Bmarchi | -0.009 | 0.008 | -1.117 |
| Baurifer | Bguifarroi | Bmarchi | Bthalassinus | 0.004 | 0.005 | 0.753 |
| Baurifer | Bmarchi | Bguifarroi | Bthalassinus | 0.035 | 0.009 | 3.761 |
| Baurifer | Bthalassinus | Bguifarroi | Bmarchi | 0.031 | 0.01 | 3.199 |
| Baurifer | Bguifarroi | Bmarchi | Bschlegelii | 0.01 | 0.008 | 1.191 |
| Baurifer | Bmarchi | Bguifarroi | Bschlegelii | -0.002 | 0.006 | -0.328 |
| Baurifer | Bschlegelii | Bguifarroi | Bmarchi | -0.012 | 0.008 | -1.488 |
| Baurifer | Bguifarroi | Bmarchi | Blateralis | 0.022 | 0.009 | 2.553 |
| Baurifer | Blateralis | Bguifarroi | Bmarchi | -0.02 | 0.009 | -2.314 |
| Baurifer | Bmarchi | Bguifarroi | Blateralis | 0.002 | 0.005 | 0.377 |
| Baurifer | Bguifarroi | Bmarchi | Bnigroviridis | 0 | 0.009 | 0.038 |
| Baurifer | Bmarchi | Bguifarroi | Bnigroviridis | -0.006 | 0.008 | -0.717 |
| Baurifer | Bnigroviridis | Bguifarroi | Bmarchi | -0.006 | 0.008 | -0.742 |
| Baurifer | Bguifarroi | Bnubestris | Browleyi | -0.024 | 0.009 | -2.756 |
| Baurifer | Bnubestris | Bguifarroi | Browleyi | -0.021 | 0.009 | -2.316 |
| Baurifer | Browleyi | Bguifarroi | Bnubestris | 0.003 | 0.006 | 0.522 |
| Baurifer | Bguifarroi | Bnubestris | Bsupraciliaris | 0.007 | 0.005 | 1.264 |
| Baurifer | Bnubestris | Bguifarroi | Bsupraciliaris | 0.029 | 0.009 | 3.095 |
| Baurifer | Bsupraciliaris | Bguifarroi | Bnubestris | 0.022 | 0.01 | 2.136 |
| Baurifer | Bguifarroi | Bnubestris | Bthalassinus | 0.002 | 0.008 | 0.228 |
| Baurifer | Bnubestris | Bguifarroi | Bthalassinus | -0.006 | 0.007 | -0.963 |
| Baurifer | Bthalassinus | Bguifarroi | Bnubestris | -0.008 | 0.007 | -1.148 |
| Baurifer | Bguifarroi | Bnubestris | Bschlegelii | 0.008 | 0.006 | 1.416 |
| Baurifer | Bnubestris | Bguifarroi | Bschlegelii | 0.031 | 0.009 | 3.294 |
| Baurifer | Bschlegelii | Bguifarroi | Bnubestris | 0.023 | 0.011 | 2.186 |
| Baurifer | Bguifarroi | Bnubestris | Blateralis | 0.02 | 0.008 | 2.612 |

| Pop 1 | Pop 2 | Pop 3 | Pop 4 | f4 | SE f4 | Z-score |
|---|---|---|---|---|---|---|
| Baurifer | Blateralis | Bguifarroi | Bnubestris | -0.022 | 0.008 | -2.833 |
| Baurifer | Bnubestris | Bguifarroi | Blateralis | -0.001 | 0.003 | -0.447 |
| Baurifer | Bguifarroi | Bnubestris | Bnigroviridis | -0.002 | 0.004 | -0.364 |
| Baurifer | Bnigroviridis | Bguifarroi | Bnubestris | 0.078 | 0.014 | 5.375 |
| Baurifer | Bnubestris | Bguifarroi | Bnigroviridis | 0.076 | 0.015 | 5.238 |
| Baurifer | Bguifarroi | Browleyi | Bsupraciliaris | 0.031 | 0.009 | 3.504 |
| Baurifer | Browleyi | Bguifarroi | Bsupraciliaris | 0.007 | 0.004 | 1.609 |
| Baurifer | Bsupraciliaris | Bguifarroi | Browleyi | -0.024 | 0.01 | -2.423 |
| Baurifer | Bguifarroi | Browleyi | Bthalassinus | 0.026 | 0.011 | 2.453 |
| Baurifer | Browleyi | Bguifarroi | Bthalassinus | -0.004 | 0.006 | -0.617 |
| Baurifer | Bthalassinus | Bguifarroi | Browleyi | -0.03 | 0.01 | -3.03 |
| Baurifer | Bguifarroi | Browleyi | Bschlegelii | 0.032 | 0.009 | 3.671 |
| Baurifer | Browleyi | Bguifarroi | Bschlegelii | 0.008 | 0.004 | 1.937 |
| Baurifer | Bschlegelii | Bguifarroi | Browleyi | -0.024 | 0.01 | -2.423 |
| Baurifer | Bguifarroi | Browleyi | Blateralis | 0.045 | 0.01 | 4.353 |
| Baurifer | Blateralis | Bguifarroi | Browleyi | -0.042 | 0.011 | -3.924 |
| Baurifer | Browleyi | Bguifarroi | Blateralis | 0.003 | 0.003 | 0.866 |
| Baurifer | Bguifarroi | Browleyi | Bnigroviridis | 0.023 | 0.009 | 2.595 |
| Baurifer | Bnigroviridis | Bguifarroi | Browleyi | -0.024 | 0.009 | -2.762 |
| Baurifer | Browleyi | Bguifarroi | Bnigroviridis | -0.001 | 0.005 | -0.22 |
| Baurifer | Bguifarroi | Bsupraciliaris | Bthalassinus | -0.005 | 0.007 | -0.649 |
| Baurifer | Bsupraciliaris | Bguifarroi | Bthalassinus | -0.007 | 0.007 | -1.138 |
| Baurifer | Bthalassinus | Bguifarroi | Bsupraciliaris | -0.003 | 0.005 | -0.503 |
| Baurifer | Bguifarroi | Bsupraciliaris | Bschlegelii | 0.001 | 0.001 | 1.151 |
| Baurifer | Bschlegelii | Bguifarroi | Bsupraciliaris | 0.145 | 0.018 | 7.97 |
| Baurifer | Bsupraciliaris | Bguifarroi | Bschlegelii | 0.147 | 0.018 | 8.059 |
| Baurifer | Bguifarroi | Bsupraciliaris | Blateralis | 0.014 | 0.006 | 2.298 |
| Baurifer | Blateralis | Bguifarroi | Bsupraciliaris | -0.009 | 0.007 | -1.387 |
| Baurifer | Bsupraciliaris | Bguifarroi | Blateralis | 0.004 | 0.004 | 1.082 |

| Pop 1 | Pop 2 | Pop 3 | Pop 4 | f4 | SE f4 | Z-score |
|---|---|---|---|---|---|---|
| Baurifer | Bguifarroi | Bsupraciliaris | Bnigroviridis | -0.008 | 0.005 | -1.614 |
| Baurifer | Bnigroviridis | Bguifarroi | Bsupraciliaris | 0.043 | 0.011 | 4.042 |
| Baurifer | Bsupraciliaris | Bguifarroi | Bnigroviridis | 0.035 | 0.012 | 2.983 |
| Baurifer | Bguifarroi | Bthalassinus | Bschlegelii | 0.006 | 0.007 | 0.821 |
| Baurifer | Bschlegelii | Bguifarroi | Bthalassinus | -0.007 | 0.007 | -1.082 |
| Baurifer | Bthalassinus | Bguifarroi | Bschlegelii | -0.001 | 0.005 | -0.223 |
| Baurifer | Bguifarroi | Bthalassinus | Blateralis | 0.019 | 0.008 | 2.306 |
| Baurifer | Blateralis | Bguifarroi | Bthalassinus | -0.017 | 0.008 | -2.126 |
| Baurifer | Bthalassinus | Bguifarroi | Blateralis | 0.001 | 0.005 | 0.242 |
| Baurifer | Bguifarroi | Bthalassinus | Bnigroviridis | -0.003 | 0.007 | -0.473 |
| Baurifer | Bnigroviridis | Bguifarroi | Bthalassinus | -0.003 | 0.006 | -0.522 |
| Baurifer | Bthalassinus | Bguifarroi | Bnigroviridis | -0.006 | 0.007 | -0.973 |
| Baurifer | Bguifarroi | Bschlegelii | Blateralis | 0.013 | 0.006 | 2.131 |
| Baurifer | Blateralis | Bguifarroi | Bschlegelii | -0.007 | 0.007 | -1.117 |
| Baurifer | Bschlegelii | Bguifarroi | Blateralis | 0.005 | 0.004 | 1.232 |
| Baurifer | Bguifarroi | Bschlegelii | Bnigroviridis | -0.009 | 0.005 | -1.75 |
| Baurifer | Bnigroviridis | Bguifarroi | Bschlegelii | 0.04 | 0.01 | 3.912 |
| Baurifer | Bschlegelii | Bguifarroi | Bnigroviridis | 0.03 | 0.011 | 2.661 |
| Baurifer | Bguifarroi | Blateralis | Bnigroviridis | -0.022 | 0.008 | -2.855 |
| Baurifer | Blateralis | Bguifarroi | Bnigroviridis | -0.018 | 0.008 | -2.133 |
| Baurifer | Bnigroviridis | Bguifarroi | Blateralis | 0.004 | 0.004 | 1.041 |
| Baurifer | Bmarchi | Bnubestris | Browleyi | -0.02 | 0.009 | -2.259 |
| Baurifer | Bnubestris | Bmarchi | Browleyi | -0.009 | 0.011 | -0.855 |
| Baurifer | Browleyi | Bmarchi | Bnubestris | 0.011 | 0.008 | 1.449 |
| Baurifer | Bmarchi | Bnubestris | Bsupraciliaris | 0.01 | 0.007 | 1.428 |
| Baurifer | Bnubestris | Bmarchi | Bsupraciliaris | 0.041 | 0.011 | 3.602 |
| Baurifer | Bsupraciliaris | Bmarchi | Bnubestris | 0.031 | 0.012 | 2.52 |
| Baurifer | Bmarchi | Bnubestris | Bthalassinus | 0.045 | 0.011 | 4.223 |
| Baurifer | Bnubestris | Bmarchi | Bthalassinus | 0.006 | 0.005 | 1.134 |

| Pop 1 | Pop 2 | Pop 3 | Pop 4 | f4 | SE f4 | Z-score |
|---|---|---|---|---|---|---|
| Baurifer | Bthalassinus | Bmarchi | Bnubestris | -0.04 | 0.011 | -3.509 |
| Baurifer | Bmarchi | Bnubestris | Bschlegelii | 0.008 | 0.006 | 1.311 |
| Baurifer | Bnubestris | Bmarchi | Bschlegelii | 0.043 | 0.011 | 3.771 |
| Baurifer | Bschlegelii | Bmarchi | Bnubestris | 0.035 | 0.012 | 2.818 |
| Baurifer | Blateralis | Bmarchi | Bnubestris | -0.001 | 0.01 | -0.138 |
| Baurifer | Bmarchi | Bnubestris | Blateralis | 0.012 | 0.009 | 1.434 |
| Baurifer | Bnubestris | Bmarchi | Blateralis | 0.011 | 0.008 | 1.344 |
| Baurifer | Bmarchi | Bnubestris | Bnigroviridis | 0.005 | 0.006 | 0.759 |
| Baurifer | Bnigroviridis | Bmarchi | Bnubestris | 0.084 | 0.016 | 5.249 |
| Baurifer | Bnubestris | Bmarchi | Bnigroviridis | 0.088 | 0.015 | 5.704 |
| Baurifer | Bmarchi | Browleyi | Bsupraciliaris | 0.03 | 0.01 | 3.013 |
| Baurifer | Browleyi | Bmarchi | Bsupraciliaris | 0.015 | 0.008 | 1.931 |
| Baurifer | Bsupraciliaris | Bmarchi | Browleyi | -0.015 | 0.012 | -1.215 |
| Baurifer | Bmarchi | Browleyi | Bthalassinus | 0.066 | 0.012 | 5.254 |
| Baurifer | Browleyi | Bmarchi | Bthalassinus | 0.004 | 0.003 | 1.27 |
| Baurifer | Bthalassinus | Bmarchi | Browleyi | -0.061 | 0.013 | -4.727 |
| Baurifer | Bmarchi | Browleyi | Bschlegelii | 0.029 | 0.01 | 3.018 |
| Baurifer | Browleyi | Bmarchi | Bschlegelii | 0.016 | 0.008 | 2.102 |
| Baurifer | Bschlegelii | Bmarchi | Browleyi | -0.012 | 0.012 | -1.042 |
| Baurifer | Blateralis | Bmarchi | Browleyi | -0.021 | 0.012 | -1.774 |
| Baurifer | Bmarchi | Browleyi | Blateralis | 0.032 | 0.01 | 3.097 |
| Baurifer | Browleyi | Bmarchi | Blateralis | 0.011 | 0.008 | 1.449 |
| Baurifer | Bmarchi | Browleyi | Bnigroviridis | 0.025 | 0.01 | 2.512 |
| Baurifer | Bnigroviridis | Bmarchi | Browleyi | -0.018 | 0.011 | -1.596 |
| Baurifer | Browleyi | Bmarchi | Bnigroviridis | 0.007 | 0.007 | 0.974 |
| Baurifer | Bmarchi | Bsupraciliaris | Bthalassinus | 0.036 | 0.011 | 3.331 |
| Baurifer | Bsupraciliaris | Bmarchi | Bthalassinus | 0.002 | 0.006 | 0.286 |
| Baurifer | Bthalassinus | Bmarchi | Bsupraciliaris | -0.034 | 0.011 | -3.15 |
| Baurifer | Bmarchi | Bsupraciliaris | Bschlegelii | -0.001 | 0.003 | -0.395 |

| Pop 1 | Pop 2 | Pop 3 | Pop 4 | f4 | SE f4 | Z-score |
|---|---|---|---|---|---|---|
| Baurifer | Bschlegelii | Bmarchi | Bsupraciliaris | 0.157 | 0.019 | 8.295 |
| Baurifer | Bsupraciliaris | Bmarchi | Bschlegelii | 0.156 | 0.019 | 8.152 |
| Baurifer | Blateralis | Bmarchi | Bsupraciliaris | 0.011 | 0.01 | 1.16 |
| Baurifer | Bmarchi | Bsupraciliaris | Blateralis | 0.003 | 0.008 | 0.333 |
| Baurifer | Bsupraciliaris | Bmarchi | Blateralis | 0.014 | 0.009 | 1.483 |
| Baurifer | Bmarchi | Bsupraciliaris | Bnigroviridis | -0.005 | 0.006 | -0.8 |
| Baurifer | Bnigroviridis | Bmarchi | Bsupraciliaris | 0.049 | 0.012 | 3.965 |
| Baurifer | Bsupraciliaris | Bmarchi | Bnigroviridis | 0.044 | 0.013 | 3.429 |
| Baurifer | Bmarchi | Bthalassinus | Bschlegelii | -0.037 | 0.01 | -3.583 |
| Baurifer | Bschlegelii | Bmarchi | Bthalassinus | 0.004 | 0.005 | 0.837 |
| Baurifer | Bthalassinus | Bmarchi | Bschlegelii | -0.032 | 0.011 | -3.021 |
| Baurifer | Blateralis | Bmarchi | Bthalassinus | 0.003 | 0.005 | 0.599 |
| Baurifer | Bmarchi | Bthalassinus | Blateralis | -0.033 | 0.009 | -3.488 |
| Baurifer | Bthalassinus | Bmarchi | Blateralis | -0.03 | 0.01 | -3.044 |
| Baurifer | Bmarchi | Bthalassinus | Bnigroviridis | -0.041 | 0.011 | -3.74 |
| Baurifer | Bnigroviridis | Bmarchi | Bthalassinus | 0.003 | 0.006 | 0.529 |
| Baurifer | Bthalassinus | Bmarchi | Bnigroviridis | -0.038 | 0.011 | -3.405 |
| Baurifer | Blateralis | Bmarchi | Bschlegelii | 0.013 | 0.009 | 1.362 |
| Baurifer | Bmarchi | Bschlegelii | Blateralis | 0.004 | 0.007 | 0.526 |
| Baurifer | Bschlegelii | Bmarchi | Blateralis | 0.017 | 0.009 | 1.896 |
| Baurifer | Bmarchi | Bschlegelii | Bnigroviridis | -0.004 | 0.007 | -0.543 |
| Baurifer | Bnigroviridis | Bmarchi | Bschlegelii | 0.046 | 0.013 | 3.637 |
| Baurifer | Bschlegelii | Bmarchi | Bnigroviridis | 0.042 | 0.013 | 3.251 |
| Baurifer | Blateralis | Bmarchi | Bnigroviridis | 0.003 | 0.01 | 0.267 |
| Baurifer | Bmarchi | Blateralis | Bnigroviridis | -0.008 | 0.009 | -0.84 |
| Baurifer | Bnigroviridis | Bmarchi | Blateralis | 0.01 | 0.009 | 1.128 |
| Baurifer | Bnubestris | Browleyi | Bsupraciliaris | 0.05 | 0.012 | 4.096 |
| Baurifer | Browleyi | Bnubestris | Bsupraciliaris | 0.004 | 0.006 | 0.76 |
| Baurifer | Bsupraciliaris | Bnubestris | Browleyi | -0.046 | 0.013 | -3.647 |

| Pop 1 | Pop 2 | Pop 3 | Pop 4 | f4 | SE f4 | Z-score |
|---|---|---|---|---|---|---|
| Baurifer | Bnubestris | Browleyi | Bthalassinus | 0.015 | 0.01 | 1.523 |
| Baurifer | Browleyi | Bnubestris | Bthalassinus | -0.007 | 0.006 | -1.095 |
| Baurifer | Bthalassinus | Bnubestris | Browleyi | -0.022 | 0.009 | -2.472 |
| Baurifer | Bnubestris | Browleyi | Bschlegelii | 0.052 | 0.012 | 4.253 |
| Baurifer | Browleyi | Bnubestris | Bschlegelii | 0.005 | 0.006 | 0.929 |
| Baurifer | Bschlegelii | Bnubestris | Browleyi | -0.047 | 0.013 | -3.664 |
| Baurifer | Blateralis | Bnubestris | Browleyi | -0.02 | 0.009 | -2.144 |
| Baurifer | Bnubestris | Browleyi | Blateralis | 0.02 | 0.009 | 2.144 |
| Baurifer | Browleyi | Bnubestris | Blateralis | 0 | 0.006 | 0 |
| Baurifer | Bnigroviridis | Bnubestris | Browleyi | -0.101 | 0.016 | -6.469 |
| Baurifer | Bnubestris | Browleyi | Bnigroviridis | 0.097 | 0.016 | 6.07 |
| Baurifer | Browleyi | Bnubestris | Bnigroviridis | -0.004 | 0.004 | -1.049 |
| Baurifer | Bnubestris | Bsupraciliaris | Bthalassinus | -0.035 | 0.011 | -3.33 |
| Baurifer | Bsupraciliaris | Bnubestris | Bthalassinus | -0.029 | 0.011 | -2.676 |
| Baurifer | Bthalassinus | Bnubestris | Bsupraciliaris | 0.006 | 0.006 | 0.973 |
| Baurifer | Bnubestris | Bsupraciliaris | Bschlegelii | 0.003 | 0.003 | 0.876 |
| Baurifer | Bschlegelii | Bnubestris | Bsupraciliaris | 0.122 | 0.017 | 7.049 |
| Baurifer | Bsupraciliaris | Bnubestris | Bschlegelii | 0.125 | 0.017 | 7.315 |
| Baurifer | Blateralis | Bnubestris | Bsupraciliaris | 0.012 | 0.006 | 2.109 |
| Baurifer | Bnubestris | Bsupraciliaris | Blateralis | -0.03 | 0.009 | -3.358 |
| Baurifer | Bsupraciliaris | Bnubestris | Blateralis | -0.017 | 0.011 | -1.659 |
| Baurifer | Bnigroviridis | Bnubestris | Bsupraciliaris | -0.035 | 0.013 | -2.658 |
| Baurifer | Bnubestris | Bsupraciliaris | Bnigroviridis | 0.048 | 0.012 | 4.062 |
| Baurifer | Bsupraciliaris | Bnubestris | Bnigroviridis | 0.013 | 0.007 | 1.86 |
| Baurifer | Bnubestris | Bthalassinus | Bschlegelii | 0.038 | 0.011 | 3.511 |
| Baurifer | Bschlegelii | Bnubestris | Bthalassinus | -0.03 | 0.011 | -2.676 |
| Baurifer | Bthalassinus | Bnubestris | Bschlegelii | 0.007 | 0.006 | 1.181 |
| Baurifer | Blateralis | Bnubestris | Bthalassinus | 0.004 | 0.009 | 0.488 |
| Baurifer | Bnubestris | Bthalassinus | Blateralis | 0.005 | 0.007 | 0.692 |

| Pop 1 | Pop 2 | Pop 3 | Pop 4 | f4 | SE f4 | Z-score |
|---|---|---|---|---|---|---|
| Baurifer | Bthalassinus | Bnubestris | Blateralis | 0.01 | 0.009 | 1.114 |
| Baurifer | Bnigroviridis | Bnubestris | Bthalassinus | -0.081 | 0.015 | -5.505 |
| Baurifer | Bnubestris | Bthalassinus | Bnigroviridis | 0.083 | 0.014 | 5.713 |
| Baurifer | Bthalassinus | Bnubestris | Bnigroviridis | 0.002 | 0.004 | 0.493 |
| Baurifer | Blateralis | Bnubestris | Bschlegelii | 0.014 | 0.006 | 2.317 |
| Baurifer | Bnubestris | Bschlegelii | Blateralis | -0.032 | 0.009 | -3.556 |
| Baurifer | Bschlegelii | Bnubestris | Blateralis | -0.018 | 0.011 | -1.66 |
| Baurifer | Bnigroviridis | Bnubestris | Bschlegelii | -0.038 | 0.013 | -2.966 |
| Baurifer | Bnubestris | Bschlegelii | Bnigroviridis | 0.045 | 0.012 | 3.721 |
| Baurifer | Bschlegelii | Bnubestris | Bnigroviridis | 0.007 | 0.007 | 1.005 |
| Baurifer | Blateralis | Bnubestris | Bnigroviridis | 0.004 | 0.005 | 0.816 |
| Baurifer | Bnigroviridis | Bnubestris | Blateralis | -0.073 | 0.015 | -4.995 |
| Baurifer | Bnubestris | Blateralis | Bnigroviridis | 0.077 | 0.014 | 5.411 |
| Baurifer | Browleyi | Bsupraciliaris | Bthalassinus | -0.011 | 0.006 | -1.691 |
| Baurifer | Bsupraciliaris | Browleyi | Bthalassinus | 0.016 | 0.011 | 1.533 |
| Baurifer | Bthalassinus | Browleyi | Bsupraciliaris | 0.027 | 0.009 | 2.997 |
| Baurifer | Browleyi | Bsupraciliaris | Bschlegelii | 0.001 | 0.001 | 1.151 |
| Baurifer | Bschlegelii | Browleyi | Bsupraciliaris | 0.169 | 0.019 | 8.715 |
| Baurifer | Bsupraciliaris | Browleyi | Bschlegelii | 0.17 | 0.019 | 8.801 |
| Baurifer | Blateralis | Browleyi | Bsupraciliaris | 0.032 | 0.009 | 3.64 |
| Baurifer | Browleyi | Bsupraciliaris | Blateralis | -0.004 | 0.003 | -1.213 |
| Baurifer | Bsupraciliaris | Browleyi | Blateralis | 0.028 | 0.009 | 2.97 |
| Baurifer | Bnigroviridis | Browleyi | Bsupraciliaris | 0.067 | 0.013 | 5.232 |
| Baurifer | Browleyi | Bsupraciliaris | Bnigroviridis | -0.008 | 0.004 | -1.916 |
| Baurifer | Bsupraciliaris | Browleyi | Bnigroviridis | 0.058 | 0.013 | 4.33 |
| Baurifer | Browleyi | Bthalassinus | Bschlegelii | 0.012 | 0.006 | 1.904 |
| Baurifer | Bschlegelii | Browleyi | Bthalassinus | 0.017 | 0.011 | 1.563 |
| Baurifer | Bthalassinus | Browleyi | Bschlegelii | 0.029 | 0.009 | 3.185 |
| Baurifer | Blateralis | Browleyi | Bthalassinus | 0.024 | 0.011 | 2.141 |

| Pop 1 | Pop 2 | Pop 3 | Pop 4 | f4 | SE f4 | Z-score |
|---|---|---|---|---|---|---|
| Baurifer | Browleyi | Bthalassinus | Blateralis | 0.007 | 0.007 | 0.999 |
| Baurifer | Bthalassinus | Browleyi | Blateralis | 0.031 | 0.01 | 3.015 |
| Baurifer | Bnigroviridis | Browleyi | Bthalassinus | 0.021 | 0.01 | 2.111 |
| Baurifer | Browleyi | Bthalassinus | Bnigroviridis | 0.003 | 0.006 | 0.479 |
| Baurifer | Bthalassinus | Browleyi | Bnigroviridis | 0.023 | 0.009 | 2.519 |
| Baurifer | Blateralis | Browleyi | Bschlegelii | 0.034 | 0.009 | 3.874 |
| Baurifer | Browleyi | Bschlegelii | Blateralis | -0.005 | 0.003 | -1.632 |
| Baurifer | Bschlegelii | Browleyi | Blateralis | 0.029 | 0.01 | 3.036 |
| Baurifer | Bnigroviridis | Browleyi | Bschlegelii | 0.063 | 0.012 | 5.129 |
| Baurifer | Browleyi | Bschlegelii | Bnigroviridis | -0.009 | 0.005 | -2.035 |
| Baurifer | Bschlegelii | Browleyi | Bnigroviridis | 0.054 | 0.013 | 4.062 |
| Baurifer | Blateralis | Browleyi | Bnigroviridis | 0.024 | 0.01 | 2.495 |
| Baurifer | Bnigroviridis | Browleyi | Blateralis | 0.028 | 0.009 | 3.082 |
| Baurifer | Browleyi | Blateralis | Bnigroviridis | -0.004 | 0.005 | -0.729 |
| Baurifer | Bschlegelii | Bsupraciliaris | Bthalassinus | -0.153 | 0.019 | -8.215 |
| Baurifer | Bsupraciliaris | Bthalassinus | Bschlegelii | 0.154 | 0.018 | 8.329 |
| Baurifer | Bthalassinus | Bsupraciliaris | Bschlegelii | 0.002 | 0.001 | 1.193 |
| Baurifer | Blateralis | Bsupraciliaris | Bthalassinus | -0.008 | 0.009 | -0.918 |
| Baurifer | Bsupraciliaris | Bthalassinus | Blateralis | 0.012 | 0.008 | 1.54 |
| Baurifer | Bthalassinus | Bsupraciliaris | Blateralis | 0.004 | 0.007 | 0.578 |
| Baurifer | Bnigroviridis | Bsupraciliaris | Bthalassinus | -0.046 | 0.011 | -4.073 |
| Baurifer | Bsupraciliaris | Bthalassinus | Bnigroviridis | 0.042 | 0.011 | 3.667 |
| Baurifer | Bthalassinus | Bsupraciliaris | Bnigroviridis | -0.004 | 0.004 | -0.831 |
| Baurifer | Blateralis | Bsupraciliaris | Bschlegelii | 0.002 | 0.001 | 1.486 |
| Baurifer | Bschlegelii | Bsupraciliaris | Blateralis | -0.14 | 0.018 | -7.792 |
| Baurifer | Bsupraciliaris | Bschlegelii | Blateralis | -0.142 | 0.018 | -7.931 |
| Baurifer | Bnigroviridis | Bsupraciliaris | Bschlegelii | -0.003 | 0.003 | -1.103 |
| Baurifer | Bschlegelii | Bsupraciliaris | Bnigroviridis | -0.115 | 0.017 | -6.968 |
| Baurifer | Bsupraciliaris | Bschlegelii | Bnigroviridis | -0.112 | 0.017 | -6.664 |

| Pop 1 | Pop 2 | Pop 3 | Pop 4 | f4 | SE f4 | Z-score |
|---|---|---|---|---|---|---|
| Baurifer | Blateralis | Bsupraciliaris | Bnigroviridis | -0.008 | 0.006 | -1.31 |
| Baurifer | Bnigroviridis | Bsupraciliaris | Blateralis | -0.039 | 0.011 | -3.598 |
| Baurifer | Bsupraciliaris | Blateralis | Bnigroviridis | 0.03 | 0.012 | 2.579 |
| Baurifer | Blateralis | Bthalassinus | Bschlegelii | 0.01 | 0.009 | 1.138 |
| Baurifer | Bschlegelii | Bthalassinus | Blateralis | 0.012 | 0.008 | 1.574 |
| Baurifer | Bthalassinus | Bschlegelii | Blateralis | 0.002 | 0.007 | 0.355 |
| Baurifer | Bnigroviridis | Bthalassinus | Bschlegelii | 0.043 | 0.011 | 3.933 |
| Baurifer | Bschlegelii | Bthalassinus | Bnigroviridis | 0.037 | 0.011 | 3.316 |
| Baurifer | Bthalassinus | Bschlegelii | Bnigroviridis | -0.005 | 0.005 | -1.074 |
| Baurifer | Blateralis | Bthalassinus | Bnigroviridis | 0 | 0.009 | -0.04 |
| Baurifer | Bnigroviridis | Bthalassinus | Blateralis | 0.007 | 0.007 | 1.024 |
| Baurifer | Bthalassinus | Blateralis | Bnigroviridis | -0.008 | 0.008 | -0.983 |
| Baurifer | Blateralis | Bschlegelii | Bnigroviridis | -0.01 | 0.006 | -1.61 |
| Baurifer | Bnigroviridis | Bschlegelii | Blateralis | -0.035 | 0.01 | -3.511 |
| Baurifer | Bschlegelii | Blateralis | Bnigroviridis | 0.025 | 0.011 | 2.195 |
| Bbicolor | Bguifarroi | Bmarchi | Bnubestris | -0.002 | 0.008 | -0.271 |
| Bbicolor | Bmarchi | Bguifarroi | Bnubestris | -0.011 | 0.007 | -1.68 |
| Bbicolor | Bnubestris | Bguifarroi | Bmarchi | -0.009 | 0.006 | -1.38 |
| Bbicolor | Bguifarroi | Bmarchi | Browleyi | -0.018 | 0.01 | -1.751 |
| Bbicolor | Bmarchi | Bguifarroi | Browleyi | -0.023 | 0.01 | -2.33 |
| Bbicolor | Browleyi | Bguifarroi | Bmarchi | -0.005 | 0.007 | -0.647 |
| Bbicolor | Bguifarroi | Bmarchi | Bsupraciliaris | -0.001 | 0.009 | -0.099 |
| Bbicolor | Bmarchi | Bguifarroi | Bsupraciliaris | -0.007 | 0.008 | -0.864 |
| Bbicolor | Bsupraciliaris | Bguifarroi | Bmarchi | -0.006 | 0.008 | -0.728 |
| Bbicolor | Bguifarroi | Bmarchi | Bthalassinus | -0.001 | 0.004 | -0.174 |
| Bbicolor | Bmarchi | Bguifarroi | Bthalassinus | 0.034 | 0.009 | 3.611 |
| Bbicolor | Bthalassinus | Bguifarroi | Bmarchi | 0.035 | 0.009 | 3.696 |
| Bbicolor | Bguifarroi | Bmarchi | Bschlegelii | 0 | 0.009 | 0 |
| Bbicolor | Bmarchi | Bguifarroi | Bschlegelii | -0.008 | 0.007 | -1.137 |

| Pop 1 | Pop 2 | Pop 3 | Pop 4 | f4 | SE f4 | Z-score |
|---|---|---|---|---|---|---|
| Bbicolor | Bschlegelii | Bguifarroi | Bmarchi | -0.008 | 0.008 | -1.087 |
| Bbicolor | Bguifarroi | Bmarchi | Blateralis | 0.015 | 0.009 | 1.652 |
| Bbicolor | Blateralis | Bguifarroi | Bmarchi | -0.017 | 0.009 | -1.886 |
| Bbicolor | Bmarchi | Bguifarroi | Blateralis | -0.002 | 0.007 | -0.232 |
| Bbicolor | Bguifarroi | Bmarchi | Bnigroviridis | -0.003 | 0.009 | -0.34 |
| Bbicolor | Bmarchi | Bguifarroi | Bnigroviridis | -0.006 | 0.009 | -0.675 |
| Bbicolor | Bnigroviridis | Bguifarroi | Bmarchi | -0.003 | 0.008 | -0.324 |
| Bbicolor | Bguifarroi | Bnubestris | Browleyi | -0.016 | 0.008 | -1.886 |
| Bbicolor | Bnubestris | Bguifarroi | Browleyi | -0.014 | 0.009 | -1.546 |
| Bbicolor | Browleyi | Bguifarroi | Bnubestris | 0.002 | 0.006 | 0.361 |
| Bbicolor | Bguifarroi | Bnubestris | Bsupraciliaris | 0.001 | 0.007 | 0.188 |
| Bbicolor | Bnubestris | Bguifarroi | Bsupraciliaris | 0.023 | 0.01 | 2.222 |
| Bbicolor | Bsupraciliaris | Bguifarroi | Bnubestris | 0.021 | 0.011 | 2.021 |
| Bbicolor | Bguifarroi | Bnubestris | Bthalassinus | 0.002 | 0.008 | 0.189 |
| Bbicolor | Bnubestris | Bguifarroi | Bthalassinus | -0.007 | 0.007 | -1.141 |
| Bbicolor | Bthalassinus | Bguifarroi | Bnubestris | -0.009 | 0.007 | -1.346 |
| Bbicolor | Bguifarroi | Bnubestris | Bschlegelii | 0.002 | 0.007 | 0.306 |
| Bbicolor | Bnubestris | Bguifarroi | Bschlegelii | 0.025 | 0.01 | 2.416 |
| Bbicolor | Bschlegelii | Bguifarroi | Bnubestris | 0.023 | 0.011 | 2.125 |
| Bbicolor | Bguifarroi | Bnubestris | Blateralis | 0.018 | 0.009 | 2.037 |
| Bbicolor | Blateralis | Bguifarroi | Bnubestris | -0.022 | 0.008 | -2.89 |
| Bbicolor | Bnubestris | Bguifarroi | Blateralis | -0.005 | 0.004 | -1.076 |
| Bbicolor | Bguifarroi | Bnubestris | Bnigroviridis | -0.001 | 0.004 | -0.217 |
| Bbicolor | Bnigroviridis | Bguifarroi | Bnubestris | 0.077 | 0.014 | 5.378 |
| Bbicolor | Bnubestris | Bguifarroi | Bnigroviridis | 0.076 | 0.014 | 5.309 |
| Bbicolor | Bguifarroi | Browleyi | Bsupraciliaris | 0.017 | 0.008 | 2.158 |
| Bbicolor | Browleyi | Bguifarroi | Bsupraciliaris | 0.001 | 0.005 | 0.246 |
| Bbicolor | Bsupraciliaris | Bguifarroi | Browleyi | -0.016 | 0.008 | -1.911 |
| Bbicolor | Bguifarroi | Browleyi | Bthalassinus | 0.017 | 0.01 | 1.688 |

| Pop 1 | Pop 2 | Pop 3 | Pop 4 | f4 | SE f4 | Z-score |
|---|---|---|---|---|---|---|
| Bbicolor | Browleyi | Bguifarroi | Bthalassinus | -0.005 | 0.007 | -0.67 |
| Bbicolor | Bthalassinus | Bguifarroi | Browleyi | -0.022 | 0.01 | -2.31 |
| Bbicolor | Bguifarroi | Browleyi | Bschlegelii | 0.018 | 0.008 | 2.275 |
| Bbicolor | Browleyi | Bguifarroi | Bschlegelii | 0.002 | 0.005 | 0.426 |
| Bbicolor | Bschlegelii | Bguifarroi | Browleyi | -0.016 | 0.008 | -1.911 |
| Bbicolor | Bguifarroi | Browleyi | Blateralis | 0.033 | 0.01 | 3.428 |
| Bbicolor | Blateralis | Bguifarroi | Browleyi | -0.034 | 0.01 | -3.486 |
| Bbicolor | Browleyi | Bguifarroi | Blateralis | -0.001 | 0.004 | -0.132 |
| Bbicolor | Bguifarroi | Browleyi | Bnigroviridis | 0.015 | 0.009 | 1.617 |
| Bbicolor | Bnigroviridis | Bguifarroi | Browleyi | -0.016 | 0.009 | -1.736 |
| Bbicolor | Browleyi | Bguifarroi | Bnigroviridis | -0.001 | 0.007 | -0.151 |
| Bbicolor | Bguifarroi | Bsupraciliaris | Bthalassinus | 0 | 0.009 | 0.02 |
| Bbicolor | Bsupraciliaris | Bguifarroi | Bthalassinus | -0.008 | 0.007 | -1.18 |
| Bbicolor | Bthalassinus | Bguifarroi | Bsupraciliaris | -0.009 | 0.007 | -1.262 |
| Bbicolor | Bguifarroi | Bsupraciliaris | Bschlegelii | 0.001 | 0.001 | 1.671 |
| Bbicolor | Bschlegelii | Bguifarroi | Bsupraciliaris | 0.139 | 0.018 | 7.768 |
| Bbicolor | Bsupraciliaris | Bguifarroi | Bschlegelii | 0.14 | 0.018 | 7.826 |
| Bbicolor | Bguifarroi | Bsupraciliaris | Blateralis | 0.016 | 0.007 | 2.225 |
| Bbicolor | Blateralis | Bguifarroi | Bsupraciliaris | -0.015 | 0.007 | -2.078 |
| Bbicolor | Bsupraciliaris | Bguifarroi | Blateralis | 0.001 | 0.004 | 0.23 |
| Bbicolor | Bguifarroi | Bsupraciliaris | Bnigroviridis | -0.002 | 0.006 | -0.36 |
| Bbicolor | Bnigroviridis | Bguifarroi | Bsupraciliaris | 0.037 | 0.011 | 3.32 |
| Bbicolor | Bsupraciliaris | Bguifarroi | Bnigroviridis | 0.035 | 0.011 | 3.031 |
| Bbicolor | Bguifarroi | Bthalassinus | Bschlegelii | 0.001 | 0.009 | 0.079 |
| Bbicolor | Bschlegelii | Bguifarroi | Bthalassinus | -0.008 | 0.007 | -1.124 |
| Bbicolor | Bthalassinus | Bguifarroi | Bschlegelii | -0.007 | 0.007 | -1.087 |
| Bbicolor | Bguifarroi | Bthalassinus | Blateralis | 0.016 | 0.009 | 1.712 |
| Bbicolor | Blateralis | Bguifarroi | Bthalassinus | -0.018 | 0.009 | -2.015 |
| Bbicolor | Bthalassinus | Bguifarroi | Blateralis | -0.002 | 0.007 | -0.338 |

| Pop 1 | Pop 2 | Pop 3 | Pop 4 | f4 | SE f4 | Z-score |
|---|---|---|---|---|---|---|
| Bbicolor | Bguifarroi | Bthalassinus | Bnigroviridis | -0.002 | 0.009 | -0.266 |
| Bbicolor | Bnigroviridis | Bguifarroi | Bthalassinus | -0.004 | 0.008 | -0.507 |
| Bbicolor | Bthalassinus | Bguifarroi | Bnigroviridis | -0.006 | 0.008 | -0.788 |
| Bbicolor | Bguifarroi | Bschlegelii | Blateralis | 0.015 | 0.007 | 2.116 |
| Bbicolor | Blateralis | Bguifarroi | Bschlegelii | -0.014 | 0.007 | -1.868 |
| Bbicolor | Bschlegelii | Bguifarroi | Blateralis | 0.002 | 0.004 | 0.379 |
| Bbicolor | Bguifarroi | Bschlegelii | Bnigroviridis | -0.003 | 0.006 | -0.499 |
| Bbicolor | Bnigroviridis | Bguifarroi | Bschlegelii | 0.033 | 0.011 | 3.152 |
| Bbicolor | Bschlegelii | Bguifarroi | Bnigroviridis | 0.03 | 0.011 | 2.762 |
| Bbicolor | Bguifarroi | Blateralis | Bnigroviridis | -0.019 | 0.009 | -2.129 |
| Bbicolor | Blateralis | Bguifarroi | Bnigroviridis | -0.018 | 0.009 | -2.026 |
| Bbicolor | Bnigroviridis | Bguifarroi | Blateralis | 0.001 | 0.006 | 0.145 |
| Bbicolor | Bmarchi | Bnubestris | Browleyi | -0.012 | 0.01 | -1.23 |
| Bbicolor | Bnubestris | Bmarchi | Browleyi | -0.005 | 0.01 | -0.458 |
| Bbicolor | Browleyi | Bmarchi | Bnubestris | 0.007 | 0.009 | 0.795 |
| Bbicolor | Bmarchi | Bnubestris | Bsupraciliaris | 0.004 | 0.008 | 0.571 |
| Bbicolor | Bnubestris | Bmarchi | Bsupraciliaris | 0.031 | 0.011 | 2.819 |
| Bbicolor | Bsupraciliaris | Bmarchi | Bnubestris | 0.027 | 0.012 | 2.288 |
| Bbicolor | Bmarchi | Bnubestris | Bthalassinus | 0.045 | 0.011 | 4.15 |
| Bbicolor | Bnubestris | Bmarchi | Bthalassinus | 0.001 | 0.004 | 0.333 |
| Bbicolor | Bthalassinus | Bmarchi | Bnubestris | -0.044 | 0.011 | -3.988 |
| Bbicolor | Bmarchi | Bnubestris | Bschlegelii | 0.003 | 0.007 | 0.399 |
| Bbicolor | Bnubestris | Bmarchi | Bschlegelii | 0.034 | 0.011 | 2.989 |
| Bbicolor | Bschlegelii | Bmarchi | Bnubestris | 0.031 | 0.012 | 2.647 |
| Bbicolor | Blateralis | Bmarchi | Bnubestris | -0.005 | 0.009 | -0.58 |
| Bbicolor | Bmarchi | Bnubestris | Blateralis | 0.01 | 0.009 | 1.043 |
| Bbicolor | Bnubestris | Bmarchi | Blateralis | 0.004 | 0.008 | 0.508 |
| Bbicolor | Bmarchi | Bnubestris | Bnigroviridis | 0.005 | 0.005 | 0.968 |
| Bbicolor | Bnigroviridis | Bmarchi | Bnubestris | 0.08 | 0.016 | 5.136 |

| Pop 1 | Pop 2 | Pop 3 | Pop 4 | f4 | SE f4 | Z-score |
|---|---|---|---|---|---|---|
| Bbicolor | Bnubestris | Bmarchi | Bnigroviridis | 0.085 | 0.015 | 5.683 |
| Bbicolor | Bmarchi | Browleyi | Bsupraciliaris | 0.016 | 0.01 | 1.692 |
| Bbicolor | Browleyi | Bmarchi | Bsupraciliaris | 0.006 | 0.008 | 0.754 |
| Bbicolor | Bsupraciliaris | Bmarchi | Browleyi | -0.01 | 0.01 | -0.984 |
| Bbicolor | Bmarchi | Browleyi | Bthalassinus | 0.057 | 0.013 | 4.381 |
| Bbicolor | Browleyi | Bmarchi | Bthalassinus | 0 | 0.006 | 0 |
| Bbicolor | Bthalassinus | Bmarchi | Browleyi | -0.057 | 0.013 | -4.381 |
| Bbicolor | Bmarchi | Browleyi | Bschlegelii | 0.015 | 0.009 | 1.596 |
| Bbicolor | Browleyi | Bmarchi | Bschlegelii | 0.007 | 0.008 | 0.862 |
| Bbicolor | Bschlegelii | Bmarchi | Browleyi | -0.008 | 0.01 | -0.778 |
| Bbicolor | Blateralis | Bmarchi | Browleyi | -0.017 | 0.01 | -1.628 |
| Bbicolor | Bmarchi | Browleyi | Blateralis | 0.021 | 0.01 | 2.134 |
| Bbicolor | Browleyi | Bmarchi | Blateralis | 0.004 | 0.007 | 0.576 |
| Bbicolor | Bmarchi | Browleyi | Bnigroviridis | 0.017 | 0.01 | 1.656 |
| Bbicolor | Bnigroviridis | Bmarchi | Browleyi | -0.013 | 0.011 | -1.239 |
| Bbicolor | Browleyi | Bmarchi | Bnigroviridis | 0.004 | 0.008 | 0.45 |
| Bbicolor | Bmarchi | Bsupraciliaris | Bthalassinus | 0.041 | 0.011 | 3.607 |
| Bbicolor | Bsupraciliaris | Bmarchi | Bthalassinus | -0.003 | 0.005 | -0.534 |
| Bbicolor | Bthalassinus | Bmarchi | Bsupraciliaris | -0.043 | 0.011 | -3.977 |
| Bbicolor | Bmarchi | Bsupraciliaris | Bschlegelii | -0.002 | 0.003 | -0.54 |
| Bbicolor | Bschlegelii | Bmarchi | Bsupraciliaris | 0.148 | 0.018 | 8.021 |
| Bbicolor | Bsupraciliaris | Bmarchi | Bschlegelii | 0.146 | 0.019 | 7.846 |
| Bbicolor | Blateralis | Bmarchi | Bsupraciliaris | 0.002 | 0.009 | 0.189 |
| Bbicolor | Bmarchi | Bsupraciliaris | Blateralis | 0.005 | 0.008 | 0.613 |
| Bbicolor | Bsupraciliaris | Bmarchi | Blateralis | 0.007 | 0.008 | 0.804 |
| Bbicolor | Bmarchi | Bsupraciliaris | Bnigroviridis | 0.001 | 0.007 | 0.127 |
| Bbicolor | Bnigroviridis | Bmarchi | Bsupraciliaris | 0.04 | 0.012 | 3.288 |
| Bbicolor | Bsupraciliaris | Bmarchi | Bnigroviridis | 0.04 | 0.012 | 3.366 |
| Bbicolor | Bmarchi | Bthalassinus | Bschlegelii | -0.042 | 0.011 | -3.877 |

| Pop 1 | Pop 2 | Pop 3 | Pop 4 | f4 | SE f4 | Z-score |
|---|---|---|---|---|---|---|
| Bbicolor | Bschlegelii | Bmarchi | Bthalassinus | 0 | 0.004 | 0 |
| Bbicolor | Bthalassinus | Bmarchi | Bschlegelii | -0.042 | 0.011 | -3.877 |
| Bbicolor | Blateralis | Bmarchi | Bthalassinus | -0.001 | 0.004 | -0.333 |
| Bbicolor | Bmarchi | Bthalassinus | Blateralis | -0.035 | 0.01 | -3.567 |
| Bbicolor | Bthalassinus | Bmarchi | Blateralis | -0.037 | 0.01 | -3.744 |
| Bbicolor | Bmarchi | Bthalassinus | Bnigroviridis | -0.04 | 0.012 | -3.437 |
| Bbicolor | Bnigroviridis | Bmarchi | Bthalassinus | -0.001 | 0.006 | -0.218 |
| Bbicolor | Bthalassinus | Bmarchi | Bnigroviridis | -0.041 | 0.011 | -3.635 |
| Bbicolor | Blateralis | Bmarchi | Bschlegelii | 0.003 | 0.009 | 0.358 |
| Bbicolor | Bmarchi | Bschlegelii | Blateralis | 0.007 | 0.008 | 0.843 |
| Bbicolor | Bschlegelii | Bmarchi | Blateralis | 0.01 | 0.008 | 1.22 |
| Bbicolor | Bmarchi | Bschlegelii | Bnigroviridis | 0.002 | 0.007 | 0.328 |
| Bbicolor | Bnigroviridis | Bmarchi | Bschlegelii | 0.036 | 0.012 | 2.959 |
| Bbicolor | Bschlegelii | Bmarchi | Bnigroviridis | 0.038 | 0.012 | 3.238 |
| Bbicolor | Blateralis | Bmarchi | Bnigroviridis | -0.001 | 0.01 | -0.067 |
| Bbicolor | Bmarchi | Blateralis | Bnigroviridis | -0.004 | 0.01 | -0.428 |
| Bbicolor | Bnigroviridis | Bmarchi | Blateralis | 0.004 | 0.01 | 0.369 |
| Bbicolor | Bnubestris | Browleyi | Bsupraciliaris | 0.036 | 0.012 | 3.077 |
| Bbicolor | Browleyi | Bnubestris | Bsupraciliaris | -0.001 | 0.007 | -0.152 |
| Bbicolor | Bsupraciliaris | Bnubestris | Browleyi | -0.037 | 0.012 | -3.173 |
| Bbicolor | Bnubestris | Browleyi | Bthalassinus | 0.006 | 0.01 | 0.605 |
| Bbicolor | Browleyi | Bnubestris | Bthalassinus | -0.007 | 0.008 | -0.86 |
| Bbicolor | Bthalassinus | Bnubestris | Browleyi | -0.013 | 0.009 | -1.417 |
| Bbicolor | Bnubestris | Browleyi | Bschlegelii | 0.038 | 0.012 | 3.244 |
| Bbicolor | Browleyi | Bnubestris | Bschlegelii | 0 | 0.007 | -0.025 |
| Bbicolor | Bschlegelii | Bnubestris | Browleyi | -0.039 | 0.012 | -3.259 |
| Bbicolor | Blateralis | Bnubestris | Browleyi | -0.012 | 0.008 | -1.376 |
| Bbicolor | Bnubestris | Browleyi | Blateralis | 0.009 | 0.009 | 0.996 |
| Bbicolor | Browleyi | Bnubestris | Blateralis | -0.003 | 0.007 | -0.377 |

| Pop 1 | Pop 2 | Pop 3 | Pop 4 | f4 | SE f4 | Z-score |
|---|---|---|---|---|---|---|
| Bbicolor | Bnigroviridis | Bnubestris | Browleyi | -0.093 | 0.016 | -5.801 |
| Bbicolor | Bnubestris | Browleyi | Bnigroviridis | 0.09 | 0.016 | 5.499 |
| Bbicolor | Browleyi | Bnubestris | Bnigroviridis | -0.003 | 0.006 | -0.527 |
| Bbicolor | Bnubestris | Bsupraciliaris | Bthalassinus | -0.03 | 0.011 | -2.757 |
| Bbicolor | Bsupraciliaris | Bnubestris | Bthalassinus | -0.03 | 0.011 | -2.709 |
| Bbicolor | Bthalassinus | Bnubestris | Bsupraciliaris | 0 | 0.007 | 0.05 |
| Bbicolor | Bnubestris | Bsupraciliaris | Bschlegelii | 0.002 | 0.003 | 0.684 |
| Bbicolor | Bschlegelii | Bnubestris | Bsupraciliaris | 0.117 | 0.017 | 6.762 |
| Bbicolor | Bsupraciliaris | Bnubestris | Bschlegelii | 0.119 | 0.017 | 6.975 |
| Bbicolor | Blateralis | Bnubestris | Bsupraciliaris | 0.007 | 0.007 | 0.987 |
| Bbicolor | Bnubestris | Bsupraciliaris | Blateralis | -0.027 | 0.01 | -2.74 |
| Bbicolor | Bsupraciliaris | Bnubestris | Blateralis | -0.02 | 0.011 | -1.829 |
| Bbicolor | Bnigroviridis | Bnubestris | Bsupraciliaris | -0.04 | 0.013 | -3.024 |
| Bbicolor | Bnubestris | Bsupraciliaris | Bnigroviridis | 0.053 | 0.012 | 4.599 |
| Bbicolor | Bsupraciliaris | Bnubestris | Bnigroviridis | 0.013 | 0.006 | 2.215 |
| Bbicolor | Bnubestris | Bthalassinus | Bschlegelii | 0.032 | 0.011 | 2.93 |
| Bbicolor | Bschlegelii | Bnubestris | Bthalassinus | -0.031 | 0.011 | -2.763 |
| Bbicolor | Bthalassinus | Bnubestris | Bschlegelii | 0.002 | 0.007 | 0.223 |
| Bbicolor | Blateralis | Bnubestris | Bthalassinus | 0.004 | 0.009 | 0.439 |
| Bbicolor | Bnubestris | Bthalassinus | Blateralis | 0.003 | 0.008 | 0.334 |
| Bbicolor | Bthalassinus | Bnubestris | Blateralis | 0.007 | 0.009 | 0.744 |
| Bbicolor | Bnigroviridis | Bnubestris | Bthalassinus | -0.081 | 0.015 | -5.378 |
| Bbicolor | Bnubestris | Bthalassinus | Bnigroviridis | 0.084 | 0.015 | 5.655 |
| Bbicolor | Bthalassinus | Bnubestris | Bnigroviridis | 0.003 | 0.005 | 0.54 |
| Bbicolor | Blateralis | Bnubestris | Bschlegelii | 0.009 | 0.007 | 1.198 |
| Bbicolor | Bnubestris | Bschlegelii | Blateralis | -0.03 | 0.01 | -2.932 |
| Bbicolor | Bschlegelii | Bnubestris | Blateralis | -0.021 | 0.011 | -1.866 |
| Bbicolor | Bnigroviridis | Bnubestris | Bschlegelii | -0.044 | 0.013 | -3.313 |
| Bbicolor | Bnubestris | Bschlegelii | Bnigroviridis | 0.051 | 0.012 | 4.19 |

| Pop 1 | Pop 2 | Pop 3 | Pop 4 | f4 | SE f4 | Z-score |
|---|---|---|---|---|---|---|
| Bbicolor | Bschlegelii | Bnubestris | Bnigroviridis | 0.008 | 0.006 | 1.235 |
| Bbicolor | Blateralis | Bnubestris | Bnigroviridis | 0.005 | 0.005 | 0.868 |
| Bbicolor | Bnigroviridis | Bnubestris | Blateralis | -0.076 | 0.015 | -5.001 |
| Bbicolor | Bnubestris | Blateralis | Bnigroviridis | 0.081 | 0.015 | 5.512 |
| Bbicolor | Browleyi | Bsupraciliaris | Bthalassinus | -0.006 | 0.007 | -0.832 |
| Bbicolor | Bsupraciliaris | Browleyi | Bthalassinus | 0.007 | 0.009 | 0.792 |
| Bbicolor | Bthalassinus | Browleyi | Bsupraciliaris | 0.013 | 0.009 | 1.574 |
| Bbicolor | Browleyi | Bsupraciliaris | Bschlegelii | 0.001 | 0.001 | 1.671 |
| Bbicolor | Bschlegelii | Browleyi | Bsupraciliaris | 0.155 | 0.019 | 8.263 |
| Bbicolor | Bsupraciliaris | Browleyi | Bschlegelii | 0.156 | 0.019 | 8.319 |
| Bbicolor | Blateralis | Browleyi | Bsupraciliaris | 0.019 | 0.008 | 2.353 |
| Bbicolor | Browleyi | Bsupraciliaris | Blateralis | -0.002 | 0.005 | -0.354 |
| Bbicolor | Bsupraciliaris | Browleyi | Blateralis | 0.017 | 0.008 | 2.021 |
| Bbicolor | Bnigroviridis | Browleyi | Bsupraciliaris | 0.053 | 0.012 | 4.329 |
| Bbicolor | Browleyi | Bsupraciliaris | Bnigroviridis | -0.002 | 0.005 | -0.462 |
| Bbicolor | Bsupraciliaris | Browleyi | Bnigroviridis | 0.051 | 0.013 | 4.046 |
| Bbicolor | Browleyi | Bthalassinus | Bschlegelii | 0.007 | 0.007 | 0.951 |
| Bbicolor | Bschlegelii | Browleyi | Bthalassinus | 0.008 | 0.009 | 0.825 |
| Bbicolor | Bthalassinus | Browleyi | Bschlegelii | 0.015 | 0.009 | 1.714 |
| Bbicolor | Blateralis | Browleyi | Bthalassinus | 0.016 | 0.01 | 1.509 |
| Bbicolor | Browleyi | Bthalassinus | Blateralis | 0.004 | 0.007 | 0.597 |
| Bbicolor | Bthalassinus | Browleyi | Blateralis | 0.02 | 0.01 | 2.055 |
| Bbicolor | Bnigroviridis | Browleyi | Bthalassinus | 0.012 | 0.009 | 1.277 |
| Bbicolor | Browleyi | Bthalassinus | Bnigroviridis | 0.004 | 0.007 | 0.569 |
| Bbicolor | Bthalassinus | Browleyi | Bnigroviridis | 0.016 | 0.009 | 1.774 |
| Bbicolor | Blateralis | Browleyi | Bschlegelii | 0.02 | 0.008 | 2.548 |
| Bbicolor | Browleyi | Bschlegelii | Blateralis | -0.003 | 0.005 | -0.537 |
| Bbicolor | Bschlegelii | Browleyi | Blateralis | 0.018 | 0.008 | 2.095 |
| Bbicolor | Bnigroviridis | Browleyi | Bschlegelii | 0.049 | 0.012 | 4.201 |

| Pop 1 | Pop 2 | Pop 3 | Pop 4 | f4 | SE f4 | Z-score |
|---|---|---|---|---|---|---|
| Bbicolor | Browleyi | Bschlegelii | Bnigroviridis | -0.003 | 0.005 | -0.641 |
| Bbicolor | Bschlegelii | Browleyi | Bnigroviridis | 0.046 | 0.012 | 3.824 |
| Bbicolor | Blateralis | Browleyi | Bnigroviridis | 0.016 | 0.009 | 1.765 |
| Bbicolor | Bnigroviridis | Browleyi | Blateralis | 0.017 | 0.009 | 1.818 |
| Bbicolor | Browleyi | Blateralis | Bnigroviridis | -0.001 | 0.007 | -0.076 |
| Bbicolor | Bschlegelii | Bsupraciliaris | Bthalassinus | -0.148 | 0.018 | -8.066 |
| Bbicolor | Bsupraciliaris | Bthalassinus | Bschlegelii | 0.149 | 0.018 | 8.15 |
| Bbicolor | Bthalassinus | Bsupraciliaris | Bschlegelii | 0.001 | 0.001 | 1.53 |
| Bbicolor | Blateralis | Bsupraciliaris | Bthalassinus | -0.003 | 0.009 | -0.344 |
| Bbicolor | Bsupraciliaris | Bthalassinus | Blateralis | 0.01 | 0.008 | 1.226 |
| Bbicolor | Bthalassinus | Bsupraciliaris | Blateralis | 0.006 | 0.007 | 0.862 |
| Bbicolor | Bnigroviridis | Bsupraciliaris | Bthalassinus | -0.041 | 0.012 | -3.382 |
| Bbicolor | Bsupraciliaris | Bthalassinus | Bnigroviridis | 0.043 | 0.012 | 3.647 |
| Bbicolor | Bthalassinus | Bsupraciliaris | Bnigroviridis | 0.002 | 0.006 | 0.352 |
| Bbicolor | Blateralis | Bsupraciliaris | Bschlegelii | 0.002 | 0.001 | 1.806 |
| Bbicolor | Bschlegelii | Bsupraciliaris | Blateralis | -0.138 | 0.018 | -7.69 |
| Bbicolor | Bsupraciliaris | Bschlegelii | Blateralis | -0.139 | 0.018 | -7.798 |
| Bbicolor | Bnigroviridis | Bsupraciliaris | Bschlegelii | -0.004 | 0.003 | -1.112 |
| Bbicolor | Bschlegelii | Bsupraciliaris | Bnigroviridis | -0.109 | 0.016 | -6.693 |
| Bbicolor | Bsupraciliaris | Bschlegelii | Bnigroviridis | -0.106 | 0.017 | -6.342 |
| Bbicolor | Blateralis | Bsupraciliaris | Bnigroviridis | -0.002 | 0.006 | -0.388 |
| Bbicolor | Bnigroviridis | Bsupraciliaris | Blateralis | -0.036 | 0.011 | -3.284 |
| Bbicolor | Bsupraciliaris | Blateralis | Bnigroviridis | 0.034 | 0.011 | 2.976 |
| Bbicolor | Blateralis | Bthalassinus | Bschlegelii | 0.005 | 0.009 | 0.515 |
| Bbicolor | Bschlegelii | Bthalassinus | Blateralis | 0.01 | 0.008 | 1.256 |
| Bbicolor | Bthalassinus | Bschlegelii | Blateralis | 0.005 | 0.007 | 0.702 |
| Bbicolor | Bnigroviridis | Bthalassinus | Bschlegelii | 0.037 | 0.012 | 3.218 |
| Bbicolor | Bschlegelii | Bthalassinus | Bnigroviridis | 0.038 | 0.011 | 3.374 |
| Bbicolor | Bthalassinus | Bschlegelii | Bnigroviridis | 0.001 | 0.006 | 0.162 |

| Pop 1 | Pop 2 | Pop 3 | Pop 4 | f4 | SE f4 | Z-score |
|---|---|---|---|---|---|---|
| Bbicolor | Blateralis | Bthalassinus | Bnigroviridis | 0.001 | 0.01 | 0.068 |
| Bbicolor | Bnigroviridis | Bthalassinus | Blateralis | 0.005 | 0.009 | 0.525 |
| Bbicolor | Bthalassinus | Blateralis | Bnigroviridis | -0.004 | 0.01 | -0.445 |
| Bbicolor | Blateralis | Bschlegelii | Bnigroviridis | -0.004 | 0.006 | -0.667 |
| Bbicolor | Bnigroviridis | Bschlegelii | Blateralis | -0.032 | 0.01 | -3.169 |
| Bbicolor | Bschlegelii | Blateralis | Bnigroviridis | 0.029 | 0.011 | 2.644 |
| Bguifarroi | Bmarchi | Bnubestris | Browleyi | 0.004 | 0.007 | 0.599 |
| Bguifarroi | Bnubestris | Bmarchi | Browleyi | 0.013 | 0.008 | 1.645 |
| Bguifarroi | Browleyi | Bmarchi | Bnubestris | 0.009 | 0.009 | 1.038 |
| Bguifarroi | Bmarchi | Bnubestris | Bsupraciliaris | 0.003 | 0.007 | 0.424 |
| Bguifarroi | Bnubestris | Bmarchi | Bsupraciliaris | 0.032 | 0.011 | 2.924 |
| Bguifarroi | Bsupraciliaris | Bmarchi | Bnubestris | 0.029 | 0.011 | 2.564 |
| Bguifarroi | Bmarchi | Bnubestris | Bthalassinus | 0.043 | 0.01 | 4.401 |
| Bguifarroi | Bnubestris | Bmarchi | Bthalassinus | 0.002 | 0.002 | 1.343 |
| Bguifarroi | Bthalassinus | Bmarchi | Bnubestris | -0.041 | 0.01 | -4.136 |
| Bguifarroi | Bmarchi | Bnubestris | Bschlegelii | 0.001 | 0.007 | 0.101 |
| Bguifarroi | Bnubestris | Bmarchi | Bschlegelii | 0.034 | 0.011 | 3.016 |
| Bguifarroi | Bschlegelii | Bmarchi | Bnubestris | 0.033 | 0.011 | 2.948 |
| Bguifarroi | Blateralis | Bmarchi | Bnubestris | -0.003 | 0.005 | -0.588 |
| Bguifarroi | Bmarchi | Bnubestris | Blateralis | -0.008 | 0.008 | -1.061 |
| Bguifarroi | Bnubestris | Bmarchi | Blateralis | -0.011 | 0.007 | -1.578 |
| Bguifarroi | Bmarchi | Bnubestris | Bnigroviridis | 0.006 | 0.005 | 1.117 |
| Bguifarroi | Bnigroviridis | Bmarchi | Bnubestris | 0.082 | 0.016 | 5.223 |
| Bguifarroi | Bnubestris | Bmarchi | Bnigroviridis | 0.088 | 0.015 | 5.832 |
| Bguifarroi | Bmarchi | Browleyi | Bsupraciliaris | -0.001 | 0.006 | -0.163 |
| Bguifarroi | Browleyi | Bmarchi | Bsupraciliaris | 0.007 | 0.008 | 0.905 |
| Bguifarroi | Bsupraciliaris | Bmarchi | Browleyi | 0.008 | 0.007 | 1.096 |
| Bguifarroi | Bmarchi | Browleyi | Bthalassinus | 0.039 | 0.01 | 3.796 |
| Bguifarroi | Browleyi | Bmarchi | Bthalassinus | 0.001 | 0.004 | 0.156 |

| Pop 1 | Pop 2 | Pop 3 | Pop 4 | f4 | SE f4 | Z-score |
|---|---|---|---|---|---|---|
| Bguifarroi | Bthalassinus | Bmarchi | Browleyi | -0.039 | 0.01 | -3.72 |
| Bguifarroi | Bmarchi | Browleyi | Bschlegelii | -0.003 | 0.006 | -0.601 |
| Bguifarroi | Browleyi | Bmarchi | Bschlegelii | 0.007 | 0.008 | 0.905 |
| Bguifarroi | Bschlegelii | Bmarchi | Browleyi | 0.01 | 0.007 | 1.542 |
| Bguifarroi | Blateralis | Bmarchi | Browleyi | 0.001 | 0.005 | 0.191 |
| Bguifarroi | Bmarchi | Browleyi | Blateralis | -0.012 | 0.008 | -1.62 |
| Bguifarroi | Browleyi | Bmarchi | Blateralis | -0.011 | 0.008 | -1.41 |
| Bguifarroi | Bmarchi | Browleyi | Bnigroviridis | 0.002 | 0.008 | 0.26 |
| Bguifarroi | Bnigroviridis | Bmarchi | Browleyi | 0.005 | 0.009 | 0.555 |
| Bguifarroi | Browleyi | Bmarchi | Bnigroviridis | 0.007 | 0.008 | 0.805 |
| Bguifarroi | Bmarchi | Bsupraciliaris | Bthalassinus | 0.04 | 0.011 | 3.807 |
| Bguifarroi | Bsupraciliaris | Bmarchi | Bthalassinus | -0.002 | 0.003 | -0.599 |
| Bguifarroi | Bthalassinus | Bmarchi | Bsupraciliaris | -0.042 | 0.01 | -4.137 |
| Bguifarroi | Bmarchi | Bsupraciliaris | Bschlegelii | -0.002 | 0.003 | -0.842 |
| Bguifarroi | Bschlegelii | Bmarchi | Bsupraciliaris | 0.148 | 0.018 | 8.095 |
| Bguifarroi | Bsupraciliaris | Bmarchi | Bschlegelii | 0.146 | 0.019 | 7.862 |
| Bguifarroi | Blateralis | Bmarchi | Bsupraciliaris | 0.003 | 0.005 | 0.464 |
| Bguifarroi | Bmarchi | Bsupraciliaris | Blateralis | -0.011 | 0.007 | -1.56 |
| Bguifarroi | Bsupraciliaris | Bmarchi | Blateralis | -0.009 | 0.008 | -1.121 |
| Bguifarroi | Bmarchi | Bsupraciliaris | Bnigroviridis | 0.003 | 0.006 | 0.502 |
| Bguifarroi | Bnigroviridis | Bmarchi | Bsupraciliaris | 0.04 | 0.012 | 3.382 |
| Bguifarroi | Bsupraciliaris | Bmarchi | Bnigroviridis | 0.043 | 0.012 | 3.747 |
| Bguifarroi | Bmarchi | Bthalassinus | Bschlegelii | -0.043 | 0.01 | -4.183 |
| Bguifarroi | Bschlegelii | Bmarchi | Bthalassinus | 0.001 | 0.002 | 0.333 |
| Bguifarroi | Bthalassinus | Bmarchi | Bschlegelii | -0.042 | 0.01 | -4.104 |
| Bguifarroi | Blateralis | Bmarchi | Bthalassinus | -0.001 | 0.001 | -1 |
| Bguifarroi | Bmarchi | Bthalassinus | Blateralis | -0.052 | 0.011 | -4.759 |
| Bguifarroi | Bthalassinus | Bmarchi | Blateralis | -0.052 | 0.011 | -4.816 |
| Bguifarroi | Bmarchi | Bthalassinus | Bnigroviridis | -0.037 | 0.011 | -3.511 |

| Pop 1 | Pop 2 | Pop 3 | Pop 4 | f4 | SE f4 | Z-score |
|---|---|---|---|---|---|---|
| Bguifarroi | Bnigroviridis | Bmarchi | Bthalassinus | -0.001 | 0.005 | -0.137 |
| Bguifarroi | Bthalassinus | Bmarchi | Bnigroviridis | -0.038 | 0.01 | -3.66 |
| Bguifarroi | Blateralis | Bmarchi | Bschlegelii | 0.003 | 0.006 | 0.583 |
| Bguifarroi | Bmarchi | Bschlegelii | Blateralis | -0.009 | 0.007 | -1.321 |
| Bguifarroi | Bschlegelii | Bmarchi | Blateralis | -0.006 | 0.007 | -0.768 |
| Bguifarroi | Bmarchi | Bschlegelii | Bnigroviridis | 0.005 | 0.007 | 0.808 |
| Bguifarroi | Bnigroviridis | Bmarchi | Bschlegelii | 0.036 | 0.012 | 2.971 |
| Bguifarroi | Bschlegelii | Bmarchi | Bnigroviridis | 0.041 | 0.011 | 3.622 |
| Bguifarroi | Blateralis | Bmarchi | Bnigroviridis | 0.002 | 0.005 | 0.433 |
| Bguifarroi | Bmarchi | Blateralis | Bnigroviridis | 0.014 | 0.008 | 1.855 |
| Bguifarroi | Bnigroviridis | Bmarchi | Blateralis | -0.012 | 0.008 | -1.449 |
| Bguifarroi | Bnubestris | Browleyi | Bsupraciliaris | 0.019 | 0.01 | 1.844 |
| Bguifarroi | Browleyi | Bnubestris | Bsupraciliaris | -0.002 | 0.007 | -0.33 |
| Bguifarroi | Bsupraciliaris | Bnubestris | Browleyi | -0.021 | 0.01 | -2.153 |
| Bguifarroi | Bnubestris | Browleyi | Bthalassinus | -0.011 | 0.008 | -1.459 |
| Bguifarroi | Browleyi | Bnubestris | Bthalassinus | -0.008 | 0.008 | -1.041 |
| Bguifarroi | Bthalassinus | Bnubestris | Browleyi | 0.003 | 0.006 | 0.426 |
| Bguifarroi | Bnubestris | Browleyi | Bschlegelii | 0.02 | 0.01 | 1.952 |
| Bguifarroi | Browleyi | Bnubestris | Bschlegelii | -0.002 | 0.007 | -0.33 |
| Bguifarroi | Bschlegelii | Bnubestris | Browleyi | -0.023 | 0.01 | -2.26 |
| Bguifarroi | Blateralis | Bnubestris | Browleyi | 0.004 | 0.005 | 0.941 |
| Bguifarroi | Bnubestris | Browleyi | Blateralis | -0.025 | 0.008 | -2.971 |
| Bguifarroi | Browleyi | Bnubestris | Blateralis | -0.02 | 0.009 | -2.248 |
| Bguifarroi | Bnigroviridis | Bnubestris | Browleyi | -0.077 | 0.015 | -5.167 |
| Bguifarroi | Bnubestris | Browleyi | Bnigroviridis | 0.075 | 0.015 | 4.917 |
| Bguifarroi | Browleyi | Bnubestris | Bnigroviridis | -0.002 | 0.006 | -0.39 |
| Bguifarroi | Bnubestris | Bsupraciliaris | Bthalassinus | -0.03 | 0.011 | -2.806 |
| Bguifarroi | Bsupraciliaris | Bnubestris | Bthalassinus | -0.031 | 0.011 | -2.973 |
| Bguifarroi | Bthalassinus | Bnubestris | Bsupraciliaris | -0.001 | 0.006 | -0.163 |

| Pop 1 | Pop 2 | Pop 3 | Pop 4 | f4 | SE f4 | Z-score |
|---|---|---|---|---|---|---|
| Bguifarroi | Bnubestris | Bsupraciliaris | Bschlegelii | 0.001 | 0.003 | 0.426 |
| Bguifarroi | Bschlegelii | Bnubestris | Bsupraciliaris | 0.115 | 0.017 | 6.759 |
| Bguifarroi | Bsupraciliaris | Bnubestris | Bschlegelii | 0.117 | 0.017 | 6.914 |
| Bguifarroi | Blateralis | Bnubestris | Bsupraciliaris | 0.006 | 0.004 | 1.502 |
| Bguifarroi | Bnubestris | Bsupraciliaris | Blateralis | -0.044 | 0.01 | -4.398 |
| Bguifarroi | Bsupraciliaris | Bnubestris | Blateralis | -0.038 | 0.011 | -3.538 |
| Bguifarroi | Bnigroviridis | Bnubestris | Bsupraciliaris | -0.041 | 0.014 | -3.067 |
| Bguifarroi | Bnubestris | Bsupraciliaris | Bnigroviridis | 0.056 | 0.012 | 4.683 |
| Bguifarroi | Bsupraciliaris | Bnubestris | Bnigroviridis | 0.014 | 0.006 | 2.355 |
| Bguifarroi | Bnubestris | Bthalassinus | Bschlegelii | 0.032 | 0.011 | 2.9 |
| Bguifarroi | Bschlegelii | Bnubestris | Bthalassinus | -0.032 | 0.011 | -3.03 |
| Bguifarroi | Bthalassinus | Bnubestris | Bschlegelii | -0.001 | 0.006 | -0.108 |
| Bguifarroi | Blateralis | Bnubestris | Bthalassinus | 0.003 | 0.005 | 0.468 |
| Bguifarroi | Bnubestris | Bthalassinus | Blateralis | -0.013 | 0.007 | -1.808 |
| Bguifarroi | Bthalassinus | Bnubestris | Blateralis | -0.011 | 0.008 | -1.374 |
| Bguifarroi | Bnigroviridis | Bnubestris | Bthalassinus | -0.083 | 0.015 | -5.42 |
| Bguifarroi | Bnubestris | Bthalassinus | Bnigroviridis | 0.086 | 0.015 | 5.761 |
| Bguifarroi | Bthalassinus | Bnubestris | Bnigroviridis | 0.003 | 0.005 | 0.714 |
| Bguifarroi | Blateralis | Bnubestris | Bschlegelii | 0.006 | 0.004 | 1.655 |
| Bguifarroi | Bnubestris | Bschlegelii | Blateralis | -0.045 | 0.01 | -4.48 |
| Bguifarroi | Bschlegelii | Bnubestris | Blateralis | -0.039 | 0.011 | -3.554 |
| Bguifarroi | Bnigroviridis | Bnubestris | Bschlegelii | -0.046 | 0.013 | -3.414 |
| Bguifarroi | Bnubestris | Bschlegelii | Bnigroviridis | 0.054 | 0.012 | 4.354 |
| Bguifarroi | Bschlegelii | Bnubestris | Bnigroviridis | 0.008 | 0.006 | 1.38 |
| Bguifarroi | Blateralis | Bnubestris | Bnigroviridis | 0.006 | 0.004 | 1.459 |
| Bguifarroi | Bnigroviridis | Bnubestris | Blateralis | -0.094 | 0.016 | -5.951 |
| Bguifarroi | Bnubestris | Blateralis | Bnigroviridis | 0.099 | 0.015 | 6.545 |
| Bguifarroi | Browleyi | Bsupraciliaris | Bthalassinus | -0.006 | 0.007 | -0.914 |
| Bguifarroi | Bsupraciliaris | Browleyi | Bthalassinus | -0.01 | 0.006 | -1.747 |

| Pop 1 | Pop 2 | Pop 3 | Pop 4 | f4 | SE f4 | Z-score |
|---|---|---|---|---|---|---|
| Bguifarroi | Bthalassinus | Browleyi | Bsupraciliaris | -0.004 | 0.005 | -0.826 |
| Bguifarroi | Browleyi | Bsupraciliaris | Bschlegelii | 0 | 0 | nan |
| Bguifarroi | Bschlegelii | Browleyi | Bsupraciliaris | 0.138 | 0.018 | 7.744 |
| Bguifarroi | Bsupraciliaris | Browleyi | Bschlegelii | 0.138 | 0.018 | 7.744 |
| Bguifarroi | Blateralis | Browleyi | Bsupraciliaris | 0.002 | 0.002 | 0.647 |
| Bguifarroi | Browleyi | Bsupraciliaris | Blateralis | -0.018 | 0.007 | -2.669 |
| Bguifarroi | Bsupraciliaris | Browleyi | Blateralis | -0.016 | 0.007 | -2.389 |
| Bguifarroi | Bnigroviridis | Browleyi | Bsupraciliaris | 0.036 | 0.011 | 3.272 |
| Bguifarroi | Browleyi | Bsupraciliaris | Bnigroviridis | 0 | 0.005 | 0 |
| Bguifarroi | Bsupraciliaris | Browleyi | Bnigroviridis | 0.036 | 0.011 | 3.272 |
| Bguifarroi | Browleyi | Bthalassinus | Bschlegelii | 0.006 | 0.007 | 0.914 |
| Bguifarroi | Bschlegelii | Browleyi | Bthalassinus | -0.01 | 0.006 | -1.677 |
| Bguifarroi | Bthalassinus | Browleyi | Bschlegelii | -0.003 | 0.005 | -0.745 |
| Bguifarroi | Blateralis | Browleyi | Bthalassinus | -0.002 | 0.005 | -0.322 |
| Bguifarroi | Browleyi | Bthalassinus | Blateralis | -0.012 | 0.008 | -1.524 |
| Bguifarroi | Bthalassinus | Browleyi | Blateralis | -0.014 | 0.007 | -1.832 |
| Bguifarroi | Bnigroviridis | Browleyi | Bthalassinus | -0.005 | 0.007 | -0.808 |
| Bguifarroi | Browleyi | Bthalassinus | Bnigroviridis | 0.006 | 0.007 | 0.914 |
| Bguifarroi | Bthalassinus | Browleyi | Bnigroviridis | 0.001 | 0.006 | 0.117 |
| Bguifarroi | Blateralis | Browleyi | Bschlegelii | 0.002 | 0.002 | 0.899 |
| Bguifarroi | Browleyi | Bschlegelii | Blateralis | -0.018 | 0.007 | -2.669 |
| Bguifarroi | Bschlegelii | Browleyi | Blateralis | -0.016 | 0.007 | -2.278 |
| Bguifarroi | Bnigroviridis | Browleyi | Bschlegelii | 0.031 | 0.01 | 3.014 |
| Bguifarroi | Browleyi | Bschlegelii | Bnigroviridis | 0 | 0.005 | 0 |
| Bguifarroi | Bschlegelii | Browleyi | Bnigroviridis | 0.031 | 0.01 | 3.014 |
| Bguifarroi | Blateralis | Browleyi | Bnigroviridis | 0.001 | 0.005 | 0.301 |
| Bguifarroi | Bnigroviridis | Browleyi | Blateralis | -0.017 | 0.008 | -2.109 |
| Bguifarroi | Browleyi | Blateralis | Bnigroviridis | 0.018 | 0.008 | 2.318 |
| Bguifarroi | Bschlegelii | Bsupraciliaris | Bthalassinus | -0.148 | 0.018 | -8.102 |

| Pop 1 | Pop 2 | Pop 3 | Pop 4 | f4 | SE f4 | Z-score |
|---|---|---|---|---|---|---|
| Bguifarroi | Bsupraciliaris | Bthalassinus | Bschlegelii | 0.148 | 0.018 | 8.128 |
| Bguifarroi | Bthalassinus | Bsupraciliaris | Bschlegelii | 0 | 0.001 | 0.447 |
| Bguifarroi | Blateralis | Bsupraciliaris | Bthalassinus | -0.003 | 0.005 | -0.592 |
| Bguifarroi | Bsupraciliaris | Bthalassinus | Blateralis | -0.007 | 0.007 | -0.936 |
| Bguifarroi | Bthalassinus | Bsupraciliaris | Blateralis | -0.01 | 0.007 | -1.512 |
| Bguifarroi | Bnigroviridis | Bsupraciliaris | Bthalassinus | -0.041 | 0.012 | -3.424 |
| Bguifarroi | Bsupraciliaris | Bthalassinus | Bnigroviridis | 0.046 | 0.011 | 3.993 |
| Bguifarroi | Bthalassinus | Bsupraciliaris | Bnigroviridis | 0.004 | 0.006 | 0.786 |
| Bguifarroi | Blateralis | Bsupraciliaris | Bschlegelii | 0.001 | 0.001 | 0.943 |
| Bguifarroi | Bschlegelii | Bsupraciliaris | Blateralis | -0.154 | 0.018 | -8.353 |
| Bguifarroi | Bsupraciliaris | Bschlegelii | Blateralis | -0.155 | 0.018 | -8.403 |
| Bguifarroi | Bnigroviridis | Bsupraciliaris | Bschlegelii | -0.004 | 0.003 | -1.38 |
| Bguifarroi | Bschlegelii | Bsupraciliaris | Bnigroviridis | -0.107 | 0.016 | -6.636 |
| Bguifarroi | Bsupraciliaris | Bschlegelii | Bnigroviridis | -0.103 | 0.016 | -6.221 |
| Bguifarroi | Blateralis | Bsupraciliaris | Bnigroviridis | 0 | 0.004 | -0.044 |
| Bguifarroi | Bnigroviridis | Bsupraciliaris | Blateralis | -0.052 | 0.012 | -4.528 |
| Bguifarroi | Bsupraciliaris | Blateralis | Bnigroviridis | 0.052 | 0.012 | 4.512 |
| Bguifarroi | Blateralis | Bthalassinus | Bschlegelii | 0.004 | 0.005 | 0.711 |
| Bguifarroi | Bschlegelii | Bthalassinus | Blateralis | -0.006 | 0.007 | -0.88 |
| Bguifarroi | Bthalassinus | Bschlegelii | Blateralis | -0.01 | 0.007 | -1.558 |
| Bguifarroi | Bnigroviridis | Bthalassinus | Bschlegelii | 0.037 | 0.012 | 3.177 |
| Bguifarroi | Bschlegelii | Bthalassinus | Bnigroviridis | 0.041 | 0.011 | 3.729 |
| Bguifarroi | Bthalassinus | Bschlegelii | Bnigroviridis | 0.004 | 0.006 | 0.717 |
| Bguifarroi | Blateralis | Bthalassinus | Bnigroviridis | 0.003 | 0.005 | 0.561 |
| Bguifarroi | Bnigroviridis | Bthalassinus | Blateralis | -0.011 | 0.008 | -1.41 |
| Bguifarroi | Bthalassinus | Blateralis | Bnigroviridis | 0.014 | 0.007 | 1.916 |
| Bguifarroi | Blateralis | Bschlegelii | Bnigroviridis | -0.001 | 0.003 | -0.249 |
| Bguifarroi | Bnigroviridis | Bschlegelii | Blateralis | -0.048 | 0.011 | -4.394 |
| Bguifarroi | Bschlegelii | Blateralis | Bnigroviridis | 0.047 | 0.011 | 4.254 |

| Pop 1 | Pop 2 | Pop 3 | Pop 4 | f4 | SE f4 | Z-score |
|---|---|---|---|---|---|---|
| Bmarchi | Bnubestris | Browleyi | Bsupraciliaris | 0.02 | 0.011 | 1.78 |
| Bmarchi | Browleyi | Bnubestris | Bsupraciliaris | -0.005 | 0.008 | -0.705 |
| Bmarchi | Bsupraciliaris | Bnubestris | Browleyi | -0.025 | 0.011 | -2.415 |
| Bmarchi | Bnubestris | Browleyi | Bthalassinus | -0.051 | 0.012 | -4.301 |
| Bmarchi | Browleyi | Bnubestris | Bthalassinus | -0.052 | 0.012 | -4.453 |
| Bmarchi | Bthalassinus | Bnubestris | Browleyi | -0.001 | 0.004 | -0.333 |
| Bmarchi | Bnubestris | Browleyi | Bschlegelii | 0.024 | 0.011 | 2.153 |
| Bmarchi | Browleyi | Bnubestris | Bschlegelii | -0.003 | 0.007 | -0.422 |
| Bmarchi | Bschlegelii | Bnubestris | Browleyi | -0.027 | 0.011 | -2.515 |
| Bmarchi | Blateralis | Bnubestris | Browleyi | 0 | 0.007 | 0.023 |
| Bmarchi | Bnubestris | Browleyi | Blateralis | -0.012 | 0.009 | -1.332 |
| Bmarchi | Browleyi | Bnubestris | Blateralis | -0.012 | 0.01 | -1.287 |
| Bmarchi | Bnigroviridis | Bnubestris | Browleyi | -0.081 | 0.015 | -5.485 |
| Bmarchi | Bnubestris | Browleyi | Bnigroviridis | 0.073 | 0.016 | 4.642 |
| Bmarchi | Browleyi | Bnubestris | Bnigroviridis | -0.008 | 0.006 | -1.389 |
| Bmarchi | Bnubestris | Bsupraciliaris | Bthalassinus | -0.071 | 0.014 | -5.192 |
| Bmarchi | Bsupraciliaris | Bnubestris | Bthalassinus | -0.075 | 0.013 | -5.66 |
| Bmarchi | Bthalassinus | Bnubestris | Bsupraciliaris | -0.004 | 0.003 | -1.343 |
| Bmarchi | Bnubestris | Bsupraciliaris | Bschlegelii | 0.004 | 0.004 | 0.878 |
| Bmarchi | Bschlegelii | Bnubestris | Bsupraciliaris | 0.112 | 0.017 | 6.476 |
| Bmarchi | Bsupraciliaris | Bnubestris | Bschlegelii | 0.116 | 0.017 | 6.864 |
| Bmarchi | Blateralis | Bnubestris | Bsupraciliaris | 0.003 | 0.007 | 0.377 |
| Bmarchi | Bnubestris | Bsupraciliaris | Blateralis | -0.032 | 0.011 | -2.923 |
| Bmarchi | Bsupraciliaris | Bnubestris | Blateralis | -0.03 | 0.011 | -2.598 |
| Bmarchi | Bnigroviridis | Bnubestris | Bsupraciliaris | -0.044 | 0.013 | -3.371 |
| Bmarchi | Bnubestris | Bsupraciliaris | Bnigroviridis | 0.053 | 0.012 | 4.3 |
| Bmarchi | Bsupraciliaris | Bnubestris | Bnigroviridis | 0.008 | 0.006 | 1.339 |
| Bmarchi | Bnubestris | Bthalassinus | Bschlegelii | 0.074 | 0.013 | 5.561 |
| Bmarchi | Bschlegelii | Bnubestris | Bthalassinus | -0.076 | 0.013 | -5.701 |

| Pop 1 | Pop 2 | Pop 3 | Pop 4 | f4 | SE f4 | Z-score |
|---|---|---|---|---|---|---|
| Bmarchi | Bthalassinus | Bnubestris | Bschlegelii | -0.001 | 0.001 | -1 |
| Bmarchi | Blateralis | Bnubestris | Bthalassinus | -0.041 | 0.01 | -4.296 |
| Bmarchi | Bnubestris | Bthalassinus | Blateralis | 0.038 | 0.01 | 3.919 |
| Bmarchi | Bthalassinus | Bnubestris | Blateralis | -0.003 | 0.002 | -1.416 |
| Bmarchi | Bnigroviridis | Bnubestris | Bthalassinus | -0.126 | 0.017 | -7.256 |
| Bmarchi | Bnubestris | Bthalassinus | Bnigroviridis | 0.123 | 0.018 | 6.993 |
| Bmarchi | Bthalassinus | Bnubestris | Bnigroviridis | -0.003 | 0.005 | -0.577 |
| Bmarchi | Blateralis | Bnubestris | Bschlegelii | 0.006 | 0.007 | 0.858 |
| Bmarchi | Bnubestris | Bschlegelii | Blateralis | -0.036 | 0.011 | -3.328 |
| Bmarchi | Bschlegelii | Bnubestris | Blateralis | -0.03 | 0.012 | -2.626 |
| Bmarchi | Bnigroviridis | Bnubestris | Bschlegelii | -0.047 | 0.013 | -3.462 |
| Bmarchi | Bnubestris | Bschlegelii | Bnigroviridis | 0.049 | 0.013 | 3.718 |
| Bmarchi | Bschlegelii | Bnubestris | Bnigroviridis | 0.002 | 0.007 | 0.326 |
| Bmarchi | Blateralis | Bnubestris | Bnigroviridis | -0.001 | 0.005 | -0.093 |
| Bmarchi | Bnigroviridis | Bnubestris | Blateralis | -0.086 | 0.015 | -5.556 |
| Bmarchi | Bnubestris | Blateralis | Bnigroviridis | 0.085 | 0.015 | 5.515 |
| Bmarchi | Browleyi | Bsupraciliaris | Bthalassinus | -0.047 | 0.012 | -3.864 |
| Bmarchi | Bsupraciliaris | Browleyi | Bthalassinus | -0.049 | 0.012 | -4.208 |
| Bmarchi | Bthalassinus | Browleyi | Bsupraciliaris | -0.003 | 0.005 | -0.534 |
| Bmarchi | Browleyi | Bsupraciliaris | Bschlegelii | 0.002 | 0.003 | 0.842 |
| Bmarchi | Bschlegelii | Browleyi | Bsupraciliaris | 0.139 | 0.018 | 7.57 |
| Bmarchi | Bsupraciliaris | Browleyi | Bschlegelii | 0.142 | 0.018 | 7.803 |
| Bmarchi | Blateralis | Browleyi | Bsupraciliaris | 0.003 | 0.007 | 0.367 |
| Bmarchi | Browleyi | Bsupraciliaris | Blateralis | -0.007 | 0.008 | -0.868 |
| Bmarchi | Bsupraciliaris | Browleyi | Blateralis | -0.004 | 0.008 | -0.527 |
| Bmarchi | Bnigroviridis | Browleyi | Bsupraciliaris | 0.037 | 0.012 | 3.113 |
| Bmarchi | Browleyi | Bsupraciliaris | Bnigroviridis | -0.003 | 0.007 | -0.424 |
| Bmarchi | Bsupraciliaris | Browleyi | Bnigroviridis | 0.034 | 0.012 | 2.774 |
| Bmarchi | Browleyi | Bthalassinus | Bschlegelii | 0.049 | 0.012 | 4.18 |

| Pop 1 | Pop 2 | Pop 3 | Pop 4 | f4 | SE f4 | Z-score |
|---|---|---|---|---|---|---|
| Bmarchi | Bschlegelii | Browleyi | Bthalassinus | -0.049 | 0.012 | -4.18 |
| Bmarchi | Bthalassinus | Browleyi | Bschlegelii | 0 | 0.004 | 0 |
| Bmarchi | Blateralis | Browleyi | Bthalassinus | -0.041 | 0.011 | -3.804 |
| Bmarchi | Browleyi | Bthalassinus | Blateralis | 0.04 | 0.011 | 3.645 |
| Bmarchi | Bthalassinus | Browleyi | Blateralis | -0.001 | 0.005 | -0.301 |
| Bmarchi | Bnigroviridis | Browleyi | Bthalassinus | -0.045 | 0.011 | -4.01 |
| Bmarchi | Browleyi | Bthalassinus | Bnigroviridis | 0.043 | 0.011 | 3.8 |
| Bmarchi | Bthalassinus | Browleyi | Bnigroviridis | -0.001 | 0.005 | -0.277 |
| Bmarchi | Blateralis | Browleyi | Bschlegelii | 0.006 | 0.006 | 0.869 |
| Bmarchi | Browleyi | Bschlegelii | Blateralis | -0.009 | 0.007 | -1.248 |
| Bmarchi | Bschlegelii | Browleyi | Blateralis | -0.004 | 0.008 | -0.441 |
| Bmarchi | Bnigroviridis | Browleyi | Bschlegelii | 0.035 | 0.012 | 2.981 |
| Bmarchi | Browleyi | Bschlegelii | Bnigroviridis | -0.005 | 0.008 | -0.701 |
| Bmarchi | Bschlegelii | Browleyi | Bnigroviridis | 0.029 | 0.012 | 2.378 |
| Bmarchi | Blateralis | Browleyi | Bnigroviridis | -0.001 | 0.009 | -0.073 |
| Bmarchi | Bnigroviridis | Browleyi | Blateralis | -0.004 | 0.01 | -0.454 |
| Bmarchi | Browleyi | Blateralis | Bnigroviridis | 0.004 | 0.01 | 0.376 |
| Bmarchi | Bschlegelii | Bsupraciliaris | Bthalassinus | -0.188 | 0.02 | -9.231 |
| Bmarchi | Bsupraciliaris | Bthalassinus | Bschlegelii | 0.191 | 0.02 | 9.482 |
| Bmarchi | Bthalassinus | Bsupraciliaris | Bschlegelii | 0.003 | 0.003 | 1 |
| Bmarchi | Blateralis | Bsupraciliaris | Bthalassinus | -0.044 | 0.011 | -3.992 |
| Bmarchi | Bsupraciliaris | Bthalassinus | Blateralis | 0.045 | 0.011 | 4.221 |
| Bmarchi | Bthalassinus | Bsupraciliaris | Blateralis | 0.001 | 0.004 | 0.378 |
| Bmarchi | Bnigroviridis | Bsupraciliaris | Bthalassinus | -0.082 | 0.015 | -5.619 |
| Bmarchi | Bsupraciliaris | Bthalassinus | Bnigroviridis | 0.083 | 0.014 | 5.746 |
| Bmarchi | Bthalassinus | Bsupraciliaris | Bnigroviridis | 0.001 | 0.004 | 0.333 |
| Bmarchi | Blateralis | Bsupraciliaris | Bschlegelii | 0.003 | 0.003 | 1.05 |
| Bmarchi | Bschlegelii | Bsupraciliaris | Blateralis | -0.143 | 0.018 | -7.725 |
| Bmarchi | Bsupraciliaris | Bschlegelii | Blateralis | -0.146 | 0.018 | -8.008 |

| Pop 1 | Pop 2 | Pop 3 | Pop 4 | f4 | SE f4 | Z-score |
|---|---|---|---|---|---|---|
| Bmarchi | Bnigroviridis | Bsupraciliaris | Bschlegelii | -0.002 | 0.002 | -1.134 |
| Bmarchi | Bschlegelii | Bsupraciliaris | Bnigroviridis | -0.11 | 0.016 | -6.751 |
| Bmarchi | Bsupraciliaris | Bschlegelii | Bnigroviridis | -0.108 | 0.016 | -6.583 |
| Bmarchi | Blateralis | Bsupraciliaris | Bnigroviridis | -0.003 | 0.007 | -0.448 |
| Bmarchi | Bnigroviridis | Bsupraciliaris | Blateralis | -0.041 | 0.012 | -3.43 |
| Bmarchi | Bsupraciliaris | Blateralis | Bnigroviridis | 0.038 | 0.012 | 3.074 |
| Bmarchi | Blateralis | Bthalassinus | Bschlegelii | 0.047 | 0.011 | 4.418 |
| Bmarchi | Bschlegelii | Bthalassinus | Blateralis | 0.045 | 0.011 | 4.248 |
| Bmarchi | Bthalassinus | Bschlegelii | Blateralis | -0.001 | 0.002 | -0.577 |
| Bmarchi | Bnigroviridis | Bthalassinus | Bschlegelii | 0.079 | 0.014 | 5.534 |
| Bmarchi | Bschlegelii | Bthalassinus | Bnigroviridis | 0.078 | 0.015 | 5.36 |
| Bmarchi | Bthalassinus | Bschlegelii | Bnigroviridis | -0.001 | 0.005 | -0.277 |
| Bmarchi | Blateralis | Bthalassinus | Bnigroviridis | 0.04 | 0.011 | 3.688 |
| Bmarchi | Bnigroviridis | Bthalassinus | Blateralis | 0.04 | 0.011 | 3.746 |
| Bmarchi | Bthalassinus | Blateralis | Bnigroviridis | 0 | 0.005 | 0 |
| Bmarchi | Blateralis | Bschlegelii | Bnigroviridis | -0.006 | 0.008 | -0.833 |
| Bmarchi | Bnigroviridis | Bschlegelii | Blateralis | -0.039 | 0.012 | -3.347 |
| Bmarchi | Bschlegelii | Blateralis | Bnigroviridis | 0.033 | 0.012 | 2.629 |
| Bnubestris | Browleyi | Bsupraciliaris | Bthalassinus | 0.024 | 0.01 | 2.344 |
| Bnubestris | Bsupraciliaris | Browleyi | Bthalassinus | 0.001 | 0.007 | 0.199 |
| Bnubestris | Bthalassinus | Browleyi | Bsupraciliaris | -0.023 | 0.01 | -2.191 |
| Bnubestris | Browleyi | Bsupraciliaris | Bschlegelii | -0.001 | 0.003 | -0.426 |
| Bnubestris | Bschlegelii | Browleyi | Bsupraciliaris | 0.119 | 0.017 | 6.985 |
| Bnubestris | Bsupraciliaris | Browleyi | Bschlegelii | 0.118 | 0.017 | 6.83 |
| Bnubestris | Blateralis | Browleyi | Bsupraciliaris | -0.017 | 0.01 | -1.741 |
| Bnubestris | Browleyi | Bsupraciliaris | Blateralis | 0.026 | 0.009 | 2.907 |
| Bnubestris | Bsupraciliaris | Browleyi | Blateralis | 0.008 | 0.006 | 1.342 |
| Bnubestris | Bnigroviridis | Browleyi | Bsupraciliaris | 0.017 | 0.008 | 2.174 |
| Bnubestris | Browleyi | Bsupraciliaris | Bnigroviridis | -0.056 | 0.013 | -4.456 |

| Pop 1 | Pop 2 | Pop 3 | Pop 4 | f4 | SE f4 | Z-score |
|---|---|---|---|---|---|---|
| Bnubestris | Bsupraciliaris | Browleyi | Bnigroviridis | -0.039 | 0.014 | -2.727 |
| Bnubestris | Browleyi | Bthalassinus | Bschlegelii | -0.025 | 0.01 | -2.446 |
| Bnubestris | Bschlegelii | Browleyi | Bthalassinus | 0.002 | 0.007 | 0.248 |
| Bnubestris | Bthalassinus | Browleyi | Bschlegelii | -0.024 | 0.011 | -2.258 |
| Bnubestris | Blateralis | Browleyi | Bthalassinus | 0.01 | 0.009 | 1.044 |
| Bnubestris | Browleyi | Bthalassinus | Blateralis | 0.002 | 0.007 | 0.216 |
| Bnubestris | Bthalassinus | Browleyi | Blateralis | 0.011 | 0.009 | 1.286 |
| Bnubestris | Bnigroviridis | Browleyi | Bthalassinus | 0.006 | 0.004 | 1.476 |
| Bnubestris | Browleyi | Bthalassinus | Bnigroviridis | -0.08 | 0.014 | -5.654 |
| Bnubestris | Bthalassinus | Browleyi | Bnigroviridis | -0.074 | 0.015 | -5.028 |
| Bnubestris | Blateralis | Browleyi | Bschlegelii | -0.018 | 0.01 | -1.78 |
| Bnubestris | Browleyi | Bschlegelii | Blateralis | 0.027 | 0.009 | 3.011 |
| Bnubestris | Bschlegelii | Browleyi | Blateralis | 0.009 | 0.006 | 1.445 |
| Bnubestris | Bnigroviridis | Browleyi | Bschlegelii | 0.011 | 0.008 | 1.405 |
| Bnubestris | Browleyi | Bschlegelii | Bnigroviridis | -0.054 | 0.013 | -4.161 |
| Bnubestris | Bschlegelii | Browleyi | Bnigroviridis | -0.043 | 0.014 | -3.051 |
| Bnubestris | Blateralis | Browleyi | Bnigroviridis | -0.073 | 0.016 | -4.728 |
| Bnubestris | Bnigroviridis | Browleyi | Blateralis | 0.008 | 0.006 | 1.314 |
| Bnubestris | Browleyi | Blateralis | Bnigroviridis | -0.081 | 0.015 | -5.545 |
| Bnubestris | Bschlegelii | Bsupraciliaris | Bthalassinus | -0.118 | 0.017 | -6.932 |
| Bnubestris | Bsupraciliaris | Bthalassinus | Bschlegelii | 0.117 | 0.017 | 6.803 |
| Bnubestris | Bthalassinus | Bsupraciliaris | Bschlegelii | -0.001 | 0.003 | -0.311 |
| Bnubestris | Blateralis | Bsupraciliaris | Bthalassinus | 0.027 | 0.011 | 2.426 |
| Bnubestris | Bsupraciliaris | Bthalassinus | Blateralis | 0.007 | 0.006 | 1.089 |
| Bnubestris | Bthalassinus | Bsupraciliaris | Blateralis | 0.034 | 0.01 | 3.338 |
| Bnubestris | Bnigroviridis | Bsupraciliaris | Bthalassinus | -0.011 | 0.007 | -1.632 |
| Bnubestris | Bsupraciliaris | Bthalassinus | Bnigroviridis | -0.04 | 0.013 | -3.038 |
| Bnubestris | Bthalassinus | Bsupraciliaris | Bnigroviridis | -0.051 | 0.012 | -4.263 |
| Bnubestris | Blateralis | Bsupraciliaris | Bschlegelii | -0.001 | 0.003 | -0.208 |

| Pop 1 | Pop 2 | Pop 3 | Pop 4 | f4 | SE f4 | Z-score |
|---|---|---|---|---|---|---|
| Bnubestris | Bschlegelii | Bsupraciliaris | Blateralis | -0.11 | 0.017 | -6.655 |
| Bnubestris | Bsupraciliaris | Bschlegelii | Blateralis | -0.11 | 0.017 | -6.549 |
| Bnubestris | Bnigroviridis | Bsupraciliaris | Bschlegelii | -0.006 | 0.004 | -1.455 |
| Bnubestris | Bschlegelii | Bsupraciliaris | Bnigroviridis | -0.163 | 0.019 | -8.47 |
| Bnubestris | Bsupraciliaris | Bschlegelii | Bnigroviridis | -0.157 | 0.02 | -7.957 |
| Bnubestris | Blateralis | Bsupraciliaris | Bnigroviridis | -0.056 | 0.013 | -4.47 |
| Bnubestris | Bnigroviridis | Bsupraciliaris | Blateralis | -0.009 | 0.006 | -1.425 |
| Bnubestris | Bsupraciliaris | Blateralis | Bnigroviridis | -0.047 | 0.013 | -3.509 |
| Bnubestris | Blateralis | Bthalassinus | Bschlegelii | -0.028 | 0.011 | -2.456 |
| Bnubestris | Bschlegelii | Bthalassinus | Blateralis | 0.007 | 0.006 | 1.132 |
| Bnubestris | Bthalassinus | Bschlegelii | Blateralis | 0.035 | 0.01 | 3.39 |
| Bnubestris | Bnigroviridis | Bthalassinus | Bschlegelii | 0.005 | 0.007 | 0.752 |
| Bnubestris | Bschlegelii | Bthalassinus | Bnigroviridis | -0.045 | 0.013 | -3.41 |
| Bnubestris | Bthalassinus | Bschlegelii | Bnigroviridis | -0.05 | 0.013 | -3.978 |
| Bnubestris | Blateralis | Bthalassinus | Bnigroviridis | -0.083 | 0.015 | -5.451 |
| Bnubestris | Bnigroviridis | Bthalassinus | Blateralis | 0.002 | 0.005 | 0.463 |
| Bnubestris | Bthalassinus | Blateralis | Bnigroviridis | -0.085 | 0.015 | -5.695 |
| Bnubestris | Blateralis | Bschlegelii | Bnigroviridis | -0.055 | 0.013 | -4.27 |
| Bnubestris | Bnigroviridis | Bschlegelii | Blateralis | -0.003 | 0.006 | -0.493 |
| Bnubestris | Bschlegelii | Blateralis | Bnigroviridis | -0.052 | 0.013 | -3.919 |
| Browleyi | Bschlegelii | Bsupraciliaris | Bthalassinus | -0.142 | 0.018 | -7.847 |
| Browleyi | Bsupraciliaris | Bthalassinus | Bschlegelii | 0.142 | 0.018 | 7.873 |
| Browleyi | Bthalassinus | Bsupraciliaris | Bschlegelii | 0 | 0.001 | 0.447 |
| Browleyi | Blateralis | Bsupraciliaris | Bthalassinus | 0.003 | 0.007 | 0.401 |
| Browleyi | Bsupraciliaris | Bthalassinus | Blateralis | 0.005 | 0.005 | 0.966 |
| Browleyi | Bthalassinus | Bsupraciliaris | Blateralis | 0.008 | 0.006 | 1.277 |
| Browleyi | Bnigroviridis | Bsupraciliaris | Bthalassinus | -0.035 | 0.012 | -3.025 |
| Browleyi | Bsupraciliaris | Bthalassinus | Bnigroviridis | 0.039 | 0.011 | 3.6 |
| Browleyi | Bthalassinus | Bsupraciliaris | Bnigroviridis | 0.004 | 0.006 | 0.786 |

| Pop 1 | Pop 2 | Pop 3 | Pop 4 | f4 | SE f4 | Z-score |
|---|---|---|---|---|---|---|
| Browleyi | Blateralis | Bsupraciliaris | Bschlegelii | 0.001 | 0.001 | 0.943 |
| Browleyi | Bschlegelii | Bsupraciliaris | Blateralis | -0.136 | 0.018 | -7.661 |
| Browleyi | Bsupraciliaris | Bschlegelii | Blateralis | -0.137 | 0.018 | -7.711 |
| Browleyi | Bnigroviridis | Bsupraciliaris | Bschlegelii | -0.004 | 0.003 | -1.38 |
| Browleyi | Bschlegelii | Bsupraciliaris | Bnigroviridis | -0.107 | 0.016 | -6.636 |
| Browleyi | Bsupraciliaris | Bschlegelii | Bnigroviridis | -0.103 | 0.016 | -6.221 |
| Browleyi | Blateralis | Bsupraciliaris | Bnigroviridis | 0 | 0.005 | -0.031 |
| Browleyi | Bnigroviridis | Bsupraciliaris | Blateralis | -0.034 | 0.011 | -3.22 |
| Browleyi | Bsupraciliaris | Blateralis | Bnigroviridis | 0.034 | 0.011 | 3.203 |
| Browleyi | Blateralis | Bthalassinus | Bschlegelii | -0.002 | 0.007 | -0.305 |
| Browleyi | Bschlegelii | Bthalassinus | Blateralis | 0.006 | 0.006 | 1.015 |
| Browleyi | Bthalassinus | Bschlegelii | Blateralis | 0.008 | 0.006 | 1.218 |
| Browleyi | Bnigroviridis | Bthalassinus | Bschlegelii | 0.031 | 0.011 | 2.758 |
| Browleyi | Bschlegelii | Bthalassinus | Bnigroviridis | 0.035 | 0.01 | 3.316 |
| Browleyi | Bthalassinus | Bschlegelii | Bnigroviridis | 0.004 | 0.006 | 0.717 |
| Browleyi | Blateralis | Bthalassinus | Bnigroviridis | -0.003 | 0.008 | -0.374 |
| Browleyi | Bnigroviridis | Bthalassinus | Blateralis | 0.001 | 0.008 | 0.089 |
| Browleyi | Bthalassinus | Blateralis | Bnigroviridis | -0.004 | 0.008 | -0.45 |
| Browleyi | Blateralis | Bschlegelii | Bnigroviridis | -0.001 | 0.005 | -0.165 |
| Browleyi | Bnigroviridis | Bschlegelii | Blateralis | -0.03 | 0.01 | -3.013 |
| Browleyi | Bschlegelii | Blateralis | Bnigroviridis | 0.029 | 0.01 | 2.878 |
| Bsupraciliaris | Blateralis | Bthalassinus | Bschlegelii | -0.144 | 0.018 | -7.964 |
| Bsupraciliaris | Bschlegelii | Bthalassinus | Blateralis | 0 | 0.001 | 0.324 |
| Bsupraciliaris | Bthalassinus | Bschlegelii | Blateralis | 0.145 | 0.018 | 7.987 |
| Bsupraciliaris | Bnigroviridis | Bthalassinus | Bschlegelii | -0.111 | 0.016 | -6.822 |
| Bsupraciliaris | Bschlegelii | Bthalassinus | Bnigroviridis | -0.005 | 0.003 | -1.462 |
| Bsupraciliaris | Bthalassinus | Bschlegelii | Bnigroviridis | 0.107 | 0.017 | 6.382 |
| Bsupraciliaris | Blateralis | Bthalassinus | Bnigroviridis | -0.042 | 0.012 | -3.618 |
| Bsupraciliaris | Bnigroviridis | Bthalassinus | Blateralis | -0.005 | 0.007 | -0.673 |

| Pop 1 | Pop 2 | Pop 3 | Pop 4 | f4 | SE f4 | Z-score |
|---|---|---|---|---|---|---|
| Bsupraciliaris | Bthalassinus | Blateralis | Bnigroviridis | -0.038 | 0.012 | -3.074 |
| Bsupraciliaris | Blateralis | Bschlegelii | Bnigroviridis | 0.102 | 0.016 | 6.201 |
| Bsupraciliaris | Bnigroviridis | Bschlegelii | Blateralis | 0.107 | 0.016 | 6.671 |
| Bsupraciliaris | Bschlegelii | Blateralis | Bnigroviridis | -0.005 | 0.003 | -1.626 |
| Bthalassinus | Blateralis | Bschlegelii | Bnigroviridis | -0.005 | 0.007 | -0.743 |
| Bthalassinus | Bnigroviridis | Bschlegelii | Blateralis | -0.038 | 0.011 | -3.393 |
| Bthalassinus | Bschlegelii | Blateralis | Bnigroviridis | 0.033 | 0.012 | 2.764 |

Table A.6: Results of D-statistic calculations of all informative combinations within *Bothriechis*, using an alignment of all SNPs (6,521) and calculated in the R package 'evobiR'.

| H1 | H2 | H3 | Out | Number ABBA | Number BABA | D | Z-score | SD D-statistic | P-value that D = 0 |
|---|---|---|---|---|---|---|---|---|---|
| Baurifer | Bbicolor | Bguifarroi | Blateralis | 17 | 14 | 0.097 | 0.097 | 0.072 | 0.177 |
| Baurifer | Bbicolor | Bguifarroi | Bmarchi | 32 | 35 | -0.045 | -0.045 | 0.096 | 0.642 |
| Baurifer | Bbicolor | Bguifarroi | Bnigroviridis | 45 | 53 | -0.082 | -0.082 | 0.038 | 0.034 |
| Baurifer | Bbicolor | Bguifarroi | Bnubestris | 42 | 71 | -0.257 | -0.257 | 0.101 | 0.011 |
| Baurifer | Bbicolor | Bguifarroi | Browleyi | 75 | 52 | 0.181 | 0.181 | 0.042 | 0 |
| Baurifer | Bbicolor | Bguifarroi | Bschlegelii | 38 | 61 | -0.232 | -0.232 | 0.04 | 0 |
| Baurifer | Bbicolor | Bguifarroi | Bsupraciliaris | 86 | 56 | 0.211 | 0.211 | 0.086 | 0.014 |
| Baurifer | Bbicolor | Bguifarroi | Bthalassinus | 94 | 22 | 0.621 | 0.621 | 0.068 | 0 |
| Baurifer | Bbicolor | Blateralis | Bnigroviridis | 36 | 47 | -0.133 | -0.133 | 0.056 | 0.019 |
| Baurifer | Bbicolor | Bmarchi | Blateralis | 32 | 88 | -0.467 | -0.467 | 0.027 | 0 |
| Baurifer | Bbicolor | Bmarchi | Bnigroviridis | 32 | 46 | -0.179 | -0.179 | 0.06 | 0.003 |
| Baurifer | Bbicolor | Bmarchi | Bnubestris | 35 | 56 | -0.231 | -0.231 | 0.065 | 0 |
| Baurifer | Bbicolor | Bmarchi | Browleyi | 111 | 66 | 0.254 | 0.254 | 0.063 | 0 |
| Baurifer | Bbicolor | Bmarchi | Bschlegelii | 39 | 54 | -0.161 | -0.161 | 0.027 | 0 |
| Baurifer | Bbicolor | Bmarchi | Bsupraciliaris | 63 | 50 | 0.115 | 0.115 | 0.071 | 0.103 |
| Baurifer | Bbicolor | Bmarchi | Bthalassinus | 18 | 17 | 0.029 | 0.029 | 0.109 | 0.793 |
| Baurifer | Bbicolor | Bnubestris | Blateralis | 46 | 39 | 0.082 | 0.082 | 0.051 | 0.107 |

| H1 | H2 | H3 | Out | Number ABBA | Number BABA | D | Z-score | SD D-statistic | P-value that D = 0 |
|---|---|---|---|---|---|---|---|---|---|
| Baurifer | Bbicolor | Bnubestris | Bnigroviridis | 21 | 11 | 0.313 | 0.313 | 0.062 | 0 |
| Baurifer | Bbicolor | Bnubestris | Browleyi | 119 | 59 | 0.337 | 0.337 | 0.058 | 0 |
| Baurifer | Bbicolor | Bnubestris | Bschlegelii | 56 | 31 | 0.287 | 0.287 | 0.155 | 0.064 |
| Baurifer | Bbicolor | Bnubestris | Bsupraciliaris | 32 | 22 | 0.185 | 0.185 | 0.057 | 0.001 |
| Baurifer | Bbicolor | Bnubestris | Bthalassinus | 63 | 56 | 0.059 | 0.059 | 0.067 | 0.379 |
| Baurifer | Bbicolor | Browleyi | Blateralis | 80 | 80 | 0 | 0 | 0.051 | 1 |
| Baurifer | Bbicolor | Browleyi | Bnigroviridis | 63 | 68 | -0.038 | -0.038 | 0.046 | 0.41 |
| Baurifer | Bbicolor | Browleyi | Bschlegelii | 86 | 120 | -0.165 | -0.165 | 0.083 | 0.046 |
| Baurifer | Bbicolor | Browleyi | Bsupraciliaris | 67 | 71 | -0.029 | -0.029 | 0.042 | 0.491 |
| Baurifer | Bbicolor | Browleyi | Bthalassinus | 79 | 66 | 0.09 | 0.09 | 0.052 | 0.087 |
| Baurifer | Bbicolor | Bschlegelii | Blateralis | 63 | 83 | -0.137 | -0.137 | 0.085 | 0.107 |
| Baurifer | Bbicolor | Bschlegelii | Bnigroviridis | 53 | 76 | -0.178 | -0.178 | 0.129 | 0.168 |
| Baurifer | Bbicolor | Bsupraciliaris | Blateralis | 45 | 80 | -0.28 | -0.28 | 0.092 | 0.002 |
| Baurifer | Bbicolor | Bsupraciliaris | Bnigroviridis | 50 | 62 | -0.107 | -0.107 | 0.195 | 0.582 |
| Baurifer | Bbicolor | Bsupraciliaris | Bschlegelii | 34 | 50 | -0.19 | -0.19 | 0.305 | 0.532 |
| Baurifer | Bbicolor | Bsupraciliaris | Bthalassinus | 93 | 48 | 0.319 | 0.319 | 0.101 | 0.002 |
| Baurifer | Bbicolor | Bthalassinus | Blateralis | 53 | 44 | 0.093 | 0.093 | 0.061 | 0.13 |
| Baurifer | Bbicolor | Bthalassinus | Bnigroviridis | 62 | 90 | -0.184 | -0.184 | 0.141 | 0.193 |
| Baurifer | Bbicolor | Bthalassinus | Bschlegelii | 55 | 58 | -0.027 | -0.027 | 0.08 | 0.741 |
| Baurifer | Bguifarroi | Bbicolor | Blateralis | 28 | 272 | -0.813 | -0.813 | 0.026 | 0 |
| Baurifer | Bguifarroi | Bbicolor | Bmarchi | 47 | 231 | -0.662 | -0.662 | 0.046 | 0 |

| H1 | H2 | H3 | Out | Number ABBA | Number BABA | D | Z-score | SD D-statistic | P-value that D = 0 |
|---|---|---|---|---|---|---|---|---|---|
| Baurifer | Bguifarroi | Bbicolor | Bnigroviridis | 54 | 153 | -0.478 | -0.478 | 0.082 | 0 |
| Baurifer | Bguifarroi | Bbicolor | Bnubestris | 43 | 157 | -0.57 | -0.57 | 0.039 | 0 |
| Baurifer | Bguifarroi | Bbicolor | Browleyi | 69 | 70 | -0.007 | -0.007 | 0.032 | 0.823 |
| Baurifer | Bguifarroi | Bbicolor | Bschlegelii | 57 | 167 | -0.491 | -0.491 | 0.033 | 0 |
| Baurifer | Bguifarroi | Bbicolor | Bsupraciliaris | 37 | 169 | -0.641 | -0.641 | 0.029 | 0 |
| Baurifer | Bguifarroi | Bbicolor | Bthalassinus | 31 | 169 | -0.69 | -0.69 | 0.036 | 0 |
| Baurifer | Bguifarroi | Blateralis | Bnigroviridis | 187 | 23 | 0.781 | 0.781 | 0.029 | 0 |
| Baurifer | Bguifarroi | Bmarchi | Blateralis | 34 | 137 | -0.602 | -0.602 | 0.031 | 0 |
| Baurifer | Bguifarroi | Bmarchi | Bnigroviridis | 96 | 69 | 0.164 | 0.164 | 0.038 | 0 |
| Baurifer | Bguifarroi | Bmarchi | Bnubestris | 86 | 78 | 0.049 | 0.049 | 0.035 | 0.161 |
| Baurifer | Bguifarroi | Bmarchi | Browleyi | 172 | 34 | 0.67 | 0.67 | 0.023 | 0 |
| Baurifer | Bguifarroi | Bmarchi | Bschlegelii | 119 | 75 | 0.227 | 0.227 | 0.037 | 0 |
| Baurifer | Bguifarroi | Bmarchi | Bsupraciliaris | 118 | 82 | 0.18 | 0.18 | 0.027 | 0 |
| Baurifer | Bguifarroi | Bmarchi | Bthalassinus | 59 | 16 | 0.573 | 0.573 | 0.131 | 0 |
| Baurifer | Bguifarroi | Bnubestris | Blateralis | 92 | 172 | -0.303 | -0.303 | 0.089 | 0.001 |
| Baurifer | Bguifarroi | Bnubestris | Bnigroviridis | 20 | 45 | -0.385 | -0.385 | 0.139 | 0.006 |
| Baurifer | Bguifarroi | Bnubestris | Browleyi | 146 | 31 | 0.65 | 0.65 | 0.034 | 0 |
| Baurifer | Bguifarroi | Bnubestris | Bschlegelii | 71 | 62 | 0.068 | 0.068 | 0.055 | 0.218 |
| Baurifer | Bguifarroi | Bnubestris | Bsupraciliaris | 81 | 41 | 0.328 | 0.328 | 0.086 | 0 |
| Baurifer | Bguifarroi | Bnubestris | Bthalassinus | 84 | 86 | -0.012 | -0.012 | 0.066 | 0.859 |
| Baurifer | Bguifarroi | Browleyi | Blateralis | 19 | 277 | -0.872 | -0.872 | 0.014 | 0 |

| H1 | H2 | H3 | Out | Number ABBA | Number BABA | D | Z-score | SD D-statistic | P-value that D = 0 |
|---|---|---|---|---|---|---|---|---|---|
| Baurifer | Bguifarroi | Browleyi | Bnigroviridis | 33 | 139 | -0.616 | -0.616 | 0.043 | 0 |
| Baurifer | Bguifarroi | Browleyi | Bschlegelii | 33 | 152 | -0.643 | -0.643 | 0.028 | 0 |
| Baurifer | Bguifarroi | Browleyi | Bsupraciliaris | 30 | 146 | -0.659 | -0.659 | 0.028 | 0 |
| Baurifer | Bguifarroi | Browleyi | Bthalassinus | 33 | 162 | -0.662 | -0.662 | 0.023 | 0 |
| Baurifer | Bguifarroi | Bschlegelii | Blateralis | 66 | 149 | -0.386 | -0.386 | 0.062 | 0 |
| Baurifer | Bguifarroi | Bschlegelii | Bnigroviridis | 49 | 52 | -0.03 | -0.03 | 0.052 | 0.565 |
| Baurifer | Bguifarroi | Bsupraciliaris | Blateralis | 34 | 167 | -0.662 | -0.662 | 0.027 | 0 |
| Baurifer | Bguifarroi | Bsupraciliaris | Bnigroviridis | 41 | 76 | -0.299 | -0.299 | 0.077 | 0 |
| Baurifer | Bguifarroi | Bsupraciliaris | Bschlegelii | 12 | 16 | -0.143 | -0.143 | 0.103 | 0.167 |
| Baurifer | Bguifarroi | Bsupraciliaris | Bthalassinus | 105 | 82 | 0.123 | 0.123 | 0.058 | 0.034 |
| Baurifer | Bguifarroi | Bthalassinus | Blateralis | 26 | 180 | -0.748 | -0.748 | 0.021 | 0 |
| Baurifer | Bguifarroi | Bthalassinus | Bnigroviridis | 90 | 75 | 0.091 | 0.091 | 0.033 | 0.007 |
| Baurifer | Bguifarroi | Bthalassinus | Bschlegelii | 192 | 82 | 0.401 | 0.401 | 0.04 | 0 |
| Baurifer | Blateralis | Bbicolor | Bguifarroi | 30 | 266 | -0.797 | -0.797 | 0.044 | 0 |
| Baurifer | Blateralis | Bbicolor | Bmarchi | 37 | 178 | -0.656 | -0.656 | 0.03 | 0 |
| Baurifer | Blateralis | Bbicolor | Bnigroviridis | 33 | 151 | -0.641 | -0.641 | 0.036 | 0 |
| Baurifer | Blateralis | Bbicolor | Bnubestris | 73 | 179 | -0.421 | -0.421 | 0.052 | 0 |
| Baurifer | Blateralis | Bbicolor | Browleyi | 77 | 82 | -0.031 | -0.031 | 0.047 | 0.507 |
| Baurifer | Blateralis | Bbicolor | Bschlegelii | 38 | 177 | -0.647 | -0.647 | 0.017 | 0 |
| Baurifer | Blateralis | Bbicolor | Bsupraciliaris | 77 | 163 | -0.358 | -0.358 | 0.04 | 0 |
| Baurifer | Blateralis | Bbicolor | Bthalassinus | 45 | 160 | -0.561 | -0.561 | 0.032 | 0 |

| H1 | H2 | H3 | Out | Number ABBA | Number BABA | D | Z-score | SD D-statistic | P-value that D = 0 |
|---|---|---|---|---|---|---|---|---|---|
| Baurifer | Blateralis | Bguifarroi | Bmarchi | 148 | 25 | 0.711 | 0.711 | 0.026 | 0 |
| Baurifer | Blateralis | Bguifarroi | Bnigroviridis | 175 | 33 | 0.683 | 0.683 | 0.018 | 0 |
| Baurifer | Blateralis | Bguifarroi | Bnubestris | 146 | 26 | 0.698 | 0.698 | 0.037 | 0 |
| Baurifer | Blateralis | Bguifarroi | Browleyi | 277 | 7 | 0.951 | 0.951 | 0.007 | 0 |
| Baurifer | Blateralis | Bguifarroi | Bschlegelii | 179 | 41 | 0.627 | 0.627 | 0.035 | 0 |
| Baurifer | Blateralis | Bguifarroi | Bsupraciliaris | 146 | 57 | 0.438 | 0.438 | 0.033 | 0 |
| Baurifer | Blateralis | Bguifarroi | Bthalassinus | 153 | 51 | 0.5 | 0.5 | 0.097 | 0 |
| Baurifer | Blateralis | Bmarchi | Bnigroviridis | 96 | 65 | 0.193 | 0.193 | 0.047 | 0 |
| Baurifer | Blateralis | Bmarchi | Bnubestris | 83 | 67 | 0.107 | 0.107 | 0.022 | 0 |
| Baurifer | Blateralis | Bmarchi | Browleyi | 157 | 94 | 0.251 | 0.251 | 0.078 | 0.001 |
| Baurifer | Blateralis | Bmarchi | Bschlegelii | 101 | 73 | 0.161 | 0.161 | 0.041 | 0 |
| Baurifer | Blateralis | Bmarchi | Bsupraciliaris | 83 | 87 | -0.024 | -0.024 | 0.029 | 0.419 |
| Baurifer | Blateralis | Bmarchi | Bthalassinus | 22 | 14 | 0.222 | 0.222 | 0.104 | 0.032 |
| Baurifer | Blateralis | Bnubestris | Bnigroviridis | 20 | 51 | -0.437 | -0.437 | 0.119 | 0 |
| Baurifer | Blateralis | Bnubestris | Browleyi | 137 | 21 | 0.734 | 0.734 | 0.035 | 0 |
| Baurifer | Blateralis | Bnubestris | Bschlegelii | 101 | 108 | -0.033 | -0.033 | 0.086 | 0.697 |
| Baurifer | Blateralis | Bnubestris | Bsupraciliaris | 91 | 49 | 0.3 | 0.3 | 0.101 | 0.003 |
| Baurifer | Blateralis | Bnubestris | Bthalassinus | 71 | 103 | -0.184 | -0.184 | 0.056 | 0.001 |
| Baurifer | Blateralis | Browleyi | Bnigroviridis | 47 | 145 | -0.51 | -0.51 | 0.098 | 0 |
| Baurifer | Blateralis | Browleyi | Bschlegelii | 28 | 155 | -0.694 | -0.694 | 0.022 | 0 |
| Baurifer | Blateralis | Browleyi | Bsupraciliaris | 93 | 159 | -0.262 | -0.262 | 0.057 | 0 |

| H1 | H2 | H3 | Out | Number ABBA | Number BABA | D | Z-score | SD D-statistic | P-value that D = 0 |
|---|---|---|---|---|---|---|---|---|---|
| Baurifer | Blateralis | Browleyi | Bthalassinus | 30 | 157 | -0.679 | -0.679 | 0.027 | 0 |
| Baurifer | Blateralis | Bschlegelii | Bnigroviridis | 82 | 89 | -0.041 | -0.041 | 0.132 | 0.756 |
| Baurifer | Blateralis | Bsupraciliaris | Bnigroviridis | 64 | 118 | -0.297 | -0.297 | 0.078 | 0 |
| Baurifer | Blateralis | Bsupraciliaris | Bschlegelii | 35 | 11 | 0.522 | 0.522 | 0.196 | 0.008 |
| Baurifer | Blateralis | Bsupraciliaris | Bthalassinus | 104 | 80 | 0.13 | 0.13 | 0.032 | 0 |
| Baurifer | Blateralis | Bthalassinus | Bnigroviridis | 92 | 71 | 0.129 | 0.129 | 0.059 | 0.029 |
| Baurifer | Blateralis | Bthalassinus | Bschlegelii | 80 | 189 | -0.405 | -0.405 | 0.038 | 0 |
| Baurifer | Bmarchi | Bbicolor | Bguifarroi | 24 | 172 | -0.755 | -0.755 | 0.03 | 0 |
| Baurifer | Bmarchi | Bbicolor | Blateralis | 40 | 167 | -0.614 | -0.614 | 0.035 | 0 |
| Baurifer | Bmarchi | Bbicolor | Bnigroviridis | 38 | 139 | -0.571 | -0.571 | 0.042 | 0 |
| Baurifer | Bmarchi | Bbicolor | Bnubestris | 36 | 131 | -0.569 | -0.569 | 0.046 | 0 |
| Baurifer | Bmarchi | Bbicolor | Browleyi | 139 | 77 | 0.287 | 0.287 | 0.092 | 0.002 |
| Baurifer | Bmarchi | Bbicolor | Bschlegelii | 55 | 134 | -0.418 | -0.418 | 0.034 | 0 |
| Baurifer | Bmarchi | Bbicolor | Bsupraciliaris | 38 | 142 | -0.578 | -0.578 | 0.041 | 0 |
| Baurifer | Bmarchi | Bbicolor | Bthalassinus | 17 | 334 | -0.903 | -0.903 | 0.012 | 0 |
| Baurifer | Bmarchi | Bguifarroi | Blateralis | 56 | 28 | 0.333 | 0.333 | 0.146 | 0.022 |
| Baurifer | Bmarchi | Bguifarroi | Bnigroviridis | 100 | 52 | 0.316 | 0.316 | 0.035 | 0 |
| Baurifer | Bmarchi | Bguifarroi | Bnubestris | 86 | 42 | 0.344 | 0.344 | 0.047 | 0 |
| Baurifer | Bmarchi | Bguifarroi | Browleyi | 165 | 26 | 0.728 | 0.728 | 0.014 | 0 |
| Baurifer | Bmarchi | Bguifarroi | Bschlegelii | 205 | 46 | 0.633 | 0.633 | 0.045 | 0 |
| Baurifer | Bmarchi | Bguifarroi | Bsupraciliaris | 93 | 78 | 0.088 | 0.088 | 0.088 | 0.318 |

| H1 | H2 | H3 | Out | Number ABBA | Number BABA | D | Z-score | SD D-statistic | P-value that D = 0 |
|---|---|---|---|---|---|---|---|---|---|
| Baurifer | Bmarchi | Bguifarroi | Bthalassinus | 22 | 218 | -0.817 | -0.817 | 0.018 | 0 |
| Baurifer | Bmarchi | Blateralis | Bnigroviridis | 108 | 46 | 0.403 | 0.403 | 0.071 | 0 |
| Baurifer | Bmarchi | Bnubestris | Blateralis | 53 | 78 | -0.191 | -0.191 | 0.034 | 0 |
| Baurifer | Bmarchi | Bnubestris | Bnigroviridis | 31 | 24 | 0.127 | 0.127 | 0.122 | 0.296 |
| Baurifer | Bmarchi | Bnubestris | Browleyi | 134 | 55 | 0.418 | 0.418 | 0.107 | 0 |
| Baurifer | Bmarchi | Bnubestris | Bschlegelii | 63 | 31 | 0.34 | 0.34 | 0.051 | 0 |
| Baurifer | Bmarchi | Bnubestris | Bsupraciliaris | 49 | 28 | 0.273 | 0.273 | 0.033 | 0 |
| Baurifer | Bmarchi | Bnubestris | Bthalassinus | 27 | 283 | -0.826 | -0.826 | 0.017 | 0 |
| Baurifer | Bmarchi | Browleyi | Blateralis | 27 | 164 | -0.717 | -0.717 | 0.018 | 0 |
| Baurifer | Bmarchi | Browleyi | Bnigroviridis | 28 | 132 | -0.65 | -0.65 | 0.036 | 0 |
| Baurifer | Bmarchi | Browleyi | Bschlegelii | 55 | 188 | -0.547 | -0.547 | 0.074 | 0 |
| Baurifer | Bmarchi | Browleyi | Bsupraciliaris | 39 | 129 | -0.536 | -0.536 | 0.042 | 0 |
| Baurifer | Bmarchi | Browleyi | Bthalassinus | 20 | 350 | -0.892 | -0.892 | 0.018 | 0 |
| Baurifer | Bmarchi | Bschlegelii | Blateralis | 46 | 113 | -0.421 | -0.421 | 0.032 | 0 |
| Baurifer | Bmarchi | Bschlegelii | Bnigroviridis | 48 | 104 | -0.368 | -0.368 | 0.111 | 0.001 |
| Baurifer | Bmarchi | Bsupraciliaris | Blateralis | 35 | 105 | -0.5 | -0.5 | 0.038 | 0 |
| Baurifer | Bmarchi | Bsupraciliaris | Bnigroviridis | 58 | 48 | 0.094 | 0.094 | 0.155 | 0.542 |
| Baurifer | Bmarchi | Bsupraciliaris | Bschlegelii | 40 | 21 | 0.311 | 0.311 | 0.123 | 0.012 |
| Baurifer | Bmarchi | Bsupraciliaris | Bthalassinus | 24 | 258 | -0.83 | -0.83 | 0.015 | 0 |
| Baurifer | Bmarchi | Bthalassinus | Blateralis | 266 | 21 | 0.854 | 0.854 | 0.012 | 0 |
| Baurifer | Bmarchi | Bthalassinus | Bnigroviridis | 275 | 39 | 0.752 | 0.752 | 0.04 | 0 |

| H1 | H2 | H3 | Out | Number ABBA | Number BABA | D | Z-score | SD D-statistic | P-value that D = 0 |
|---|---|---|---|---|---|---|---|---|---|
| Baurifer | Bmarchi | Bthalassinus | Bschlegelii | 379 | 38 | 0.818 | 0.818 | 0.034 | 0 |
| Baurifer | Bnigroviridis | Bbicolor | Bguifarroi | 127 | 146 | -0.07 | -0.07 | 0.066 | 0.294 |
| Baurifer | Bnigroviridis | Bbicolor | Blateralis | 64 | 169 | -0.451 | -0.451 | 0.055 | 0 |
| Baurifer | Bnigroviridis | Bbicolor | Bmarchi | 49 | 160 | -0.531 | -0.531 | 0.039 | 0 |
| Baurifer | Bnigroviridis | Bbicolor | Bnubestris | 43 | 551 | -0.855 | -0.855 | 0.017 | 0 |
| Baurifer | Bnigroviridis | Bbicolor | Browleyi | 77 | 73 | 0.027 | 0.027 | 0.041 | 0.515 |
| Baurifer | Bnigroviridis | Bbicolor | Bschlegelii | 24 | 317 | -0.859 | -0.859 | 0.014 | 0 |
| Baurifer | Bnigroviridis | Bbicolor | Bsupraciliaris | 25 | 320 | -0.855 | -0.855 | 0.012 | 0 |
| Baurifer | Bnigroviridis | Bbicolor | Bthalassinus | 74 | 179 | -0.415 | -0.415 | 0.069 | 0 |
| Baurifer | Bnigroviridis | Bguifarroi | Blateralis | 37 | 44 | -0.086 | -0.086 | 0.05 | 0.082 |
| Baurifer | Bnigroviridis | Bguifarroi | Bmarchi | 66 | 43 | 0.211 | 0.211 | 0.047 | 0 |
| Baurifer | Bnigroviridis | Bguifarroi | Bnubestris | 45 | 430 | -0.811 | -0.811 | 0.042 | 0 |
| Baurifer | Bnigroviridis | Bguifarroi | Browleyi | 142 | 50 | 0.479 | 0.479 | 0.045 | 0 |
| Baurifer | Bnigroviridis | Bguifarroi | Bschlegelii | 38 | 198 | -0.678 | -0.678 | 0.025 | 0 |
| Baurifer | Bnigroviridis | Bguifarroi | Bsupraciliaris | 43 | 196 | -0.64 | -0.64 | 0.022 | 0 |
| Baurifer | Bnigroviridis | Bguifarroi | Bthalassinus | 62 | 66 | -0.031 | -0.031 | 0.108 | 0.772 |
| Baurifer | Bnigroviridis | Bmarchi | Blateralis | 99 | 75 | 0.138 | 0.138 | 0.073 | 0.059 |
| Baurifer | Bnigroviridis | Bmarchi | Bnubestris | 23 | 503 | -0.913 | -0.913 | 0.007 | 0 |
| Baurifer | Bnigroviridis | Bmarchi | Browleyi | 165 | 65 | 0.435 | 0.435 | 0.054 | 0 |
| Baurifer | Bnigroviridis | Bmarchi | Bschlegelii | 47 | 225 | -0.654 | -0.654 | 0.038 | 0 |
| Baurifer | Bnigroviridis | Bmarchi | Bsupraciliaris | 46 | 219 | -0.653 | -0.653 | 0.026 | 0 |

| H1 | H2 | H3 | Out | Number ABBA | Number BABA | D | Z-score | SD D-statistic | P-value that D = 0 |
|---|---|---|---|---|---|---|---|---|---|
| Baurifer | Bnigroviridis | Bmarchi | Bthalassinus | 54 | 25 | 0.367 | 0.367 | 0.132 | 0.005 |
| Baurifer | Bnigroviridis | Bnubestris | Blateralis | 430 | 37 | 0.842 | 0.842 | 0.055 | 0 |
| Baurifer | Bnigroviridis | Bnubestris | Browleyi | 535 | 17 | 0.938 | 0.938 | 0.005 | 0 |
| Baurifer | Bnigroviridis | Bnubestris | Bschlegelii | 313 | 25 | 0.852 | 0.852 | 0.011 | 0 |
| Baurifer | Bnigroviridis | Bnubestris | Bsupraciliaris | 300 | 50 | 0.714 | 0.714 | 0.054 | 0 |
| Baurifer | Bnigroviridis | Bnubestris | Bthalassinus | 471 | 12 | 0.95 | 0.95 | 0.006 | 0 |
| Baurifer | Bnigroviridis | Browleyi | Blateralis | 37 | 137 | -0.575 | -0.575 | 0.017 | 0 |
| Baurifer | Bnigroviridis | Browleyi | Bschlegelii | 35 | 340 | -0.813 | -0.813 | 0.03 | 0 |
| Baurifer | Bnigroviridis | Browleyi | Bsupraciliaris | 24 | 267 | -0.835 | -0.835 | 0.019 | 0 |
| Baurifer | Bnigroviridis | Browleyi | Bthalassinus | 50 | 128 | -0.438 | -0.438 | 0.028 | 0 |
| Baurifer | Bnigroviridis | Bschlegelii | Blateralis | 210 | 88 | 0.409 | 0.409 | 0.06 | 0 |
| Baurifer | Bnigroviridis | Bsupraciliaris | Blateralis | 204 | 43 | 0.652 | 0.652 | 0.027 | 0 |
| Baurifer | Bnigroviridis | Bsupraciliaris | Bschlegelii | 101 | 24 | 0.616 | 0.616 | 0.061 | 0 |
| Baurifer | Bnigroviridis | Bsupraciliaris | Bthalassinus | 263 | 48 | 0.691 | 0.691 | 0.034 | 0 |
| Baurifer | Bnigroviridis | Bthalassinus | Blateralis | 50 | 66 | -0.138 | -0.138 | 0.052 | 0.007 |
| Baurifer | Bnigroviridis | Bthalassinus | Bschlegelii | 47 | 220 | -0.648 | -0.648 | 0.043 | 0 |
| Baurifer | Bnubestris | Bbicolor | Bguifarroi | 65 | 181 | -0.472 | -0.472 | 0.07 | 0 |
| Baurifer | Bnubestris | Bbicolor | Blateralis | 69 | 151 | -0.373 | -0.373 | 0.038 | 0 |
| Baurifer | Bnubestris | Bbicolor | Bmarchi | 51 | 178 | -0.555 | -0.555 | 0.051 | 0 |
| Baurifer | Bnubestris | Bbicolor | Bnigroviridis | 18 | 568 | -0.939 | -0.939 | 0.012 | 0 |
| Baurifer | Bnubestris | Bbicolor | Browleyi | 77 | 96 | -0.11 | -0.11 | 0.048 | 0.022 |

| H1 | H2 | H3 | Out | Number ABBA | Number BABA | D | Z-score | SD D-statistic | P-value that D = 0 |
|---|---|---|---|---|---|---|---|---|---|
| Baurifer | Bnubestris | Bbicolor | Bschlegelii | 116 | 317 | -0.464 | -0.464 | 0.057 | 0 |
| Baurifer | Bnubestris | Bbicolor | Bsupraciliaris | 64 | 301 | -0.649 | -0.649 | 0.085 | 0 |
| Baurifer | Bnubestris | Bbicolor | Bthalassinus | 56 | 150 | -0.456 | -0.456 | 0.05 | 0 |
| Baurifer | Bnubestris | Bguifarroi | Blateralis | 32 | 55 | -0.264 | -0.264 | 0.167 | 0.113 |
| Baurifer | Bnubestris | Bguifarroi | Bmarchi | 71 | 54 | 0.136 | 0.136 | 0.037 | 0 |
| Baurifer | Bnubestris | Bguifarroi | Bnigroviridis | 21 | 461 | -0.913 | -0.913 | 0.007 | 0 |
| Baurifer | Bnubestris | Bguifarroi | Browleyi | 180 | 41 | 0.629 | 0.629 | 0.025 | 0 |
| Baurifer | Bnubestris | Bguifarroi | Bschlegelii | 42 | 195 | -0.646 | -0.646 | 0.028 | 0 |
| Baurifer | Bnubestris | Bguifarroi | Bsupraciliaris | 70 | 188 | -0.457 | -0.457 | 0.052 | 0 |
| Baurifer | Bnubestris | Bguifarroi | Bthalassinus | 76 | 67 | 0.063 | 0.063 | 0.136 | 0.643 |
| Baurifer | Bnubestris | Blateralis | Bnigroviridis | 52 | 470 | -0.801 | -0.801 | 0.039 | 0 |
| Baurifer | Bnubestris | Bmarchi | Blateralis | 66 | 79 | -0.09 | -0.09 | 0.035 | 0.011 |
| Baurifer | Bnubestris | Bmarchi | Bnigroviridis | 50 | 457 | -0.803 | -0.803 | 0.043 | 0 |
| Baurifer | Bnubestris | Bmarchi | Browleyi | 190 | 48 | 0.597 | 0.597 | 0.018 | 0 |
| Baurifer | Bnubestris | Bmarchi | Bschlegelii | 102 | 214 | -0.354 | -0.354 | 0.08 | 0 |
| Baurifer | Bnubestris | Bmarchi | Bsupraciliaris | 48 | 216 | -0.636 | -0.636 | 0.023 | 0 |
| Baurifer | Bnubestris | Bmarchi | Bthalassinus | 41 | 18 | 0.39 | 0.39 | 0.107 | 0 |
| Baurifer | Bnubestris | Browleyi | Blateralis | 52 | 151 | -0.488 | -0.488 | 0.02 | 0 |
| Baurifer | Bnubestris | Browleyi | Bnigroviridis | 29 | 565 | -0.902 | -0.902 | 0.022 | 0 |
| Baurifer | Bnubestris | Browleyi | Bschlegelii | 32 | 306 | -0.811 | -0.811 | 0.021 | 0 |
| Baurifer | Bnubestris | Browleyi | Bsupraciliaris | 26 | 289 | -0.835 | -0.835 | 0.013 | 0 |

| H1 | H2 | H3 | Out | Number ABBA | Number BABA | D | Z-score | SD D-statistic | P-value that D = 0 |
|---|---|---|---|---|---|---|---|---|---|
| Baurifer | Bnubestris | Browleyi | Bthalassinus | 89 | 125 | -0.168 | -0.168 | 0.073 | 0.02 |
| Baurifer | Bnubestris | Bschlegelii | Blateralis | 214 | 58 | 0.574 | 0.574 | 0.044 | 0 |
| Baurifer | Bnubestris | Bschlegelii | Bnigroviridis | 28 | 301 | -0.83 | -0.83 | 0.023 | 0 |
| Baurifer | Bnubestris | Bsupraciliaris | Blateralis | 190 | 72 | 0.45 | 0.45 | 0.082 | 0 |
| Baurifer | Bnubestris | Bsupraciliaris | Bnigroviridis | 31 | 296 | -0.81 | -0.81 | 0.022 | 0 |
| Baurifer | Bnubestris | Bsupraciliaris | Bschlegelii | 42 | 13 | 0.527 | 0.527 | 0.217 | 0.015 |
| Baurifer | Bnubestris | Bsupraciliaris | Bthalassinus | 245 | 48 | 0.672 | 0.672 | 0.026 | 0 |
| Baurifer | Bnubestris | Bthalassinus | Blateralis | 50 | 70 | -0.167 | -0.167 | 0.037 | 0 |
| Baurifer | Bnubestris | Bthalassinus | Bnigroviridis | 40 | 462 | -0.841 | -0.841 | 0.052 | 0 |
| Baurifer | Bnubestris | Bthalassinus | Bschlegelii | 132 | 277 | -0.355 | -0.355 | 0.061 | 0 |
| Baurifer | Browleyi | Bbicolor | Bguifarroi | 65 | 64 | 0.008 | 0.008 | 0.057 | 0.891 |
| Baurifer | Browleyi | Bbicolor | Blateralis | 83 | 72 | 0.071 | 0.071 | 0.095 | 0.457 |
| Baurifer | Browleyi | Bbicolor | Bmarchi | 81 | 75 | 0.038 | 0.038 | 0.12 | 0.75 |
| Baurifer | Browleyi | Bbicolor | Bnigroviridis | 65 | 90 | -0.161 | -0.161 | 0.066 | 0.014 |
| Baurifer | Browleyi | Bbicolor | Bnubestris | 101 | 90 | 0.058 | 0.058 | 0.069 | 0.405 |
| Baurifer | Browleyi | Bbicolor | Bschlegelii | 77 | 78 | -0.006 | -0.006 | 0.056 | 0.908 |
| Baurifer | Browleyi | Bbicolor | Bsupraciliaris | 54 | 102 | -0.308 | -0.308 | 0.046 | 0 |
| Baurifer | Browleyi | Bbicolor | Bthalassinus | 105 | 79 | 0.141 | 0.141 | 0.068 | 0.038 |
| Baurifer | Browleyi | Bguifarroi | Blateralis | 26 | 11 | 0.405 | 0.405 | 0.077 | 0 |
| Baurifer | Browleyi | Bguifarroi | Bmarchi | 34 | 30 | 0.063 | 0.063 | 0.077 | 0.415 |
| Baurifer | Browleyi | Bguifarroi | Bnigroviridis | 31 | 56 | -0.287 | -0.287 | 0.066 | 0 |

| H1 | H2 | H3 | Out | Number ABBA | Number BABA | D | Z-score | SD D-statistic | P-value that D = 0 |
|---|---|---|---|---|---|---|---|---|---|
| Baurifer | Browleyi | Bguifarroi | Bnubestris | 30 | 79 | -0.45 | -0.45 | 0.083 | 0 |
| Baurifer | Browleyi | Bguifarroi | Bschlegelii | 29 | 48 | -0.247 | -0.247 | 0.043 | 0 |
| Baurifer | Browleyi | Bguifarroi | Bsupraciliaris | 33 | 45 | -0.154 | -0.154 | 0.067 | 0.021 |
| Baurifer | Browleyi | Bguifarroi | Bthalassinus | 43 | 46 | -0.034 | -0.034 | 0.189 | 0.859 |
| Baurifer | Browleyi | Blateralis | Bnigroviridis | 22 | 47 | -0.362 | -0.362 | 0.069 | 0 |
| Baurifer | Browleyi | Bmarchi | Blateralis | 24 | 94 | -0.593 | -0.593 | 0.044 | 0 |
| Baurifer | Browleyi | Bmarchi | Bnigroviridis | 71 | 68 | 0.022 | 0.022 | 0.13 | 0.869 |
| Baurifer | Browleyi | Bmarchi | Bnubestris | 55 | 52 | 0.028 | 0.028 | 0.149 | 0.851 |
| Baurifer | Browleyi | Bmarchi | Bschlegelii | 35 | 95 | -0.462 | -0.462 | 0.053 | 0 |
| Baurifer | Browleyi | Bmarchi | Bsupraciliaris | 40 | 52 | -0.13 | -0.13 | 0.04 | 0.001 |
| Baurifer | Browleyi | Bmarchi | Bthalassinus | 24 | 8 | 0.5 | 0.5 | 0.195 | 0.01 |
| Baurifer | Browleyi | Bnubestris | Blateralis | 106 | 30 | 0.559 | 0.559 | 0.079 | 0 |
| Baurifer | Browleyi | Bnubestris | Bnigroviridis | 13 | 23 | -0.278 | -0.278 | 0.236 | 0.239 |
| Baurifer | Browleyi | Bnubestris | Bschlegelii | 76 | 53 | 0.178 | 0.178 | 0.228 | 0.433 |
| Baurifer | Browleyi | Bnubestris | Bsupraciliaris | 32 | 37 | -0.072 | -0.072 | 0.096 | 0.452 |
| Baurifer | Browleyi | Bnubestris | Bthalassinus | 75 | 29 | 0.442 | 0.442 | 0.106 | 0 |
| Baurifer | Browleyi | Bschlegelii | Blateralis | 38 | 107 | -0.476 | -0.476 | 0.053 | 0 |
| Baurifer | Browleyi | Bschlegelii | Bnigroviridis | 28 | 46 | -0.243 | -0.243 | 0.148 | 0.1 |
| Baurifer | Browleyi | Bsupraciliaris | Blateralis | 39 | 47 | -0.093 | -0.093 | 0.131 | 0.477 |
| Baurifer | Browleyi | Bsupraciliaris | Bnigroviridis | 25 | 85 | -0.545 | -0.545 | 0.079 | 0 |
| Baurifer | Browleyi | Bsupraciliaris | Bschlegelii | 32 | 7 | 0.641 | 0.641 | 0.282 | 0.023 |

| H1 | H2 | H3 | Out | Number ABBA | Number BABA | D | Z-score | SD D-statistic | P-value that D = 0 |
|---|---|---|---|---|---|---|---|---|---|
| Baurifer | Browleyi | Bsupraciliaris | Bthalassinus | 53 | 65 | -0.102 | -0.102 | 0.087 | 0.24 |
| Baurifer | Browleyi | Bthalassinus | Blateralis | 27 | 66 | -0.419 | -0.419 | 0.077 | 0 |
| Baurifer | Browleyi | Bthalassinus | Bnigroviridis | 29 | 51 | -0.275 | -0.275 | 0.058 | 0 |
| Baurifer | Browleyi | Bthalassinus | Bschlegelii | 74 | 60 | 0.104 | 0.104 | 0.089 | 0.238 |
| Baurifer | Bschlegelii | Bbicolor | Bguifarroi | 118 | 179 | -0.205 | -0.205 | 0.109 | 0.059 |
| Baurifer | Bschlegelii | Bbicolor | Blateralis | 47 | 178 | -0.582 | -0.582 | 0.044 | 0 |
| Baurifer | Bschlegelii | Bbicolor | Bmarchi | 65 | 131 | -0.337 | -0.337 | 0.07 | 0 |
| Baurifer | Bschlegelii | Bbicolor | Bnigroviridis | 28 | 267 | -0.81 | -0.81 | 0.019 | 0 |
| Baurifer | Bschlegelii | Bbicolor | Bnubestris | 27 | 300 | -0.835 | -0.835 | 0.024 | 0 |
| Baurifer | Bschlegelii | Bbicolor | Browleyi | 95 | 89 | 0.033 | 0.033 | 0.033 | 0.321 |
| Baurifer | Bschlegelii | Bbicolor | Bsupraciliaris | 26 | 996 | -0.949 | -0.949 | 0.005 | 0 |
| Baurifer | Bschlegelii | Bbicolor | Bthalassinus | 77 | 137 | -0.28 | -0.28 | 0.046 | 0 |
| Baurifer | Bschlegelii | Bguifarroi | Blateralis | 33 | 58 | -0.275 | -0.275 | 0.118 | 0.02 |
| Baurifer | Bschlegelii | Bguifarroi | Bmarchi | 78 | 43 | 0.289 | 0.289 | 0.034 | 0 |
| Baurifer | Bschlegelii | Bguifarroi | Bnigroviridis | 61 | 192 | -0.518 | -0.518 | 0.042 | 0 |
| Baurifer | Bschlegelii | Bguifarroi | Bnubestris | 44 | 232 | -0.681 | -0.681 | 0.03 | 0 |
| Baurifer | Bschlegelii | Bguifarroi | Browleyi | 157 | 38 | 0.61 | 0.61 | 0.016 | 0 |
| Baurifer | Bschlegelii | Bguifarroi | Bsupraciliaris | 40 | 911 | -0.916 | -0.916 | 0.012 | 0 |
| Baurifer | Bschlegelii | Bguifarroi | Bthalassinus | 79 | 38 | 0.35 | 0.35 | 0.05 | 0 |
| Baurifer | Bschlegelii | Blateralis | Bnigroviridis | 60 | 194 | -0.528 | -0.528 | 0.039 | 0 |
| Baurifer | Bschlegelii | Bmarchi | Blateralis | 39 | 108 | -0.469 | -0.469 | 0.053 | 0 |

| H1 | H2 | H3 | Out | Number ABBA | Number BABA | D | Z-score | SD D-statistic | P-value that D = 0 |
|---|---|---|---|---|---|---|---|---|---|
| Baurifer | Bschlegelii | Bmarchi | Bnigroviridis | 35 | 238 | -0.744 | -0.744 | 0.02 | 0 |
| Baurifer | Bschlegelii | Bmarchi | Bnubestris | 34 | 233 | -0.745 | -0.745 | 0.024 | 0 |
| Baurifer | Bschlegelii | Bmarchi | Browleyi | 135 | 59 | 0.392 | 0.392 | 0.028 | 0 |
| Baurifer | Bschlegelii | Bmarchi | Bsupraciliaris | 44 | 955 | -0.912 | -0.912 | 0.011 | 0 |
| Baurifer | Bschlegelii | Bmarchi | Bthalassinus | 28 | 21 | 0.143 | 0.143 | 0.068 | 0.035 |
| Baurifer | Bschlegelii | Bnubestris | Blateralis | 226 | 44 | 0.674 | 0.674 | 0.03 | 0 |
| Baurifer | Bschlegelii | Bnubestris | Bnigroviridis | 42 | 59 | -0.168 | -0.168 | 0.102 | 0.098 |
| Baurifer | Bschlegelii | Bnubestris | Browleyi | 335 | 25 | 0.861 | 0.861 | 0.016 | 0 |
| Baurifer | Bschlegelii | Bnubestris | Bsupraciliaris | 35 | 767 | -0.913 | -0.913 | 0.018 | 0 |
| Baurifer | Bschlegelii | Bnubestris | Bthalassinus | 212 | 81 | 0.447 | 0.447 | 0.072 | 0 |
| Baurifer | Bschlegelii | Browleyi | Blateralis | 42 | 145 | -0.551 | -0.551 | 0.018 | 0 |
| Baurifer | Bschlegelii | Browleyi | Bnigroviridis | 25 | 270 | -0.831 | -0.831 | 0.017 | 0 |
| Baurifer | Bschlegelii | Browleyi | Bsupraciliaris | 9 | 994 | -0.982 | -0.982 | 0.003 | 0 |
| Baurifer | Bschlegelii | Browleyi | Bthalassinus | 48 | 119 | -0.425 | -0.425 | 0.044 | 0 |
| Baurifer | Bschlegelii | Bsupraciliaris | Blateralis | 903 | 14 | 0.969 | 0.969 | 0.005 | 0 |
| Baurifer | Bschlegelii | Bsupraciliaris | Bnigroviridis | 780 | 32 | 0.921 | 0.921 | 0.015 | 0 |
| Baurifer | Bschlegelii | Bsupraciliaris | Bthalassinus | 933 | 34 | 0.93 | 0.93 | 0.013 | 0 |
| Baurifer | Bschlegelii | Bthalassinus | Blateralis | 65 | 97 | -0.198 | -0.198 | 0.077 | 0.01 |
| Baurifer | Bschlegelii | Bthalassinus | Bnigroviridis | 32 | 237 | -0.762 | -0.762 | 0.019 | 0 |
| Baurifer | Bsupraciliaris | Bbicolor | Bguifarroi | 84 | 150 | -0.282 | -0.282 | 0.097 | 0.004 |
| Baurifer | Bsupraciliaris | Bbicolor | Blateralis | 40 | 159 | -0.598 | -0.598 | 0.035 | 0 |

| H1 | H2 | H3 | Out | Number ABBA | Number BABA | D | Z-score | SD D-statistic | P-value that D = 0 |
|---|---|---|---|---|---|---|---|---|---|
| Baurifer | Bsupraciliaris | Bbicolor | Bmarchi | 61 | 132 | -0.368 | -0.368 | 0.043 | 0 |
| Baurifer | Bsupraciliaris | Bbicolor | Bnigroviridis | 28 | 304 | -0.831 | -0.831 | 0.015 | 0 |
| Baurifer | Bsupraciliaris | Bbicolor | Bnubestris | 24 | 316 | -0.859 | -0.859 | 0.014 | 0 |
| Baurifer | Bsupraciliaris | Bbicolor | Browleyi | 100 | 109 | -0.043 | -0.043 | 0.077 | 0.578 |
| Baurifer | Bsupraciliaris | Bbicolor | Bschlegelii | 34 | 1007 | -0.935 | -0.935 | 0.015 | 0 |
| Baurifer | Bsupraciliaris | Bbicolor | Bthalassinus | 55 | 133 | -0.415 | -0.415 | 0.057 | 0 |
| Baurifer | Bsupraciliaris | Bguifarroi | Blateralis | 28 | 79 | -0.477 | -0.477 | 0.11 | 0 |
| Baurifer | Bsupraciliaris | Bguifarroi | Bmarchi | 73 | 43 | 0.259 | 0.259 | 0.04 | 0 |
| Baurifer | Bsupraciliaris | Bguifarroi | Bnigroviridis | 51 | 193 | -0.582 | -0.582 | 0.026 | 0 |
| Baurifer | Bsupraciliaris | Bguifarroi | Bnubestris | 53 | 191 | -0.566 | -0.566 | 0.027 | 0 |
| Baurifer | Bsupraciliaris | Bguifarroi | Browleyi | 143 | 77 | 0.3 | 0.3 | 0.081 | 0 |
| Baurifer | Bsupraciliaris | Bguifarroi | Bschlegelii | 17 | 909 | -0.963 | -0.963 | 0.007 | 0 |
| Baurifer | Bsupraciliaris | Bguifarroi | Bthalassinus | 73 | 40 | 0.292 | 0.292 | 0.04 | 0 |
| Baurifer | Bsupraciliaris | Blateralis | Bnigroviridis | 91 | 197 | -0.368 | -0.368 | 0.091 | 0 |
| Baurifer | Bsupraciliaris | Bmarchi | Blateralis | 43 | 90 | -0.353 | -0.353 | 0.042 | 0 |
| Baurifer | Bsupraciliaris | Bmarchi | Bnigroviridis | 39 | 207 | -0.683 | -0.683 | 0.023 | 0 |
| Baurifer | Bsupraciliaris | Bmarchi | Bnubestris | 57 | 227 | -0.599 | -0.599 | 0.043 | 0 |
| Baurifer | Bsupraciliaris | Bmarchi | Browleyi | 156 | 60 | 0.444 | 0.444 | 0.053 | 0 |
| Baurifer | Bsupraciliaris | Bmarchi | Bschlegelii | 19 | 920 | -0.96 | -0.96 | 0.005 | 0 |
| Baurifer | Bsupraciliaris | Bmarchi | Bthalassinus | 60 | 27 | 0.379 | 0.379 | 0.09 | 0 |
| Baurifer | Bsupraciliaris | Bnubestris | Blateralis | 189 | 56 | 0.543 | 0.543 | 0.028 | 0 |

| H1 | H2 | H3 | Out | Number ABBA | Number BABA | D | Z-score | SD D-statistic | P-value that D = 0 |
|---|---|---|---|---|---|---|---|---|---|
| Baurifer | Bsupraciliaris | Bnubestris | Bnigroviridis | 35 | 65 | -0.3 | -0.3 | 0.047 | 0 |
| Baurifer | Bsupraciliaris | Bnubestris | Browleyi | 271 | 48 | 0.699 | 0.699 | 0.069 | 0 |
| Baurifer | Bsupraciliaris | Bnubestris | Bschlegelii | 36 | 780 | -0.912 | -0.912 | 0.019 | 0 |
| Baurifer | Bsupraciliaris | Bnubestris | Bthalassinus | 220 | 32 | 0.746 | 0.746 | 0.023 | 0 |
| Baurifer | Bsupraciliaris | Browleyi | Blateralis | 43 | 176 | -0.607 | -0.607 | 0.048 | 0 |
| Baurifer | Bsupraciliaris | Browleyi | Bnigroviridis | 29 | 286 | -0.816 | -0.816 | 0.017 | 0 |
| Baurifer | Bsupraciliaris | Browleyi | Bschlegelii | 66 | 988 | -0.875 | -0.875 | 0.028 | 0 |
| Baurifer | Bsupraciliaris | Browleyi | Bthalassinus | 62 | 147 | -0.407 | -0.407 | 0.067 | 0 |
| Baurifer | Bsupraciliaris | Bschlegelii | Blateralis | 932 | 10 | 0.979 | 0.979 | 0.002 | 0 |
| Baurifer | Bsupraciliaris | Bschlegelii | Bnigroviridis | 768 | 19 | 0.952 | 0.952 | 0.003 | 0 |
| Baurifer | Bsupraciliaris | Bthalassinus | Blateralis | 43 | 137 | -0.522 | -0.522 | 0.043 | 0 |
| Baurifer | Bsupraciliaris | Bthalassinus | Bnigroviridis | 58 | 219 | -0.581 | -0.581 | 0.08 | 0 |
| Baurifer | Bsupraciliaris | Bthalassinus | Bschlegelii | 53 | 919 | -0.891 | -0.891 | 0.03 | 0 |
| Baurifer | Bthalassinus | Bbicolor | Bguifarroi | 29 | 180 | -0.722 | -0.722 | 0.034 | 0 |
| Baurifer | Bthalassinus | Bbicolor | Blateralis | 72 | 169 | -0.402 | -0.402 | 0.097 | 0 |
| Baurifer | Bthalassinus | Bbicolor | Bmarchi | 26 | 352 | -0.862 | -0.862 | 0.04 | 0 |
| Baurifer | Bthalassinus | Bbicolor | Bnigroviridis | 42 | 144 | -0.548 | -0.548 | 0.062 | 0 |
| Baurifer | Bthalassinus | Bbicolor | Bnubestris | 74 | 138 | -0.302 | -0.302 | 0.116 | 0.009 |
| Baurifer | Bthalassinus | Bbicolor | Browleyi | 56 | 71 | -0.118 | -0.118 | 0.043 | 0.006 |
| Baurifer | Bthalassinus | Bbicolor | Bschlegelii | 80 | 136 | -0.259 | -0.259 | 0.09 | 0.004 |
| Baurifer | Bthalassinus | Bbicolor | Bsupraciliaris | 39 | 188 | -0.656 | -0.656 | 0.042 | 0 |

| H1 | H2 | H3 | Out | Number ABBA | Number BABA | D | Z-score | SD D-statistic | P-value that D = 0 |
|---|---|---|---|---|---|---|---|---|---|
| Baurifer | Bthalassinus | Bguifarroi | Blateralis | 38 | 26 | 0.188 | 0.188 | 0.05 | 0 |
| Baurifer | Bthalassinus | Bguifarroi | Bmarchi | 15 | 225 | -0.875 | -0.875 | 0.017 | 0 |
| Baurifer | Bthalassinus | Bguifarroi | Bnigroviridis | 91 | 46 | 0.328 | 0.328 | 0.06 | 0 |
| Baurifer | Bthalassinus | Bguifarroi | Bnubestris | 72 | 52 | 0.161 | 0.161 | 0.053 | 0.002 |
| Baurifer | Bthalassinus | Bguifarroi | Browleyi | 167 | 18 | 0.805 | 0.805 | 0.014 | 0 |
| Baurifer | Bthalassinus | Bguifarroi | Bschlegelii | 84 | 39 | 0.366 | 0.366 | 0.047 | 0 |
| Baurifer | Bthalassinus | Bguifarroi | Bsupraciliaris | 89 | 59 | 0.203 | 0.203 | 0.133 | 0.127 |
| Baurifer | Bthalassinus | Blateralis | Bnigroviridis | 84 | 81 | 0.018 | 0.018 | 0.078 | 0.815 |
| Baurifer | Bthalassinus | Bmarchi | Blateralis | 231 | 17 | 0.863 | 0.863 | 0.013 | 0 |
| Baurifer | Bthalassinus | Bmarchi | Bnigroviridis | 257 | 75 | 0.548 | 0.548 | 0.075 | 0 |
| Baurifer | Bthalassinus | Bmarchi | Bnubestris | 261 | 31 | 0.788 | 0.788 | 0.019 | 0 |
| Baurifer | Bthalassinus | Bmarchi | Browleyi | 347 | 42 | 0.784 | 0.784 | 0.066 | 0 |
| Baurifer | Bthalassinus | Bmarchi | Bschlegelii | 304 | 19 | 0.882 | 0.882 | 0.014 | 0 |
| Baurifer | Bthalassinus | Bmarchi | Bsupraciliaris | 269 | 27 | 0.818 | 0.818 | 0.018 | 0 |
| Baurifer | Bthalassinus | Bnubestris | Blateralis | 49 | 75 | -0.21 | -0.21 | 0.047 | 0 |
| Baurifer | Bthalassinus | Bnubestris | Bnigroviridis | 13 | 33 | -0.435 | -0.435 | 0.182 | 0.017 |
| Baurifer | Bthalassinus | Bnubestris | Browleyi | 175 | 63 | 0.471 | 0.471 | 0.073 | 0 |
| Baurifer | Bthalassinus | Bnubestris | Bschlegelii | 65 | 37 | 0.275 | 0.275 | 0.067 | 0 |
| Baurifer | Bthalassinus | Bnubestris | Bsupraciliaris | 40 | 32 | 0.111 | 0.111 | 0.032 | 0.001 |
| Baurifer | Bthalassinus | Browleyi | Blateralis | 25 | 159 | -0.728 | -0.728 | 0.02 | 0 |
| Baurifer | Bthalassinus | Browleyi | Bnigroviridis | 40 | 184 | -0.643 | -0.643 | 0.037 | 0 |

| H1 | H2 | H3 | Out | Number ABBA | Number BABA | D | Z-score | SD D-statistic | P-value that D = 0 |
|---|---|---|---|---|---|---|---|---|---|
| Baurifer | Bthalassinus | Browleyi | Bschlegelii | 87 | 159 | -0.293 | -0.293 | 0.127 | 0.022 |
| Baurifer | Bthalassinus | Browleyi | Bsupraciliaris | 81 | 125 | -0.214 | -0.214 | 0.09 | 0.017 |
| Baurifer | Bthalassinus | Bschlegelii | Blateralis | 60 | 115 | -0.314 | -0.314 | 0.055 | 0 |
| Baurifer | Bthalassinus | Bschlegelii | Bnigroviridis | 31 | 44 | -0.173 | -0.173 | 0.039 | 0 |
| Baurifer | Bthalassinus | Bsupraciliaris | Blateralis | 42 | 113 | -0.458 | -0.458 | 0.056 | 0 |
| Baurifer | Bthalassinus | Bsupraciliaris | Bnigroviridis | 58 | 45 | 0.126 | 0.126 | 0.117 | 0.28 |
| Baurifer | Bthalassinus | Bsupraciliaris | Bschlegelii | 95 | 18 | 0.681 | 0.681 | 0.057 | 0 |
| Bbicolor | Bguifarroi | Blateralis | Bnigroviridis | 155 | 40 | 0.59 | 0.59 | 0.036 | 0 |
| Bbicolor | Bguifarroi | Bmarchi | Blateralis | 49 | 142 | -0.487 | -0.487 | 0.036 | 0 |
| Bbicolor | Bguifarroi | Bmarchi | Bnigroviridis | 93 | 60 | 0.216 | 0.216 | 0.043 | 0 |
| Bbicolor | Bguifarroi | Bmarchi | Bnubestris | 89 | 60 | 0.195 | 0.195 | 0.045 | 0 |
| Bbicolor | Bguifarroi | Bmarchi | Browleyi | 182 | 32 | 0.701 | 0.701 | 0.039 | 0 |
| Bbicolor | Bguifarroi | Bmarchi | Bschlegelii | 104 | 81 | 0.124 | 0.124 | 0.033 | 0 |
| Bbicolor | Bguifarroi | Bmarchi | Bsupraciliaris | 95 | 67 | 0.173 | 0.173 | 0.028 | 0 |
| Bbicolor | Bguifarroi | Bmarchi | Bthalassinus | 25 | 26 | -0.02 | -0.02 | 0.105 | 0.851 |
| Bbicolor | Bguifarroi | Bnubestris | Blateralis | 26 | 152 | -0.708 | -0.708 | 0.028 | 0 |
| Bbicolor | Bguifarroi | Bnubestris | Bnigroviridis | 29 | 8 | 0.568 | 0.568 | 0.112 | 0 |
| Bbicolor | Bguifarroi | Bnubestris | Browleyi | 183 | 68 | 0.458 | 0.458 | 0.109 | 0 |
| Bbicolor | Bguifarroi | Bnubestris | Bschlegelii | 74 | 57 | 0.13 | 0.13 | 0.075 | 0.084 |
| Bbicolor | Bguifarroi | Bnubestris | Bsupraciliaris | 46 | 51 | -0.052 | -0.052 | 0.055 | 0.345 |
| Bbicolor | Bguifarroi | Bnubestris | Bthalassinus | 104 | 95 | 0.045 | 0.045 | 0.095 | 0.634 |

| H1 | H2 | H3 | Out | Number ABBA | Number BABA | D | Z-score | SD D-statistic | P-value that D = 0 |
|---|---|---|---|---|---|---|---|---|---|
| Bbicolor | Bguifarroi | Browleyi | Blateralis | 56 | 244 | -0.627 | -0.627 | 0.08 | 0 |
| Bbicolor | Bguifarroi | Browleyi | Bnigroviridis | 89 | 135 | -0.205 | -0.205 | 0.094 | 0.029 |
| Bbicolor | Bguifarroi | Browleyi | Bschlegelii | 42 | 150 | -0.563 | -0.563 | 0.037 | 0 |
| Bbicolor | Bguifarroi | Browleyi | Bsupraciliaris | 47 | 165 | -0.557 | -0.557 | 0.062 | 0 |
| Bbicolor | Bguifarroi | Browleyi | Bthalassinus | 82 | 156 | -0.311 | -0.311 | 0.095 | 0.001 |
| Bbicolor | Bguifarroi | Bschlegelii | Blateralis | 28 | 158 | -0.699 | -0.699 | 0.025 | 0 |
| Bbicolor | Bguifarroi | Bschlegelii | Bnigroviridis | 61 | 44 | 0.162 | 0.162 | 0.064 | 0.011 |
| Bbicolor | Bguifarroi | Bsupraciliaris | Blateralis | 73 | 161 | -0.376 | -0.376 | 0.088 | 0 |
| Bbicolor | Bguifarroi | Bsupraciliaris | Bnigroviridis | 47 | 59 | -0.113 | -0.113 | 0.068 | 0.096 |
| Bbicolor | Bguifarroi | Bsupraciliaris | Bschlegelii | 15 | 18 | -0.091 | -0.091 | 0.068 | 0.18 |
| Bbicolor | Bguifarroi | Bsupraciliaris | Bthalassinus | 70 | 140 | -0.333 | -0.333 | 0.054 | 0 |
| Bbicolor | Bguifarroi | Bthalassinus | Blateralis | 52 | 144 | -0.469 | -0.469 | 0.067 | 0 |
| Bbicolor | Bguifarroi | Bthalassinus | Bnigroviridis | 91 | 88 | 0.017 | 0.017 | 0.049 | 0.735 |
| Bbicolor | Bguifarroi | Bthalassinus | Bschlegelii | 96 | 69 | 0.164 | 0.164 | 0.02 | 0 |
| Bbicolor | Blateralis | Bguifarroi | Bmarchi | 177 | 34 | 0.678 | 0.678 | 0.023 | 0 |
| Bbicolor | Blateralis | Bguifarroi | Bnigroviridis | 160 | 28 | 0.702 | 0.702 | 0.02 | 0 |
| Bbicolor | Blateralis | Bguifarroi | Bnubestris | 155 | 39 | 0.598 | 0.598 | 0.041 | 0 |
| Bbicolor | Blateralis | Bguifarroi | Browleyi | 295 | 12 | 0.922 | 0.922 | 0.008 | 0 |
| Bbicolor | Blateralis | Bguifarroi | Bschlegelii | 174 | 61 | 0.481 | 0.481 | 0.069 | 0 |
| Bbicolor | Blateralis | Bguifarroi | Bsupraciliaris | 197 | 53 | 0.576 | 0.576 | 0.041 | 0 |
| Bbicolor | Blateralis | Bguifarroi | Bthalassinus | 181 | 37 | 0.661 | 0.661 | 0.027 | 0 |

| H1 | H2 | H3 | Out | Number ABBA | Number BABA | D | Z-score | SD D-statistic | P-value that D = 0 |
|---|---|---|---|---|---|---|---|---|---|
| Bbicolor | Blateralis | Bmarchi | Bnigroviridis | 88 | 69 | 0.121 | 0.121 | 0.043 | 0.005 |
| Bbicolor | Blateralis | Bmarchi | Bnubestris | 86 | 64 | 0.147 | 0.147 | 0.033 | 0 |
| Bbicolor | Blateralis | Bmarchi | Browleyi | 193 | 47 | 0.608 | 0.608 | 0.054 | 0 |
| Bbicolor | Blateralis | Bmarchi | Bschlegelii | 122 | 84 | 0.184 | 0.184 | 0.044 | 0 |
| Bbicolor | Blateralis | Bmarchi | Bsupraciliaris | 92 | 144 | -0.22 | -0.22 | 0.046 | 0 |
| Bbicolor | Blateralis | Bmarchi | Bthalassinus | 40 | 24 | 0.25 | 0.25 | 0.215 | 0.244 |
| Bbicolor | Blateralis | Bnubestris | Bnigroviridis | 9 | 12 | -0.143 | -0.143 | 0.111 | 0.2 |
| Bbicolor | Blateralis | Bnubestris | Browleyi | 147 | 37 | 0.598 | 0.598 | 0.037 | 0 |
| Bbicolor | Blateralis | Bnubestris | Bschlegelii | 60 | 43 | 0.165 | 0.165 | 0.078 | 0.034 |
| Bbicolor | Blateralis | Bnubestris | Bsupraciliaris | 41 | 44 | -0.035 | -0.035 | 0.048 | 0.462 |
| Bbicolor | Blateralis | Bnubestris | Bthalassinus | 71 | 92 | -0.129 | -0.129 | 0.039 | 0.001 |
| Bbicolor | Blateralis | Browleyi | Bnigroviridis | 65 | 132 | -0.34 | -0.34 | 0.109 | 0.002 |
| Bbicolor | Blateralis | Browleyi | Bschlegelii | 34 | 146 | -0.622 | -0.622 | 0.033 | 0 |
| Bbicolor | Blateralis | Browleyi | Bsupraciliaris | 37 | 142 | -0.587 | -0.587 | 0.04 | 0 |
| Bbicolor | Blateralis | Browleyi | Bthalassinus | 42 | 153 | -0.569 | -0.569 | 0.062 | 0 |
| Bbicolor | Blateralis | Bschlegelii | Bnigroviridis | 46 | 43 | 0.034 | 0.034 | 0.058 | 0.564 |
| Bbicolor | Blateralis | Bsupraciliaris | Bnigroviridis | 43 | 100 | -0.399 | -0.399 | 0.099 | 0 |
| Bbicolor | Blateralis | Bsupraciliaris | Bschlegelii | 35 | 20 | 0.273 | 0.273 | 0.16 | 0.089 |
| Bbicolor | Blateralis | Bsupraciliaris | Bthalassinus | 119 | 93 | 0.123 | 0.123 | 0.054 | 0.022 |
| Bbicolor | Blateralis | Bthalassinus | Bnigroviridis | 103 | 88 | 0.079 | 0.079 | 0.076 | 0.301 |
| Bbicolor | Blateralis | Bthalassinus | Bschlegelii | 95 | 125 | -0.136 | -0.136 | 0.065 | 0.036 |

| H1 | H2 | H3 | Out | Number ABBA | Number BABA | D | Z-score | SD D-statistic | P-value that D = 0 |
|---|---|---|---|---|---|---|---|---|---|
| Bbicolor | Bmarchi | Bguifarroi | Blateralis | 35 | 46 | -0.136 | -0.136 | 0.12 | 0.26 |
| Bbicolor | Bmarchi | Bguifarroi | Bnigroviridis | 89 | 51 | 0.271 | 0.271 | 0.035 | 0 |
| Bbicolor | Bmarchi | Bguifarroi | Bnubestris | 91 | 51 | 0.282 | 0.282 | 0.035 | 0 |
| Bbicolor | Bmarchi | Bguifarroi | Browleyi | 170 | 25 | 0.744 | 0.744 | 0.018 | 0 |
| Bbicolor | Bmarchi | Bguifarroi | Bschlegelii | 129 | 44 | 0.491 | 0.491 | 0.068 | 0 |
| Bbicolor | Bmarchi | Bguifarroi | Bsupraciliaris | 97 | 75 | 0.128 | 0.128 | 0.101 | 0.205 |
| Bbicolor | Bmarchi | Bguifarroi | Bthalassinus | 24 | 227 | -0.809 | -0.809 | 0.019 | 0 |
| Bbicolor | Bmarchi | Blateralis | Bnigroviridis | 87 | 57 | 0.208 | 0.208 | 0.044 | 0 |
| Bbicolor | Bmarchi | Bnubestris | Blateralis | 44 | 89 | -0.338 | -0.338 | 0.049 | 0 |
| Bbicolor | Bmarchi | Bnubestris | Bnigroviridis | 10 | 8 | 0.111 | 0.111 | 0.05 | 0.025 |
| Bbicolor | Bmarchi | Bnubestris | Browleyi | 126 | 49 | 0.44 | 0.44 | 0.064 | 0 |
| Bbicolor | Bmarchi | Bnubestris | Bschlegelii | 50 | 31 | 0.235 | 0.235 | 0.047 | 0 |
| Bbicolor | Bmarchi | Bnubestris | Bsupraciliaris | 46 | 74 | -0.233 | -0.233 | 0.101 | 0.021 |
| Bbicolor | Bmarchi | Bnubestris | Bthalassinus | 19 | 287 | -0.876 | -0.876 | 0.014 | 0 |
| Bbicolor | Bmarchi | Browleyi | Blateralis | 27 | 176 | -0.734 | -0.734 | 0.013 | 0 |
| Bbicolor | Bmarchi | Browleyi | Bnigroviridis | 69 | 160 | -0.397 | -0.397 | 0.05 | 0 |
| Bbicolor | Bmarchi | Browleyi | Bschlegelii | 66 | 120 | -0.29 | -0.29 | 0.065 | 0 |
| Bbicolor | Bmarchi | Browleyi | Bsupraciliaris | 80 | 114 | -0.175 | -0.175 | 0.09 | 0.051 |
| Bbicolor | Bmarchi | Browleyi | Bthalassinus | 11 | 358 | -0.94 | -0.94 | 0.009 | 0 |
| Bbicolor | Bmarchi | Bschlegelii | Blateralis | 50 | 97 | -0.32 | -0.32 | 0.061 | 0 |
| Bbicolor | Bmarchi | Bschlegelii | Bnigroviridis | 52 | 63 | -0.096 | -0.096 | 0.115 | 0.404 |

| H1 | H2 | H3 | Out | Number ABBA | Number BABA | D | Z-score | SD D-statistic | P-value that D = 0 |
|---|---|---|---|---|---|---|---|---|---|
| Bbicolor | Bmarchi | Bsupraciliaris | Blateralis | 49 | 122 | -0.427 | -0.427 | 0.109 | 0 |
| Bbicolor | Bmarchi | Bsupraciliaris | Bnigroviridis | 50 | 69 | -0.16 | -0.16 | 0.091 | 0.078 |
| Bbicolor | Bmarchi | Bsupraciliaris | Bschlegelii | 45 | 18 | 0.429 | 0.429 | 0.267 | 0.108 |
| Bbicolor | Bmarchi | Bsupraciliaris | Bthalassinus | 42 | 289 | -0.746 | -0.746 | 0.038 | 0 |
| Bbicolor | Bmarchi | Bthalassinus | Blateralis | 228 | 23 | 0.817 | 0.817 | 0.013 | 0 |
| Bbicolor | Bmarchi | Bthalassinus | Bnigroviridis | 291 | 45 | 0.732 | 0.732 | 0.048 | 0 |
| Bbicolor | Bmarchi | Bthalassinus | Bschlegelii | 313 | 17 | 0.897 | 0.897 | 0.008 | 0 |
| Bbicolor | Bnigroviridis | Bguifarroi | Blateralis | 23 | 27 | -0.08 | -0.08 | 0.05 | 0.113 |
| Bbicolor | Bnigroviridis | Bguifarroi | Bmarchi | 68 | 53 | 0.124 | 0.124 | 0.046 | 0.007 |
| Bbicolor | Bnigroviridis | Bguifarroi | Bnubestris | 48 | 436 | -0.802 | -0.802 | 0.048 | 0 |
| Bbicolor | Bnigroviridis | Bguifarroi | Browleyi | 131 | 50 | 0.448 | 0.448 | 0.02 | 0 |
| Bbicolor | Bnigroviridis | Bguifarroi | Bschlegelii | 60 | 178 | -0.496 | -0.496 | 0.057 | 0 |
| Bbicolor | Bnigroviridis | Bguifarroi | Bsupraciliaris | 45 | 201 | -0.634 | -0.634 | 0.035 | 0 |
| Bbicolor | Bnigroviridis | Bguifarroi | Bthalassinus | 82 | 54 | 0.206 | 0.206 | 0.052 | 0 |
| Bbicolor | Bnigroviridis | Bmarchi | Blateralis | 77 | 59 | 0.132 | 0.132 | 0.074 | 0.072 |
| Bbicolor | Bnigroviridis | Bmarchi | Bnubestris | 42 | 454 | -0.831 | -0.831 | 0.038 | 0 |
| Bbicolor | Bnigroviridis | Bmarchi | Browleyi | 160 | 46 | 0.553 | 0.553 | 0.037 | 0 |
| Bbicolor | Bnigroviridis | Bmarchi | Bschlegelii | 80 | 213 | -0.454 | -0.454 | 0.062 | 0 |
| Bbicolor | Bnigroviridis | Bmarchi | Bsupraciliaris | 46 | 207 | -0.636 | -0.636 | 0.023 | 0 |
| Bbicolor | Bnigroviridis | Bmarchi | Bthalassinus | 21 | 66 | -0.517 | -0.517 | 0.069 | 0 |
| Bbicolor | Bnigroviridis | Bnubestris | Blateralis | 443 | 21 | 0.909 | 0.909 | 0.012 | 0 |

| H1 | H2 | H3 | Out | Number ABBA | Number BABA | D | Z-score | SD D-statistic | P-value that D = 0 |
|---|---|---|---|---|---|---|---|---|---|
| Bbicolor | Bnigroviridis | Bnubestris | Browleyi | 535 | 11 | 0.96 | 0.96 | 0.003 | 0 |
| Bbicolor | Bnigroviridis | Bnubestris | Bschlegelii | 363 | 59 | 0.72 | 0.72 | 0.04 | 0 |
| Bbicolor | Bnigroviridis | Bnubestris | Bsupraciliaris | 319 | 32 | 0.818 | 0.818 | 0.033 | 0 |
| Bbicolor | Bnigroviridis | Bnubestris | Bthalassinus | 463 | 22 | 0.909 | 0.909 | 0.01 | 0 |
| Bbicolor | Bnigroviridis | Browleyi | Blateralis | 51 | 149 | -0.49 | -0.49 | 0.062 | 0 |
| Bbicolor | Bnigroviridis | Browleyi | Bschlegelii | 26 | 270 | -0.824 | -0.824 | 0.013 | 0 |
| Bbicolor | Bnigroviridis | Browleyi | Bsupraciliaris | 32 | 256 | -0.778 | -0.778 | 0.02 | 0 |
| Bbicolor | Bnigroviridis | Browleyi | Bthalassinus | 61 | 155 | -0.435 | -0.435 | 0.056 | 0 |
| Bbicolor | Bnigroviridis | Bschlegelii | Blateralis | 190 | 57 | 0.538 | 0.538 | 0.051 | 0 |
| Bbicolor | Bnigroviridis | Bsupraciliaris | Blateralis | 183 | 47 | 0.591 | 0.591 | 0.026 | 0 |
| Bbicolor | Bnigroviridis | Bsupraciliaris | Bschlegelii | 39 | 20 | 0.322 | 0.322 | 0.104 | 0.002 |
| Bbicolor | Bnigroviridis | Bsupraciliaris | Bthalassinus | 194 | 121 | 0.232 | 0.232 | 0.062 | 0 |
| Bbicolor | Bnigroviridis | Bthalassinus | Blateralis | 108 | 80 | 0.149 | 0.149 | 0.053 | 0.005 |
| Bbicolor | Bnigroviridis | Bthalassinus | Bschlegelii | 60 | 219 | -0.57 | -0.57 | 0.024 | 0 |
| Bbicolor | Bnubestris | Bguifarroi | Blateralis | 34 | 29 | 0.079 | 0.079 | 0.069 | 0.253 |
| Bbicolor | Bnubestris | Bguifarroi | Bmarchi | 70 | 54 | 0.129 | 0.129 | 0.038 | 0.001 |
| Bbicolor | Bnubestris | Bguifarroi | Bnigroviridis | 28 | 434 | -0.879 | -0.879 | 0.018 | 0 |
| Bbicolor | Bnubestris | Bguifarroi | Browleyi | 148 | 58 | 0.437 | 0.437 | 0.062 | 0 |
| Bbicolor | Bnubestris | Bguifarroi | Bschlegelii | 64 | 187 | -0.49 | -0.49 | 0.054 | 0 |
| Bbicolor | Bnubestris | Bguifarroi | Bsupraciliaris | 79 | 178 | -0.385 | -0.385 | 0.065 | 0 |
| Bbicolor | Bnubestris | Bguifarroi | Bthalassinus | 66 | 50 | 0.138 | 0.138 | 0.056 | 0.014 |

| H1 | H2 | H3 | Out | Number ABBA | Number BABA | D | Z-score | SD D-statistic | P-value that D = 0 |
|---|---|---|---|---|---|---|---|---|---|
| Bbicolor | Bnubestris | Blateralis | Bnigroviridis | 27 | 432 | -0.882 | -0.882 | 0.019 | 0 |
| Bbicolor | Bnubestris | Bmarchi | Blateralis | 50 | 66 | -0.138 | -0.138 | 0.043 | 0.001 |
| Bbicolor | Bnubestris | Bmarchi | Bnigroviridis | 9 | 442 | -0.96 | -0.96 | 0.005 | 0 |
| Bbicolor | Bnubestris | Bmarchi | Browleyi | 140 | 66 | 0.359 | 0.359 | 0.047 | 0 |
| Bbicolor | Bnubestris | Bmarchi | Bschlegelii | 48 | 205 | -0.621 | -0.621 | 0.021 | 0 |
| Bbicolor | Bnubestris | Bmarchi | Bsupraciliaris | 46 | 242 | -0.681 | -0.681 | 0.02 | 0 |
| Bbicolor | Bnubestris | Bmarchi | Bthalassinus | 83 | 19 | 0.627 | 0.627 | 0.081 | 0 |
| Bbicolor | Bnubestris | Browleyi | Blateralis | 71 | 169 | -0.408 | -0.408 | 0.064 | 0 |
| Bbicolor | Bnubestris | Browleyi | Bnigroviridis | 59 | 531 | -0.8 | -0.8 | 0.035 | 0 |
| Bbicolor | Bnubestris | Browleyi | Bschlegelii | 77 | 283 | -0.572 | -0.572 | 0.051 | 0 |
| Bbicolor | Bnubestris | Browleyi | Bsupraciliaris | 35 | 280 | -0.778 | -0.778 | 0.014 | 0 |
| Bbicolor | Bnubestris | Browleyi | Bthalassinus | 63 | 164 | -0.445 | -0.445 | 0.059 | 0 |
| Bbicolor | Bnubestris | Bschlegelii | Blateralis | 206 | 85 | 0.416 | 0.416 | 0.102 | 0 |
| Bbicolor | Bnubestris | Bschlegelii | Bnigroviridis | 31 | 305 | -0.815 | -0.815 | 0.018 | 0 |
| Bbicolor | Bnubestris | Bsupraciliaris | Blateralis | 223 | 69 | 0.527 | 0.527 | 0.075 | 0 |
| Bbicolor | Bnubestris | Bsupraciliaris | Bnigroviridis | 26 | 335 | -0.856 | -0.856 | 0.014 | 0 |
| Bbicolor | Bnubestris | Bsupraciliaris | Bschlegelii | 22 | 16 | 0.158 | 0.158 | 0.064 | 0.014 |
| Bbicolor | Bnubestris | Bsupraciliaris | Bthalassinus | 196 | 83 | 0.405 | 0.405 | 0.039 | 0 |
| Bbicolor | Bnubestris | Bthalassinus | Blateralis | 79 | 66 | 0.09 | 0.09 | 0.071 | 0.208 |
| Bbicolor | Bnubestris | Bthalassinus | Bnigroviridis | 11 | 455 | -0.953 | -0.953 | 0.004 | 0 |
| Bbicolor | Bnubestris | Bthalassinus | Bschlegelii | 54 | 241 | -0.634 | -0.634 | 0.03 | 0 |

| H1 | H2 | H3 | Out | Number ABBA | Number BABA | D | Z-score | SD D-statistic | P-value that D = 0 |
|---|---|---|---|---|---|---|---|---|---|
| Bbicolor | Browleyi | Bguifarroi | Blateralis | 50 | 19 | 0.449 | 0.449 | 0.124 | 0 |
| Bbicolor | Browleyi | Bguifarroi | Bmarchi | 56 | 25 | 0.383 | 0.383 | 0.058 | 0 |
| Bbicolor | Browleyi | Bguifarroi | Bnigroviridis | 39 | 51 | -0.133 | -0.133 | 0.096 | 0.164 |
| Bbicolor | Browleyi | Bguifarroi | Bnubestris | 44 | 47 | -0.033 | -0.033 | 0.067 | 0.623 |
| Bbicolor | Browleyi | Bguifarroi | Bschlegelii | 43 | 64 | -0.196 | -0.196 | 0.103 | 0.058 |
| Bbicolor | Browleyi | Bguifarroi | Bsupraciliaris | 70 | 40 | 0.273 | 0.273 | 0.116 | 0.019 |
| Bbicolor | Browleyi | Bguifarroi | Bthalassinus | 33 | 28 | 0.082 | 0.082 | 0.064 | 0.2 |
| Bbicolor | Browleyi | Blateralis | Bnigroviridis | 57 | 42 | 0.152 | 0.152 | 0.07 | 0.032 |
| Bbicolor | Browleyi | Bmarchi | Blateralis | 25 | 59 | -0.405 | -0.405 | 0.116 | 0 |
| Bbicolor | Browleyi | Bmarchi | Bnigroviridis | 82 | 63 | 0.131 | 0.131 | 0.111 | 0.239 |
| Bbicolor | Browleyi | Bmarchi | Bnubestris | 69 | 60 | 0.07 | 0.07 | 0.114 | 0.539 |
| Bbicolor | Browleyi | Bmarchi | Bschlegelii | 51 | 89 | -0.271 | -0.271 | 0.083 | 0.001 |
| Bbicolor | Browleyi | Bmarchi | Bsupraciliaris | 78 | 54 | 0.182 | 0.182 | 0.062 | 0.003 |
| Bbicolor | Browleyi | Bmarchi | Bthalassinus | 48 | 25 | 0.315 | 0.315 | 0.21 | 0.133 |
| Bbicolor | Browleyi | Bnubestris | Blateralis | 80 | 32 | 0.429 | 0.429 | 0.123 | 0 |
| Bbicolor | Browleyi | Bnubestris | Bnigroviridis | 33 | 10 | 0.535 | 0.535 | 0.159 | 0.001 |
| Bbicolor | Browleyi | Bnubestris | Bschlegelii | 60 | 41 | 0.188 | 0.188 | 0.216 | 0.384 |
| Bbicolor | Browleyi | Bnubestris | Bsupraciliaris | 57 | 46 | 0.107 | 0.107 | 0.157 | 0.496 |
| Bbicolor | Browleyi | Bnubestris | Bthalassinus | 87 | 53 | 0.243 | 0.243 | 0.119 | 0.042 |
| Bbicolor | Browleyi | Bschlegelii | Blateralis | 70 | 40 | 0.273 | 0.273 | 0.112 | 0.015 |
| Bbicolor | Browleyi | Bschlegelii | Bnigroviridis | 22 | 95 | -0.624 | -0.624 | 0.072 | 0 |

| H1 | H2 | H3 | Out | Number ABBA | Number BABA | D | Z-score | SD D-statistic | P-value that D = 0 |
|---|---|---|---|---|---|---|---|---|---|
| Bbicolor | Browleyi | Bsupraciliaris | Blateralis | 114 | 37 | 0.51 | 0.51 | 0.073 | 0 |
| Bbicolor | Browleyi | Bsupraciliaris | Bnigroviridis | 51 | 34 | 0.2 | 0.2 | 0.109 | 0.067 |
| Bbicolor | Browleyi | Bsupraciliaris | Bschlegelii | 31 | 15 | 0.348 | 0.348 | 0.19 | 0.068 |
| Bbicolor | Browleyi | Bsupraciliaris | Bthalassinus | 102 | 46 | 0.378 | 0.378 | 0.059 | 0 |
| Bbicolor | Browleyi | Bthalassinus | Blateralis | 31 | 118 | -0.584 | -0.584 | 0.045 | 0 |
| Bbicolor | Browleyi | Bthalassinus | Bnigroviridis | 41 | 52 | -0.118 | -0.118 | 0.107 | 0.27 |
| Bbicolor | Browleyi | Bthalassinus | Bschlegelii | 45 | 46 | -0.011 | -0.011 | 0.05 | 0.826 |
| Bbicolor | Bschlegelii | Bguifarroi | Blateralis | 63 | 66 | -0.023 | -0.023 | 0.145 | 0.873 |
| Bbicolor | Bschlegelii | Bguifarroi | Bmarchi | 68 | 38 | 0.283 | 0.283 | 0.043 | 0 |
| Bbicolor | Bschlegelii | Bguifarroi | Bnigroviridis | 44 | 192 | -0.627 | -0.627 | 0.036 | 0 |
| Bbicolor | Bschlegelii | Bguifarroi | Bnubestris | 48 | 182 | -0.583 | -0.583 | 0.028 | 0 |
| Bbicolor | Bschlegelii | Bguifarroi | Browleyi | 164 | 50 | 0.533 | 0.533 | 0.044 | 0 |
| Bbicolor | Bschlegelii | Bguifarroi | Bsupraciliaris | 33 | 866 | -0.927 | -0.927 | 0.012 | 0 |
| Bbicolor | Bschlegelii | Bguifarroi | Bthalassinus | 78 | 72 | 0.04 | 0.04 | 0.098 | 0.682 |
| Bbicolor | Bschlegelii | Blateralis | Bnigroviridis | 57 | 172 | -0.502 | -0.502 | 0.031 | 0 |
| Bbicolor | Bschlegelii | Bmarchi | Blateralis | 37 | 72 | -0.321 | -0.321 | 0.061 | 0 |
| Bbicolor | Bschlegelii | Bmarchi | Bnigroviridis | 74 | 198 | -0.456 | -0.456 | 0.062 | 0 |
| Bbicolor | Bschlegelii | Bmarchi | Bnubestris | 34 | 271 | -0.777 | -0.777 | 0.024 | 0 |
| Bbicolor | Bschlegelii | Bmarchi | Browleyi | 117 | 61 | 0.315 | 0.315 | 0.041 | 0 |
| Bbicolor | Bschlegelii | Bmarchi | Bsupraciliaris | 18 | 933 | -0.962 | -0.962 | 0.004 | 0 |
| Bbicolor | Bschlegelii | Bmarchi | Bthalassinus | 17 | 71 | -0.614 | -0.614 | 0.097 | 0 |

| H1 | H2 | H3 | Out | Number ABBA | Number BABA | D | Z-score | SD D-statistic | P-value that D = 0 |
|---|---|---|---|---|---|---|---|---|---|
| Bbicolor | Bschlegelii | Bnubestris | Blateralis | 184 | 62 | 0.496 | 0.496 | 0.027 | 0 |
| Bbicolor | Bschlegelii | Bnubestris | Bnigroviridis | 55 | 45 | 0.1 | 0.1 | 0.109 | 0.361 |
| Bbicolor | Bschlegelii | Bnubestris | Browleyi | 256 | 58 | 0.631 | 0.631 | 0.064 | 0 |
| Bbicolor | Bschlegelii | Bnubestris | Bsupraciliaris | 33 | 750 | -0.916 | -0.916 | 0.013 | 0 |
| Bbicolor | Bschlegelii | Bnubestris | Bthalassinus | 193 | 57 | 0.544 | 0.544 | 0.061 | 0 |
| Bbicolor | Bschlegelii | Browleyi | Blateralis | 54 | 142 | -0.449 | -0.449 | 0.026 | 0 |
| Bbicolor | Bschlegelii | Browleyi | Bnigroviridis | 63 | 259 | -0.609 | -0.609 | 0.044 | 0 |
| Bbicolor | Bschlegelii | Browleyi | Bsupraciliaris | 11 | 983 | -0.978 | -0.978 | 0.003 | 0 |
| Bbicolor | Bschlegelii | Browleyi | Bthalassinus | 44 | 126 | -0.482 | -0.482 | 0.05 | 0 |
| Bbicolor | Bschlegelii | Bsupraciliaris | Blateralis | 876 | 30 | 0.934 | 0.934 | 0.017 | 0 |
| Bbicolor | Bschlegelii | Bsupraciliaris | Bnigroviridis | 790 | 75 | 0.827 | 0.827 | 0.041 | 0 |
| Bbicolor | Bschlegelii | Bsupraciliaris | Bthalassinus | 920 | 24 | 0.949 | 0.949 | 0.006 | 0 |
| Bbicolor | Bschlegelii | Bthalassinus | Blateralis | 83 | 83 | 0 | 0 | 0.117 | 1 |
| Bbicolor | Bschlegelii | Bthalassinus | Bnigroviridis | 44 | 227 | -0.675 | -0.675 | 0.035 | 0 |
| Bbicolor | Bsupraciliaris | Bguifarroi | Blateralis | 30 | 43 | -0.178 | -0.178 | 0.05 | 0 |
| Bbicolor | Bsupraciliaris | Bguifarroi | Bmarchi | 73 | 41 | 0.281 | 0.281 | 0.034 | 0 |
| Bbicolor | Bsupraciliaris | Bguifarroi | Bnigroviridis | 77 | 193 | -0.43 | -0.43 | 0.079 | 0 |
| Bbicolor | Bsupraciliaris | Bguifarroi | Bnubestris | 44 | 195 | -0.632 | -0.632 | 0.025 | 0 |
| Bbicolor | Bsupraciliaris | Bguifarroi | Browleyi | 162 | 38 | 0.62 | 0.62 | 0.028 | 0 |
| Bbicolor | Bsupraciliaris | Bguifarroi | Bschlegelii | 41 | 887 | -0.912 | -0.912 | 0.015 | 0 |
| Bbicolor | Bsupraciliaris | Bguifarroi | Bthalassinus | 83 | 41 | 0.339 | 0.339 | 0.06 | 0 |

| H1 | H2 | H3 | Out | Number ABBA | Number BABA | D | Z-score | SD D-statistic | P-value that D = 0 |
|---|---|---|---|---|---|---|---|---|---|
| Bbicolor | Bsupraciliaris | Blateralis | Bnigroviridis | 47 | 187 | -0.598 | -0.598 | 0.022 | 0 |
| Bbicolor | Bsupraciliaris | Bmarchi | Blateralis | 37 | 75 | -0.339 | -0.339 | 0.047 | 0 |
| Bbicolor | Bsupraciliaris | Bmarchi | Bnigroviridis | 43 | 207 | -0.656 | -0.656 | 0.06 | 0 |
| Bbicolor | Bsupraciliaris | Bmarchi | Bnubestris | 29 | 201 | -0.748 | -0.748 | 0.027 | 0 |
| Bbicolor | Bsupraciliaris | Bmarchi | Browleyi | 163 | 51 | 0.523 | 0.523 | 0.025 | 0 |
| Bbicolor | Bsupraciliaris | Bmarchi | Bschlegelii | 15 | 946 | -0.969 | -0.969 | 0.005 | 0 |
| Bbicolor | Bsupraciliaris | Bmarchi | Bthalassinus | 33 | 28 | 0.082 | 0.082 | 0.137 | 0.55 |
| Bbicolor | Bsupraciliaris | Bnubestris | Blateralis | 204 | 55 | 0.575 | 0.575 | 0.037 | 0 |
| Bbicolor | Bsupraciliaris | Bnubestris | Bnigroviridis | 64 | 33 | 0.32 | 0.32 | 0.183 | 0.081 |
| Bbicolor | Bsupraciliaris | Bnubestris | Browleyi | 261 | 31 | 0.788 | 0.788 | 0.016 | 0 |
| Bbicolor | Bsupraciliaris | Bnubestris | Bschlegelii | 21 | 759 | -0.946 | -0.946 | 0.004 | 0 |
| Bbicolor | Bsupraciliaris | Bnubestris | Bthalassinus | 200 | 31 | 0.732 | 0.732 | 0.033 | 0 |
| Bbicolor | Bsupraciliaris | Browleyi | Blateralis | 57 | 138 | -0.415 | -0.415 | 0.046 | 0 |
| Bbicolor | Bsupraciliaris | Browleyi | Bnigroviridis | 66 | 261 | -0.596 | -0.596 | 0.07 | 0 |
| Bbicolor | Bsupraciliaris | Browleyi | Bschlegelii | 69 | 972 | -0.867 | -0.867 | 0.014 | 0 |
| Bbicolor | Bsupraciliaris | Browleyi | Bthalassinus | 65 | 117 | -0.286 | -0.286 | 0.045 | 0 |
| Bbicolor | Bsupraciliaris | Bschlegelii | Blateralis | 868 | 14 | 0.968 | 0.968 | 0.004 | 0 |
| Bbicolor | Bsupraciliaris | Bschlegelii | Bnigroviridis | 757 | 60 | 0.853 | 0.853 | 0.033 | 0 |
| Bbicolor | Bsupraciliaris | Bthalassinus | Blateralis | 40 | 135 | -0.543 | -0.543 | 0.05 | 0 |
| Bbicolor | Bsupraciliaris | Bthalassinus | Bnigroviridis | 32 | 267 | -0.786 | -0.786 | 0.023 | 0 |
| Bbicolor | Bsupraciliaris | Bthalassinus | Bschlegelii | 45 | 985 | -0.913 | -0.913 | 0.018 | 0 |

| H1 | H2 | H3 | Out | Number ABBA | Number BABA | D | Z-score | SD D-statistic | P-value that D = 0 |
|---|---|---|---|---|---|---|---|---|---|
| Bbicolor | Bthalassinus | Bguifarroi | Blateralis | 28 | 27 | 0.018 | 0.018 | 0.067 | 0.785 |
| Bbicolor | Bthalassinus | Bguifarroi | Bmarchi | 22 | 221 | -0.819 | -0.819 | 0.022 | 0 |
| Bbicolor | Bthalassinus | Bguifarroi | Bnigroviridis | 107 | 59 | 0.289 | 0.289 | 0.065 | 0 |
| Bbicolor | Bthalassinus | Bguifarroi | Bnubestris | 93 | 57 | 0.24 | 0.24 | 0.04 | 0 |
| Bbicolor | Bthalassinus | Bguifarroi | Browleyi | 148 | 35 | 0.617 | 0.617 | 0.019 | 0 |
| Bbicolor | Bthalassinus | Bguifarroi | Bschlegelii | 99 | 41 | 0.414 | 0.414 | 0.049 | 0 |
| Bbicolor | Bthalassinus | Bguifarroi | Bsupraciliaris | 118 | 41 | 0.484 | 0.484 | 0.03 | 0 |
| Bbicolor | Bthalassinus | Blateralis | Bnigroviridis | 106 | 105 | 0.005 | 0.005 | 0.077 | 0.951 |
| Bbicolor | Bthalassinus | Bmarchi | Blateralis | 235 | 24 | 0.815 | 0.815 | 0.018 | 0 |
| Bbicolor | Bthalassinus | Bmarchi | Bnigroviridis | 291 | 27 | 0.83 | 0.83 | 0.016 | 0 |
| Bbicolor | Bthalassinus | Bmarchi | Bnubestris | 268 | 24 | 0.836 | 0.836 | 0.014 | 0 |
| Bbicolor | Bthalassinus | Bmarchi | Browleyi | 387 | 43 | 0.8 | 0.8 | 0.035 | 0 |
| Bbicolor | Bthalassinus | Bmarchi | Bschlegelii | 307 | 18 | 0.889 | 0.889 | 0.011 | 0 |
| Bbicolor | Bthalassinus | Bmarchi | Bsupraciliaris | 296 | 17 | 0.891 | 0.891 | 0.009 | 0 |
| Bbicolor | Bthalassinus | Bnubestris | Blateralis | 61 | 92 | -0.203 | -0.203 | 0.054 | 0 |
| Bbicolor | Bthalassinus | Bnubestris | Bnigroviridis | 16 | 36 | -0.385 | -0.385 | 0.115 | 0.001 |
| Bbicolor | Bthalassinus | Bnubestris | Browleyi | 127 | 41 | 0.512 | 0.512 | 0.046 | 0 |
| Bbicolor | Bthalassinus | Bnubestris | Bschlegelii | 76 | 77 | -0.007 | -0.007 | 0.144 | 0.964 |
| Bbicolor | Bthalassinus | Bnubestris | Bsupraciliaris | 61 | 33 | 0.298 | 0.298 | 0.059 | 0 |
| Bbicolor | Bthalassinus | Browleyi | Blateralis | 31 | 149 | -0.656 | -0.656 | 0.019 | 0 |
| Bbicolor | Bthalassinus | Browleyi | Bnigroviridis | 43 | 144 | -0.54 | -0.54 | 0.048 | 0 |

| H1 | H2 | H3 | Out | Number ABBA | Number BABA | D | Z-score | SD D-statistic | P-value that D = 0 |
|---|---|---|---|---|---|---|---|---|---|
| Bbicolor | Bthalassinus | Browleyi | Bschlegelii | 55 | 125 | -0.389 | -0.389 | 0.037 | 0 |
| Bbicolor | Bthalassinus | Browleyi | Bsupraciliaris | 55 | 154 | -0.474 | -0.474 | 0.068 | 0 |
| Bbicolor | Bthalassinus | Bschlegelii | Blateralis | 99 | 97 | 0.01 | 0.01 | 0.054 | 0.851 |
| Bbicolor | Bthalassinus | Bschlegelii | Bnigroviridis | 90 | 50 | 0.286 | 0.286 | 0.105 | 0.006 |
| Bbicolor | Bthalassinus | Bsupraciliaris | Blateralis | 54 | 159 | -0.493 | -0.493 | 0.069 | 0 |
| Bbicolor | Bthalassinus | Bsupraciliaris | Bnigroviridis | 47 | 79 | -0.254 | -0.254 | 0.09 | 0.005 |
| Bbicolor | Bthalassinus | Bsupraciliaris | Bschlegelii | 23 | 30 | -0.132 | -0.132 | 0.192 | 0.491 |
| Bguifarroi | Blateralis | Bmarchi | Bnigroviridis | 31 | 44 | -0.173 | -0.173 | 0.063 | 0.006 |
| Bguifarroi | Blateralis | Bmarchi | Bnubestris | 33 | 37 | -0.057 | -0.057 | 0.074 | 0.443 |
| Bguifarroi | Blateralis | Bmarchi | Browleyi | 29 | 104 | -0.564 | -0.564 | 0.057 | 0 |
| Bguifarroi | Blateralis | Bmarchi | Bschlegelii | 38 | 50 | -0.136 | -0.136 | 0.052 | 0.009 |
| Bguifarroi | Blateralis | Bmarchi | Bsupraciliaris | 34 | 49 | -0.181 | -0.181 | 0.047 | 0 |
| Bguifarroi | Blateralis | Bmarchi | Bthalassinus | 11 | 53 | -0.656 | -0.656 | 0.113 | 0 |
| Bguifarroi | Blateralis | Bnubestris | Bnigroviridis | 8 | 11 | -0.158 | -0.158 | 0.148 | 0.285 |
| Bguifarroi | Blateralis | Bnubestris | Browleyi | 31 | 35 | -0.061 | -0.061 | 0.068 | 0.375 |
| Bguifarroi | Blateralis | Bnubestris | Bschlegelii | 24 | 29 | -0.094 | -0.094 | 0.076 | 0.214 |
| Bguifarroi | Blateralis | Bnubestris | Bsupraciliaris | 16 | 26 | -0.238 | -0.238 | 0.066 | 0 |
| Bguifarroi | Blateralis | Bnubestris | Bthalassinus | 37 | 40 | -0.039 | -0.039 | 0.071 | 0.581 |
| Bguifarroi | Blateralis | Browleyi | Bnigroviridis | 24 | 30 | -0.111 | -0.111 | 0.057 | 0.053 |
| Bguifarroi | Blateralis | Browleyi | Bschlegelii | 55 | 37 | 0.196 | 0.196 | 0.148 | 0.185 |
| Bguifarroi | Blateralis | Browleyi | Bsupraciliaris | 24 | 41 | -0.262 | -0.262 | 0.049 | 0 |

| H1 | H2 | H3 | Out | Number ABBA | Number BABA | D | Z-score | SD D-statistic | P-value that D = 0 |
|---|---|---|---|---|---|---|---|---|---|
| Bguifarroi | Blateralis | Browleyi | Bthalassinus | 104 | 23 | 0.638 | 0.638 | 0.052 | 0 |
| Bguifarroi | Blateralis | Bschlegelii | Bnigroviridis | 24 | 20 | 0.091 | 0.091 | 0.063 | 0.149 |
| Bguifarroi | Blateralis | Bsupraciliaris | Bnigroviridis | 21 | 14 | 0.2 | 0.2 | 0.049 | 0 |
| Bguifarroi | Blateralis | Bsupraciliaris | Bschlegelii | 19 | 49 | -0.441 | -0.441 | 0.088 | 0 |
| Bguifarroi | Blateralis | Bsupraciliaris | Bthalassinus | 50 | 42 | 0.087 | 0.087 | 0.061 | 0.151 |
| Bguifarroi | Blateralis | Bthalassinus | Bnigroviridis | 44 | 51 | -0.074 | -0.074 | 0.061 | 0.224 |
| Bguifarroi | Blateralis | Bthalassinus | Bschlegelii | 44 | 43 | 0.011 | 0.011 | 0.064 | 0.858 |
| Bguifarroi | Bmarchi | Blateralis | Bnigroviridis | 34 | 141 | -0.611 | -0.611 | 0.029 | 0 |
| Bguifarroi | Bmarchi | Bnubestris | Blateralis | 140 | 36 | 0.591 | 0.591 | 0.027 | 0 |
| Bguifarroi | Bmarchi | Bnubestris | Bnigroviridis | 10 | 59 | -0.71 | -0.71 | 0.054 | 0 |
| Bguifarroi | Bmarchi | Bnubestris | Browleyi | 50 | 54 | -0.038 | -0.038 | 0.056 | 0.496 |
| Bguifarroi | Bmarchi | Bnubestris | Bschlegelii | 43 | 25 | 0.265 | 0.265 | 0.044 | 0 |
| Bguifarroi | Bmarchi | Bnubestris | Bsupraciliaris | 36 | 23 | 0.22 | 0.22 | 0.046 | 0 |
| Bguifarroi | Bmarchi | Bnubestris | Bthalassinus | 24 | 241 | -0.819 | -0.819 | 0.011 | 0 |
| Bguifarroi | Bmarchi | Browleyi | Blateralis | 172 | 24 | 0.755 | 0.755 | 0.021 | 0 |
| Bguifarroi | Bmarchi | Browleyi | Bnigroviridis | 92 | 49 | 0.305 | 0.305 | 0.068 | 0 |
| Bguifarroi | Bmarchi | Browleyi | Bschlegelii | 101 | 36 | 0.474 | 0.474 | 0.053 | 0 |
| Bguifarroi | Bmarchi | Browleyi | Bsupraciliaris | 68 | 38 | 0.283 | 0.283 | 0.039 | 0 |
| Bguifarroi | Bmarchi | Browleyi | Bthalassinus | 12 | 219 | -0.896 | -0.896 | 0.009 | 0 |
| Bguifarroi | Bmarchi | Bschlegelii | Blateralis | 118 | 39 | 0.503 | 0.503 | 0.028 | 0 |
| Bguifarroi | Bmarchi | Bschlegelii | Bnigroviridis | 22 | 39 | -0.279 | -0.279 | 0.029 | 0 |

| H1 | H2 | H3 | Out | Number ABBA | Number BABA | D | Z-score | SD D-statistic | P-value that D = 0 |
|---|---|---|---|---|---|---|---|---|---|
| Bguifarroi | Bmarchi | Bsupraciliaris | Blateralis | 148 | 33 | 0.635 | 0.635 | 0.044 | 0 |
| Bguifarroi | Bmarchi | Bsupraciliaris | Bnigroviridis | 19 | 32 | -0.255 | -0.255 | 0.034 | 0 |
| Bguifarroi | Bmarchi | Bsupraciliaris | Bschlegelii | 9 | 11 | -0.1 | -0.1 | 0.09 | 0.264 |
| Bguifarroi | Bmarchi | Bsupraciliaris | Bthalassinus | 18 | 293 | -0.884 | -0.884 | 0.015 | 0 |
| Bguifarroi | Bmarchi | Bthalassinus | Blateralis | 323 | 11 | 0.934 | 0.934 | 0.013 | 0 |
| Bguifarroi | Bmarchi | Bthalassinus | Bnigroviridis | 236 | 21 | 0.837 | 0.837 | 0.021 | 0 |
| Bguifarroi | Bmarchi | Bthalassinus | Bschlegelii | 263 | 26 | 0.82 | 0.82 | 0.026 | 0 |
| Bguifarroi | Bnigroviridis | Bmarchi | Blateralis | 133 | 58 | 0.393 | 0.393 | 0.043 | 0 |
| Bguifarroi | Bnigroviridis | Bmarchi | Bnubestris | 13 | 474 | -0.947 | -0.947 | 0.007 | 0 |
| Bguifarroi | Bnigroviridis | Bmarchi | Browleyi | 47 | 103 | -0.373 | -0.373 | 0.036 | 0 |
| Bguifarroi | Bnigroviridis | Bmarchi | Bschlegelii | 44 | 232 | -0.681 | -0.681 | 0.029 | 0 |
| Bguifarroi | Bnigroviridis | Bmarchi | Bsupraciliaris | 40 | 265 | -0.738 | -0.738 | 0.016 | 0 |
| Bguifarroi | Bnigroviridis | Bmarchi | Bthalassinus | 25 | 85 | -0.545 | -0.545 | 0.085 | 0 |
| Bguifarroi | Bnigroviridis | Bnubestris | Blateralis | 581 | 10 | 0.966 | 0.966 | 0.006 | 0 |
| Bguifarroi | Bnigroviridis | Bnubestris | Browleyi | 437 | 13 | 0.942 | 0.942 | 0.007 | 0 |
| Bguifarroi | Bnigroviridis | Bnubestris | Bschlegelii | 322 | 42 | 0.769 | 0.769 | 0.027 | 0 |
| Bguifarroi | Bnigroviridis | Bnubestris | Bsupraciliaris | 310 | 23 | 0.862 | 0.862 | 0.011 | 0 |
| Bguifarroi | Bnigroviridis | Bnubestris | Bthalassinus | 479 | 15 | 0.939 | 0.939 | 0.007 | 0 |
| Bguifarroi | Bnigroviridis | Browleyi | Blateralis | 163 | 28 | 0.707 | 0.707 | 0.014 | 0 |
| Bguifarroi | Bnigroviridis | Browleyi | Bschlegelii | 41 | 172 | -0.615 | -0.615 | 0.03 | 0 |
| Bguifarroi | Bnigroviridis | Browleyi | Bsupraciliaris | 58 | 179 | -0.511 | -0.511 | 0.026 | 0 |

| H1 | H2 | H3 | Out | Number ABBA | Number BABA | D | Z-score | SD D-statistic | P-value that D = 0 |
|---|---|---|---|---|---|---|---|---|---|
| Bguifarroi | Bnigroviridis | Browleyi | Bthalassinus | 87 | 46 | 0.308 | 0.308 | 0.04 | 0 |
| Bguifarroi | Bnigroviridis | Bschlegelii | Blateralis | 310 | 22 | 0.867 | 0.867 | 0.018 | 0 |
| Bguifarroi | Bnigroviridis | Bsupraciliaris | Blateralis | 290 | 14 | 0.908 | 0.908 | 0.01 | 0 |
| Bguifarroi | Bnigroviridis | Bsupraciliaris | Bschlegelii | 37 | 19 | 0.321 | 0.321 | 0.09 | 0 |
| Bguifarroi | Bnigroviridis | Bsupraciliaris | Bthalassinus | 231 | 70 | 0.535 | 0.535 | 0.057 | 0 |
| Bguifarroi | Bnigroviridis | Bthalassinus | Blateralis | 158 | 66 | 0.411 | 0.411 | 0.055 | 0 |
| Bguifarroi | Bnigroviridis | Bthalassinus | Bschlegelii | 92 | 226 | -0.421 | -0.421 | 0.09 | 0 |
| Bguifarroi | Bnubestris | Blateralis | Bnigroviridis | 8 | 610 | -0.974 | -0.974 | 0.005 | 0 |
| Bguifarroi | Bnubestris | Bmarchi | Blateralis | 126 | 41 | 0.509 | 0.509 | 0.037 | 0 |
| Bguifarroi | Bnubestris | Bmarchi | Bnigroviridis | 10 | 478 | -0.959 | -0.959 | 0.005 | 0 |
| Bguifarroi | Bnubestris | Bmarchi | Browleyi | 46 | 135 | -0.492 | -0.492 | 0.049 | 0 |
| Bguifarroi | Bnubestris | Bmarchi | Bschlegelii | 41 | 267 | -0.734 | -0.734 | 0.021 | 0 |
| Bguifarroi | Bnubestris | Bmarchi | Bsupraciliaris | 36 | 225 | -0.724 | -0.724 | 0.02 | 0 |
| Bguifarroi | Bnubestris | Bmarchi | Bthalassinus | 29 | 30 | -0.017 | -0.017 | 0.1 | 0.865 |
| Bguifarroi | Bnubestris | Browleyi | Blateralis | 176 | 26 | 0.743 | 0.743 | 0.024 | 0 |
| Bguifarroi | Bnubestris | Browleyi | Bnigroviridis | 10 | 439 | -0.955 | -0.955 | 0.005 | 0 |
| Bguifarroi | Bnubestris | Browleyi | Bschlegelii | 45 | 184 | -0.607 | -0.607 | 0.034 | 0 |
| Bguifarroi | Bnubestris | Browleyi | Bsupraciliaris | 47 | 194 | -0.61 | -0.61 | 0.031 | 0 |
| Bguifarroi | Bnubestris | Browleyi | Bthalassinus | 83 | 42 | 0.328 | 0.328 | 0.037 | 0 |
| Bguifarroi | Bnubestris | Bschlegelii | Blateralis | 292 | 58 | 0.669 | 0.669 | 0.074 | 0 |
| Bguifarroi | Bnubestris | Bschlegelii | Bnigroviridis | 80 | 310 | -0.59 | -0.59 | 0.063 | 0 |

| H1 | H2 | H3 | Out | Number ABBA | Number BABA | D | Z-score | SD D-statistic | P-value that D = 0 |
|---|---|---|---|---|---|---|---|---|---|
| Bguifarroi | Bnubestris | Bsupraciliaris | Blateralis | 298 | 20 | 0.874 | 0.874 | 0.02 | 0 |
| Bguifarroi | Bnubestris | Bsupraciliaris | Bnigroviridis | 29 | 307 | -0.827 | -0.827 | 0.022 | 0 |
| Bguifarroi | Bnubestris | Bsupraciliaris | Bschlegelii | 25 | 19 | 0.136 | 0.136 | 0.053 | 0.01 |
| Bguifarroi | Bnubestris | Bsupraciliaris | Bthalassinus | 231 | 69 | 0.54 | 0.54 | 0.074 | 0 |
| Bguifarroi | Bnubestris | Bthalassinus | Blateralis | 151 | 39 | 0.589 | 0.589 | 0.027 | 0 |
| Bguifarroi | Bnubestris | Bthalassinus | Bnigroviridis | 12 | 516 | -0.955 | -0.955 | 0.006 | 0 |
| Bguifarroi | Bnubestris | Bthalassinus | Bschlegelii | 45 | 211 | -0.648 | -0.648 | 0.032 | 0 |
| Bguifarroi | Browleyi | Blateralis | Bnigroviridis | 22 | 173 | -0.774 | -0.774 | 0.016 | 0 |
| Bguifarroi | Browleyi | Bmarchi | Blateralis | 120 | 39 | 0.509 | 0.509 | 0.031 | 0 |
| Bguifarroi | Browleyi | Bmarchi | Bnigroviridis | 51 | 89 | -0.271 | -0.271 | 0.041 | 0 |
| Bguifarroi | Browleyi | Bmarchi | Bnubestris | 56 | 96 | -0.263 | -0.263 | 0.031 | 0 |
| Bguifarroi | Browleyi | Bmarchi | Bschlegelii | 68 | 111 | -0.24 | -0.24 | 0.023 | 0 |
| Bguifarroi | Browleyi | Bmarchi | Bsupraciliaris | 62 | 171 | -0.468 | -0.468 | 0.033 | 0 |
| Bguifarroi | Browleyi | Bmarchi | Bthalassinus | 14 | 33 | -0.404 | -0.404 | 0.064 | 0 |
| Bguifarroi | Browleyi | Bnubestris | Blateralis | 174 | 27 | 0.731 | 0.731 | 0.02 | 0 |
| Bguifarroi | Browleyi | Bnubestris | Bnigroviridis | 15 | 28 | -0.302 | -0.302 | 0.09 | 0.001 |
| Bguifarroi | Browleyi | Bnubestris | Bschlegelii | 75 | 38 | 0.327 | 0.327 | 0.077 | 0 |
| Bguifarroi | Browleyi | Bnubestris | Bsupraciliaris | 41 | 44 | -0.035 | -0.035 | 0.064 | 0.581 |
| Bguifarroi | Browleyi | Bnubestris | Bthalassinus | 93 | 56 | 0.248 | 0.248 | 0.044 | 0 |
| Bguifarroi | Browleyi | Bschlegelii | Blateralis | 156 | 27 | 0.705 | 0.705 | 0.02 | 0 |
| Bguifarroi | Browleyi | Bschlegelii | Bnigroviridis | 49 | 45 | 0.043 | 0.043 | 0.068 | 0.53 |

| H1 | H2 | H3 | Out | Number ABBA | Number BABA | D | Z-score | SD D-statistic | P-value that D = 0 |
|---|---|---|---|---|---|---|---|---|---|
| Bguifarroi | Browleyi | Bsupraciliaris | Blateralis | 160 | 86 | 0.301 | 0.301 | 0.074 | 0 |
| Bguifarroi | Browleyi | Bsupraciliaris | Bnigroviridis | 110 | 43 | 0.438 | 0.438 | 0.063 | 0 |
| Bguifarroi | Browleyi | Bsupraciliaris | Bschlegelii | 39 | 11 | 0.56 | 0.56 | 0.214 | 0.009 |
| Bguifarroi | Browleyi | Bsupraciliaris | Bthalassinus | 132 | 76 | 0.269 | 0.269 | 0.048 | 0 |
| Bguifarroi | Browleyi | Bthalassinus | Blateralis | 128 | 37 | 0.552 | 0.552 | 0.023 | 0 |
| Bguifarroi | Browleyi | Bthalassinus | Bnigroviridis | 55 | 95 | -0.267 | -0.267 | 0.033 | 0 |
| Bguifarroi | Browleyi | Bthalassinus | Bschlegelii | 71 | 96 | -0.15 | -0.15 | 0.03 | 0 |
| Bguifarroi | Bschlegelii | Blateralis | Bnigroviridis | 28 | 310 | -0.834 | -0.834 | 0.016 | 0 |
| Bguifarroi | Bschlegelii | Bmarchi | Blateralis | 114 | 49 | 0.399 | 0.399 | 0.031 | 0 |
| Bguifarroi | Bschlegelii | Bmarchi | Bnigroviridis | 23 | 261 | -0.838 | -0.838 | 0.012 | 0 |
| Bguifarroi | Bschlegelii | Bmarchi | Bnubestris | 24 | 221 | -0.804 | -0.804 | 0.017 | 0 |
| Bguifarroi | Bschlegelii | Bmarchi | Browleyi | 41 | 130 | -0.52 | -0.52 | 0.041 | 0 |
| Bguifarroi | Bschlegelii | Bmarchi | Bsupraciliaris | 11 | 941 | -0.977 | -0.977 | 0.003 | 0 |
| Bguifarroi | Bschlegelii | Bmarchi | Bthalassinus | 18 | 37 | -0.345 | -0.345 | 0.11 | 0.002 |
| Bguifarroi | Bschlegelii | Bnubestris | Blateralis | 304 | 25 | 0.848 | 0.848 | 0.012 | 0 |
| Bguifarroi | Bschlegelii | Bnubestris | Bnigroviridis | 26 | 24 | 0.04 | 0.04 | 0.073 | 0.585 |
| Bguifarroi | Bschlegelii | Bnubestris | Browleyi | 207 | 45 | 0.643 | 0.643 | 0.027 | 0 |
| Bguifarroi | Bschlegelii | Bnubestris | Bsupraciliaris | 19 | 782 | -0.953 | -0.953 | 0.003 | 0 |
| Bguifarroi | Bschlegelii | Bnubestris | Bthalassinus | 225 | 34 | 0.737 | 0.737 | 0.022 | 0 |
| Bguifarroi | Bschlegelii | Browleyi | Blateralis | 200 | 38 | 0.681 | 0.681 | 0.028 | 0 |
| Bguifarroi | Bschlegelii | Browleyi | Bnigroviridis | 62 | 186 | -0.5 | -0.5 | 0.094 | 0 |

| H1 | H2 | H3 | Out | Number ABBA | Number BABA | D | Z-score | SD D-statistic | P-value that D = 0 |
|---|---|---|---|---|---|---|---|---|---|
| Bguifarroi | Bschlegelii | Browleyi | Bsupraciliaris | 19 | 882 | -0.958 | -0.958 | 0.004 | 0 |
| Bguifarroi | Bschlegelii | Browleyi | Bthalassinus | 129 | 59 | 0.372 | 0.372 | 0.072 | 0 |
| Bguifarroi | Bschlegelii | Bsupraciliaris | Blateralis | 1034 | 7 | 0.987 | 0.987 | 0.002 | 0 |
| Bguifarroi | Bschlegelii | Bsupraciliaris | Bnigroviridis | 761 | 25 | 0.936 | 0.936 | 0.006 | 0 |
| Bguifarroi | Bschlegelii | Bsupraciliaris | Bthalassinus | 926 | 66 | 0.867 | 0.867 | 0.032 | 0 |
| Bguifarroi | Bschlegelii | Bthalassinus | Blateralis | 132 | 41 | 0.526 | 0.526 | 0.037 | 0 |
| Bguifarroi | Bschlegelii | Bthalassinus | Bnigroviridis | 22 | 226 | -0.823 | -0.823 | 0.015 | 0 |
| Bguifarroi | Bsupraciliaris | Blateralis | Bnigroviridis | 30 | 318 | -0.828 | -0.828 | 0.021 | 0 |
| Bguifarroi | Bsupraciliaris | Bmarchi | Blateralis | 148 | 58 | 0.437 | 0.437 | 0.034 | 0 |
| Bguifarroi | Bsupraciliaris | Bmarchi | Bnigroviridis | 23 | 229 | -0.817 | -0.817 | 0.008 | 0 |
| Bguifarroi | Bsupraciliaris | Bmarchi | Bnubestris | 26 | 230 | -0.797 | -0.797 | 0.012 | 0 |
| Bguifarroi | Bsupraciliaris | Bmarchi | Browleyi | 39 | 173 | -0.632 | -0.632 | 0.042 | 0 |
| Bguifarroi | Bsupraciliaris | Bmarchi | Bschlegelii | 9 | 943 | -0.981 | -0.981 | 0.003 | 0 |
| Bguifarroi | Bsupraciliaris | Bmarchi | Bthalassinus | 16 | 31 | -0.319 | -0.319 | 0.096 | 0.001 |
| Bguifarroi | Bsupraciliaris | Bnubestris | Blateralis | 297 | 61 | 0.659 | 0.659 | 0.064 | 0 |
| Bguifarroi | Bsupraciliaris | Bnubestris | Bnigroviridis | 37 | 22 | 0.254 | 0.254 | 0.047 | 0 |
| Bguifarroi | Bsupraciliaris | Bnubestris | Browleyi | 222 | 44 | 0.669 | 0.669 | 0.03 | 0 |
| Bguifarroi | Bsupraciliaris | Bnubestris | Bschlegelii | 24 | 803 | -0.942 | -0.942 | 0.004 | 0 |
| Bguifarroi | Bsupraciliaris | Bnubestris | Bthalassinus | 226 | 30 | 0.766 | 0.766 | 0.016 | 0 |
| Bguifarroi | Bsupraciliaris | Browleyi | Blateralis | 192 | 34 | 0.699 | 0.699 | 0.036 | 0 |
| Bguifarroi | Bsupraciliaris | Browleyi | Bnigroviridis | 40 | 169 | -0.617 | -0.617 | 0.031 | 0 |

| H1 | H2 | H3 | Out | Number ABBA | Number BABA | D | Z-score | SD D-statistic | P-value that D = 0 |
|---|---|---|---|---|---|---|---|---|---|
| Bguifarroi | Bsupraciliaris | Browleyi | Bschlegelii | 19 | 874 | -0.957 | -0.957 | 0.006 | 0 |
| Bguifarroi | Bsupraciliaris | Browleyi | Bthalassinus | 129 | 38 | 0.545 | 0.545 | 0.069 | 0 |
| Bguifarroi | Bsupraciliaris | Bschlegelii | Blateralis | 994 | 82 | 0.848 | 0.848 | 0.019 | 0 |
| Bguifarroi | Bsupraciliaris | Bschlegelii | Bnigroviridis | 805 | 24 | 0.942 | 0.942 | 0.004 | 0 |
| Bguifarroi | Bsupraciliaris | Bthalassinus | Blateralis | 121 | 91 | 0.142 | 0.142 | 0.076 | 0.063 |
| Bguifarroi | Bsupraciliaris | Bthalassinus | Bnigroviridis | 28 | 229 | -0.782 | -0.782 | 0.013 | 0 |
| Bguifarroi | Bsupraciliaris | Bthalassinus | Bschlegelii | 54 | 967 | -0.894 | -0.894 | 0.024 | 0 |
| Bguifarroi | Bthalassinus | Blateralis | Bnigroviridis | 40 | 158 | -0.596 | -0.596 | 0.03 | 0 |
| Bguifarroi | Bthalassinus | Bmarchi | Blateralis | 320 | 10 | 0.939 | 0.939 | 0.008 | 0 |
| Bguifarroi | Bthalassinus | Bmarchi | Bnigroviridis | 238 | 85 | 0.474 | 0.474 | 0.077 | 0 |
| Bguifarroi | Bthalassinus | Bmarchi | Bnubestris | 241 | 62 | 0.591 | 0.591 | 0.087 | 0 |
| Bguifarroi | Bthalassinus | Bmarchi | Browleyi | 222 | 21 | 0.827 | 0.827 | 0.013 | 0 |
| Bguifarroi | Bthalassinus | Bmarchi | Bschlegelii | 253 | 25 | 0.82 | 0.82 | 0.018 | 0 |
| Bguifarroi | Bthalassinus | Bmarchi | Bsupraciliaris | 284 | 27 | 0.826 | 0.826 | 0.013 | 0 |
| Bguifarroi | Bthalassinus | Bnubestris | Blateralis | 142 | 35 | 0.605 | 0.605 | 0.029 | 0 |
| Bguifarroi | Bthalassinus | Bnubestris | Bnigroviridis | 10 | 36 | -0.565 | -0.565 | 0.135 | 0 |
| Bguifarroi | Bthalassinus | Bnubestris | Browleyi | 45 | 94 | -0.353 | -0.353 | 0.062 | 0 |
| Bguifarroi | Bthalassinus | Bnubestris | Bschlegelii | 43 | 52 | -0.095 | -0.095 | 0.085 | 0.264 |
| Bguifarroi | Bthalassinus | Bnubestris | Bsupraciliaris | 41 | 63 | -0.212 | -0.212 | 0.112 | 0.06 |
| Bguifarroi | Bthalassinus | Browleyi | Blateralis | 124 | 28 | 0.632 | 0.632 | 0.016 | 0 |
| Bguifarroi | Bthalassinus | Browleyi | Bnigroviridis | 53 | 62 | -0.078 | -0.078 | 0.116 | 0.499 |

| H1 | H2 | H3 | Out | Number ABBA | Number BABA | D | Z-score | SD D-statistic | P-value that D = 0 |
|---|---|---|---|---|---|---|---|---|---|
| Bguifarroi | Bthalassinus | Browleyi | Bschlegelii | 58 | 52 | 0.055 | 0.055 | 0.085 | 0.523 |
| Bguifarroi | Bthalassinus | Browleyi | Bsupraciliaris | 67 | 41 | 0.241 | 0.241 | 0.051 | 0 |
| Bguifarroi | Bthalassinus | Bschlegelii | Blateralis | 178 | 34 | 0.679 | 0.679 | 0.038 | 0 |
| Bguifarroi | Bthalassinus | Bschlegelii | Bnigroviridis | 22 | 60 | -0.463 | -0.463 | 0.092 | 0 |
| Bguifarroi | Bthalassinus | Bsupraciliaris | Blateralis | 116 | 40 | 0.487 | 0.487 | 0.031 | 0 |
| Bguifarroi | Bthalassinus | Bsupraciliaris | Bnigroviridis | 24 | 90 | -0.579 | -0.579 | 0.06 | 0 |
| Bguifarroi | Bthalassinus | Bsupraciliaris | Bschlegelii | 56 | 11 | 0.672 | 0.672 | 0.088 | 0 |
| Bmarchi | Blateralis | Bnubestris | Bnigroviridis | 47 | 9 | 0.679 | 0.679 | 0.13 | 0 |
| Bmarchi | Blateralis | Bnubestris | Browleyi | 74 | 62 | 0.088 | 0.088 | 0.043 | 0.038 |
| Bmarchi | Blateralis | Bnubestris | Bschlegelii | 20 | 40 | -0.333 | -0.333 | 0.048 | 0 |
| Bmarchi | Blateralis | Bnubestris | Bsupraciliaris | 24 | 68 | -0.478 | -0.478 | 0.079 | 0 |
| Bmarchi | Blateralis | Bnubestris | Bthalassinus | 251 | 29 | 0.793 | 0.793 | 0.013 | 0 |
| Bmarchi | Blateralis | Browleyi | Bnigroviridis | 42 | 52 | -0.106 | -0.106 | 0.043 | 0.013 |
| Bmarchi | Blateralis | Browleyi | Bschlegelii | 64 | 63 | 0.008 | 0.008 | 0.084 | 0.925 |
| Bmarchi | Blateralis | Browleyi | Bsupraciliaris | 39 | 70 | -0.284 | -0.284 | 0.032 | 0 |
| Bmarchi | Blateralis | Browleyi | Bthalassinus | 248 | 23 | 0.83 | 0.83 | 0.015 | 0 |
| Bmarchi | Blateralis | Bschlegelii | Bnigroviridis | 62 | 26 | 0.409 | 0.409 | 0.043 | 0 |
| Bmarchi | Blateralis | Bsupraciliaris | Bnigroviridis | 43 | 21 | 0.344 | 0.344 | 0.041 | 0 |
| Bmarchi | Blateralis | Bsupraciliaris | Bschlegelii | 36 | 7 | 0.674 | 0.674 | 0.149 | 0 |
| Bmarchi | Blateralis | Bsupraciliaris | Bthalassinus | 269 | 21 | 0.855 | 0.855 | 0.013 | 0 |
| Bmarchi | Blateralis | Bthalassinus | Bnigroviridis | 37 | 253 | -0.745 | -0.745 | 0.015 | 0 |

| H1 | H2 | H3 | Out | Number ABBA | Number BABA | D | Z-score | SD D-statistic | P-value that D = 0 |
|---|---|---|---|---|---|---|---|---|---|
| Bmarchi | Blateralis | Bthalassinus | Bschlegelii | 54 | 253 | -0.648 | -0.648 | 0.079 | 0 |
| Bmarchi | Bnigroviridis | Bnubestris | Blateralis | 474 | 7 | 0.971 | 0.971 | 0.004 | 0 |
| Bmarchi | Bnigroviridis | Bnubestris | Browleyi | 468 | 23 | 0.906 | 0.906 | 0.028 | 0 |
| Bmarchi | Bnigroviridis | Bnubestris | Bschlegelii | 289 | 29 | 0.818 | 0.818 | 0.012 | 0 |
| Bmarchi | Bnigroviridis | Bnubestris | Bsupraciliaris | 280 | 26 | 0.83 | 0.83 | 0.014 | 0 |
| Bmarchi | Bnigroviridis | Bnubestris | Bthalassinus | 687 | 9 | 0.974 | 0.974 | 0.005 | 0 |
| Bmarchi | Bnigroviridis | Browleyi | Blateralis | 129 | 54 | 0.41 | 0.41 | 0.054 | 0 |
| Bmarchi | Bnigroviridis | Browleyi | Bschlegelii | 44 | 217 | -0.663 | -0.663 | 0.033 | 0 |
| Bmarchi | Bnigroviridis | Browleyi | Bsupraciliaris | 34 | 189 | -0.695 | -0.695 | 0.023 | 0 |
| Bmarchi | Bnigroviridis | Browleyi | Bthalassinus | 268 | 18 | 0.874 | 0.874 | 0.014 | 0 |
| Bmarchi | Bnigroviridis | Bschlegelii | Blateralis | 241 | 63 | 0.586 | 0.586 | 0.074 | 0 |
| Bmarchi | Bnigroviridis | Bsupraciliaris | Blateralis | 217 | 20 | 0.831 | 0.831 | 0.014 | 0 |
| Bmarchi | Bnigroviridis | Bsupraciliaris | Bschlegelii | 30 | 35 | -0.077 | -0.077 | 0.208 | 0.711 |
| Bmarchi | Bnigroviridis | Bsupraciliaris | Bthalassinus | 432 | 33 | 0.858 | 0.858 | 0.039 | 0 |
| Bmarchi | Bnigroviridis | Bthalassinus | Blateralis | 47 | 253 | -0.687 | -0.687 | 0.056 | 0 |
| Bmarchi | Bnigroviridis | Bthalassinus | Bschlegelii | 14 | 420 | -0.935 | -0.935 | 0.01 | 0 |
| Bmarchi | Bnubestris | Blateralis | Bnigroviridis | 12 | 460 | -0.949 | -0.949 | 0.006 | 0 |
| Bmarchi | Bnubestris | Browleyi | Blateralis | 87 | 94 | -0.039 | -0.039 | 0.079 | 0.627 |
| Bmarchi | Bnubestris | Browleyi | Bnigroviridis | 10 | 430 | -0.955 | -0.955 | 0.006 | 0 |
| Bmarchi | Bnubestris | Browleyi | Bschlegelii | 32 | 215 | -0.741 | -0.741 | 0.026 | 0 |
| Bmarchi | Bnubestris | Browleyi | Bsupraciliaris | 29 | 194 | -0.74 | -0.74 | 0.025 | 0 |

| H1 | H2 | H3 | Out | Number ABBA | Number BABA | D | Z-score | SD D-statistic | P-value that D = 0 |
|---|---|---|---|---|---|---|---|---|---|
| Bmarchi | Bnubestris | Browleyi | Bthalassinus | 277 | 17 | 0.884 | 0.884 | 0.013 | 0 |
| Bmarchi | Bnubestris | Bschlegelii | Blateralis | 219 | 25 | 0.795 | 0.795 | 0.02 | 0 |
| Bmarchi | Bnubestris | Bschlegelii | Bnigroviridis | 26 | 290 | -0.835 | -0.835 | 0.022 | 0 |
| Bmarchi | Bnubestris | Bsupraciliaris | Blateralis | 217 | 22 | 0.816 | 0.816 | 0.02 | 0 |
| Bmarchi | Bnubestris | Bsupraciliaris | Bnigroviridis | 66 | 289 | -0.628 | -0.628 | 0.064 | 0 |
| Bmarchi | Bnubestris | Bsupraciliaris | Bschlegelii | 21 | 14 | 0.2 | 0.2 | 0.118 | 0.089 |
| Bmarchi | Bnubestris | Bsupraciliaris | Bthalassinus | 467 | 10 | 0.958 | 0.958 | 0.004 | 0 |
| Bmarchi | Bnubestris | Bthalassinus | Blateralis | 44 | 261 | -0.711 | -0.711 | 0.027 | 0 |
| Bmarchi | Bnubestris | Bthalassinus | Bnigroviridis | 9 | 720 | -0.975 | -0.975 | 0.004 | 0 |
| Bmarchi | Bnubestris | Bthalassinus | Bschlegelii | 10 | 422 | -0.954 | -0.954 | 0.005 | 0 |
| Bmarchi | Browleyi | Blateralis | Bnigroviridis | 40 | 105 | -0.448 | -0.448 | 0.024 | 0 |
| Bmarchi | Browleyi | Bnubestris | Blateralis | 89 | 87 | 0.011 | 0.011 | 0.09 | 0.9 |
| Bmarchi | Browleyi | Bnubestris | Bnigroviridis | 10 | 19 | -0.31 | -0.31 | 0.074 | 0 |
| Bmarchi | Browleyi | Bnubestris | Bschlegelii | 38 | 45 | -0.084 | -0.084 | 0.047 | 0.074 |
| Bmarchi | Browleyi | Bnubestris | Bsupraciliaris | 39 | 48 | -0.103 | -0.103 | 0.055 | 0.062 |
| Bmarchi | Browleyi | Bnubestris | Bthalassinus | 278 | 24 | 0.841 | 0.841 | 0.012 | 0 |
| Bmarchi | Browleyi | Bschlegelii | Blateralis | 114 | 41 | 0.471 | 0.471 | 0.032 | 0 |
| Bmarchi | Browleyi | Bschlegelii | Bnigroviridis | 99 | 29 | 0.547 | 0.547 | 0.05 | 0 |
| Bmarchi | Browleyi | Bsupraciliaris | Blateralis | 102 | 32 | 0.522 | 0.522 | 0.045 | 0 |
| Bmarchi | Browleyi | Bsupraciliaris | Bnigroviridis | 50 | 46 | 0.042 | 0.042 | 0.081 | 0.607 |
| Bmarchi | Browleyi | Bsupraciliaris | Bschlegelii | 16 | 13 | 0.103 | 0.103 | 0.114 | 0.365 |

| H1 | H2 | H3 | Out | Number ABBA | Number BABA | D | Z-score | SD D-statistic | P-value that D = 0 |
|---|---|---|---|---|---|---|---|---|---|
| Bmarchi | Browleyi | Bsupraciliaris | Bthalassinus | 351 | 20 | 0.892 | 0.892 | 0.007 | 0 |
| Bmarchi | Browleyi | Bthalassinus | Blateralis | 21 | 303 | -0.87 | -0.87 | 0.012 | 0 |
| Bmarchi | Browleyi | Bthalassinus | Bnigroviridis | 69 | 273 | -0.596 | -0.596 | 0.053 | 0 |
| Bmarchi | Browleyi | Bthalassinus | Bschlegelii | 20 | 292 | -0.872 | -0.872 | 0.012 | 0 |
| Bmarchi | Bschlegelii | Blateralis | Bnigroviridis | 63 | 215 | -0.547 | -0.547 | 0.033 | 0 |
| Bmarchi | Bschlegelii | Bnubestris | Blateralis | 213 | 50 | 0.62 | 0.62 | 0.02 | 0 |
| Bmarchi | Bschlegelii | Bnubestris | Bnigroviridis | 24 | 35 | -0.186 | -0.186 | 0.133 | 0.159 |
| Bmarchi | Bschlegelii | Bnubestris | Browleyi | 193 | 52 | 0.576 | 0.576 | 0.02 | 0 |
| Bmarchi | Bschlegelii | Bnubestris | Bsupraciliaris | 9 | 766 | -0.977 | -0.977 | 0.005 | 0 |
| Bmarchi | Bschlegelii | Bnubestris | Bthalassinus | 418 | 10 | 0.953 | 0.953 | 0.011 | 0 |
| Bmarchi | Bschlegelii | Browleyi | Blateralis | 133 | 78 | 0.261 | 0.261 | 0.056 | 0 |
| Bmarchi | Bschlegelii | Browleyi | Bnigroviridis | 45 | 183 | -0.605 | -0.605 | 0.027 | 0 |
| Bmarchi | Bschlegelii | Browleyi | Bsupraciliaris | 16 | 901 | -0.965 | -0.965 | 0.005 | 0 |
| Bmarchi | Bschlegelii | Browleyi | Bthalassinus | 312 | 29 | 0.83 | 0.83 | 0.019 | 0 |
| Bmarchi | Bschlegelii | Bsupraciliaris | Blateralis | 946 | 12 | 0.975 | 0.975 | 0.002 | 0 |
| Bmarchi | Bschlegelii | Bsupraciliaris | Bnigroviridis | 763 | 23 | 0.941 | 0.941 | 0.014 | 0 |
| Bmarchi | Bschlegelii | Bsupraciliaris | Bthalassinus | 1168 | 25 | 0.958 | 0.958 | 0.015 | 0 |
| Bmarchi | Bschlegelii | Bthalassinus | Blateralis | 39 | 276 | -0.752 | -0.752 | 0.044 | 0 |
| Bmarchi | Bschlegelii | Bthalassinus | Bnigroviridis | 16 | 410 | -0.925 | -0.925 | 0.012 | 0 |
| Bmarchi | Bsupraciliaris | Blateralis | Bnigroviridis | 56 | 215 | -0.587 | -0.587 | 0.029 | 0 |
| Bmarchi | Bsupraciliaris | Bnubestris | Blateralis | 240 | 60 | 0.6 | 0.6 | 0.028 | 0 |

| H1 | H2 | H3 | Out | Number ABBA | Number BABA | D | Z-score | SD D-statistic | P-value that D = 0 |
|---|---|---|---|---|---|---|---|---|---|
| Bmarchi | Bsupraciliaris | Bnubestris | Bnigroviridis | 39 | 31 | 0.114 | 0.114 | 0.103 | 0.265 |
| Bmarchi | Bsupraciliaris | Bnubestris | Browleyi | 194 | 112 | 0.268 | 0.268 | 0.052 | 0 |
| Bmarchi | Bsupraciliaris | Bnubestris | Bschlegelii | 22 | 769 | -0.944 | -0.944 | 0.005 | 0 |
| Bmarchi | Bsupraciliaris | Bnubestris | Bthalassinus | 433 | 16 | 0.929 | 0.929 | 0.008 | 0 |
| Bmarchi | Bsupraciliaris | Browleyi | Blateralis | 102 | 66 | 0.214 | 0.214 | 0.034 | 0 |
| Bmarchi | Bsupraciliaris | Browleyi | Bnigroviridis | 49 | 233 | -0.652 | -0.652 | 0.021 | 0 |
| Bmarchi | Bsupraciliaris | Browleyi | Bschlegelii | 80 | 906 | -0.838 | -0.838 | 0.022 | 0 |
| Bmarchi | Bsupraciliaris | Browleyi | Bthalassinus | 293 | 19 | 0.878 | 0.878 | 0.011 | 0 |
| Bmarchi | Bsupraciliaris | Bschlegelii | Blateralis | 933 | 13 | 0.973 | 0.973 | 0.003 | 0 |
| Bmarchi | Bsupraciliaris | Bschlegelii | Bnigroviridis | 757 | 16 | 0.959 | 0.959 | 0.003 | 0 |
| Bmarchi | Bsupraciliaris | Bthalassinus | Blateralis | 95 | 258 | -0.462 | -0.462 | 0.093 | 0 |
| Bmarchi | Bsupraciliaris | Bthalassinus | Bnigroviridis | 16 | 432 | -0.929 | -0.929 | 0.005 | 0 |
| Bmarchi | Bsupraciliaris | Bthalassinus | Bschlegelii | 8 | 1170 | -0.986 | -0.986 | 0.002 | 0 |
| Bmarchi | Bthalassinus | Blateralis | Bnigroviridis | 29 | 47 | -0.237 | -0.237 | 0.141 | 0.093 |
| Bmarchi | Bthalassinus | Bnubestris | Blateralis | 38 | 36 | 0.027 | 0.027 | 0.091 | 0.765 |
| Bmarchi | Bthalassinus | Bnubestris | Bnigroviridis | 38 | 10 | 0.583 | 0.583 | 0.183 | 0.001 |
| Bmarchi | Bthalassinus | Bnubestris | Browleyi | 46 | 23 | 0.333 | 0.333 | 0.2 | 0.095 |
| Bmarchi | Bthalassinus | Bnubestris | Bschlegelii | 11 | 47 | -0.621 | -0.621 | 0.084 | 0 |
| Bmarchi | Bthalassinus | Bnubestris | Bsupraciliaris | 16 | 12 | 0.143 | 0.143 | 0.083 | 0.084 |
| Bmarchi | Bthalassinus | Browleyi | Blateralis | 22 | 23 | -0.022 | -0.022 | 0.088 | 0.801 |
| Bmarchi | Bthalassinus | Browleyi | Bnigroviridis | 33 | 36 | -0.043 | -0.043 | 0.145 | 0.764 |

| H1 | H2 | H3 | Out | Number ABBA | Number BABA | D | Z-score | SD D-statistic | P-value that D = 0 |
|---|---|---|---|---|---|---|---|---|---|
| Bmarchi | Bthalassinus | Browleyi | Bschlegelii | 25 | 71 | -0.479 | -0.479 | 0.152 | 0.002 |
| Bmarchi | Bthalassinus | Browleyi | Bsupraciliaris | 27 | 58 | -0.365 | -0.365 | 0.139 | 0.009 |
| Bmarchi | Bthalassinus | Bschlegelii | Blateralis | 27 | 16 | 0.256 | 0.256 | 0.106 | 0.016 |
| Bmarchi | Bthalassinus | Bschlegelii | Bnigroviridis | 67 | 18 | 0.576 | 0.576 | 0.127 | 0 |
| Bmarchi | Bthalassinus | Bsupraciliaris | Blateralis | 26 | 47 | -0.288 | -0.288 | 0.138 | 0.037 |
| Bmarchi | Bthalassinus | Bsupraciliaris | Bnigroviridis | 60 | 13 | 0.644 | 0.644 | 0.071 | 0 |
| Bmarchi | Bthalassinus | Bsupraciliaris | Bschlegelii | 7 | 6 | 0.077 | 0.077 | 0.153 | 0.614 |
| Bnubestris | Blateralis | Browleyi | Bnigroviridis | 424 | 60 | 0.752 | 0.752 | 0.048 | 0 |
| Bnubestris | Blateralis | Browleyi | Bschlegelii | 221 | 46 | 0.655 | 0.655 | 0.018 | 0 |
| Bnubestris | Blateralis | Browleyi | Bsupraciliaris | 243 | 58 | 0.615 | 0.615 | 0.035 | 0 |
| Bnubestris | Blateralis | Browleyi | Bthalassinus | 52 | 85 | -0.241 | -0.241 | 0.03 | 0 |
| Bnubestris | Blateralis | Bschlegelii | Bnigroviridis | 330 | 38 | 0.793 | 0.793 | 0.039 | 0 |
| Bnubestris | Blateralis | Bsupraciliaris | Bnigroviridis | 344 | 37 | 0.806 | 0.806 | 0.024 | 0 |
| Bnubestris | Blateralis | Bsupraciliaris | Bschlegelii | 17 | 24 | -0.171 | -0.171 | 0.055 | 0.002 |
| Bnubestris | Blateralis | Bsupraciliaris | Bthalassinus | 78 | 222 | -0.48 | -0.48 | 0.056 | 0 |
| Bnubestris | Blateralis | Bthalassinus | Bnigroviridis | 463 | 8 | 0.966 | 0.966 | 0.004 | 0 |
| Bnubestris | Blateralis | Bthalassinus | Bschlegelii | 215 | 40 | 0.686 | 0.686 | 0.02 | 0 |
| Bnubestris | Bnigroviridis | Browleyi | Blateralis | 54 | 16 | 0.543 | 0.543 | 0.147 | 0 |
| Bnubestris | Bnigroviridis | Browleyi | Bschlegelii | 43 | 32 | 0.147 | 0.147 | 0.115 | 0.203 |
| Bnubestris | Bnigroviridis | Browleyi | Bsupraciliaris | 31 | 24 | 0.127 | 0.127 | 0.054 | 0.017 |
| Bnubestris | Bnigroviridis | Browleyi | Bthalassinus | 11 | 48 | -0.627 | -0.627 | 0.085 | 0 |

| H1 | H2 | H3 | Out | Number ABBA | Number BABA | D | Z-score | SD D-statistic | P-value that D = 0 |
|---|---|---|---|---|---|---|---|---|---|
| Bnubestris | Bnigroviridis | Bschlegelii | Blateralis | 28 | 25 | 0.057 | 0.057 | 0.072 | 0.432 |
| Bnubestris | Bnigroviridis | Bsupraciliaris | Blateralis | 65 | 25 | 0.444 | 0.444 | 0.099 | 0 |
| Bnubestris | Bnigroviridis | Bsupraciliaris | Bschlegelii | 64 | 10 | 0.73 | 0.73 | 0.064 | 0 |
| Bnubestris | Bnigroviridis | Bsupraciliaris | Bthalassinus | 30 | 50 | -0.25 | -0.25 | 0.097 | 0.01 |
| Bnubestris | Bnigroviridis | Bthalassinus | Blateralis | 11 | 41 | -0.577 | -0.577 | 0.166 | 0 |
| Bnubestris | Bnigroviridis | Bthalassinus | Bschlegelii | 81 | 48 | 0.256 | 0.256 | 0.145 | 0.078 |
| Bnubestris | Browleyi | Blateralis | Bnigroviridis | 420 | 56 | 0.765 | 0.765 | 0.058 | 0 |
| Bnubestris | Browleyi | Bschlegelii | Blateralis | 72 | 174 | -0.415 | -0.415 | 0.059 | 0 |
| Bnubestris | Browleyi | Bschlegelii | Bnigroviridis | 352 | 41 | 0.791 | 0.791 | 0.036 | 0 |
| Bnubestris | Browleyi | Bsupraciliaris | Blateralis | 40 | 183 | -0.641 | -0.641 | 0.027 | 0 |
| Bnubestris | Browleyi | Bsupraciliaris | Bnigroviridis | 310 | 37 | 0.787 | 0.787 | 0.024 | 0 |
| Bnubestris | Browleyi | Bsupraciliaris | Bschlegelii | 42 | 20 | 0.355 | 0.355 | 0.218 | 0.103 |
| Bnubestris | Browleyi | Bsupraciliaris | Bthalassinus | 82 | 209 | -0.436 | -0.436 | 0.049 | 0 |
| Bnubestris | Browleyi | Bthalassinus | Blateralis | 54 | 42 | 0.125 | 0.125 | 0.045 | 0.006 |
| Bnubestris | Browleyi | Bthalassinus | Bnigroviridis | 435 | 49 | 0.798 | 0.798 | 0.052 | 0 |
| Bnubestris | Browleyi | Bthalassinus | Bschlegelii | 239 | 70 | 0.547 | 0.547 | 0.062 | 0 |
| Bnubestris | Bschlegelii | Blateralis | Bnigroviridis | 314 | 81 | 0.59 | 0.59 | 0.056 | 0 |
| Bnubestris | Bschlegelii | Browleyi | Blateralis | 41 | 76 | -0.299 | -0.299 | 0.064 | 0 |
| Bnubestris | Bschlegelii | Browleyi | Bnigroviridis | 334 | 27 | 0.85 | 0.85 | 0.009 | 0 |
| Bnubestris | Bschlegelii | Browleyi | Bsupraciliaris | 91 | 782 | -0.792 | -0.792 | 0.028 | 0 |
| Bnubestris | Bschlegelii | Browleyi | Bthalassinus | 71 | 64 | 0.052 | 0.052 | 0.138 | 0.706 |

| H1 | H2 | H3 | Out | Number ABBA | Number BABA | D | Z-score | SD D-statistic | P-value that D = 0 |
|---|---|---|---|---|---|---|---|---|---|
| Bnubestris | Bschlegelii | Bsupraciliaris | Blateralis | 752 | 39 | 0.901 | 0.901 | 0.021 | 0 |
| Bnubestris | Bschlegelii | Bsupraciliaris | Bnigroviridis | 1051 | 28 | 0.948 | 0.948 | 0.013 | 0 |
| Bnubestris | Bschlegelii | Bsupraciliaris | Bthalassinus | 801 | 40 | 0.905 | 0.905 | 0.019 | 0 |
| Bnubestris | Bschlegelii | Bthalassinus | Blateralis | 30 | 107 | -0.562 | -0.562 | 0.048 | 0 |
| Bnubestris | Bschlegelii | Bthalassinus | Bnigroviridis | 299 | 23 | 0.857 | 0.857 | 0.01 | 0 |
| Bnubestris | Bsupraciliaris | Blateralis | Bnigroviridis | 321 | 23 | 0.866 | 0.866 | 0.014 | 0 |
| Bnubestris | Bsupraciliaris | Browleyi | Blateralis | 44 | 45 | -0.011 | -0.011 | 0.075 | 0.881 |
| Bnubestris | Bsupraciliaris | Browleyi | Bnigroviridis | 321 | 30 | 0.829 | 0.829 | 0.015 | 0 |
| Bnubestris | Bsupraciliaris | Browleyi | Bschlegelii | 21 | 764 | -0.946 | -0.946 | 0.007 | 0 |
| Bnubestris | Bsupraciliaris | Browleyi | Bthalassinus | 105 | 34 | 0.511 | 0.511 | 0.06 | 0 |
| Bnubestris | Bsupraciliaris | Bschlegelii | Blateralis | 740 | 40 | 0.897 | 0.897 | 0.013 | 0 |
| Bnubestris | Bsupraciliaris | Bschlegelii | Bnigroviridis | 1008 | 55 | 0.897 | 0.897 | 0.023 | 0 |
| Bnubestris | Bsupraciliaris | Bthalassinus | Blateralis | 28 | 54 | -0.317 | -0.317 | 0.027 | 0 |
| Bnubestris | Bsupraciliaris | Bthalassinus | Bnigroviridis | 357 | 37 | 0.812 | 0.812 | 0.042 | 0 |
| Bnubestris | Bsupraciliaris | Bthalassinus | Bschlegelii | 25 | 765 | -0.937 | -0.937 | 0.01 | 0 |
| Bnubestris | Bthalassinus | Blateralis | Bnigroviridis | 468 | 20 | 0.918 | 0.918 | 0.02 | 0 |
| Bnubestris | Bthalassinus | Browleyi | Blateralis | 62 | 117 | -0.307 | -0.307 | 0.052 | 0 |
| Bnubestris | Bthalassinus | Browleyi | Bnigroviridis | 468 | 14 | 0.942 | 0.942 | 0.007 | 0 |
| Bnubestris | Bthalassinus | Browleyi | Bschlegelii | 191 | 42 | 0.639 | 0.639 | 0.045 | 0 |
| Bnubestris | Bthalassinus | Browleyi | Bsupraciliaris | 202 | 33 | 0.719 | 0.719 | 0.028 | 0 |
| Bnubestris | Bthalassinus | Bschlegelii | Blateralis | 43 | 210 | -0.66 | -0.66 | 0.037 | 0 |

| H1 | H2 | H3 | Out | Number ABBA | Number BABA | D | Z-score | SD D-statistic | P-value that D = 0 |
|---|---|---|---|---|---|---|---|---|---|
| Bnubestris | Bthalassinus | Bschlegelii | Bnigroviridis | 288 | 95 | 0.504 | 0.504 | 0.058 | 0 |
| Bnubestris | Bthalassinus | Bsupraciliaris | Blateralis | 31 | 253 | -0.782 | -0.782 | 0.026 | 0 |
| Bnubestris | Bthalassinus | Bsupraciliaris | Bnigroviridis | 286 | 50 | 0.702 | 0.702 | 0.035 | 0 |
| Bnubestris | Bthalassinus | Bsupraciliaris | Bschlegelii | 17 | 53 | -0.514 | -0.514 | 0.059 | 0 |
| Browleyi | Blateralis | Bschlegelii | Bnigroviridis | 37 | 33 | 0.057 | 0.057 | 0.069 | 0.408 |
| Browleyi | Blateralis | Bsupraciliaris | Bnigroviridis | 56 | 76 | -0.152 | -0.152 | 0.117 | 0.194 |
| Browleyi | Blateralis | Bsupraciliaris | Bschlegelii | 39 | 15 | 0.444 | 0.444 | 0.214 | 0.038 |
| Browleyi | Blateralis | Bsupraciliaris | Bthalassinus | 67 | 96 | -0.178 | -0.178 | 0.03 | 0 |
| Browleyi | Blateralis | Bthalassinus | Bnigroviridis | 82 | 67 | 0.101 | 0.101 | 0.027 | 0 |
| Browleyi | Blateralis | Bthalassinus | Bschlegelii | 93 | 60 | 0.216 | 0.216 | 0.027 | 0 |
| Browleyi | Bnigroviridis | Bschlegelii | Blateralis | 222 | 50 | 0.632 | 0.632 | 0.031 | 0 |
| Browleyi | Bnigroviridis | Bsupraciliaris | Blateralis | 177 | 58 | 0.506 | 0.506 | 0.027 | 0 |
| Browleyi | Bnigroviridis | Bsupraciliaris | Bschlegelii | 32 | 29 | 0.049 | 0.049 | 0.072 | 0.495 |
| Browleyi | Bnigroviridis | Bsupraciliaris | Bthalassinus | 194 | 76 | 0.437 | 0.437 | 0.078 | 0 |
| Browleyi | Bnigroviridis | Bthalassinus | Blateralis | 51 | 89 | -0.271 | -0.271 | 0.066 | 0 |
| Browleyi | Bnigroviridis | Bthalassinus | Bschlegelii | 85 | 207 | -0.418 | -0.418 | 0.038 | 0 |
| Browleyi | Bschlegelii | Blateralis | Bnigroviridis | 39 | 166 | -0.62 | -0.62 | 0.03 | 0 |
| Browleyi | Bschlegelii | Bsupraciliaris | Blateralis | 880 | 23 | 0.949 | 0.949 | 0.005 | 0 |
| Browleyi | Bschlegelii | Bsupraciliaris | Bnigroviridis | 751 | 16 | 0.958 | 0.958 | 0.004 | 0 |
| Browleyi | Bschlegelii | Bsupraciliaris | Bthalassinus | 913 | 17 | 0.963 | 0.963 | 0.004 | 0 |
| Browleyi | Bschlegelii | Bthalassinus | Blateralis | 31 | 102 | -0.534 | -0.534 | 0.044 | 0 |

| H1 | H2 | H3 | Out | Number ABBA | Number BABA | D | Z-score | SD D-statistic | P-value that D = 0 |
|---|---|---|---|---|---|---|---|---|---|
| Browleyi | Bschlegelii | Bthalassinus | Bnigroviridis | 44 | 182 | -0.611 | -0.611 | 0.063 | 0 |
| Browleyi | Bsupraciliaris | Blateralis | Bnigroviridis | 43 | 179 | -0.613 | -0.613 | 0.034 | 0 |
| Browleyi | Bsupraciliaris | Bschlegelii | Blateralis | 950 | 40 | 0.919 | 0.919 | 0.023 | 0 |
| Browleyi | Bsupraciliaris | Bschlegelii | Bnigroviridis | 792 | 62 | 0.855 | 0.855 | 0.03 | 0 |
| Browleyi | Bsupraciliaris | Bthalassinus | Blateralis | 40 | 81 | -0.339 | -0.339 | 0.03 | 0 |
| Browleyi | Bsupraciliaris | Bthalassinus | Bnigroviridis | 33 | 194 | -0.709 | -0.709 | 0.031 | 0 |
| Browleyi | Bsupraciliaris | Bthalassinus | Bschlegelii | 70 | 903 | -0.856 | -0.856 | 0.028 | 0 |
| Browleyi | Bthalassinus | Blateralis | Bnigroviridis | 129 | 44 | 0.491 | 0.491 | 0.046 | 0 |
| Browleyi | Bthalassinus | Bschlegelii | Blateralis | 115 | 86 | 0.144 | 0.144 | 0.085 | 0.088 |
| Browleyi | Bthalassinus | Bschlegelii | Bnigroviridis | 66 | 52 | 0.119 | 0.119 | 0.088 | 0.18 |
| Browleyi | Bthalassinus | Bsupraciliaris | Blateralis | 79 | 86 | -0.042 | -0.042 | 0.107 | 0.692 |
| Browleyi | Bthalassinus | Bsupraciliaris | Bnigroviridis | 42 | 64 | -0.208 | -0.208 | 0.072 | 0.004 |
| Browleyi | Bthalassinus | Bsupraciliaris | Bschlegelii | 10 | 100 | -0.818 | -0.818 | 0.029 | 0 |
| Bsupraciliaris | Blateralis | Bschlegelii | Bnigroviridis | 19 | 741 | -0.95 | -0.95 | 0.003 | 0 |
| Bsupraciliaris | Blateralis | Bthalassinus | Bnigroviridis | 228 | 28 | 0.781 | 0.781 | 0.018 | 0 |
| Bsupraciliaris | Blateralis | Bthalassinus | Bschlegelii | 920 | 7 | 0.985 | 0.985 | 0.003 | 0 |
| Bsupraciliaris | Bnigroviridis | Bschlegelii | Blateralis | 50 | 759 | -0.876 | -0.876 | 0.017 | 0 |
| Bsupraciliaris | Bnigroviridis | Bthalassinus | Blateralis | 64 | 22 | 0.488 | 0.488 | 0.094 | 0 |
| Bsupraciliaris | Bnigroviridis | Bthalassinus | Bschlegelii | 784 | 13 | 0.967 | 0.967 | 0.004 | 0 |
| Bsupraciliaris | Bschlegelii | Blateralis | Bnigroviridis | 29 | 30 | -0.017 | -0.017 | 0.144 | 0.906 |
| Bsupraciliaris | Bschlegelii | Bthalassinus | Blateralis | 14 | 10 | 0.167 | 0.167 | 0.067 | 0.013 |

| H1 | H2 | H3 | Out | Number ABBA | Number BABA | D | Z-score | SD D-statistic | P-value that D = 0 |
|---|---|---|---|---|---|---|---|---|---|
| Bsupraciliaris | Bschlegelii | Bthalassinus | Bnigroviridis | 34 | 13 | 0.447 | 0.447 | 0.1 | 0 |
| Bsupraciliaris | Bthalassinus | Blateralis | Bnigroviridis | 218 | 64 | 0.546 | 0.546 | 0.057 | 0 |
| Bsupraciliaris | Bthalassinus | Bschlegelii | Blateralis | 32 | 930 | -0.933 | -0.933 | 0.013 | 0 |
| Bsupraciliaris | Bthalassinus | Bschlegelii | Bnigroviridis | 74 | 776 | -0.826 | -0.826 | 0.022 | 0 |
| Bthalassinus | Blateralis | Bschlegelii | Bnigroviridis | 48 | 59 | -0.103 | -0.103 | 0.148 | 0.487 |
| Bthalassinus | Bnigroviridis | Bschlegelii | Blateralis | 235 | 72 | 0.531 | 0.531 | 0.038 | 0 |
| Bthalassinus | Bschlegelii | Blateralis | Bnigroviridis | 91 | 233 | -0.438 | -0.438 | 0.08 | 0 |

## A.7 Supplementary discussion of differences in the performance of reticulation tests



Among the three approaches used here for reticulate analyses, each had their own strengths and weakness. The speed, computational efficiency, and reproducibility of TreeMix's algorithmic approach is an attractive advantage of this method. However, its basis in allele frequencies and theoretical basis in inferring migration among populations may make it less appropriate for phylogenomic datasets with hundreds rather than thousands of independent loci. In contrast, the network-based approaches of PhyloNet and SNaQ, which explicitly account for ILS and reticulation can use many types of input, but at a high computational cost. These costs were especially apparent in our PhyloNet analyses, where memory limitations prohibited inference of networks with more than two reticulations. Moreover, the "best networks" recovered from PhyloNet were highly variable, indicating that robust network estimate in PhyloNet may require a very high number of searches. SNaQ's more restrictive search allowed it to reach network convergence much more quickly, albeit still requiring at least 100 searches. In fact, the number of searches necessary for resolving our dataset generally exceeded program defaults and those used by other published studies (Burbrink and Gehara, 2018; Grummer et al., 2018; Thom et al., 2018) underscoring the singular nature of analytical requirements for different datasets.

# Appendix B Supplemental Figures for Chapter 3: Trait differentiation and modular toxin expression in palm-pitvipers

## B.1 Module Assignment

Table B.1: Module assignment for orthologous transcripts from *Bothriechis nigroviridis* and *B. nubestris* passing VST transformation and filtering by CEMiTool.

| Module | *Bnubestris* genes | *Bnigroviridis* genes |
|---|---|---|
| M1 | Bnubes-BPP-1 | Bnigro-BPP-1 |
| M1 | Bnubes-GRP78 | Bnigro-GRP78 |
| M1 | Bnubes-Parvalbumin | Bnigro-Parvalbumin |
| M1 | Bnubes-Galectin1 | Bnigro-Galectin1 |
| M1 | Bnubes-MyosinLight | Bnigro-MyosinLight |
| M1 | Bnubes-Endoplasmin | Bnigro-Endoplasmin |
| M1 | Bnubes-PDI-A4 | Bnigro-PDI-A4 |
| M1 | Bnubes-Peroxiredoxin6 | Bnigro-Peroxiredoxin6 |
| M1 | Bnubes-CreatineKin | Bnigro-CreatineKin |
| M1 | Bnubes-Actin-a | Bnigro-Actin-a |
| M1 | Bnubes-TroponinC | Bnigro-TroponinC |
| M1 | Bnubes-TF-LIM-LMO4 | Bnigro-TF-LIM-LMO4 |
| M1 | Bnubes-Calglandulin | Bnigro-Calglandulin |
| M1 | Bnubes-Calmod | Bnigro-Calmod |
| M1 | Bnubes-TropI | Bnigro-TropI |
| M1 | Bnubes-AdenylosuccinateLyase | Bnigro-AdenylosuccinateLyase |
| M1 | Bnubes-Rab-18 | Bnigro-Rab-18 |
| M1 | Bnubes-TIF-1b | Bnigro-TIF-1b |
| M1 | Bnubes-PepMethSulfRed | Bnigro-PepMethSulfRed |
| M1 | Bnubes-SC35B1 | Bnigro-SC35B1 |

| Module | *Bnubestris* genes | *Bnigroviridis* genes |
|---|---|---|
| M2 | Bnubes-SVMPIII-5 | Bnigro-SVMPIII-5 |
| M2 | Bnubes-CTL-1 | Bnigro-CTL-1 |
| M2 | Bnubes-SVMPIII-3 | Bnigro-SVMPIII-3 |
| M2 | Bnubes-SVSP-1 | Bnigro-SVSP-1 |
| M2 | Bnubes-SVSP-8 | Bnigro-SVSP-8 |
| M2 | Bnubes-SVMPII-1 | Bnigro-SVMPII-1 |
| M2 | Bnubes-LAAO-1 | Bnigro-LAAO-1 |
| M2 | Bnubes-SVMPII-2 | Bnigro-SVMPII-2 |
| M2 | Bnubes-SVMPIII-2 | Bnigro-SVMPIII-2 |
| M2 | Bnubes-SVSP-7 | Bnigro-SVSP-7 |
| M2 | Bnubes-ErythMem | Bnigro-ErythMem |
| M2 | Bnubes-d3PGDH | Bnigro-d3PGDH |
| M2 | Bnubes-HYAL-1 | Bnigro-HYAL-1 |
| M2 | Bnubes-SPARC | Bnigro-SPARC |
| M2 | Bnubes-TIF-4E1 | Bnigro-TIF-4E1 |
| M2 | Bnubes-ATOX1 | Bnigro-ATOX1 |
| M2 | Bnubes-EpididymalSecretory-E1 | Bnigro-EpididymalSecretory-E1 |
| M3 | Bnubes-PLA2-2 | Bnigro-PLA2-2 |
| M3 | Bnubes-PLA2-1 | Bnigro-PLA2-1 |
| M3 | Bnubes-NGF-1 | Bnigro-NGF-1 |
| M3 | Bnubes-SVSP-5 | Bnigro-SVSP-5 |
| M3 | Bnubes-GST-t1 | Bnigro-GST-t1 |
| M3 | Bnubes-poly-rC-2 | Bnigro-Vigilin-1 |
| M3 | Bnubes-Translocator | Bnigro-Translocator |
| M3 | Bnubes-SuperoxideDismutase | Bnigro-SuperoxideDismutase |
| M3 | Bnubes-NucGTP1 | Bnigro-NucGTP1 |
| M3 | Bnubes-GlutamineSyn | Bnigro-GlutamineSyn |
| M3 | Bnubes-MatrixGla | Bnigro-MatrixGla |
| M3 | Bnubes-Tetraspanin31 | Bnigro-Tetraspanin31 |

| Module | *Bnubestris* genes | *Bnigroviridis* genes |
|---|---|---|
| M3 | Bnubes-Leydig | Bnigro-Leydig |
| M3 | Bnubes-RAB11a-2 | Bnigro-RAB11a-2 |
| M3 | Bnubes-AffCuUp2 | Bnigro-AffCuUp2 |
| M3 | Bnubes-selenoproteinU | Bnigro-selenoproteinU |
| M4 | Bnubes-SVSP-4 | Bnigro-SVSP-4 |
| M4 | Bnubes-VEGF-1 | Bnigro-VEGF-1 |
| M4 | Bnubes-SVMPII-3 | Bnigro-SVMPII-3 |
| M4 | Bnubes-Actin2 | Bnigro-Actin2 |
| M4 | Bnubes-CREGF | Bnigro-CREGF |
| M4 | Bnubes-OrnithinAminoTrans | Bnigro-OrnithinAminoTrans |
| M4 | Bnubes-tom5 | Bnigro-tom5$_{t}rinContig$36585 |
| M4 | Bnubes-Tetraspanin13$_{t}rinContig$2931 | Bnigro-Tetraspanin13 |
| M4 | Bnubes-IPDPDIsomerase | Bnigro-IPDPDIsomerase |
| M4 | Bnubes-Bifunctional-PURH | Bnigro-Bifunctional-PURH |
| M4 | Bnubes-C19orf60 | Bnigro-C19orf60 |
| M4 | Bnubes-DehydrocholesterolRed | Bnigro-DehydrocholesterolRed |
| M5 | Bnubes-Plasminogen | Bnigro-Plasminogen |
| M5 | Bnubes-LOC100329601 | Bnigro-LOC100329601 |
| M5 | Bnubes-HypPro1 | Bnigro-HypPro1 |
| M5 | Bnubes-AminopeptidaseA | Bnigro-AminopeptidaseA |
| M5 | Bnubes-FAM3D | Bnigro-FAM3D |
| M5 | Bnubes-Reticulocalbin1 | Bnigro-Reticulocalbin1 |
| M5 | Bnubes-Thiolase | Bnigro-Thiolase |
| M5 | Bnubes-GILT | Bnigro-GILT |
| M5 | Bnubes-SVMPIII-1 | Bnigro-SVMPIII-1 |
| M6 | Bnubes-CTL-2 | Bnigro-CTL-2 |
| M6 | Bnubes-MannosidaseIB | Bnigro-MannosidaseIB |
| M6 | Bnubes-MCFD2 | Bnigro-MCFD2 |
| M6 | Bnubes-CytC | Bnigro-CytC |

| Module | *Bnubestris* genes | *Bnigroviridis* genes |
|---|---|---|
| M6 | Bnubes-VEGF-3 | Bnigro-VEGF-3 |
| M6 | Bnubes-FKBP7 | Bnigro-FKBP7 |
| M6 | Bnubes-Neurocalcin-d | Bnigro-Neurocalcin-d |
| M6 | Bnubes-mRpL55 | Bnigro-mRpL55 |
| M6 | Bnubes-InsulinInd1 | Bnigro-InsulinInd1 |

## B.2 OrthoFinder phylogenies

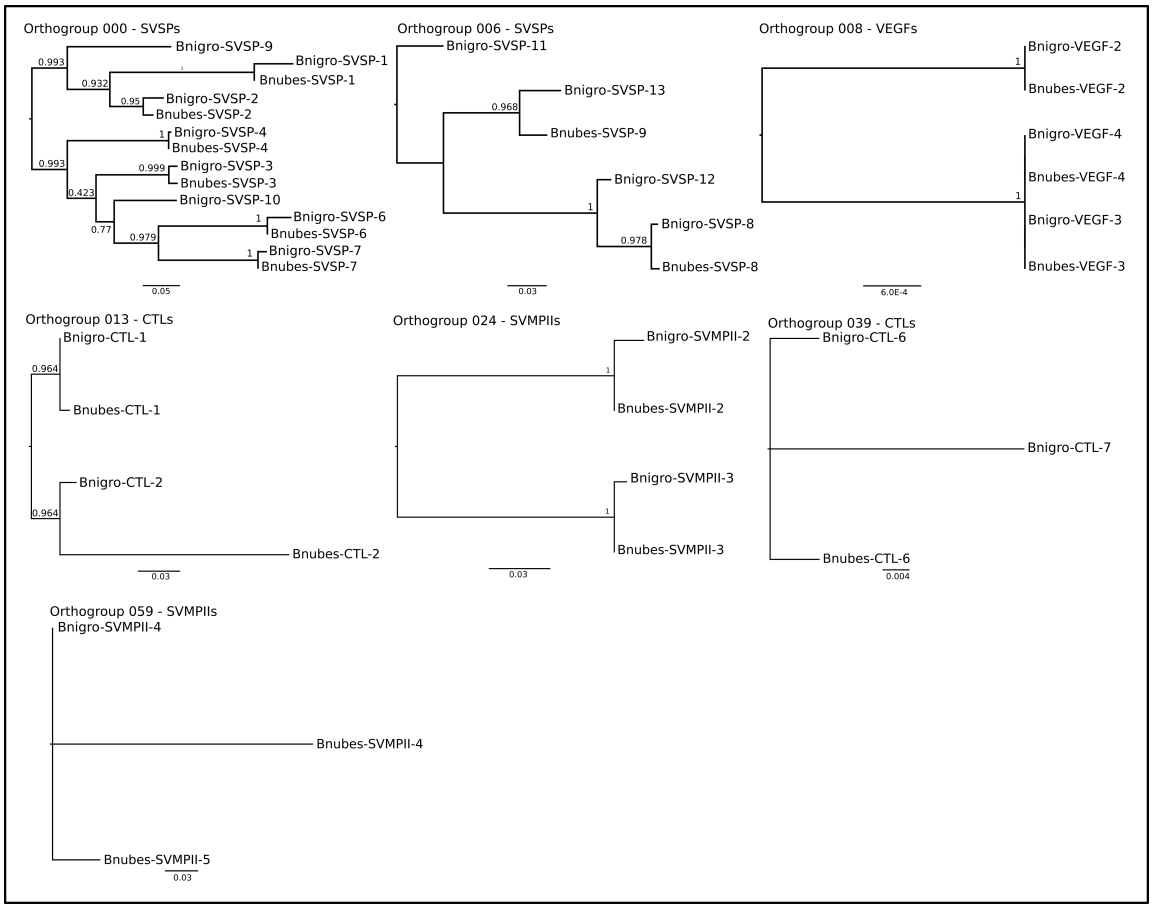


Figure B.1: Toxin orthogroup trees inferred by OrthoFinder from amino acid sequences of *Bothriechis nigroviridis* and *B. nubestris* transcripts

# Appendix C Supplemental Figures for Chapter 4: Evolution of gene expression in snake toxin families

| Species | Specimen ID | Museum ID | SRR | Locality | Country |
|---|---|---|---|---|---|
| *Bothriechis aurifer* | CLP2481 | CHFCB-0416 | TBD | "Santiago Gualatao, Chiapas" | Mexico |
| *Bothriechis aurifer* | CRVA3759 | TBD | TBD | "Biotopo de Quetzal, Baja Verapaz" | Guatemala |
| *Bothriechis bicolor* | CLP2365 | CHFCB-0277 | TBD | "Chiquihuites, Chiapas" | Mexico |
| *Bothriechis guifarroi* | CLP2537 | FLMNH-190202 | TBD | "Pico Pijol, Yoro" | Honduras |
| *Bothriechis guifarroi* | CLP2613 | FLMNH-190224 | TBD | "Reserva Texiguat, Atlantida" | Honduras |
| *Bothriechis lateralis* | CLP1858 | MZUCR-23266 | TBD | "Orosi, Cartago" | Costa Rica |
| *Bothriechis lateralis* | LIAP0080 | MZUCR-23274 | TBD | "Palmichal de Acosta, Despamparados, San José" | Costa Rica |
| *Bothriechis marchi* | CLP2545 | FLMNH-190206 | TBD | "El Merendon, Cortés" | Honduras |
| *Bothriechis marchi* | CLP2565 | FLMNH-190213 | TBD | "El Merendon, Cortés" | Honduras |
| *Bothriechis nigroviridis* | CLP1856 | MZUCR-23264 | TBD | "Sitio Las Tablas, Puntarenas" | Costa Rica |
| *Bothriechis nigroviridis* | CLP1864 | MZUCR-23270 | TBD | "La Esperanza, Cartago" | Costa Rica |
| *Bothriechis nubestris* | CLP1859 | MZUCR-23267 | TBD | "San Gerado de Dota, San José" | Costa Rica |
| *Bothriechis nubestris* | CLP1865 | MZUCR-23271 | TBD | "San Gerado de Dota, San José" | Costa Rica |
| *Bothriechis rowleyi* | CLP2475 | CHFCB-0410 | TBD | "Selva Negra, Chiapas" | Mexico |
| *Bothriechis rowleyi* | CLP2482 | CHFCB-0417 | TBD | "Selva Negra, Chiapas" | Mexico |
| *Bothriechis schlegelii* | LIAP068 | MZUCR-23274 | TBD | "Buena Vista, Cartago" | Costa Rica |
| *Bothriechis schlegelii* | CLP2568 | FLMNH-90216 | TBD | "Pico Bonito, Atlántida" | Honduras |
| *Bothriechis supraciliaris* | CLP1855 | MZUCR-23263 | TBD | Las Cruces. Puntarenas | Costa Rica |
| *Bothriechis supraciliaris* | CLP1857 | MZUCR-23265 | TBD | Las Cruces. Puntarenas | Costa Rica |
| *Bothriechis thalassinus* | CRVA3763 | TBD | TBD | "Union Zacapa, Zacapa" | Guatemala |
| *Bothriechis thalassinus* | CRVA3764 | TBD | TBD | "Union Zacapa, Zacapa" | Guatemala |

Table C.1: Specimen information for *Bothriechis* individuals used in transcriptome assembly and expression analyses

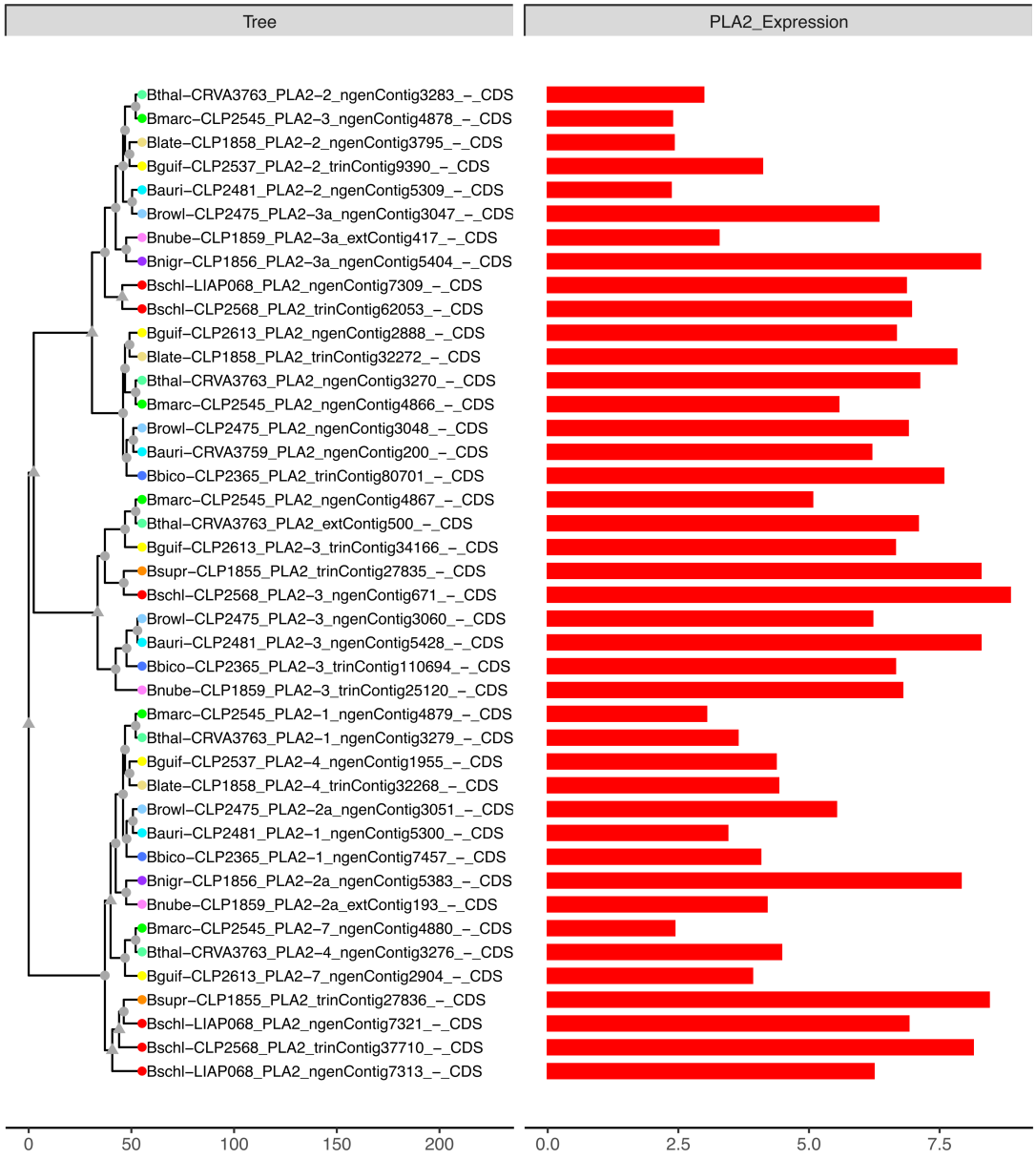


Figure C.1: Gene specific toxin expression of $PLA_2$s in centered log-ratio transformed TPM. Terminal colors correspond to tip labels in Fig. 4.1A. Node shapes indicate whether divergence was the result of a gene duplication (triangle) or speciation (circle) event.

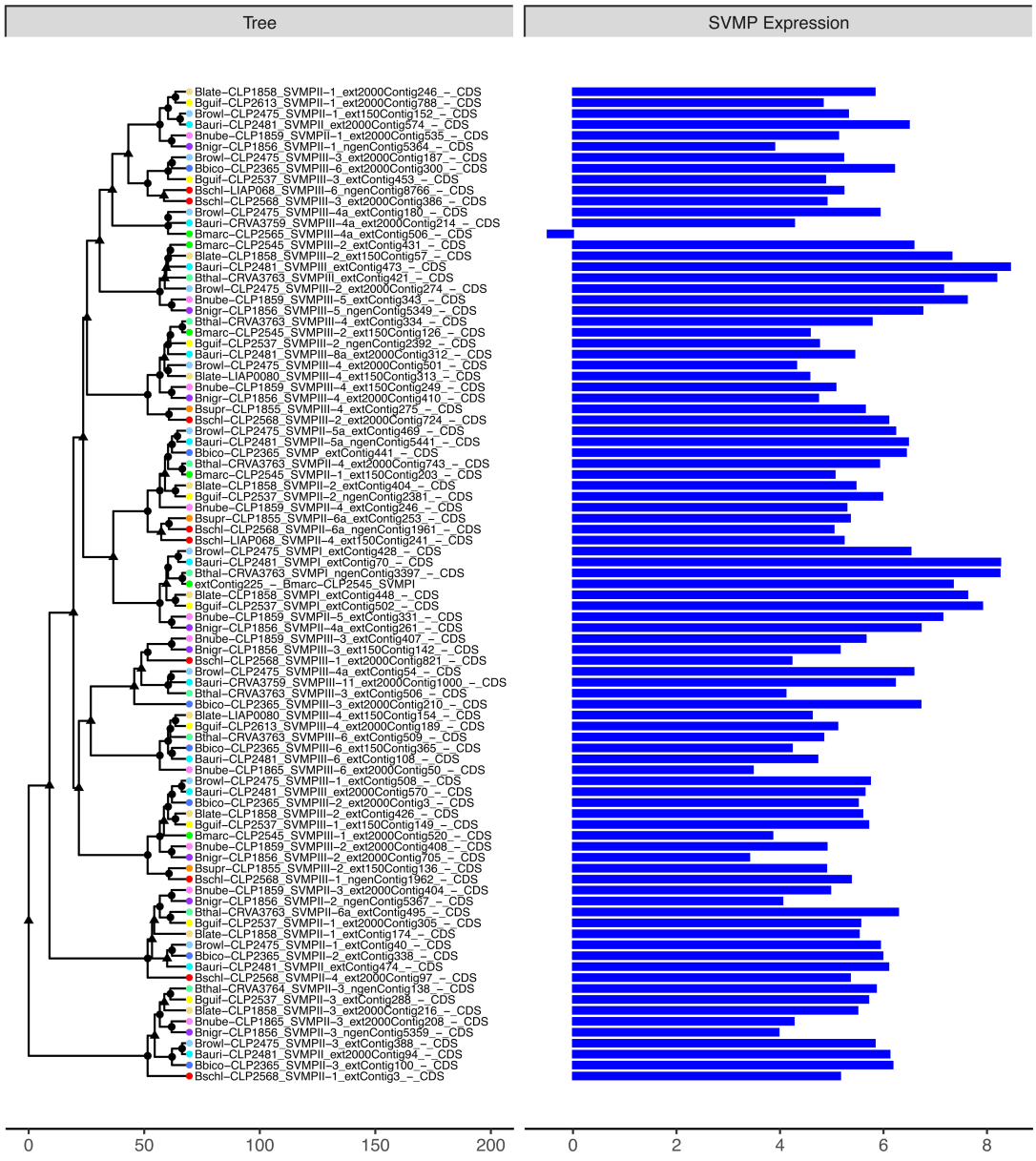


Figure C.2: Gene specific toxin expression of SVMPs in centered log-ratio transformed TPM (negative values indicate expression below the geometric mean of transcript expression). Terminal colors correspond to tip labels in Fig. 4.1A. Node shapes indicate whether divergence was the result of a gene duplication (triangle) or speciation (circle) event.

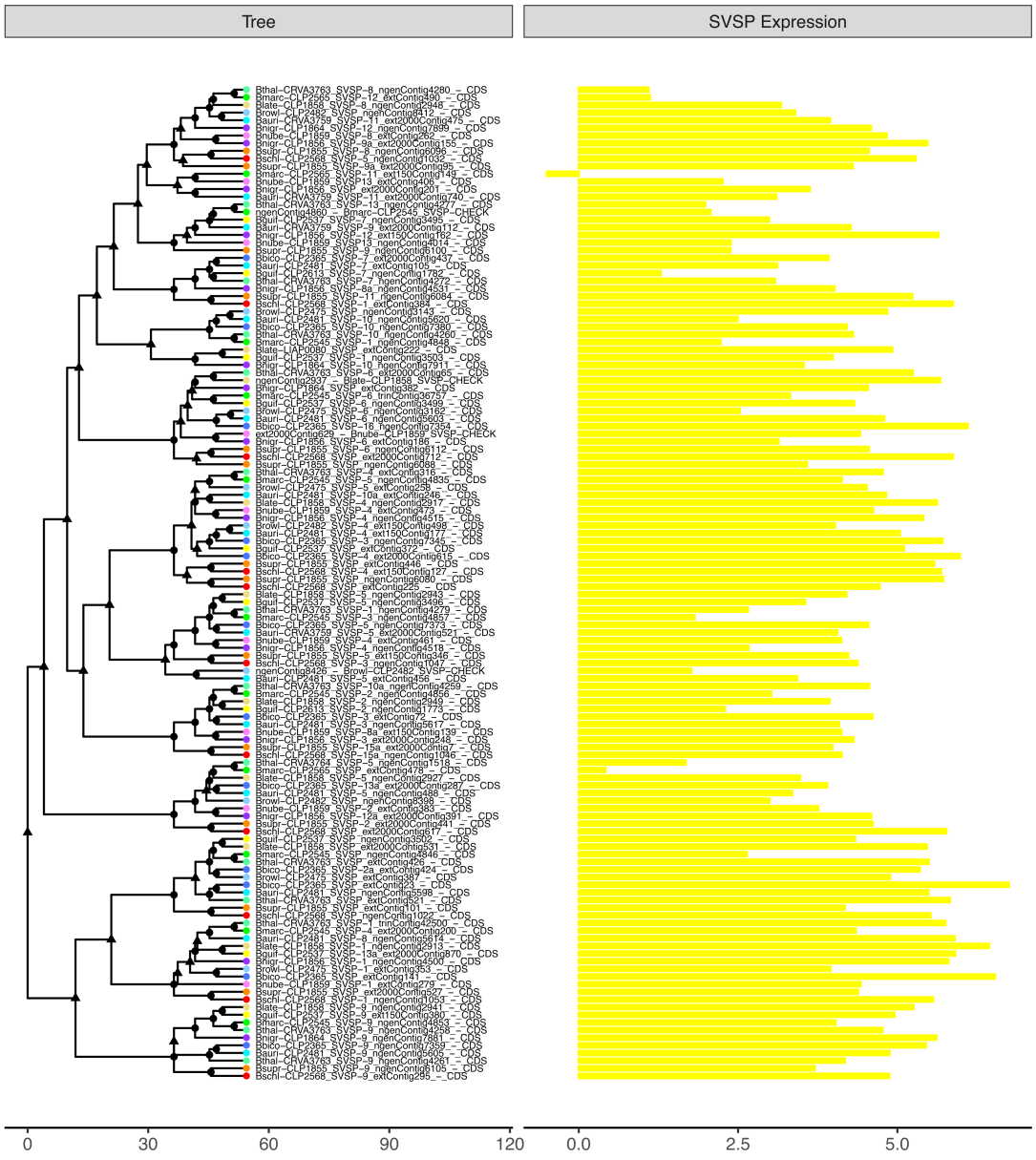


Figure C.3: Gene specific toxin expression of SVSPs in centered log-ratio transformed TPM (negative values indicate expression below the geometric mean of transcript expression). Terminal colors correspond to tip labels in Fig. 4.1A. Node shapes indicate whether divergence was the result of a gene duplication (triangle) or speciation (circle) event.

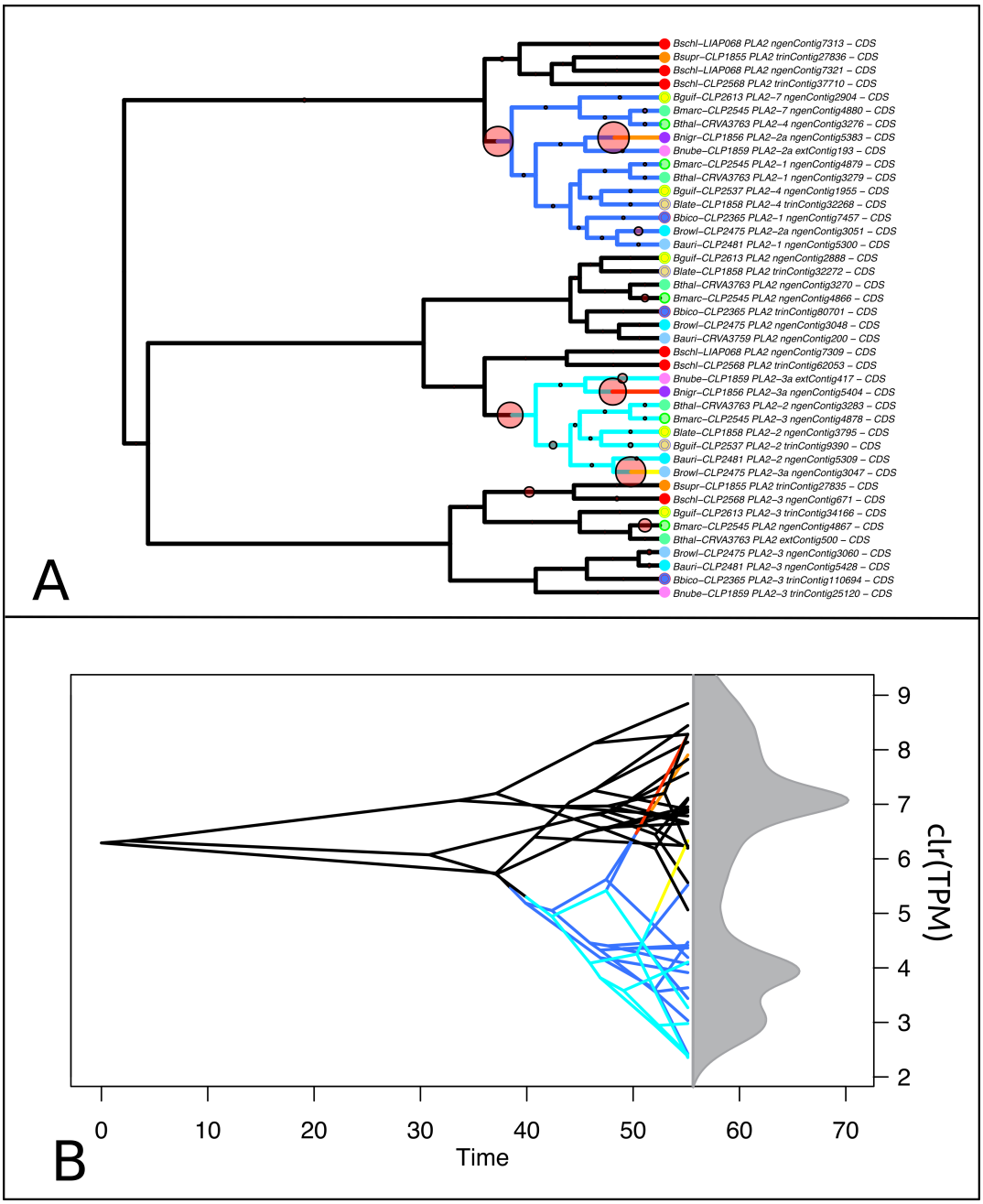


Figure C.4: $PLA_2$ gene family phylogeny (A) and density-phenograms (B) displaying evolutionary regimes and phenotypic variation identified with bayou. Lineage colors denote unique evolutionary regimes and correspond between phylogenies and phenograms. Red circles on phylogenies denote identified rate shifts with circle size corresponding to posterior probability of a shift occurring. Grey distributions to the right of phenograms show density of phenotypes.

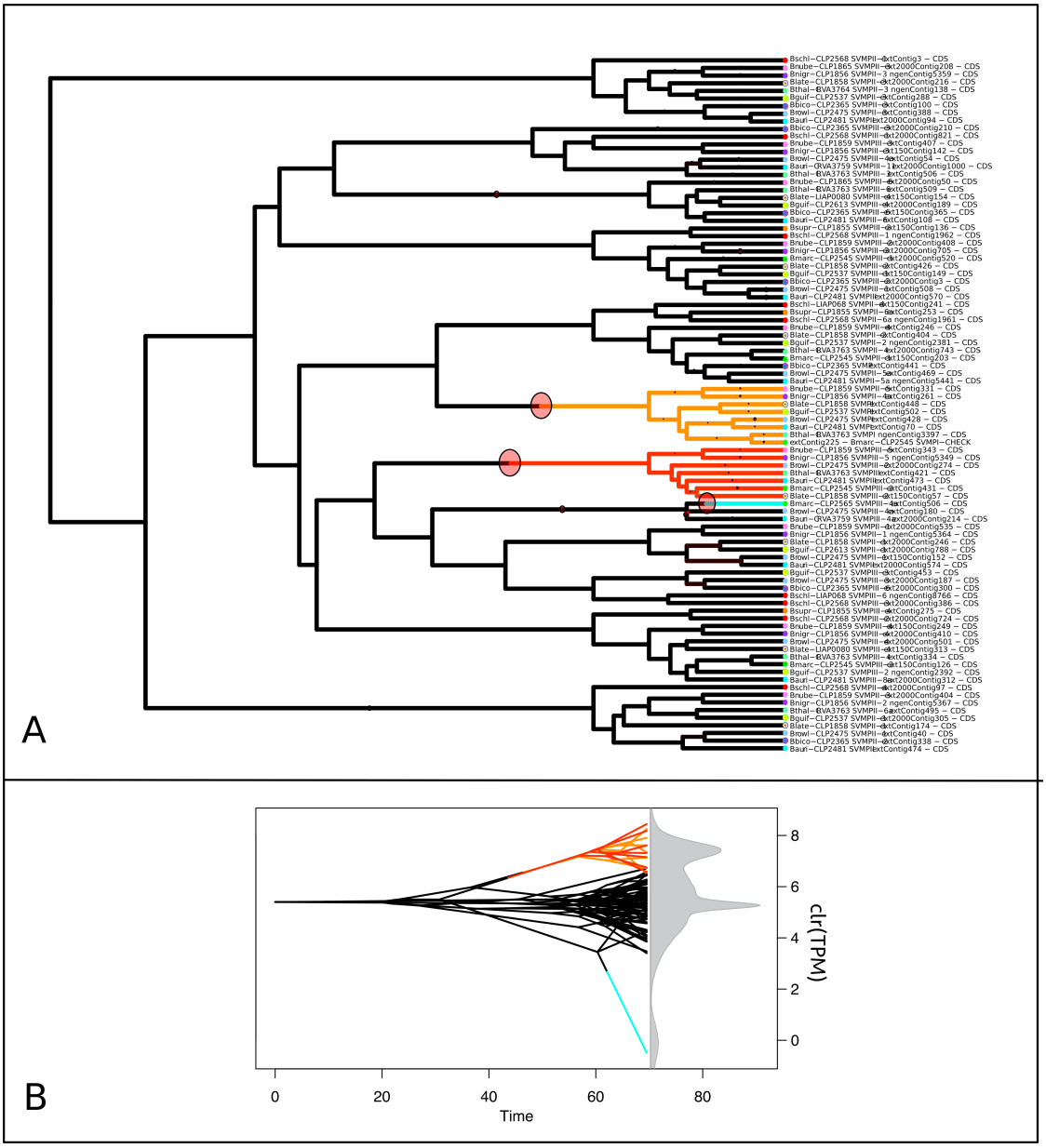


Figure C.5: SVMP gene family phylogeny (A) and density-phenograms (B) displaying evolutionary regimes and phenotypic variation identified with bayou. Lineage colors denote unique evolutionary regimes and correspond between phylogenies and phenograms. Red circles on phylogenies denote identified rate shifts with circle size corresponding to posterior probability of a shift occurring. Grey distributions to the right of phenograms show density of phenotypes.

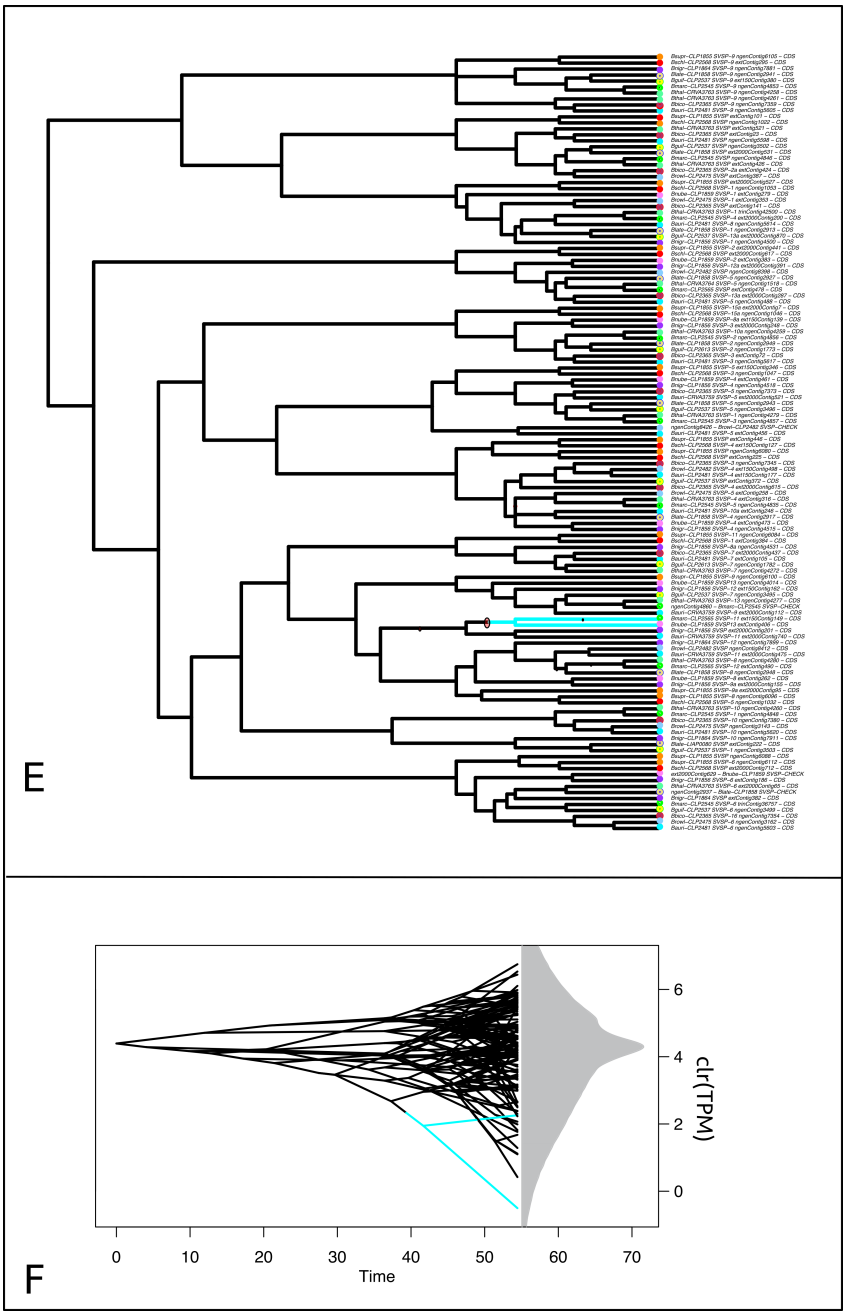


Figure C.6: SVSP gene family phylogeny (A) and density-phenograms (B) displaying evolutionary regimes and phenotypic variation identified with bayou. Lineage colors denote unique evolutionary regimes and correspond between phylogenies and phenograms. Red circles on phylogenies denote identified rate shifts with circle size corresponding to posterior probability of a shift occurring. Grey distributions to the right of phenograms show density of phenotypes.

# Appendix D John Wiley and Sons License Terms and Conditions

# JOHN WILEY AND SONS LICENSE TERMS AND CONDITIONS

Apr 08, 2020

This Agreement between Andrew Mason ("You") and John Wiley and Sons ("John Wiley and Sons") consists of your license details and the terms and conditions provided by John Wiley and Sons and Copyright Clearance Center.

| | |
|---|---|
| License Number | 4804430320738 |
| License date | Apr 08, 2020 |
| Licensed Content Publisher | John Wiley and Sons |
| Licensed Content Publication | Journal of Biogeography |
| Licensed Content Title | Reticulate evolution in nuclear Middle America causes discordance in the phylogeny of palm-pitvipers (Viperidae: Bothriechis) |
| Licensed Content Author | Andrew J. Mason, Felipe G. Grazziotin, Hussam Zaher, et al |
| Licensed Content Date | Mar 19, 2019 |
| Licensed Content Volume | 46 |
| Licensed Content Issue | 5 |
| Licensed Content Pages | 12 |
| Type of Use | Dissertation/Thesis |
| Requestor type | Author of this Wiley article |
| Format | Print and electronic |
| Portion | Full article |
| Will you be translating? | No |
| Title | Patterns and Processes of Speciation and Phenotypic Diversification in Palm-Pitvipers |
| Institution name | Clemson University |
| Expected presentation date | May 2020 |
| Requestor Location | Andrew Mason<br>57 Greenleaf Ct.<br><br>SENECA, SC 29678<br>United States<br>Attn: Andrew Mason |
| Publisher Tax ID | EU826007151 |
| Total | **0.00 USD** |
| Terms and Conditions | |

**TERMS AND CONDITIONS**

This copyrighted material is owned by or exclusively licensed to John Wiley & Sons, Inc. or one of its group companies (each a"Wiley Company") or handled on behalf of a society with which a Wiley Company has exclusive publishing rights in relation to a particular work (collectively "WILEY"). By clicking "accept" in connection with completing this licensing transaction, you agree that the following terms and conditions apply to this transaction (along with the billing and payment terms and conditions established by the Copyright Clearance Center Inc., ("CCC's Billing and Payment terms and conditions"), at the time that you opened your RightsLink account (these are available at any time at http://myaccount.copyright.com).

**Terms and Conditions**

- The materials you have requested permission to reproduce or reuse (the "Wiley Materials") are protected by copyright.
- You are hereby granted a personal, non-exclusive, non-sub licensable (on a stand-alone basis), non-transferable, worldwide, limited license to reproduce the Wiley Materials for the purpose specified in the licensing process. This license, **and any**

**CONTENT (PDF or image file) purchased as part of your order,** is for a one-time use only and limited to any maximum distribution number specified in the license. The first instance of republication or reuse granted by this license must be completed within two years of the date of the grant of this license (although copies prepared before the end date may be distributed thereafter). The Wiley Materials shall not be used in any other manner or for any other purpose, beyond what is granted in the license. Permission is granted subject to an appropriate acknowledgement given to the author, title of the material/book/journal and the publisher. You shall also duplicate the copyright notice that appears in the Wiley publication in your use of the Wiley Material. Permission is also granted on the understanding that nowhere in the text is a previously published source acknowledged for all or part of this Wiley Material. Any third party content is expressly excluded from this permission.

- With respect to the Wiley Materials, all rights are reserved. Except as expressly granted by the terms of the license, no part of the Wiley Materials may be copied, modified, adapted (except for minor reformatting required by the new Publication), translated, reproduced, transferred or distributed, in any form or by any means, and no derivative works may be made based on the Wiley Materials without the prior permission of the respective copyright owner.**For STM Signatory Publishers clearing permission under the terms of the STM Permissions Guidelines only, the terms of the license are extended to include subsequent editions and for editions in other languages, provided such editions are for the work as a whole in situ and does not involve the separate exploitation of the permitted figures or extracts,** You may not alter, remove or suppress in any manner any copyright, trademark or other notices displayed by the Wiley Materials. You may not license, rent, sell, loan, lease, pledge, offer as security, transfer or assign the Wiley Materials on a stand-alone basis, or any of the rights granted to you hereunder to any other person.

- The Wiley Materials and all of the intellectual property rights therein shall at all times remain the exclusive property of John Wiley & Sons Inc, the Wiley Companies, or their respective licensors, and your interest therein is only that of having possession of and the right to reproduce the Wiley Materials pursuant to Section 2 herein during the continuance of this Agreement. You agree that you own no right, title or interest in or to the Wiley Materials or any of the intellectual property rights therein. You shall have no rights hereunder other than the license as provided for above in Section 2. No right, license or interest to any trademark, trade name, service mark or other branding ("Marks") of WILEY or its licensors is granted hereunder, and you agree that you shall not assert any such right, license or interest with respect thereto

- NEITHER WILEY NOR ITS LICENSORS MAKES ANY WARRANTY OR REPRESENTATION OF ANY KIND TO YOU OR ANY THIRD PARTY, EXPRESS, IMPLIED OR STATUTORY, WITH RESPECT TO THE MATERIALS OR THE ACCURACY OF ANY INFORMATION CONTAINED IN THE MATERIALS, INCLUDING, WITHOUT LIMITATION, ANY IMPLIED WARRANTY OF MERCHANTABILITY, ACCURACY, SATISFACTORY QUALITY, FITNESS FOR A PARTICULAR PURPOSE, USABILITY, INTEGRATION OR NON-INFRINGEMENT AND ALL SUCH WARRANTIES ARE HEREBY EXCLUDED BY WILEY AND ITS LICENSORS AND WAIVED BY YOU.

- WILEY shall have the right to terminate this Agreement immediately upon breach of this Agreement by you.

- You shall indemnify, defend and hold harmless WILEY, its Licensors and their respective directors, officers, agents and employees, from and against any actual or threatened claims, demands, causes of action or proceedings arising from any breach of this Agreement by you.

- IN NO EVENT SHALL WILEY OR ITS LICENSORS BE LIABLE TO YOU OR ANY OTHER PARTY OR ANY OTHER PERSON OR ENTITY FOR ANY SPECIAL, CONSEQUENTIAL, INCIDENTAL, INDIRECT, EXEMPLARY OR PUNITIVE DAMAGES, HOWEVER CAUSED, ARISING OUT OF OR IN CONNECTION WITH THE DOWNLOADING, PROVISIONING, VIEWING OR USE OF THE MATERIALS REGARDLESS OF THE FORM OF ACTION, WHETHER FOR BREACH OF CONTRACT, BREACH OF WARRANTY, TORT, NEGLIGENCE, INFRINGEMENT OR OTHERWISE (INCLUDING, WITHOUT LIMITATION, DAMAGES BASED ON LOSS OF PROFITS, DATA, FILES, USE, BUSINESS OPPORTUNITY OR CLAIMS OF THIRD PARTIES), AND WHETHER OR NOT THE PARTY HAS BEEN ADVISED OF THE POSSIBILITY OF SUCH DAMAGES. THIS LIMITATION SHALL APPLY NOTWITHSTANDING ANY FAILURE OF ESSENTIAL PURPOSE OF ANY LIMITED REMEDY PROVIDED HEREIN.

- Should any provision of this Agreement be held by a court of competent jurisdiction to be illegal, invalid, or unenforceable, that provision shall be deemed amended to achieve as nearly as possible the same economic effect as the original provision, and the legality, validity and enforceability of the remaining provisions of this Agreement shall not be affected or impaired thereby.

- The failure of either party to enforce any term or condition of this Agreement shall not constitute a waiver of either party's right to enforce each and every term and condition of this Agreement. No breach under this agreement shall be deemed waived or excused by either party unless such waiver or consent is in writing signed by the party granting such waiver or consent. The waiver by or consent of a party to a breach of any provision of this Agreement shall not operate or be construed as a waiver of

or consent to any other or subsequent breach by such other party.

- This Agreement may not be assigned (including by operation of law or otherwise) by you without WILEY's prior written consent.
- Any fee required for this permission shall be non-refundable after thirty (30) days from receipt by the CCC.
- These terms and conditions together with CCC's Billing and Payment terms and conditions (which are incorporated herein) form the entire agreement between you and WILEY concerning this licensing transaction and (in the absence of fraud) supersedes all prior agreements and representations of the parties, oral or written. This Agreement may not be amended except in writing signed by both parties. This Agreement shall be binding upon and inure to the benefit of the parties' successors, legal representatives, and authorized assigns.
- In the event of any conflict between your obligations established by these terms and conditions and those established by CCC's Billing and Payment terms and conditions, these terms and conditions shall prevail.
- WILEY expressly reserves all rights not specifically granted in the combination of (i) the license details provided by you and accepted in the course of this licensing transaction, (ii) these terms and conditions and (iii) CCC's Billing and Payment terms and conditions.
- This Agreement will be void if the Type of Use, Format, Circulation, or Requestor Type was misrepresented during the licensing process.
- This Agreement shall be governed by and construed in accordance with the laws of the State of New York, USA, without regards to such state's conflict of law rules. Any legal action, suit or proceeding arising out of or relating to these Terms and Conditions or the breach thereof shall be instituted in a court of competent jurisdiction in New York County in the State of New York in the United States of America and each party hereby consents and submits to the personal jurisdiction of such court, waives any objection to venue in such court and consents to service of process by registered or certified mail, return receipt requested, at the last known address of such party.

**WILEY OPEN ACCESS TERMS AND CONDITIONS**

Wiley Publishes Open Access Articles in fully Open Access Journals and in Subscription journals offering Online Open. Although most of the fully Open Access journals publish open access articles under the terms of the Creative Commons Attribution (CC BY) License only, the subscription journals and a few of the Open Access Journals offer a choice of Creative Commons Licenses. The license type is clearly identified on the article.

**The Creative Commons Attribution License**

The Creative Commons Attribution License (CC-BY) allows users to copy, distribute and transmit an article, adapt the article and make commercial use of the article. The CC-BY license permits commercial and non-

**Creative Commons Attribution Non-Commercial License**

The Creative Commons Attribution Non-Commercial (CC-BY-NC)License permits use, distribution and reproduction in any medium, provided the original work is properly cited and is not used for commercial purposes.(see below)

**Creative Commons Attribution-Non-Commercial-NoDerivs License**

The Creative Commons Attribution Non-Commercial-NoDerivs License (CC-BY-NC-ND) permits use, distribution and reproduction in any medium, provided the original work is properly cited, is not used for commercial purposes and no modifications or adaptations are made. (see below)

**Use by commercial "for-profit" organizations**

Use of Wiley Open Access articles for commercial, promotional, or marketing purposes requires further explicit permission from Wiley and will be subject to a fee.

Further details can be found on Wiley Online Library http://olabout.wiley.com/WileyCDA/Section/id-410895.html

**Other Terms and Conditions:**

**v1.10 Last updated September 2015**

**Questions? customercare@copyright.com or +1-855-239-3415 (toll free in the US) or +1-978-646-2777.**